DISSERTATION

NOVEL POLYNUCLEAR COPPER COMPOUNDS OF HALIDES AND PSEUDO–HALIDES

Submitted by

Joseph Henry Reibenspies

Department of Chemistry

In partial fulfillment of the requirements

for the Degree of Dotor of Philosophy

Colorado State University

Fort Collins, Colorado

Spring, 1987

COLORADO STATE UNIVERSITY

December 23, 1986

WE HEREBY RECOMMEND THAT THE THESIS PREPARED UNDER OUR SUPERVISION BY JOSEPH HENRY REIBENSPIES ENTITLED NOVEL POLYNUCLEAR COPPER COMPOUNDS OF HALIDES AND PSEUDO HALIDES BE ACCEPTED AS FULFILLING IN PART REQUIREMENTS FOR THE DEGREE OF DOCTOR OF PHILOSOPHY.

Committee on Graduate Work

Advisor

Department Head

ABSTRACT OF DISSERTATION

NOVEL POLYNUCLEAR COPPER COMPOUNDS OF HALIDES AND PSEUDO–HALIDES

Mixed-valence compounds (one trinuclear (**4**) and two polymeric (**5**,**6**)) of copper(I,II) containing bridging cyano ligands and the ligands **1** (Pre–H) and **2** (cyclops) have been synthesized and characterized by single crystal X-ray diffraction. For **4**, $[Cu(\mathbf{1})(\mu\text{-}NC)]_2Cu(CN) \cdot H_2O$, a = 9.723(2) Å, b = 10.908(2) Å, c = 16.184(3) Å, α = 97.82(1)°, β = 103.64(2)°, γ = 92.21(2)°. Compound **5** ($[Cu(\mathbf{1})(\mu\text{-}NC)Cu(\mu\text{-}CN)]_n$) occurs in three structural modifications. For **5a**, a = 7.755(2) Å, b = 13.179(3) Å, c = 16.508(5) Å. For **5b**, a = 7.878(2) Å, b = 8.418(2) Å, c = 25.874(4) Å, β = 94.15(2)°. For **5c**, a = 8.85(1) Å, b = 20.755(8) Å, c = 23.081(8) Å. For **6**, $[Cu(\mathbf{2})(\mu\text{-}NC)Cu(\mu\text{-}CN)\cdot(1/2C_6H_6)]_n$, a = 11.667(2) Å, b = 8.962(2) Å, c = 19.895(5) Å, β= 97.58(2)°. The discrete molecules of **4** contain a trigonal planar $[Cu(CN)_3]^{2-}$ unit, which bridges between two $[Cu(\mathbf{1})]^+$ complexes through two cyano ligands. Each of the polymeric species **5a**, **5b**, **5c**, and **6** consists of a chain of $[Cu(CN)_2]^-$ units joined by bridging cyano ligands. A cyano ligand also bridges between the copper(I) atoms of the chain and $[Cu(\mathbf{1})]^+$ or $[Cu(\mathbf{2})]^+$ complexes.

The structures of three dinuclear copper(II) complexes, in which the Cu(II) atoms are bridged by azido and hydroxo ligands and by either the phenolate oxygen atom of N_6OH or $N_6'OH$ have been determined by single crystal X-ray diffraction. The compound $[Cu_2(\mu\text{-}1,3\text{-}N_3)(N_6O)](ClO_4)_2\cdot THF$ (**7**) crystallized in the orthorhombic space group $P2_12_12_1$, with a = 12.977(2) Å, b = 13.188(3) Å, c = 22.033(6) Å. The compound $[Cu_2(\mu\text{-}$

1,1-N_3)(N_6'O)]$(BF_4)_2$·THF (**8**) crystallized in the orthorhombic space group $P2_1cn$, with a = 10.222(2) Å, b = 16.683(4) Å, c = 23.517(7) Å. The compound [Cu_2(μ-OH)(N_6'O)]$(BF_4)_2$ · THF (**9a**) crystallized in the monoclinic space group $P2_1/n$, with a = 12.457(3) Å, b = 10.222(3) Å, c = 30.397(10) Å, β = 91.63(2). In these complexes each copper(II) atom is five-coordinate and is bound to three nitrogen atoms and the bridging phenoxo oxygen atom of either N_6O^- or N_6'O^-. The fifth coordination site on each copper(II) atom is occupied by an atom of the bridging azido or hydroxo ligand.

A dinuclear copper(II) complex which contains a bridging iodo ligand and two [Cu(**2**)]$^+$ moieties has been characterized by X-ray crystallography. [Cu_2(**2**)$_2$I](ClO_4) · 2MeOH (**10**) crystallized in the monoclinic system, space group $C2/c$, with Z = 4 and a = 21.564(3) Å, b = 11.920(2) Å, c = 14.831(2) Å, β = 96.83(1)°. Each of the copper(II) atoms in the dimer is coordinated to four nitrogen atoms of ligand **2** and to the bridging iodo ligand.

The structures of two phases of the perchlorate salt of the copper(II) complex of **1** and methanol have been characterized by X-ray crystallography. For the room temperature phase {[Cu(**1**)]ClO_4 · 1/2 MeOH}$_n$ (**11a**), a = 23.018(3) Å, b = 6.903(1) Å, c = 22.511(3) Å, β = 105.48(1)°. For the low temperature phase {[Cu(**1**)]ClO_4 · 1/2 MeOH}$_2$ ((**11b**), a = 6.850(2) Å, b = 11.886(3) Å, c = 22.303(5) Å, α = 75.26(2)°, β = 88.97(2)°, γ = 73.38(2)°. When cooled, the crystalline solid **11** undergoes a reversible structural change. **11a** is polymeric in nature, with bridging between copper atoms accomplished by an oxime oxygen atom of ligand **1**. **11b** is best described as dimeric.

Joseph Henry Reibenspies
Department of Chemistry
Colorado State University
Fort Collins, CO 80523
Spring, 1987

Acknowledgments

As I prepare for these final pages of my dissertation I am reminded how blessed I was to find such warm hearted people who, in one way or another, have helped me to fulfill a dream I began so long ago. A list of such people would easily fill a text this size and more, but still there are a few good people I wish to acknowledge.

To my classmates Cindy, Mike, and Bob. We began the race not knowing where the path would lead or to what end our efforts would repay us; still we ran together and if one should stumble the others would lift him up. Never did I run alone. Cindy, your wisdom and warm smile shall always be remembered and when time comes when I shall advise I shall follow your lead and yes, we are still the shuffle-board champs. Bob I shall keep your common sense chemistry with me and every Friday I shall raise a can or two of beer to that end. Mike, my friend, I cannot begin to thank-you. You have truly said in words and deeds what it means to be friends. With out your trust I would not have reached my goal. Have a beer for me sometime and remember.

To Kevin, Lu, and Suzy, well its all yours now. I know that you'll grow to love that old machine. Treat her well. I leave Colorado knowing that she could be in no better care for I see in you the best there is. Take care.

To Dr. Paul Norman and Dr. Richard Cornelius. Dick, you sparked my interest and advised me toward new goals, new dreams. You gave to me more than just your advise but your desire for knowledge for this I shall be forever thankful. Paul I wish we could lift a 'pint' or two again and talk of science and life. Paul, keep the pubs open I shall see you again.

To my parents John and Claire, you brought me into life, with love, and showed me how to read and to ask why. I owe you everything. I remember the kind words and

the faith that kept my spirit alive. Someday I may be asked to give as you have given and I shall respond with love, as you two would respond, for I have had the best of teachers.

To Dr. Oren Anderson, you have been not only a guide and a teacher but a friend as well. For all your labors in particular your help in the preparation of this thesis I shall be eternally grateful. I can truly say that you are the best instructor that I know. You teach not just by your words but by your deeds.

Finally to Lisa my wife, how could I tell you what help and encouragement you have shown to me. Not only for typing most of this dissertation but by giving me the hope and love that I need so desperately. Our lives are just beginning to blossom. I give you this work of my hands for without you it would be but words without meaning, an empty dream, a wish left unspoken.

TABLE OF CONTENTS

LIST OF TABLES

LIST OF FIGURES

Chapter 1

Cyano-Bridged Mixed-Valence Compounds of Copper(I,II) Utilizing the Ligands Pre–H and Cyclops

Introduction

The cyanide ion coordinates to transition metals as either a terminal or a bridging ligand. The C–N distance of 1.16 Å[1–6] in cyano ligands is consistent with the existence of a triple bond between carbon and nitrogen. The highest filled orbital of the cyanide ion has σ_z symmetry and is localized on the carbon atom.[7,8] A lower filled orbital that is localized on the nitrogen atom has σ_s^* symmetry. Comparison of orbital energies dictates that the carbon atom of the cyanide ion is more basic than the nitrogen atom. Thus the coordination of cyanide ion to transition metals, as a terminal ligand, occurs through the carbon atom. Overlap of the orbitals on the cyano ligand with the nd_σ, (n+1)*s* and $(n+1)p_\sigma$ metal orbitals creates the sigma bond, while the empty π^* orbitals of the cyano group are available for backbonding.[7]

Electronic transitions in complexes containing carbon-bound cyano ligands lie higher in energy than similar transitions in complexes containing nitrogen-bound cyano ligands.[8] As a result, carbon-bound cyano ligands are at the same position in the spectrochemical series as carbon-bound carbonyl compounds, while nitrogen-bound cyano compounds are approximately at the level of N- bound thiocyanate and cyanate ligands. The degenerate π_x and π_y orbitals of the cyanide ion fall between the sigma orbitals in energy. These orbitals are potentially basic, but "side-on" binding of the cyanide ion is unknown.

Bridging cyano ligands display cyanide's ambidentate character by binding to one metal atom through the carbon atom and to a second metal atom through the nitrogen atom.[7,9,10] Distortions from linearity are uncommon for terminal M–C–N bonds, but have been reported for M–C–N–M bridges. Such distortions commonly involve bending of the bridge at the nitrogen atom.[11–13]

Copper(I) forms a variety of cyano adducts. CuCN is a diamagnetic solid and crystallizes in the orthorhombic system with 36 formula units per unit cell.[14] The structure of CuCN has not been determined. The copper(I) atoms of CuCN can form adducts with a variety of nitrogen donor ligands. These moieties are often one-, two- or three-dimensional cyano-bridged polymers in which the coordination environment about the copper(I) atoms is influenced by packing requirements along and between the polymeric chains.

The structures of one-dimensional $[Cu(L)(\mu\text{-}CN)]_n$ ploymers (where L = diethylamine,[2] triethylamine,[2] 1,10-phenanthroline,[2] 2,9-dimethyl-1,10-phenanthroline,[3] 4-methylpyridine,[2] and biquinoline[15]) show the influence of ligand bulk. The three-coordinate copper(I) atoms in the diethylamine and triethylamine adducts of CuCN exhibit trigonal planar geometry, with two sites occupied by atoms of bridging cyano ligands and the remaining site occupied by the amine nitrogen atom. The polymer chain displays a high degree of flexibility in adjusting to binding of the amine base. The bond angle at copper(I) between the bridging cyano ligands reflects the degree of distortion caused by the coordination of the amine base to the copper(I) atom. For ideal trigonal planar geometry, this angle (N–Cu–C) would be 120°, but in the diethylamine adduct this angle is 133.3(4)°.[2] Coordination of the stericly bulkier triethlyamine base widens the (N–Cu–C) angle to 148.9(5)°.[2]

The structures of CuCN adducts of 1,10-phenanthroline[2] and 2,9-dimethyl-1,10-phenanthroline,[3] which have similar formulas, differ as a result of the different packing requirements of the bidentate ligands. The geometry about the copper atom is tetrahedral in each case, with two sites occupied by nitrogen atoms of the bidentate ligand and two sites

occupied by atoms of bridging cyanide groups. In the 1,10-phenanthroline adduct the chain is helical and coils around a threefold screw axis. The CuCN chain in the 2,9-dimethyl-1,10-phenanthroline adduct is nearly planar and is propagated along a twofold screw axis parallel to the crystallographic *b* axis.

The 4-methylpyridine adduct of CuCN contains three- and four-coordinate copper(I) atoms that are bridged by cyano ligands. The coordination geometry about the copper atoms is either trigonal planar or tetrahedral. Two sites in the tetrahedral case and one site in the trigonal planar case are occupied by nitrogen atoms of the 4-methylpyridine base while two sites in each case are occupied by atoms of bridging cyano ligands.

Both two- and four-coordinate copper(I) atoms occur in $[Cu(L)(\mu\text{-}NC)Cu(\mu\text{-}CN)Cu(L)(\mu\text{-}NC)]_n$ (L = biquinoline).[15] This compound contains dimeric $[Cu(L)(\mu\text{-}NC)Cu(L)]^+$ moieties in which the bridging cyano group is disordered; these dimers are linked by linear $[Cu(CN)_2]^-$ complex ions. The bidentate biquinoline ligand stacks along and between the polymeric chains thus formed.

Compounds containing dicyanocuprate(I) units may contain a polymer chain in which only one of the two cyano ligands bridges between copper(I) atoms. The second cyano ligand, which is bound to the copper(I) in a terminal fashion, is then available for other bridging interactions. The simplest such compounds are $Na[Cu(CN)(\mu\text{-}CN)]\cdot 2H_2O$[1] and $K[Cu(CN)(\mu\text{-}CN)]$.[13] In the sodium salt, the dicyanocuprate(I) polymer chain is planar, and is propagated by the *c* glide operation. The cyano bridges between the copper(I) atoms are linear. In the potassium salt, the dicyanocuprate(I) polymer chain is coiled about a twofold screw axis parallel to the crystallographic *b* axis; the cyano bridges between the copper(I) atoms are nonlinear. The sodium ion in $Na[Cu(CN)(\mu\text{-}CN)]\cdot 2H_2O$ and the potassium ion in $K[Cu(CN)(\mu\text{-}CN)]$ interact weakly with the nitrogen atom of the terminal cyano ligand of the polymeric chain.

The mixed-valence compound $[Cu_3(NH_3)_3(CN)_4]$[16] also contains one-dimensional chains composed of $[Cu(CN)(\mu\text{-}CN)]^-$ units. In this case the terminal cyano ligands of the

chain bind to $[Cu(NH_3)_3]^{2+}$ groups to form planar pentagonal moieties containing four Cu(I) atoms and one Cu(II) atom, all bridged by cyano ligands. Each such pentagon shares two edges with adjacent reversed pentagons to form the polymeric chain. Spectroscopic studies of the mixed-valence polymer $[Cu(NCMe)_4][Cu_2(\mu\text{-}CN)_2]$[17] suggest that the compound contains a structure similar to the one-dimensional $Cu_3(NH_3)_3(CN)_4$ compound. A detailed structural analysis has not been reported.

Polymers involving two dimensional sheets occur in copper(I) cyanide adducts of hydrazine-*N*,*N*',[18] 4-cyanopyridine-*N*,*N*',[19] pyridazine-*N*,*N*',[19] dimethylthioformamide-*S*,[20], and selenocyanato-*Se*,*N*·1/2$[Cu(en)_2(OH_2)]^{2+}$.[21] The hydrazine and 4-cyanopyridine adducts consist of a chain of CuCN units bridged by cyanide ions. The chains are connected by ambidentate hydrazine or 4-cyanopyridine ligands to form a two-dimensional sheet of repeating units. The coordination geometry about the copper(I) atom in these cases is distorted tetrahedral, with two sites occupied by nitrogen atoms of the bases and two sites occupied by atoms of the bridging cyano ligands. The pyridazine[19] and dimethylthioformamide[20] adducts also contain one-dimensional cyanocuprate(I) chains. The chains are joined by the bifunctional bases in such a way as to form rings involving two copper atoms and two bases. The coordination geometry about the copper(I) atoms are roughly tetrahedral, with two sites occupied by atoms of the base molecules and two sites occupied by atoms of the bridging cyano ligands. The structure of the selenocyanide adduct (SeCN·1/2$[Cu(en)_2OH_2]^{2+}$) is similar to that of the pyridazine and dimethylthioformamide adducts except that the bridging selenocyante ion is charged. The selenocyanide ligand bridges between the copper atoms in such a way as to form a ring with corners occupied by copper(I) atoms and by the selenium and nitroge atoms of the selenocyante ligands. Every two repeat units are accompanied by a discrete complex counter ion ($[Cu(en)_2H_2O]^{2+}$).

Two-dimensional mixed-valence copper(I,II) polymers occur in $Cu_5(NH_3)_2(CN)_6$[22] and $Cu_4(NH_3)_2(OH_2)(CN)_5$.[22] Each compound contains CuCN

repeat units and $[Cu(NH_3)_2]^{2+}$ complex ions. In each repeat unit, two cyano ligands bridge between copper(I) atoms to form a one-dimensional polymeric chain, while one cyano ligand is terminal. The $[Cu(NH_3)_2]^{2+}$ units bridge between the one-dimensional chains by means of *trans* coordination of the terminal cyano ligands. The one-dimensional polymer in the structure of $Cu_5(NH_3)_2(CN)_6$ contains planar $[Cu_2(CN)_4]^{2-}$ units, which are bridged by linear $[Cu_2(CN)_2]$ units through their cyano ligands. The chains are connected by $[Cu(NH_3)_2]^{2+}$ complexes, which coordinate to the terminal cyano ligands in the $[Cu_2(CN)_4]^-$ units. The one-dimensional polymer in $Cu_4(NH_3)_2(OH_2)(CN)_5$ contains planar $[Cu_2(CN)_4]^-$ units, which are bridged by linear [Cu(CN)] units through cyano ligands. The chains are bridged by $[Cu(NH_3)_2(OH_2)]^{2+}$ complexes, which coordinate to the terminal cyano ligands in the $[Cu_2(CN)_4]^-$ units. The copper(II) atoms display square pyramidal coordination geometries with *trans* basal sites occupied by the nitrogen atoms of the bridging cyano ligands and the remaining basal sites occupied by nitrogen atoms of the amine ligands. The apical site is occupied by a coordinated water molecule.

The three-dimensional mixed-valence polymer $Cu_5(DMF)_4(CN)_6$ (DMF = dimethylformamide)[9] contains linear $[Cu(\mu\text{-}CN)_2]^-$ units which bridge between moieties that contain dimeric $[Cu_2(CN)_2]$ units. The bridging nature of the cyano ligands in the dimeric units is similar to that seen in the ammine adduct of CuCN[10] in that the copper(I) atoms are bridged by the carbon atoms of the cyano ligands. The nitrogen atoms of the cyano ligands in the dimeric unit thus are available to bridge to $[Cu(DMF)_4]^{2+}$ complexes. The coordination geometry about the copper(I) atoms in the dimeric unit is roughly tetrahedral, with two sites occupied by nitrogen atoms of cyano ligands of the linear dicyanocuprate(I) unit, and two sites occupied by cyano carbon atoms. The coordination geometry about the copper(II) atom is distorted octahedral, with *trans* sites occupied by nitrogen atoms of bridging cyano ligands.

Nonpolymeric copper(I) cyano compounds have been reported; the sodium[6] and $\{[Cu([9]aneN_3)_2]^{2+}\}$[5] salts of the $[Cu(CN)_3]^{2-}$ anion and the potassium salt[23] of the

$[Cu(CN)_4]^{3-}$ anion contain discrete anions. The copper(I) atoms in the tricyanocuprate anions exhibit trigonal planar coordination, with carbon-bound cyano ligands occupying the three coordination sites. $[Cu(en)_2][Cu(CN)_3]$ has also been synthesized,[24] but its structure was not determined. The coordination geometry in the tetracyanocuprate(I) anion is tetrahedral, with carbon-bound cyano ligands occupying the four sites. No instances of bridging between the tricyanocuprate(I) anion and other metal ion complexes have been reported, although the possibility of such bridging through the terminal cyano ligands would seem to exist.

Discrete copper(II) complexes of the formula Cu(**L**)CN (where **L** = cyclops[25] and PnAO–H[26]) have been reported. The cyano ligands in these complexes are carbon-bound. The coordination geometry about the copper(II) atoms is square pyramidal in each case, with the basal sites occupied by nitrogen atoms of the tetradentate ligands and the apical site occupied by the cyano ligand.

A discrete dimeric copper(II) complex $\{[Cu(\mathbf{L})]_2CN\}ClO_4$ (where **L** = [14]-4,11-diene-N_4) has been reported.[27] The dimer consists of two Cu(**L**) complexes bridged by a cyano ligand. The cyano ligand is disordered in the solid state. The coordination geometry about the copper(II) atoms is square pyramidal, with the basal sites occupied by nitrogen atoms of ligand **L** and the apical site occupied by an atom of the bridging cyano ligand.

This dissertation reports the synthesis of mixed-valence copper(I,II) compounds in which bridging by cyano ligands is common. $\{[Cu(CN)(\mu\text{-}CN)]^-\}$ chains and $[Cu(CN)_3]^{2-}$ anions have been utilized to bind reduction-resistant Cu(II) complexes through cyano bridges. Copper(II) complexes of ligand **1** (4,8-diaza-3,9-dimethylundeca-3,8-diene-2,10-dione dioxime, Pre–H) and **2** ($Me_4BO_2F_2$[14]teteneN$_4$, cyclops) are such

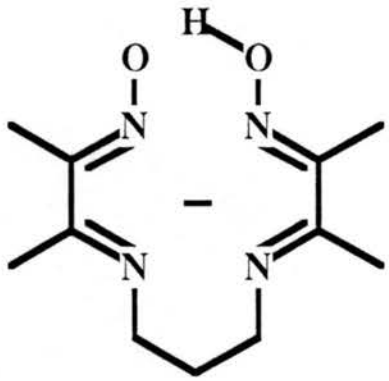

Pre-H, 1

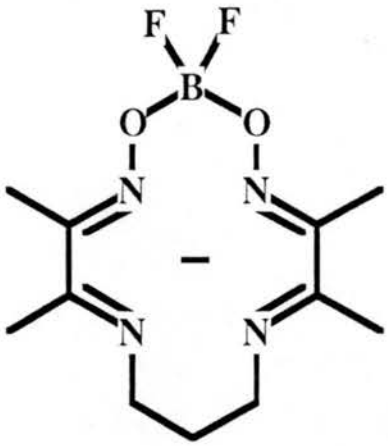

cyclops, 2

reduction-resistant complexes. The cyano adduct of the copper(II) complex of **2**[25] and the copper(II) complex of a ligand similar to **1** (PnAO–H)[26] have been structurally characterized. The strong sigma donor properties of these ligands is a major factor in the inability of cyanide to reduce copper(II) in these systems.[28] A trinuclear complex and two one-dimensional polymeric compounds are reported herin. One of the one-dimensional polymers occurs as three structural variations of the same formula unit. These complexes offer further examples of rare mixed-valence cyano-bridged copper compounds.

Experimental

EPR and Magnetic Susceptibility Measurements. Samples for EPR and magnetic susceptibility experiments were ground to a fine powder. Infrared spectra of the powders confirmed that the structures did not change upon grinding. Small samples of less than 10 mg were used in the EPR experiments, while larger samples of approximately 20 mg were required for the magnetic susceptibility experiments.

All EPR spectra were recorded on a Varian E-9 X-band EPR spectrometer, located in the laboratory of Professor Gareth Eaton at the University of Denver. The sample compartment was maintained at a temperature of –174 °C. The individual spectra were calibrated against a DPPH standard; its spectrum was recorded immediately following the recordinag of the sample spectra.

The magnetic susceptibility measurements were made at room temperature on a Cahn Faraday balance with $Hg[Co(NCS)_4]$ as calibrant. The room temperature magnetic susceptibility was corrected by applying Pascal's constants.[29] The magnetic moment, μ_{eff}, was calculated from

$$\mu_{eff} = 2.828(\chi T)^{1/2}$$

Synthesis of $Na_2Cu(CN)_3 \cdot 3H_2O$. A 2.5 g sample (0.050 mol) of NaCN (Aldrich) was added to 2.25 g (0.025 mol) of CuCN (Aldrich) dissolved in 50 mL of water. The solvent was evaporated at low heat until white crystals formed. The solution was allowed to slowly cool to room temperature. The crystals were collected by filtration and washed with cold water. (see reference 6)

Synthesis of 4,8-diaza-3,9-dimethylundeca-3,8-diene-2,10-dione dioxime, (Pre). A 20.6 mL (0.10 mol) aliquot of 1,3-diaminopropane (Aldrich) was

added to 125 mL of a hot (~60 °C) solution containing 50 g (0.50 mol) of 2,3 butanedione monoxime (Aldrich) in 90% ethanol. The colorless solution of 2,3-butanedione monoxime turned pale yellow immediately upon mixing with the 1,3-diaminopropane . The solution was stirred while the temperature was slowly lowered to room temperature. The resulting solution was further cooled in an ice bath to 0° C. Fine white crystals of **Pre** formed slowly over 20 min; the crystals were collected by filtration and washed with cold ethanol. Yield 26 g (47%), m.p. 75 °C.

Synthesis of $[Cu(1)(OH_2)]BF_4$ (3). A 3.7 mL sample of 48% HBF_4 was added to 40 mL of an aqueous solution containing 8.0 g (40 mmol) of $Cu(CH_3CO_2)_2{\cdot}H_2O$ (Baker and Adamson). 40 mL of a solution of 4.8 g (20.0 mmol) of **Pre** in methanol was then added drop by drop. The resulting dark brown solution was stirred at room temperature for 20 min, after which its volume was reduced to approximately 20 mL on a rotary evaporator. Over the course of 12 h, at 0 °C a brown crystalline solid formed. The solid was collected by filtration and washed with ether. Yield 1.50 g (18.4%).

Synthesis of $[Cu(1)(OH_2)]ClO_4$. A solution of 4.9 g of **Pre** (0.020 mol) in 20 mL of acetone was slowly added to a hot (~50 °C) solution of 3.9 g (0.01 mol) of $[Cu(H_2O)_6](ClO_4)_2$ (Pfaltz & Bauer) in 20 mL of acetone. The resulting solution was stirred for 10 min and slowly cooled to ice temperature. Dark red crystals were collected by filtration and washed with ether. The compound was recrystallized from 95% ethanol. Yield 2.8 grams (45%).

Synthesis of $[Cu(2)(OH_2)]ClO_4$. A sample of 8.8 g (0.021 mol) of $[Cu(\mathbf{1})H_2O]ClO_4$ was dissolved in 60 mL of 98% boron trifluoride diethyletherate. The solution was refluxed for one h and allowed to cool to room temperature. The cooled solution was poured into a mixture of 800 g of ice and 200 grams of sodium acetate. This mixture was allowed to warm to room temperature; its volume was then reduced on a rotary evaporator without heat to one-fourth of its original value. $NaClO_4$ (20 g) was

dissolved in the resulting solution. After 2 h, deep purple crystals were collected by filtration and washed with ethanol. Yield 1.5 g (17%).

Synthesis of [Cu(1)(μ-NC)]$_2$CuCN (4). 0.16 g (0.39 mmol) of **3** was dissolved in 20 mL of methanol; the solution was diluted to 40 mL with benzene. Dropwise addition of a second solution of NaCN (0.02 g, 0.4 mmol) and $Na_2Cu(CN)_3 \cdot 3H_2O$ (0.04 g, 0.17 mmol) in 40 mL of a 50/50 mixture of benzene and methanol resulted in an immediate color change from pale brown to dark green. The volume of the solution was slowly reduced with a dry air flush to approximately 8 mL. A dark green crystalline solid formed during the course of 12 h at 0 °C. The product was collected by filtration and washed with 95% ethanol. Yield 30 mg (23%)). Elemental analysis: calculated for $C_{25}H_{38}N_{11}O_4Cu_3 \cdot H_2O$, C 39.24%, H 5.27%, N 20.13%, O 10.45%; found, C 39.43%, H 5.04%, N 19.80%, O 9.98% (Galbraith Laboratories). $\chi_g^{294K} = 4.15 \times 10^{-6}$ cgs/g, $\mu_{eff} = 2.82$.

Compound **4** may also be synthesized by using $Na_3Cu(CN)_4$.[23] In this alternative procedure 0.16 g (0.39 mmol) of **3** was dissolved in 40 mL of a 50/50 mixture of methanol and benzene. Addition of a solution of 0.010 g (0.20 mmol) of NaCN and 0.040 g (0.20 mmol) of $Na_3Cu(CN)_4$ dissolved in 40 mL of a 50/50 mixture of methanol and benzene was followed by reduction of the solution volume to 10 mL under a dry air flush. Cooling the resultant solution to 0° C for 12 h resulted in the isolation of crystals of compound **4**.

Synthesis of [Cu(1)(μ-NC)Cu(μ-CN)$_n$ (5a). 0.15 g (0.36 mmol) of [Cu(**1**)OH_2]ClO_4 was added to 20 mL of methanol. Rapid addition of a solution of $Na_2Cu(CN)_3 \cdot 3H_2O$ (0.04 g, 0.17 mmol in 15 mL of methanol) resulted in an immediate color change from brown to dark green. The [Cu(**1**)OH_2]ClO_4 powder dissolved, with stirring, over a period of 24 h. The solvent was allowed to evaporate slowly from the resulting solution at room temperature until the volume was approximately 5 mL. Large prismatic crystals formed during this process. The crystals were collected by filtration and

washed with methanol. Yield 10 mg (14%). $\chi_g^{294K} = 2.81 \times 10^{-6}$ cgs/g, $\mu_{eff} = 1.75$, $g_{ave} = 2.085$.

Synthesis of [Cu(1)(μ-NC)Cu(μ-CN)]$_n$ (5b). 0.15 g (0.36 mmol) of **3** was dissolved in 50 mL of methanol. Rapid addition of a solution of $Na_2Cu(CN)_3 \cdot 3H_2O$ (0.04 g, 0.17 mmol in 15 mL of methanol) resulted in an immediate color change from brown to dark green. The solution was stirred, at room temperature, for 1 h and then rapidly reduced in volume to 20 mL under a dry air flush. The resulting solution was cooled to –19 °C. Crystals (large dark green parallelepipeds) formed overnight. The crystals were collected by filtration and washed with methanol. Yield 20 mg (28%). Elemental analysis: calculated for $C_{13}H_{19}N_6Cu_2O_2$, C 37.32%, H 4.58%, N 20.09%, O 7.65%; found, C 37.41%, H 4.33%, N 20.08%, O 9.56% (Galbraith Laboratories). $\chi_g^{294K} = 2.80 \times 10^{-6}$ cgs/g, $\mu_{eff} = 1.75$, $g_{ave} = 2.109$.

Synthesis of [Cu(1)(μ-NC)Cu(μ-CN)]$_n$ (5c). 0.082 g (0.20 mmol) of **3** was dissolved in 10 mL of methanol; this solution was diluted to 20 mL by addition of benzene. Slow addition of a solution of $Na_2Cu(CN)_3 \cdot 3H_2O$ (0.022 g, 0.10 mmol, in 20 mL of a mixture of 50/50 methanol/benzene) resulted in an immediate color change from brown to dark green. The solvent was rapidly evaporated by a dry air flush until the solution volume was 20 mL. Large dark green crystals formed during storage at –19 °C overnight; These crystals were collected by filtration and washed with methanol. Yield 13 mg (31%). $\chi_g^{294K} = 2.42 \times 10^{-6}$ cgs/g, $\mu_{eff} = 1.63$, $g_{ave} = 2.087$.

Synthesis of [Cu(2)(μ-NC)Cu(μ-CN) · 1/2 C$_6$H$_6$]$_n$ (6). 0.040 g (0.080 mmol) of [Cu(**2**)H_2O]ClO_4 was dissolved in 10 mL of methanol; this solution was diluted to 20 mL by addition of benzene. Rapid addition of a solution of $Na_2Cu(CN)_3 \cdot 3H_2O$ (0.02 g, 0.09 mmol, in 10 mL of a 50/50 mixture of methanol and benzene) resulted in an immediate color change from violet to blue. The solution was cooled to –19 °C. Thin, plate-like, light blue crystals formed over a two week period; these crystals were collected and washed in cold ethanol. Yield 10 mg (50%). Elemental analysis: calculated for

$C_{16}H_{21}N_6BF_2Cu_2O_2$, C 38.03%, H 4.19%, N 16.63%, O 6.33%; found, C 38.78%, H 4.87%, N 20.02%, O 8.09% (Galbraith Laboratories). $\chi_g^{294K} = 2.86 \times 10^{-6}$ cgs/g, $\mu_{eff} = 1.87$, $g_{ave} = 2.079$.

X-ray Structure Determinations. The crystallographic experiments were carried out on a Nicolet *R3m* X-ray diffractometer utilizing the software provided with the instrument. The SHELXTL program package (rev. 4.1, 1983, written by G. M. Sheldrick and supplied by Nicolet XRD for the Data General Eclipse S/140 computer) was used for data reduction, structure solution, refinement, and plotting. Neutral atom scattering factors and anomalous dispersion terms were taken from reference 39.

Structure Determination for 4. A wedge-shaped crystal of **4** was mounted on a glass fiber and centered on the X-ray diffractometer. The cell constants reported in Table 1.1 were calculated from a least squares fit to the setting angles for 12 independent reflections ($2\theta_{ave} = 14.3°$). Three control reflections monitored every 200 reflections showed no significant variation in intensity during the data collection. Data were corrected for Lorentz and polarization factors but not for absorption.

The structure was solved by Patterson map interpretation. All nonhydrogen atoms were refined using anisotropic thermal parameters. Hydrogen atoms bound to carbon were placed in idealized positions (C–H = 0.96 Å, $U_{iso}(H) = 1.2 \times U_{iso}(C)$). Weighted [$w = (\sigma^2(F) + g(F)^2)^{-1}$] least squares refinement on F yielded the residual values listed in Table 1.1 at convergence (for the last 20 cycles, mean shift/e.s.d = 0.027, max. shift/e.s.d. = 0.28 for rotation of the methyl group C28 about the C21 – C28 bond). The height of the highest peak in the final ΔF map was +0.47 e Å^{-3} (near C25), while the minimum was –0.41 e Å^{-3}.

Structure Determination for 5a. A crystal of **5a** was mounted on a glass fiber and centered on the X-ray diffractometer. The cell constants reported in Table 1.2 were calculated from a least squares fit to the setting angles for 22 independent reflections ($2\theta_{ave} = 18.0°$). Three control reflections monitored every 197 reflections showed no

Table 1.1. Details of the Crystallographic Experiment and Computations for **4**.

Formula	$C_{25}H_{40}N_{11}Cu_3O_5$
Formula weight (g mol^{-1})	765.3
Crystal system	triclinic
Space group	$P\bar{1}$
Lattice constants	
a (Å)	9.723(2)
b (Å)	10.908(2)
c (Å)	16.184(3)
α (deg)	97.82(1)
β (deg)	103.64(2)
γ (deg)	92.21(2)
V (Å^3)	1648
Temperature (°C)	20(1)
Z	2
ρ(calculated, g cm^{-3})	1.54
ρ(observed, g cm^{-3})[a]	1.53
Crystal dimensions	0.32 mm × 0.26 mm × 0.16 mm × 0.04 mm
Radiation	MoK_α(λ = 0.71073 Å)
Monochromator	graphite
μ (cm^{-1})	20.5
Scan type	θ-2θ
Geometry	bisecting
Scan speed (deg min^{-1})	2.0 – 29.3
2θ range (deg)	3.5 – 50.0
Index restrictions	$0 \le h \le 12$; $-13 \le k \le 13$; $-20 \le l \le 20$
Total number of reflections	6200
Number of unique, observed reflections	4375
Observed reflection criterion	$\lvert F\rvert \ge 4.0\ \sigma\lvert F\rvert$
Data to parameter ratio	9.8
R	0.039
R_w	0.051
S	1.53
g (refined)	5.0×10^{-4}
Slope, normal probability plot	1.28

[a] Determined by neutral buoyancy in methylene chloride/1,2-dibromoethylene at 20 °C.

Table 1.2. Details of the Crystallographic Experiments and Computations for **5a**, **5b**, and **5c**.

	5a	**5b**	**5c**
Formula	$C_{13}H_{19}N_6Cu_2O_2$	$C_{13}H_{19}N_6Cu_2O_2$	$C_{13}H_{19}N_6Cu_2O_2$
Molecular weight (g mol^{-1})	418.4	418.4	418.4
Crystal system	orthorhombic	monoclinic	orthorhombic
Space group	$Pn2_1a$	$P2_1/c$	$Pcab$
Lattice constants			
a (Å)	7.755(2)	7.878(2)	8.85(1)
b (Å)	13.179(3)	8.418(2)	20.755(8)
c (Å)	16.508(5)	25.874(4)	23.081(8)
β (deg)		94.15(2)	
V (Å^3)	1687(1)	1711(1)	4220(1)
Temperature (°C)	−128(1)	20(1)	−125(1)
Z	4	4	8
ρ (calculated, g cm^{-3})	1.65	1.62	1.31
ρ (observed, g cm^{-3})[a]		1.64	1.59
Crystal dimensions	0.30 mm (001→ 0$\bar{1}\bar{1}$) × 0.30 mm (001→ 01$\bar{1}$) × 0.31mm (010 → 0$\bar{1}$0) × 0.34 mm (100 → $\bar{1}$00)	0.18 mm (0$\bar{1}$1 → 0$\bar{1}\bar{1}$) × 0.16 mm (011 → 01$\bar{1}$) × 0.10 mm (100 → $\bar{1}$00)	0.36 mm (001 → 00$\bar{1}$) × 0.20 mm (010 → 0$\bar{1}$0) × 0.02 mm (100 → $\bar{1}$00)

Table 1.2. (continued)

Radiation	$MoK_\alpha(\lambda = 0.71073$ Å)	MoK_α	MoK_α
Monochromator	graphite	graphite	graphite
Scan type	θ-2θ	θ-2θ	θ-2θ
Geometry	bisecting	bisecting	bisecting
μ (cm^{-1})	26.3	25.9	20.3
Scan speed (deg min^{-1})	5.0 – 29.3	2.0 – 29.3	2.0 – 29.3
2θ range (deg)	3.5 – 50.0	3.5 – 50.0	3.5 to 50.0
Index restrictions	$0 \le h \le 10$; $0 \le k \le 16$; $0 \le l \le 20$	$-10 \le h \le 10$; $-11 \le k \le 0$; $-31 \le l \le 0$	$-11 \le h \le 11$; $0 \le k \le 25$; $0 \le l \le 28$
Total number of reflections	1782	3268	5935
Number of unique, observed reflections	1531	2454	1621
Observed reflection criterion	$\|F\| \ge 3.0\ \sigma\|F\|$	$\|F\| \ge 3.0\ \sigma\|F\|$	$\|F\| \ge 2.5\ \sigma\|F\|$
Data to parameter ratio	6.8	11.2	7.8
R	0.023	0.058	0.115
R_w	0.025	0.069	0.108
S	1.13	1.53	2.28
g	6.1×10^{-4} (refined)	1.0×10^{-4} (fixed)	5.0×10^{-4} (fixed)
Slope, normal probability plot	0.97	1.37	1.53

[a] Determined in each case by flotation in methlyene chloride/1,2-dibromoethylene at 20 °C.

significant variation in intensity during data collection. Data were corrected for Lorentz and polarization factors, as well as for absorption effects. The numerical absorption correction resulted in $T_{min} = 0.50$ and $T_{max} = 0.61$. Systematic reflection conditions suggested that the space group was either *Pnma* or $Pn2_1a$. Attempts to solve the structure in the centrosymmetric space group failed. Statistical tests ($|E^2 - 1|$) suggested that the noncentrosymmetric space group was the correct choice.

The structure was solved readily in $Pn2_1a$ (a variant of $Pna2_1$, No. 33) by Patterson map interpretation. All nonhydrogen atoms were refined with anisotropic thermal parameters. Hydrogen atoms bound to carbon were placed in idealized positions (C–H = 0.96 Å, $U_{iso}(H) = 1.2 \times U_{iso}(C)$). H1(the oxime hydrogen atom) was located in a ΔF map and included (with isotropic thermal parameter) in the refinement. The weighted [$w = (\sigma^2(F) + g(F)^2)^{-1}$] least squares refinement on F yielded the residual values listed in Table 1.2 at convergence (for the last ten cycles, mean shift/e.s.d = 0.008, max. shift/e.s.d. = 0.059 for rotation of the C11 methyl group). The height of the highest peak found in the final ΔF map was +0.24 e Å^{-3} (near C5), while the minimum was –0.46 e Å^{-3}.

Structure Determination for 5b. A parallelepiped of **5b** was mounted on a glass fiber and centered on the X-ray diffractometer. The cell constants reported in Table 1.2 were calculated from a least squares fit to the setting angles for 19 independent reflections ($2\theta_{ave} = 14.0°$). Three control reflections monitored every 97 reflections showed no significant variation in intensity during data collection. Data were corrected for Lorentz and polarization factors, as well as for absorption effects. The numerical absorption correction resulted in $T_{min} = 0.60$ and $T_{max} = 0.78$.

The structure was solved by Patterson map interpretation. All nonhydrogen atoms were refined with anisotropic thermal parameters. Hydrogen atoms bound to carbon were placed in idealized positions (C–H = 0.96 Å, $U_{iso}(H) = 1.2 \times U_{iso}(C)$). The weighted [$w = (\sigma^2(F) + g(F)^2)^{-1}$] least squares refinement on F yielded the residual values listed in

Table 1.2 at convergence (for the last ten least squares cycles, mean shift/e.s.d. = 0.007, max. shift/e.s.d. = 0.06 for U_{33} of O1). The height of the highest peak in the final ΔF map was +0.61 e Å^{-3} (near C6), while the minimum was –0.76 e Å^{-3}. The carbon atom C6 is disordered (50/50) between two positions in the propylene group of ligand **1**.

Structure Determination for 5c. A very thin plate of **5c** was mounted on a glass fiber and centered on the X-ray diffractometer. Initial cell reduction routines indicated that the unit cell might be monoclinic. Axial photographs, however, indicated the presence of a mirror plane perpendicular to both the *a* and *c* crystallographic axes. Twelve crystals were examined; all exhibited this phenomenon. It was concluded that the crystals were twinned. Attempts to identify the twin plane and to slice crystals along this plane so as to isolate a single fragment failed.

A search of reciprocal space identified a set of reflections which gave the best fit to the proposed orthorhombic lattice. These reflections were then used to calculate the cell constants. The cell constants reported in Table 1.2 were calculated from a least squares fit to the setting angle for 10 independent reflections ($2\theta_{ave} = 18.0°$). The data set that was collected contained reflections from each twin fragment. Three control reflections monitored every 97 reflections showed no significant variation in intensity during data collection. Data were corrected for Lorentz and polarization factors, but not for absorption. Data reduction indicated clear systematic absences (*0kl*, $l = 2n$; *h0l*, $h = 2n$; *hk0*, $k = 2n$) which identified the space group as *Pcab* .

The structure was solved by Patterson map interpretation. The cyanocuprate(I) chain and the copper(II) atom were readily identified in the ΔF maps generated during the structure refinement, but the position of the atoms in ligand **1** could not be assigned reliably. Although all of the atoms of the ligand were eventually located, large deviations in bond lengths and angles from acceptable values were common for ligand **1**. Hydrogen atoms were not included in the model, due to the problems in modeling ligand **1**. The weighted [$w = (\sigma^2(F) + g(F)^2)^{-1}$] least squares refinement on F yielded the residual values

listed in Table 1.2 at convergence (for the last twenty least squares cycles, mean shift/e.s.d. = 0.062, max. shift/e.s.d. = 0.417 for *z/c* of C9). The height of the highest peak in the final ΔF map was +0.90 e Å^{-3} (3.8 Å from Cu2), while the minimum was –0.82 e Å^{-3}.

The calculated density of **5c** was much less than that observed (ρ(observed) = 1.59 g cm^{-3}; ρ(calculated) = 1.31 g cm^{-3} Unlike the densitiy reported for **5b**, the calculated density for **5c** may be the result of the combination of the two twinned fragment volumes. If this is true the volume of the untwinned unit cell must be less than the volume of the reported cell. An unaccounted for molecule of solvation would tend to increase the calculated density in relation to the observed density. Inclusion of three molecules of methanol or a molecule of benzene into the density calculation would return a calculated density of 1.60 g cm^{-3}.

Structure Determination for 6. A very thin plate of **6** was mounted on a glass fiber and centered on the X-ray diffractometer. The cell constants reported in Table 1.3 were calculated from a least squares fit to the setting angles for 25 independent reflections ($2\theta_{ave}$ = 18.5°). Three control reflections monitored every 97 reflections showed no significant variation in intensity during data collection. Data were corrected for Lorentz and polarization factors.

The structure was solved by Patterson map interpretation. Hydrogen atoms bound to carbon were placed in idealized positions (C–H = 0.96 Å, U_{iso}(H) = 1.2 × U_{iso}(C)). The atoms of the cyano ligand which bridges between the copper(I) atoms of the polymer were found to be disordered about a crystallographic inversion center. Two uniquely disordered atoms were seen (labeled C1(N1) and N1(C1)). Each disordered atom was treated in such a way as to allow for its site occupancy factor (S.O.F) to refine. Each disordered atom was assigned as a carbon atom. The S.O.F. of C1(N1) refined to 1.18(8), while N1(C1) refined to 1.19(8).

The weighted [$w = (\sigma^2(F) + g(F)^2)^{-1}$] least squares refinement on F yielded the residual values listed in Table 1.3 at convergence (for the last twenty least squares cycles,

Table 1.3. Details of the Crystallographic Experiment and Computations for **6**.

Formula	$C_{16}H_{23}N_6BCu_2F_2O_2$
Formula weight (g mol^{-1})	507.3
Crystal system	monoclinic
Space group	$P\,2_1/n$
Lattice constants	
a (Å)	11.667(2)
b (Å)	8.962(2)
c (Å)	19.895(5)
β (deg)	97.58(2)
V (Å^3)	2062(1)
Temperature (°C)	20(1)
Z	4
ρ(calculated, g cm^{-3})	1.63
ρ(observed, g cm^{-3})[a]	1.61
Crystal dimensions	0.22 mm (010→010) × 0.16 mm (001→001) × 0.04 mm (100→100)
Radiation	MoK_α(λ = 0.71073 Å)
Monochromator	graphite
μ (cm^{-1})	21.9
Scan type	θ–2θ
Geometry	bisecting
Scan speed (deg min^{-1})	2.0 – 29.3
2θ range (deg)	3.5 – 50.0
Index restrictions	$-14 \le h \le 14;\ 0 \le k \le 11;\ 0 \le l \le 24$
Total number of reflections	4022
Number of unique, observed reflections	3118
Observed reflection criterion	$\lvert F\rvert \ge 2.5\ \sigma\lvert F\rvert$
Data to parameter ratio	11.3
R	0.040
R_w	0.047
S	1.39
g	5.3×10^{-4} (refined)
Slope, normal probability plot	1.22

[a] Determined by neutral buoyancy in methlyene chloride/1,2-dibromoethylene at 20 °C.

mean shift/e.s.d. = 0.011, max shift/e.s.d. = 0.048 for rotation of the C10 methyl group). The height of the highest peak in the final ΔF map was +0.51 e $Å^{-3}$ (near Cu2), while the minimum was –0.46 e $Å^{-3}$.

Near the end of the least squares refinement, a molecule of benzene was located in the asymmetric unit. The atoms of this occluded benzene molecule were given anisotropic thermal parameters; hydrogen atoms associated with this molecule were included in the final structural model. The occluded molecule resides at an inversion center; only one-half of the benzene ring is unique.

Assignment of the Identities of Atoms of Cyano Ligands in 4, 5a, 5b, 5c and 6. In structures **4**, **5a**, **5b**, **5c**, and **6**, the atom in each cyano ligand which formed the shorter bond to copper(I) was assigned as carbon.[2] Cu(I)–C(cyanide) bond lengths have been reported to be shorter than Cu(I)–N(cyanide) bond lengths in cyanocuprates that contain ordered bridging cyano ligands.[1–3,13]

Fourier Transform Infrared Spectroscopy. A single crystal of **6** was mounted on a glass fiber and centered on the *R*3*m* X-ray diffractometer. Cell constants were calculated for this crystal; they agreed with those from the crystal used for data collection in the crystallographic study. The crystal was mounted in an infrared cell holder so that the predominant face (001) was perpendicular to the infrared beam. The holder was placed in the microchamber of a 60-SX Nicolet FT-IR spectrometer and the cell was translated into the micro IR beam. Five hundred double sided interferograms[30–32] were collected at a resolution of 4 cm^{-1}. The data was ratioed against background, consisting of five hundred scans taken with an identical experimental arrangement, but without the single crystal in place. The resulting spectrum was not smoothed or flattened. This method worked best for small, very thin, nonopaque crystals, for which the path length through the crystal was short. Although single crystal spectra contain the desired vibrational information, they are harder to interpret due to their origin in a oriented sample.[33,34]

In separate experiments, single crystals of **4**, **5a**, **5b**, **5c**, and **6** were mounted on glass fibers and centered on the X-ray diffractometer to verify that their cell constants matched those of the previously characterized crystals. Each crystal was subsequently suspended in a very small drop of mineral oil placed on a sodium chloride plate. A second plate was placed on top of the crystal, and the crystal was ground between the plates until a mull with an approximate diameter of 1 mm was formed. The plates were then placed in a cell holder and positioned in the microchamber of a 60-SX Nicolet FT-IR spectrometer. The cell holder was translated until the mulled sample was positioned in the microbeam. One hundred double sided interferograms were collected at a resolution of 1 cm^{-1} and ratioed against background. This method produced spectra that can be straightfowardly compared to the bulk sample IR spectra. Standard mulls of the bulk samples were also prepared for **4**, **5a**, **5b**, **5c**, and **6**. Spectra of the bulk samples were recorded on the 60-SX Nicolet FT-IR spectrometer in the normal manner.[30–32]

Results and Discussion

Tables 1.4 through 1.8 contain the atomic coordinates for **4**, **5a**, **5b**,**5c**, and for **6**, respectively. Tables 1.9 contains bond lengths for **4**, while Table 1.11 contain bond lengths for **5a**, **5b**, and **6**, as well as selected bond lengths for **5c**. Bond angles for **4** are contained in Table 1.10, while Table 1.12 contains bond angles for **5a**, **5b**, and **6**, as well as selected bond angles for **5c**. Hydrogen atom coordinates and anisotropic thermal parameters for **4**, **5a**, **5b**, and **6** are included in the Appendix as Tables S-1.1 through S-1.9. Table S-1.10 in the Appendix contains selected least-squares planes for **4**, **5a**, **5b**, and **6**.

The powder EPR spectra for **5a**, **5b**, **5c**, and **6** are given in the Appendix as Figures S-1.1 through S-1.4. As expected from examination of the structural results (see below) the magnetic orbitals on the copper (II) atoms are isolated from each other. Magnetic coupling between the copper(II) atoms is not seen.

The Structure of 4. The structure of **4** consists of discrete, trinuclear, mixed-valence moieties (see Figure 1.1). Each trinuclear unit consists of a tricyanocuprate(I) complex anion that bridges between two $[Cu(\mathbf{1})]^+$ moieties by means of end-on cyano ligands.

The coordination geometry about the copper(I) atom is approximately trigonal planar, with each of the three coordination sites occupied by carbon-bound cyano ligands. The three carbon atoms of the cyano ligands and the copper(I) atom form a plane $(5.80(7)x - 8.29(14)y + 4.39(8)z = 2.02(2)$; $\Sigma\Delta^2 = 0.016$; $\sigma^2 = 0.02)$; deviations from that plane are as follows: Cu1, –0.034(1) Å; C11, 0.012(4) Å; C12, 0.012(4) Å; C13, 0.108(4) Å. The smallest C–Cu(I)–C bond angle involves the bridging cyano ligands (C11–Cu1–C13 =

Table 1.4. Atomic coordinates ($\times 10^4$) and isotropic thermal parameters ($Å^2 \times 10^3$)[a] for **4**.

atom	*x*	*y*	*z*	U_{iso}[b]
Cu1	2770(1)	878(1)	2401(1)	46(1)
C11	4234(5)	1568(4)	1935(3)	49(1)
N11	5099(4)	2006(3)	1682(2)	60(1)
C12	1373(5)	–449(4)	1798(3)	63(2)
N12	614(6)	–1280(5)	1473(4)	110(3)
C13	2852(4)	1515(4)	3587(3)	46(1)
N13	2954(4)	1860(3)	4299(2)	51(1)
Cu2	2873(1)	2546(1)	5547(1)	35(1)
N21	863(3)	2181(3)	5497(2)	41(1)
N22	3008(3)	1091(3)	6174(2)	41(1)
N23	4814(3)	3292(3)	6113(2)	40(1)
N24	2613(3)	4306(3)	5441(2)	40(1)
O21	–171(3)	2841(2)	5122(2)	55(1)
O22	1370(3)	4709(3)	5057(2)	55(1)
C21	551(4)	1283(3)	5878(3)	43(1)
C22	1825(4)	650(3)	6264(2)	44(1)
C23	4381(5)	574(4)	6503(3)	59(2)
C24	5591(7)	1198(6)	6185(5)	40(3)
C24'	5478(12)	1618(12)	6934(9)	96(6)
C25	5959(4)	2543(4)	6489(3)	63(2)
C26	4963(4)	4475(3)	6177(2)	40(1)
C27	3691(4)	5084(3)	5777(2)	38(1)
C28	–899(5)	953(4)	5965(3)	64(2)
C29	1628(6)	–454(4)	6702(3)	66(2)
C30	6298(4)	5248(4)	6629(3)	57(2)
C31	3638(5)	6457(4)	5803(3)	56(2)
Cu3	6008(1)	3193(1)	988(1)	46(1)
N31	7024(4)	4473(3)	1925(2)	51(1)
N32	7958(4)	2673(3)	1099(2)	50(1)
N33	5172(4)	2318(3)	–182(2)	54(1)
N34	4310(4)	4107(3)	685(2)	56(1)
O31	6363(4)	5396(3)	2281(2)	72(1)
O32	4005(4)	5045(4)	1217(3)	70(2)
C32	8358(4)	4396(4)	2203(3)	52(2)
C33	8890(4)	3326(4)	1711(3)	53(2)
C34	8314(5)	1604(4)	540(3)	67(2)
C35	6985(5)	809(4)	44(3)	67(2)
C36	5934(5)	1382(4)	–603(3)	68(2)
C37	3933(5)	2617(4)	–518(3)	58(2)
C38	3390(5)	3627(5)	–12(3)	60(2)
C39	9284(6)	5269(5)	2912(3)	86(2)

Table 1.4 (continued)

atom	*x*	*y*	*z*	U_{iso}[b]
C40	10426(5)	3108(5)	1945(4)	88(2)
C41	3021(6)	2050(6)	–1371(3)	83(2)
C42	1919(6)	4036(7)	–264(4)	93(3)
O51	8562(6)	3887(5)	8390(4)	128(3)

[a] Estimated standard deviations in the least significant digits are given in parentheses.
[b] The equivalent isotropic U_{iso} is defined as one-third of the trace of the U_{ij} tensor.

Table 1.5. Atomic coordinates ($\times 10^4$) and isotropic thermal parameters ($Å^2 \times 10^3$)[a] for **5a**.

atom	*x*	*y*	*z*	U_{iso}[b]
Cu1	1104(1)	–4088(1)	6559(1)	22(1)
Cu2	4477(1)	–3898(1)	3885(1)	18(1)
C1	3911(4)	–4044(4)	7924(2)	23(1)
N1	2778(4)	–4055(3)	7469(2)	33(1)
C2	2209(5)	–4159(3)	5535(2)	24(1)
N2	2993(4)	–4181(3)	4949(2)	27(1)
O1	2704(4)	–5503(2)	3000(2)	29(1)
O2	1346(3)	–3802(2)	2909(2)	27(1)
N3	4177(4)	–5225(3)	3373(2)	24(1)
N4	6762(4)	–4495(3)	4126(2)	24(1)
N5	5043(4)	–2464(3)	4098(2)	21(1)
N6	2550(4)	–3263(2)	3299(2)	20(1)
C3	5398(5)	–5874(3)	3490(2)	26(1)
C4	6931(5)	–5407(3)	3884(2)	27(1)
C5	8138(4)	–3895(4)	4497(2)	30(1)
C6	7422(6)	–3015(4)	4992(3)	34(1)
C7	6622(5)	–2147(3)	4525(3)	30(1)
C8	3902(5)	–1839(3)	3830(2)	19(1)
C9	2419(5)	–2284(3)	3389(2)	23(1)
C10	5332(7)	–6964(3)	3237(3)	37(1)
C11	8531(6)	–6035(4)	3980(3)	39(1)
C12	3982(5)	–702(3)	3913(2)	28(1)
C13	968(6)	–1684(4)	3052(3)	35(1)

[a] Estimated standard deviations in the least significant digits are given in parentheses.
[b] The equivalent isotropic U_{iso} is defined as one-third of the trace of the U_{ij} tensor.

Table 1.6. Atomic coordinates ($\times 10^4$) and isotropic thermal parameters ($Å^2 \times 10^3$)[a] for **5b**.

atom	*x*	*y*	*z*	U_{iso}[b]
Cu1	1001(1)	1170(1)	2115(1)	54(1)
Cu2	4257(1)	3447(1)	771(1)	44(1)
C1	126(7)	4360(6)	2632(2)	51(2)
N1	673(7)	3178(6)	2482(2)	70(2)
C2	2322(8)	1310(6)	1527(2)	54(2)
N2	3075(7)	1543(5)	1177(2)	64(2)
N3	3731(5)	2910(5)	42(2)	48(1)
N4	6454(5)	2540(6)	614(2)	54(2)
N5	4988(6)	4595(5)	1413(2)	54(2)
N6	2345(5)	4927(5)	809(2)	46(1)
O1	2235(5)	3207(5)	–207(1)	61(1)
O2	1055(4)	4990(5)	445(1)	59(1)
C3	4907(7)	2177(6)	–187(2)	48(2)
C4	6480(7)	1990(6)	147(2)	53(2)
C5	7915(8)	2482(9)	994(3)	78(3)
C6	7202(18)	2657(19)	1579(5)	78(6)
C6'	8079(15)	3991(18)	1276(5)	77(5)
C7	6647(9)	4226(10)	1699(3)	83(3)
C8	3893(7)	5551(7)	1571(2)	56(2)
C9	2325(7)	5799(6)	1217(2)	50(2)
C10	4617(8)	1603(7)	–732(2)	63(2)
C11	7987(8)	1183(8)	–64(3)	73(3)
C12	4033(11)	6477(10)	2060(3)	90(3)
C13	930(9)	6889(8)	1331(3)	73(3)

[a] Estimated standard deviations in the least significant digits are given in parentheses.
[b] The equivalent isotropic U_{iso} is defined as one-third of the trace of the U_{ij} tensor.

Table 1.7. Atomic coordinates ($\times 10^4$) and isotropic thermal parameters ($Å^2 \times 10^3$)[a] for **5c**.

atom	*x*	*y*	*z*	U_{iso}[b]
Cu1	2080(2)	–1930(1)	3802(1)	68(1)
Cu2	2266(2)	532(1)	3768(1)	57(1)
N1	4053(15)	–2362(6)	3784(8)	66(6)
C1	5183(16)	–2586(7)	3801(9)	100(7)
C2	2039(16)	–983(8)	3873(9)	66(7)
N2	2055(15)	–449(6)	3768(8)	75(6)
O1	5462(13)	545(9)	4016(10)	189(11)
O2	4721(27)	501(9)	2983(9)	184(11)
N3	4108(15)	660(8)	4238(7)	92(7)
C3	3889(29)	784(9)	4719(8)	99(10)
C4	2422(22)	934(7)	4871(8)	66(6)
N4	1405(16)	825(6)	4522(7)	61(6)
C5	–161(34)	970(11)	4583(14)	141(14)
C6	–829(50)	652(20)	4334(29)	331(47)
C7	–1099(27)	644(26)	3709(26)	344(41)
N5	447(33)	753(8)	3289(11)	144(13)
C8	1091(56)	889(12)	2707(17)	166(21)
C9	2659(82)	804(16)	2582(10)	289(44)
N6	3125(36)	655(11)	3007(10)	139(12)
C10	5380(37)	888(49)	5136(23)	830(96)
C11	2187(33)	1161(14)	5510(10)	141(13)
C12	3728(152)	417(56)	1845(23)	964(104)
C13	–208(69)	968(21)	2148(24)	379(37)

[a] Estimated standard deviations in the least significant digits are given in parentheses.

[b] The equivalent isotropic U_{iso} is defined as one-third of the trace of the U_{ij} tensor.

Table 1.8. Atomic coordinates ($\times 10^4$) and isotropic thermal parameters ($Å^2 \times 10^3$)[a] for **6**.

atom	*x*	*y*	*z*	U_{iso}[b]
Cu1	148(1)	7506(1)	9430(1)	47(1)
Cu2	243(1)	7708(1)	6885(1)	34(1)
C1(N1)	25(3)	9405(3)	9882(2)	54(1)
N1(C1)	21(3)	5595(3)	9884(2)	62(1)
C2	418(3)	7414(3)	8493(2)	43(1)
N2	505(3)	7351(3)	7933(1)	48(1)
O1	181(2)	4905(3)	6092(1)	60(1)
O2	–1730(2)	5818(3)	6317(1)	59(1)
B	–859(4)	4637(5)	6430(2)	59(2)
F1	–534(2)	4438(2)	7115(1)	69(1)
F2	–1367(2)	3389(3)	6126(1)	91(1)
N3	817(2)	6109(3)	6339(1)	42(1)
N4	1755(2)	8535(3)	6743(1)	46(1)
N5	–533(2)	9646(3)	6975(1)	43(1)
N6	–1364(2)	7150(3)	6587(1)	39(1)
C3	1768(3)	6345(4)	6108(2)	50(1)
C4	2339(3)	7759(4)	6378(2)	51(1)
C5	2143(4)	9971(4)	7058(2)	77(2)
C6	1213(4)	11136(4)	6965(2)	80(2)
C7	140(4)	10913(4)	7277(2)	69(2)
C8	–1625(3)	9625(4)	6848(2)	45(1)
C9	–2127(3)	8193(4)	6583(2)	44(1)
C10	2247(4)	5356(6)	5613(2)	84(2)
C11	3513(3)	8159(6)	6204(3)	87(2)
C12	–2439(4)	10879(5)	6943(2)	79(2)
C13	–3375(3)	7992(6)	6340(3)	80(2)
C14	991(7)	853(8)	4957(2)	115(3)
C15	–17(8)	1497(6)	5101(3)	117(3)
C16	985(7)	–680(8)	4852(3)	111(3)

[a] Estimated standard deviations in the least significant digits are given in parentheses.
[b] The equivalent isotropic U_{iso} is defined as one-third of the trace of the U_{ij} tensor.

Table 1.9. Bond lengths (Å)[a] for **4**.

Cu1–C11	1.933(5)	Cu1–C12	1.931(4)
Cu1–C13	1.933(4)	C11–N11	1.136(6)
N11–Cu3	2.120(4)	C12–N12	1.131(7)
C13–N13	1.142(6)	N13–Cu2	2.079(4)
Cu2–N21	1.960(3)	Cu2–N22	1.990(3)
Cu2–N23	1.981(3)	Cu2–N24	1.971(3)
N21–O21	1.336(4)	N21–C21	1.288(5)
N22–C22	1.277(5)	N22–C23	1.479(5)
N23–C25	1.470(5)	N23–C26	1.280(5)
N24–O22	1.342(4)	N24–C27	1.285(4)
C21–C22	1.490(5)	C21–C28	1.485(6)
C22–C29	1.506(7)	C23–C24	1.558(9)
C23–C24'	1.504(12)	C24–C25	1.484(8)
C24'–C25	1.440(16)	C26–C27	1.481(5)
C26–C30	1.494(5)	C27–C31	1.495(5)
Cu3–N31	1.959(3)	Cu3–N32	1.975(4)
Cu3–N33	1.969(3)	Cu3–N34	1.959(4)
N31–O31	1.351(5)	N31–C32	1.279(5)
N32–C33	1.282(5)	N32–C34	1.479(6)
N33–C36	1.471(6)	N33–C37	1.274(6)
N34–O32	1.334(5)	N34–C38	1.294(5)
C32–C33	1.500(6)	C32–C39	1.478(6)
C33–C40	1.489(7)	C34–C35	1.517(6)
C35–C36	1.501(7)	C37–C38	1.472(7)
C37–C41	1.490(6)	C38–C42	1.495(7)

[a] Estimated standard deviations in the least significant digits are given in parentheses.

Table 1.10. Bond angles (deg)[a] for **4**.

C11–Cu1–C12	124.8(2)	C11–Cu1–C13	115.4(2)
C12–Cu1–C13	119.6(2)	Cu1–C11–N11	177.8(4)
C11–N11–Cu3	157.2(4)	Cu1–C12–N12	175.3(5)
Cu1–C13–N13	176.8(4)	C13–N13–Cu2	172.7(3)
N13–Cu2–N21	101.2(1)	N13–Cu2–N22	105.9(1)
N21–Cu2–N22	79.9(1)	N13–Cu2–N23	104.9(1)
N21–Cu2–N23	153.7(1)	N22–Cu2–N23	95.8(1)
N13–Cu2–N24	100.2(1)	N21–Cu2–N24	92.8(1)
N22–Cu2–N22	153.8(1)	N23–Cu2–N24	79.6(1)
Cu2–N21–O21	123.4(2)	Cu2–N21–C21	117.2(3)
O21–N21–C21	119.3(3)	Cu2–N22–C22	114.7(3)
Cu2–N22–C23	121.8(3)	C22–N22–C23	123.5(4)
Cu2–N23–C25	121.9(2)	Cu2–N23–C26	114.9(2)
C25–N23–C26	123.0(3)	Cu2–N24–O22	122.9(2)
Cu2–N24–C27	117.1(2)	O22–N24–C27	120.0(3)
N21–C21–C22	112.4(3)	N21–C21–C28	124.1(4)
C22–C21–C28	123.5(4)	N22–C22–C21	115.8(4)
N22–C22–C29	125.4(4)	C21–C22–C29	118.8(4)
N22–C23–C24	111.1(4)	N22–C23–C24'	109.3(6)
C23–C24–C25	117.1(6)	C23–C24'–C25	123.7(10)
N23–C25–C24	111.5(4)	N23–C25–C24'	112.6(6)
N23–C26–C27	115.8(3)	N23–C26–C30	124.6(3)
C27–C26–C30	119.6(3)	N24–C27–C26	112.4(3)
N24–C27–C31	123.5(3)	C26–C27–C31	124.0(3)
N11–Cu3–N31	100.7(1)	N11–Cu3–N32	104.0(2)
N31–Cu3–N32	80.5(1)	N11–Cu3–N33	98.4(1)
N31–Cu3–N33	160.6(2)	N32–Cu3–N33	97.8(1)
N11–Cu3–N34	94.6(2)	N31–Cu3–N34	95.0(1)
N32–Cu3–N34	161.4(2)	N33–Cu3–N34	80.3(1)
Cu3–N31–O31	122.5(3)	Cu3–N31–C32	117.2(3)
O31–N31–C32	120.4(3)	Cu3–N32–C33	114.2(3)
Cu3–N32–C34	123.1(3)	C33–N32–C34	122.7(4)
Cu3–N33–C36	121.3(3)	Cu3–N33–C37	114.3(3)
C36–N33–C37	124.3(3)	Cu3–N34–O32	122.8(3)
Cu3–N34–C38	115.3(3)	O32–N34–C38	121.1(4)
N31–C32–C33	112.1(3)	N31–C32–C39	124.4(4)
C33–C32–C39	123.5(4)	N32–C33–C32	116.0(4)
N32–C33–C40	124.9(4)	C32–C33–C40	119.2(4)
N32–C34–C35	110.9(4)	C34–C35–C36	117.4(4)
N33–C36–C35	111.5(4)	N33–C37–C38	115.9(4)
N33–C37–C41	125.7(4)	C38–C37–C41	118.4(4)
N34–C38–C37	112.9(4)	N34–C38–C42	123.4(4)
C37–C38–C42	123.7(4)		

[a] Estimated standard deviations in the least significant digits are given in parentheses.

Table 1.11. Bond lengths (Å)[a] for **5a**, **5b**, and **6**, and selected bond lengths for **5c**.

Bond	**5a**	**5a**	**5c**	**6**
Cu1–C1(N1)				1.938(3)
Cu1–N1(C1)				1.951(3)
Cu1–N1	1.986(3)	1.967(5)	1.96(1)	
Cu1–C2	1.897(4)	1.908(6)	1.97(1)	1.934(4)
Cu1–C1	1.903(3)	1.906(5)	1.96(1)	
Cu2–N2	2.134(3)	2.165(5)	2.04(1)	2.091(3)
Cu2–N3	1.956(4)	1.958(4)	1.98(1)	1.968(3)
Cu2–N4	1.979(3)	1.962(4)	1.99(2)	1.968(3)
Cu2–N5	1.972(3)	1.972(4)	2.01(3)	1.978(3)
Cu2–N6	1.967(3)	1.964(4)	1.93(3)	1.955(2)
C1(N1)–C1(N1)				1.170(6)
N1(C1)–N1(C1)				1.166(6)
C1–N1	1.156(5)	1.164(8)	1.10(2)	
C1–Cu1	1.903(3)	1.906(5)	1.96(1)	
C2–N2	1.143(5)	1.137(8)	1.13(2)	1.133(4)
O1–N3	1.348(4)	1.327(6)		1.364(3)
O2–N6	1.338(4)	1.336(5)		1.354(3)
O1–B				1.482(6)
O2–B				1.464(5)
B–F1				1.377(5)
B–F2				1.369(5)
N3–C3	1.290(5)	1.293(7)		1.274(4)
N4–C4	1.274(6)	1.298(7)		1.268(5)
N4–C5	1.462(5)	1.461(8)		1.476(5)
N5–C7	1.473(5)	1.489(8)		1.463(5)
N5–C8	1.288(5)	1.270(7)		1.267(4)
N6–C9	1.303(5)	1.289(7)		1.290(4)
C3–C4	1.489(6)	1.469(7)		1.497(5)
C3–C10	1.497(6)	1.492(7)		1.488(6)
C4–C11	1.500(7)	1.504(9)		1.499(5)
C5–C6	1.524(6)	1.660(16)		1.498(6)
C5–C6'		1.469(17)		
C6–C7	1.512(6)	1.434(18)		1.483(6)
C6'–C7		1.640(15)		
C8–C9	1.482(5)	1.499(8)		1.478(5)
C8–C12	1.506(6)	1.485(9)		1.499(5)
C9–C13	1.483(6)	1.479(9)		1.484(5)
H1–O1	0.94(5)			

[a] Estimated standard deviations in the least significant digits are given in parentheses.

Table 1.12. Bond angles (deg)[a] for **5a**, **5b**, and **6**, and selected bond angles for **5c**.

Bonds	**5a**	**5b**	**5c**	**6**
C1(N1)–Cu1–N1(C1)				122.8(1)
C1(N1)–Cu1–C2				121.1(1)
N1(C1)–Cu1–C2				116.1(1)
N1–Cu1–C2	112.3(1)	115.5(2)	118.3(6)	
N1–Cu1–C1	104.2(1)	116.2(2)	121.8(6)	
C2–Cu1–C1	143.5(1)	128.2(2)	119.8(6)	
N2–Cu–N3	97.7(1)	103.2(2)	102.1(6)	115.0(1)
N2–Cu2–N4	104.3(1)	103.2(2)	105.6(6)	100.6(1)
N3–Cu2–N4	80.7(1)	80.7(2)	78.1(6)	79.5(1)
N2–Cu2–N5	98.1(1)	93.7(2)	98.9(6)	93.0(1)
N3–Cu2–N5	163.9(1)	162.7(2)	158.9(7)	151.9(1)
N4–Cu2–N5	98.4(1)	99.0(2)	95.9(8)	96.4(1)
N2–Cu2–N6	94.0(1)	95.1(2)	99.7(8)	105.8(1)
N3–Cu2–N6	94.5(1)	94.8(2)	99(1)	91.7(1)
N4–Cu2–N6	161.5(1)	161.7(2)	154.6(8)	153.4(1)
N5–Cu2–N6	81.3(1)	80.0(2)	77(1)	79.6(1)
N1–C1–Cu1a	165.9(3)	173.5(5)	173(1)	
Cu1–N1(C1)–N1(C1)				175.6(4)
Cu1–C1(N1)–C1(N1)				175.0(4)
Cu1–N1–C1	171.3(3)	164.4(5)	176(2)	
Cu1–C2–N2	174.6(3)	173.5(5)	163(2)	175.8(3)
Cu2–N2–C2	168.4(4)	141.5(4)	167(2)	162.2(3)
Cu2–N3–O1	122.7(2)	123.0(3)		124.5(2)
F1–B–F2				112.3(3)
B–O1–N3				113.8(3)
B–O2–N6				113.7(3)
O1–B–O2				114.0(3)
O1–B–F1				109.5(3)
O2–B–F1				109.9(3)
O1–B–F2				105.3(3)
O2–B–F2				105.8(3)
O1–N3–C3	120.7(3)	120.5(4)		117.4(3)
Cu2–N3–C3	116.2(3)	116.4(3)		117.0(2)
Cu2–N4–C4	113.8(3)	113.9(3)		115.8(2)
Cu2–N4–C5	121.5(3)	122.6(4)		119.9(2)
C4–N4–C5	124.5(3)	123.5(5)		124.3(3)
Cu2–N5–C7	122.8(3)	120.7(4)		119.5(2)
Cu2–N5–C8	113.5(3)	114.8(4)		115.4(2)
C7–N5–C8	123.7(3)	124.4(5)		124.4(3)
Cu2–N6–O2	122.7(2)	122.6(3)		125.8(2)
Cu2–N6–C9	115.1(3)	117.2(3)		116.7(2)
O2–N6–C9	121.8(3)	120.1(4)		117.1(2)
N3–C3–C4	112.1(4)	112.5(5)		112.3(3)

Table 1.12. (continued)

Bonds	**5a**	**5b**	**6**
N3–C3–C10	124.7(4)	121.5(5)	124.1(3)
C4–C3–C10	123.1(4)	126.0(5)	123.6(3)
N4–C4–C3	116.5(4)	116.2(5)	114.9(3)
N4–C4–C11	125.0(4)	124.4(5)	125.3(4)
C3–C4–C11	118.6(4)	119.4(5)	119.8(3)
N4–C5–C6	111.7(3)	108.0(6)	112.2(3)
N4–C5–C6'		110.1(7)	
C5–C6–C7	116.9(4)	114.2(10)	119.4(4)
C5–C6'–C7		113.4(9)	
N5–C7–C6	111.7(3)	110.8(7)	111.7(3)
N5–C7–C6'		108.3(6)	
N5–C8–C9	116.7(4)	116.2(5)	115.2(3)
N5–C8–C12	125.2(3)	126.7(6)	126.9(3)
C9–C8–C12	118.0(3)	117.1(6)	117.9(3)
N6–C9–C8	112.8(3)	111.4(5)	112.7(3)
N6–C9–C13	123.0(4)	124.8(5)	124.1(3)
C8–C9–C13	124.2(4)	123.8(5)	123.2(3)

[a] Estimated standard deviations in the least significant digits are given in parentheses.

Figure 1.1. Thermal ellipsoid plot (50% probability) and the numbering scheme of $[Cu(\mathbf{1})(\mu\text{-}NC)]_2Cu(CN) \cdot H_2O$ (**4**). Hydrogen atoms have been omited for clarity.

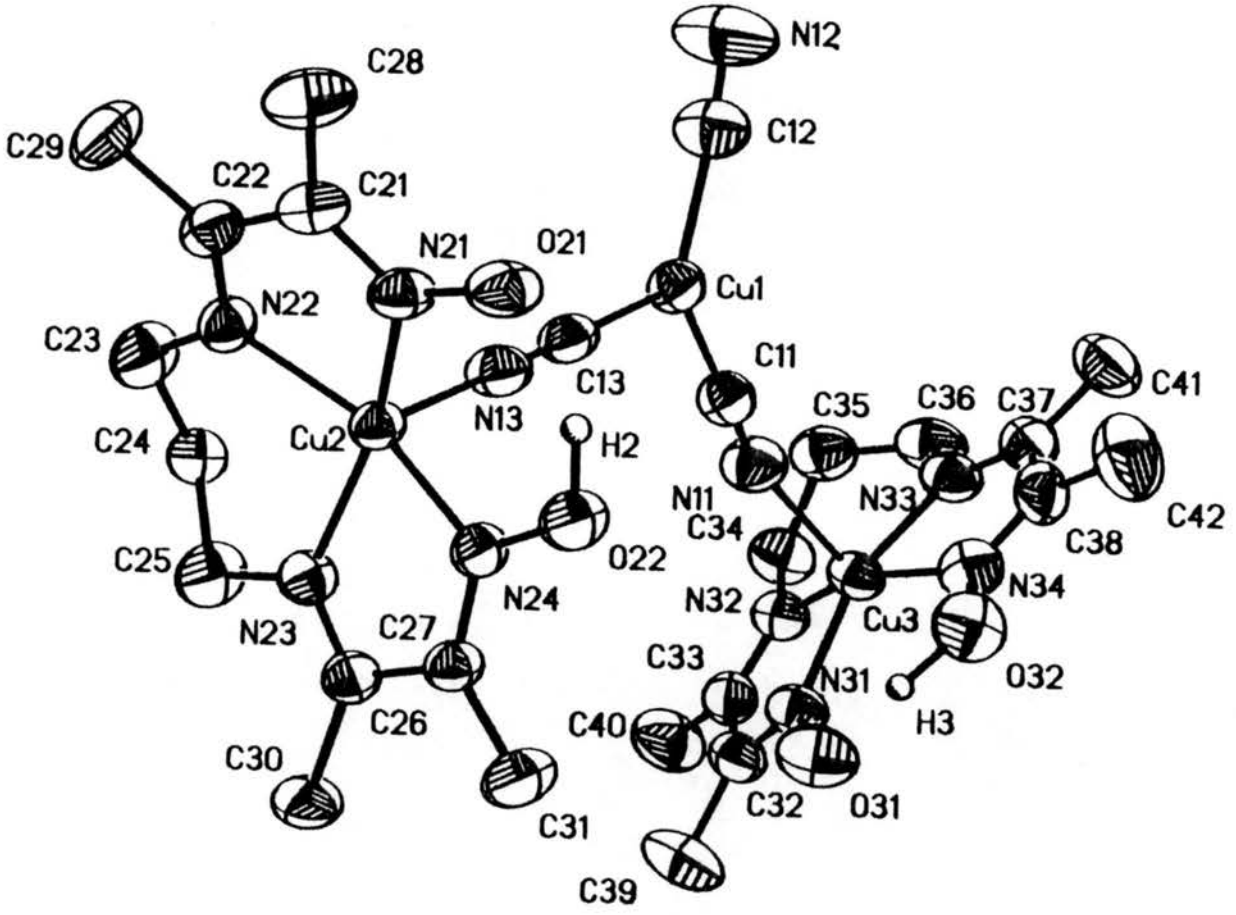
N12
C28
C12
C29
C22
C21
N21
O21
Cu1
N22
C23
C11
C13
C35
C36
C37
C41
N13
H2
C24
Cu2
N11
N33
C42
C34
C38
C25
O22
N34
N24
N32
Cu3
N23
C27
C33
O32
N31
H3
C40
C26
C30
C32
O31
C31
C39

115.4(2)°); the largest such angle (C11–Cu1–C12 = 124.8(2)°) is only 9° larger. Despite the fact that one cyano ligand is coordinated in a terminal fashion (C12/N12) while the other two bridge metal atoms, the three Cu(I)–C bond lengths do not differ significantly (Cu(I)–C_{ave} = 1.932(3) Å). The same is true for the three C–N bond lengths (C–N_{ave} = 1.136(4) Å). Each of the three Cu(I)–C–N bond angles is approximately linear.

The coordination geometry in each of the copper(II) complexes is square pyramidal. In each complex a nitrogen atom of a cyano group occupies an apical site, while four nitrogen atoms of ligand **1** occupy the basal positions. The four basal nitrogen atoms of each [Cu(**1**)]$^+$ complex form a plane (see Table S-1.10). The Cu(II)–N(cyano) bond lengths differ significantly between the two copper(II) complexes (Cu2–N13 = 2.079(4) Å, Cu3–N11 = 2.120(4) Å). The shorter bond results in a greater displacement of the copper(II) atom from the plane formed by the basal nitrogen atoms (0.448(1) Å for Cu2, 0.323(1) Å for Cu3).

The two Cu(II)–N–C angles differ. The larger deviation from linearity involves Cu3 (C11–N11–Cu3 = 157.2(4)°) and the longer Cu3–N11 bond. The other bridging cyano ligand is more nearly linear (Cu2–N13–C13 = 172.7(3)°).

An occluded water molecule was also found in the asymmetric unit of the unit cell. The shortest distance between this atom and any atom of the trimeric species was 3.003(1) Å (O51 to N12 of the terminal cyano ligand) and 3.022(1) Å (O51 to O32 an oxime oxygen atom). The water molecule may function to link separate trinuclear complexes by very weak hydrogen bonds (–N12···H–O51–H···O32–). The weakly bonded hydrogen chain thus formed discriminates between the [Cu3(**1**)]$^+$ unit, which is involved in the hydrogen bonding chain by supplying O32, and the [Cu2(**1**)]$^+$ unit, which is not involved in the hydrogen bonding scheme.

The packing diagram (Figure 1.2) displays the hydrogen bonding and also illustrates the different packing environments for [Cu3(**1**)]$^+$ and [Cu2(**1**)]$^+$ units. The former unit packs along and between the hydrogen bonded chains so as to present a face,

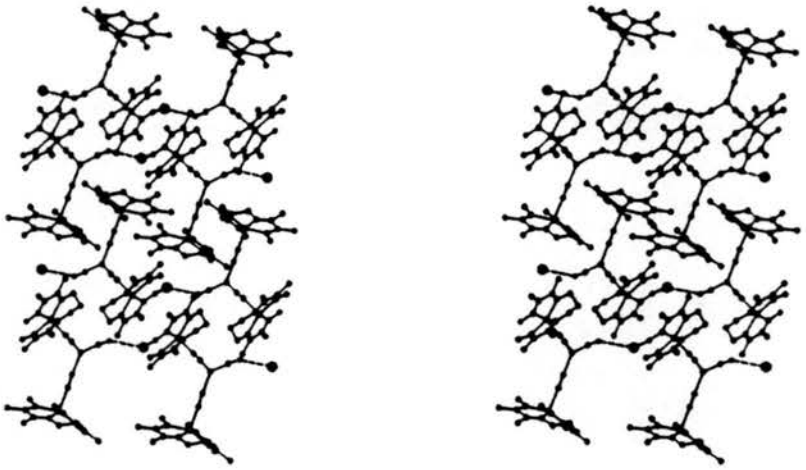

Figure 1.2. Stereoview of the structure of $[Cu(\mathbf{1})(\mu\text{-}NC)]_2Cu(CN) \cdot H_2O$ (**4**), viewed parallel to the *c* axis. Bonds are represented as solid lines. Hydrogen bonds are represented as dashed lines. The water molecule is represented as a large sphere, while the remaining atoms are represented as small dots.

defined by the plane of the atoms of ligand **1**, toward a face of a $[Cu3(\mathbf{1})]^+$ unit in an adjacent chain. These two $[Cu3(\mathbf{1})]^+$ units are related by a center of inversion at (1/2, 0, 0). The space between the $[Cu3(\mathbf{1})]^+$ unit and the terminal cyano ligand (C12/N12) is occupied by a $[Cu3(\mathbf{1})]^+$ unit of an adjacent chain, which are related by the center of inversion at (0, 0, 0). The $[Cu2(\mathbf{1})]^+$ unit is not involved in any way in the chain propagation. The packing environment about the $[Cu2(\mathbf{1})]^+$ unit consists of four symmetry-related $[Cu2(\mathbf{1})]^+$ units which fill spaces along the hydrogen bonded chain. The packing environment of each of the $[Cu(\mathbf{1})]^+$ units leaves open the possibility for a different orientation of this otherwise equivalent moiety, which in turn results in a difference in the bonding between this unit and the tricyanocuprate unit. The differences seen in the bonding between the copper(II) complex ions and the tricyanocuprate complex are the direct result of packing forces in the unit cell.

The oxime hydrogen atoms were located in each of the two ligands **1** and refined with isotropic thermal parameters. The hydrogen bonds are unsymmetrical (H2–O22 = 0.95(6) Å ; H2-O21 = 1.67(6) Å; H3–O32 = 1.11(6) Å; H3–O31 = 1.47(5) Å). The intramolecular separation of the oxime oxygen atoms (O22···O21 = 2.511(4) Å, O32···O31 = 2.509(4) Å) indicates that these hydrogen bonds are strong.

The Structure of 5a. The structure of **5a** consists of $[Cu(CN)_2]^-$ repeat units, bridged by one of the two cyano ligands in each unit to form an infinite polymeric chain. Each such unit is connected to a $[Cu(\mathbf{1})]^+$ complex via the second cyano ligand (see Figure 1.3). The coordination geometry about each copper(I) atom is roughly trigonal planar with two of the three coordination sites occupied by carbon-bound cyano ligands. The third coordination site is occupied by a nitrogen-bound cyano ligand from an adjacent symmetry-related repeat unit. The copper(I) atom and the ligand atoms bound to it form a plane ($0.11(4)x + 13.16(2)y - 0.74(1)z = -5.857(7)$; $\Sigma\Delta^2 = 0.000$, $\sigma^2 = 0.002$); deviations of atoms from that plane are as follows: Cu1, 0.003(1) Å; C1, –0.001(5) Å; C2, 0.001(4) Å; N1, –0.001(4) Å. The angle between the carbon-bound cyano ligands (C2–Cu1–C1 =

Figure 1.3. Thermal ellipsoid plot (50% probability) and the numbering scheme of $[Cu(\mathbf{1})(\mu\text{-NC})Cu(\mu\text{-CN})]_n$ (**5a**). Hydrogen atoms have been included as spheres of fixed, arbitary radius. Only the repeat unit of the polymer chain is represented.

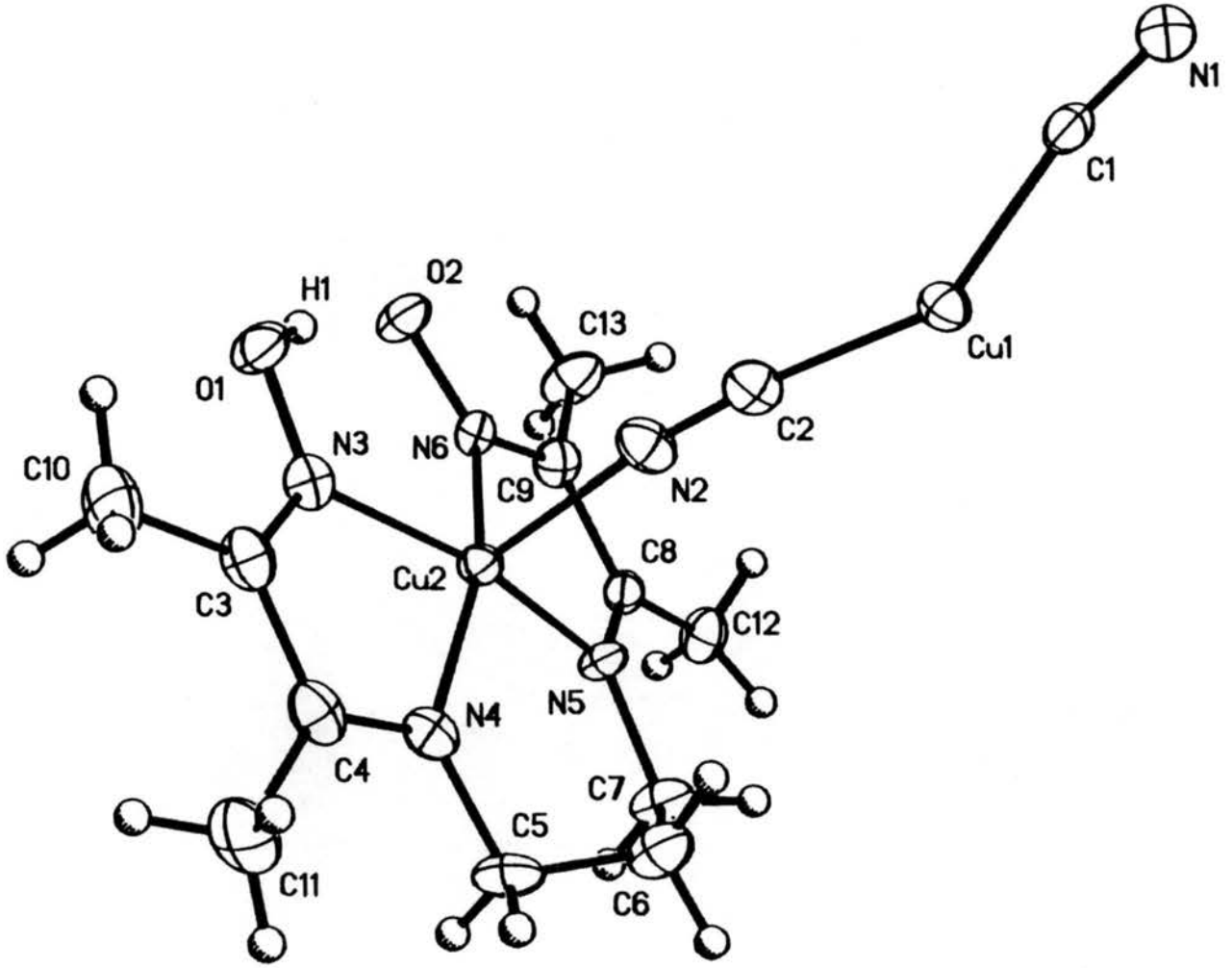
N1
C1
Cu1
C2
N2
C13
O2
H1
O1
N3
N6
C9
C10
C8
Cu2
C3
C12
N5
N4
C4
C7
C5
C11
C6

143.5(1)°) is far from the ideal angle of 120° for trigonal planar coordination. At the same time, the C1–Cu1–N1 angle has been compressed to 104.2(1)°. As would be expected, the Cu(I)–N and Cu(I)–C bond lengths differ appreciably (Cu1–N1 = 1.986(3) Å, Cu1–C1 = 1.903(3) Å, Cu1–C2 = 1.897(4) Å). Neither the Cu(I)–C bond lengths nor the C–N bond lengths differ significantly (C1–N1 = 1.156(5) Å, C2–N2 = 1.143(5) Å). The carbon-bound and nitrogen-bound cyano ligands form bonds to copper(I) that are nearly linear (N1–C1–Cu1 = 165.9(3)°, Cu1–C2–N2 = 174.6(3)°, Cu1–N1–C1 = 171.3(3)°). The repeat units are related by an *a* glide plane (with reflection through the *ab* face of the unit cell). Thus, propagation of the chain occurs parallel to the *a* axis.

The geometry about the copper(II) atom is distorted square pyramidal, with the nitrogen atom of the bridging cyano ligand occupying the apical position, and the nitrogen atoms of ligand **1** occupying basal sites. The four basal nitrogen atoms form a plane (see Table S-1.10). The copper(II) atom is displaced 0.294(2) Å from the basal plane toward the apical ligand. The apical Cu(II)–N bond length (Cu2–N2 = 2.134(3)) is significantly longer than the basal Cu(II)–N bond lengths ($Cu2–N(basal)_{ave}$ = 1.969(9) Å) and the Cu(I)–N(cyano) bond length (Cu1–N1 = 1.986(3) Å). The bond between the copper(II) atom and the cyano ligand is almost linear (Cu2–N2–C3 = 168.4(2)°).

The packing environment along the chain is sterically restrictive, and binding the large $[Cu(\mathbf{1})]^+$ complexes creates distortions from the ideal dicyanocuprate(I) geometry (see Figure 1.4). The $[Cu(\mathbf{1})]^+$ complex is too large to bind to the terminal cyano ligands of the dicyanocuprate(I) polymer without distortion. To accommodate the bulky copper(II) complex, the polymer distorts by enlarging the C(cyano)–Cu(I)–C(cyano) bond angle (C1–Cu1–C2 = 143.5(1)°). The distortion allows the $[Cu(1)]^+$ units to stack along the chain without interference and effectively fill the intrachain voids. The chain itself shortens and widens as a result of this change.

A twist angle can be used to describe the orientation of the $[Cu(\mathbf{1})]^+$ complex relative to the plane of the dicyanocuprate(I) polymer. In this case, the twist angle is the

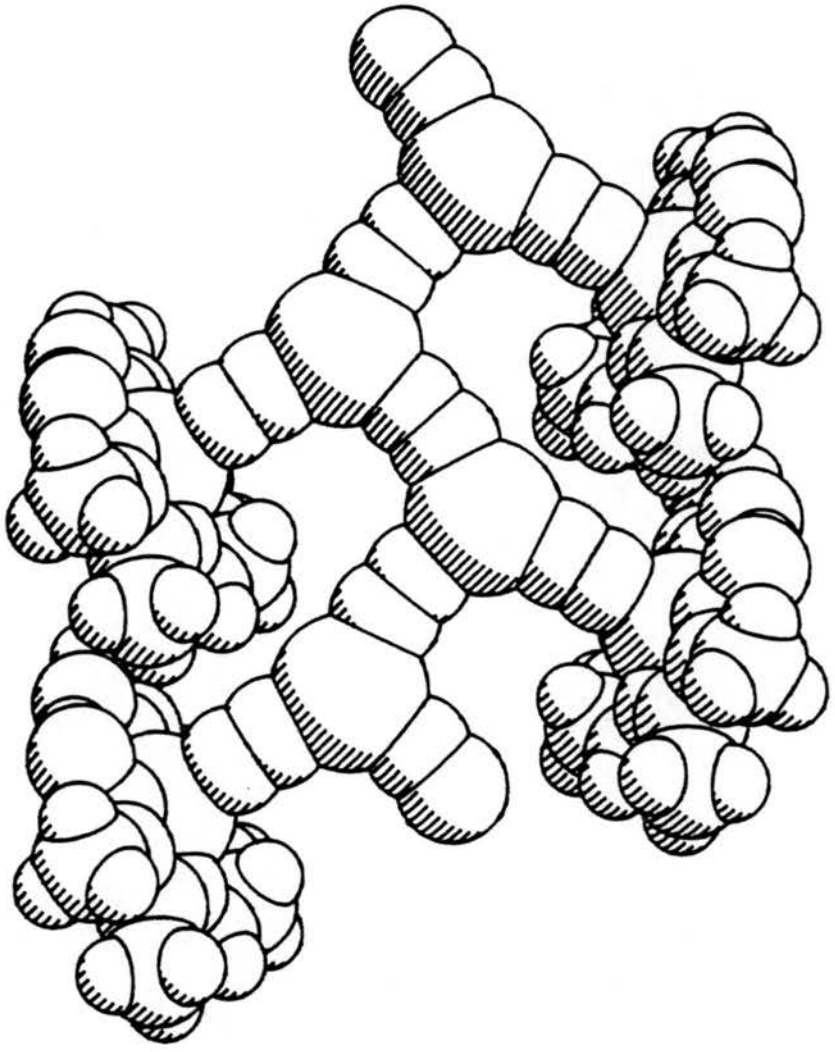

Figure 1.4. Space-filling plot of a portion of the chain in Cu(**1**)(μ-NC)Cu(μ-CN)]$_n$ (**5a**), viewed parallel to the *b* axis.

angle formed between the normals of the plane of the elbow carbon of the propylene group of ligand **1**, the copper(II) atom, and the copper(I) atom, and the plane of the copper(II) atom, the copper(I) atom, and the carbon atom of the cyano ligand which bridges between copper(I) atoms. A twist angle of 0° describes a situation in which the oxime oxygen atoms of **1** are coincident with the chain propagation axis. An angle of 90° indicates that the oxime oxygen atoms of **1** are perpendicular to chain axis. The twist angle for **5a** is 19.9°, and thus the oxime oxygen atoms are nearly coincident with the chain axis.

A stereo plot of the packing environment viewed down the crystallographic *a* axis (Figure 1.5) displays the packing scheme for the polymeric chains. The chains are related by a twofold screw axis parallel to*b* and a *n* glide plane (with reflection through the *ac* face) along the direction (*a* + *b*). The *n* glide plane relates two $[Cu(\mathbf{1})]^+$ complexes of adjacent polymers in such a way as to stack the units along the *a* axis with an oxime oxygen atom of one complex close to a copper(II) atom of a related complex. The *n* glide and the 2_1 screw operations give rise to alternating polymer layers along *b*. Each layer fills the cavities formed by the layers below and above it.

The oxime hydrogen atom of ligand **1** was located and refined with an isotropic thermal parameter. As expected based on the O1···O2 distance of 2.481(3) Å, the hydrogen bond is unsymmetrical; the shorter H–O bond length is 0.94(5) Å (O1–H1), while the longer H···O bond length is 1.58(4) Å.

The Structure of 5b. The structure of **5b** consists of $[Cu(CN)_2]^-$ repeat units (see Figure 1.6), bridged by one of the two cyano ligands in each unit to form polymeric chain. Each such unit is connected to a $[Cu(\mathbf{1})]^+$ complex via the second cyano ligand. The coordination geometry about each copper(I) atom is roughly trigonal planar, with two of the three coordination sites occupied by carbon-bound cyano ligands. The copper(I) atom, together with the carbon atoms and the nitrogen atom which are bound to copper(I), form a plane ($6.13(1)x - 1.69(7)y + 13.93(6)z = 3.34(1)$; $\Sigma\Delta^2 = 0.001$, $\sigma^2 = 0.014$); deviations of the atoms from this plane are as follows: Cu1, 0.024(2) Å; C1, –0.008(5) Å;

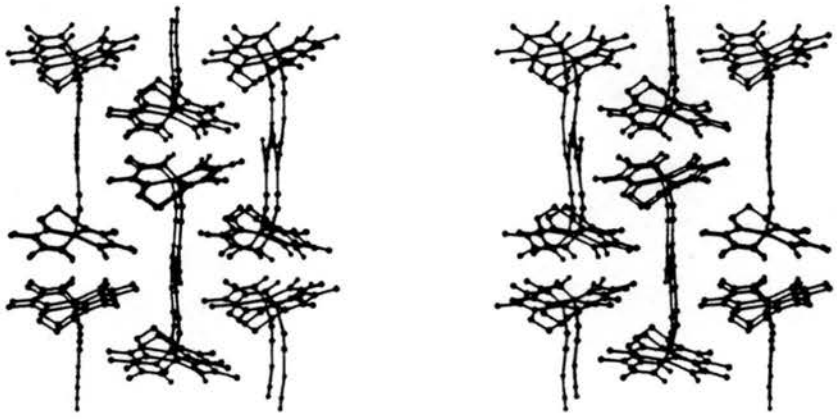

Figure 1.5. Stereoview of the structure of $[Cu(\mathbf{1})(\mu\text{-NC})Cu(\mu\text{-CN})]_n$ (**5a**), viewed parallel to the *a* axis. Bonds are represented as solid lines. Atoms are represented as solid circles.

Figure 1.6. Thermal ellipsoid plot (50% probability) and the numbering scheme of $[Cu(\mathbf{1})(\mu\text{-NC})Cu(\mu\text{-CN})]_n$ (**5b**). Hydrogen atoms have been included as spheres of fixed, arbitary radius. Only the repeat unit of the polymer chain is represented.

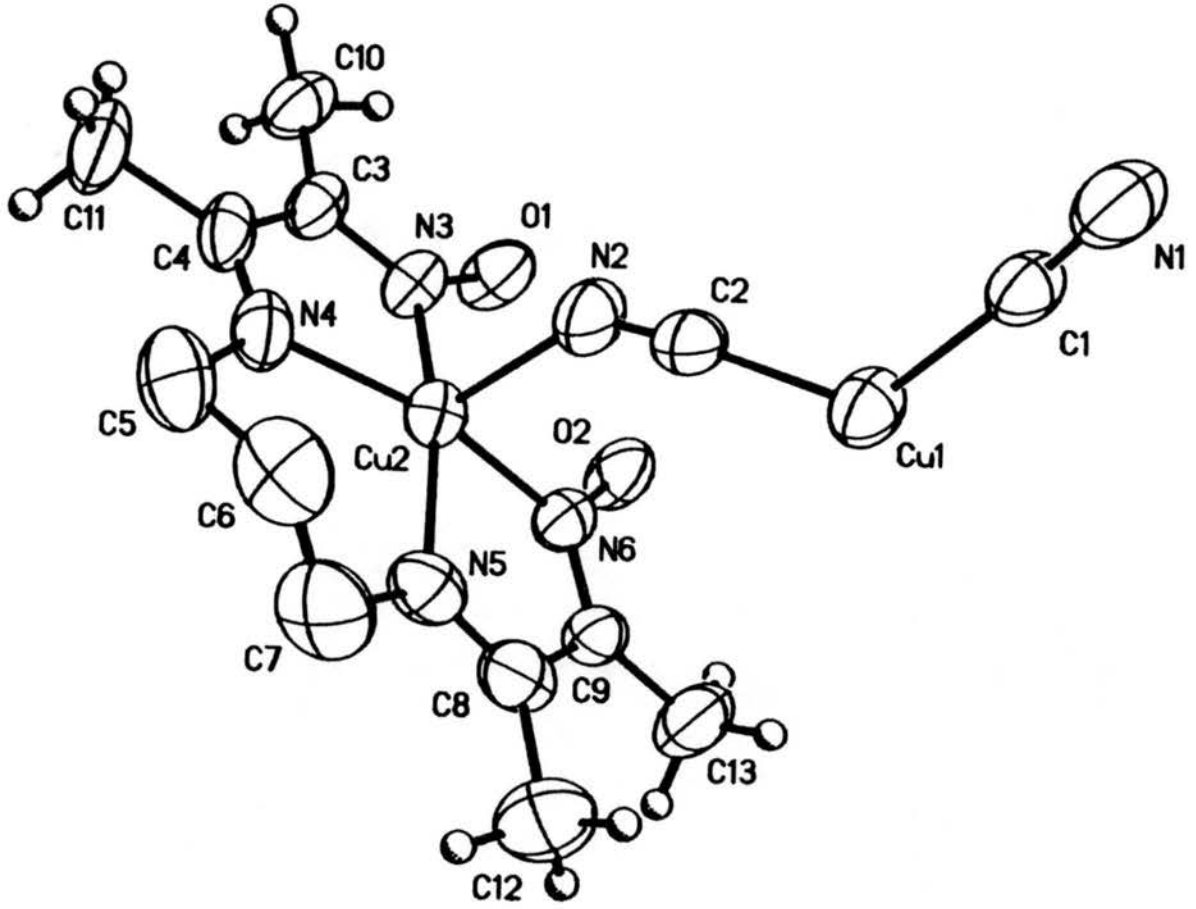
C10
C3
C11
C4
N3
O1
N2
C2
N1
N4
C1
C5
Cu2
O2
Cu1
C6
N5
N6
C7
C8
C9
C13
C12

C2, –0.008(6) Å; N1, 0.007(5) Å. The third coordination site is occupied by a nitrogen-bound cyano ligand from an adjacent symmetry-related repeat unit. The angles about copper(I) (C2–Cu1–C1 = 128.2(2)°; C2–Cu1–N1 = 115.5(2)°; C1–Cu1–N1 = 116.2(2)°) are close to the ideal angle of 120° for trigonal planar coordination. The Cu(I)–N and Cu(I)–C bond lengths differ appreciably (Cu1–N1 = 1.967(5) Å; Cu1–C1 = 1.906(5) Å; Cu1–C2 = 1.908(6) Å), although the Cu(I)–C bond lengths do not. The C1–N1 bond (1.164(8) Å) may be longer than the C2–N2 bond (1.137(8) Å). The carbon-bound and nitrogen-bound cyano ligands form bonds to copper(I) that deviate sightly from linearity (N1–C1–Cu1 = 173.5(5)°; Cu1–C2–N2 = 173.5(5))°; Cu1–N1–C1 = 164.4(5)°). The repeat units are related by the 2_1 screw axis, and thus propagation of the chain occurs parallel to the *b* axis.

The coordination sphere about the copper(II) atom is distorted square pyramidal, with the nitrogen atom of the bridging cyano ligand occupying the apical site and the nitrogen atoms of ligand **1** occupying basal sites. The four basal nitrogen atoms form a plane (see Table S-1.10), with the copper(II) atom displaced from this plane by 0.301(1) Å in the direction of the apical ligand. The apical bond length is long (Cu2–N2 = 2.165(5) Å), and is significantly longer than the Cu(I)–N bond length. The Cu(II)–N–C(cyano) bond angle is nonlinear; the value of 141.5(4)° for Cu2–N2–C2 represents an extremely large deviation from linearity for a bridging cyano ligand.

As was the case for **5a**, the chain is sterically restrictive, and binding the large $[Cu(\mathbf{1})]^+$ complexes creates distortions (see Figure 1.7). To accommodate the bulky copper(II) complex in this case, the Cu(II)–N–C(cyano) bond angle distorts dramatically from linearity. The distortion allows the $[Cu(\mathbf{1})]^+$ units to swing in towards the chain and fill the space between the terminal cyano ligands. By this means the chain effectively stacks the $[Cu(\mathbf{1})]^+$ complexes and fills the intrachain voids.

A plot of the packing environment viewed down the *b* axis (Figure 1.8) displays the packing scheme for the polymeric chains. Each repeat unit in an isolated chain is related to

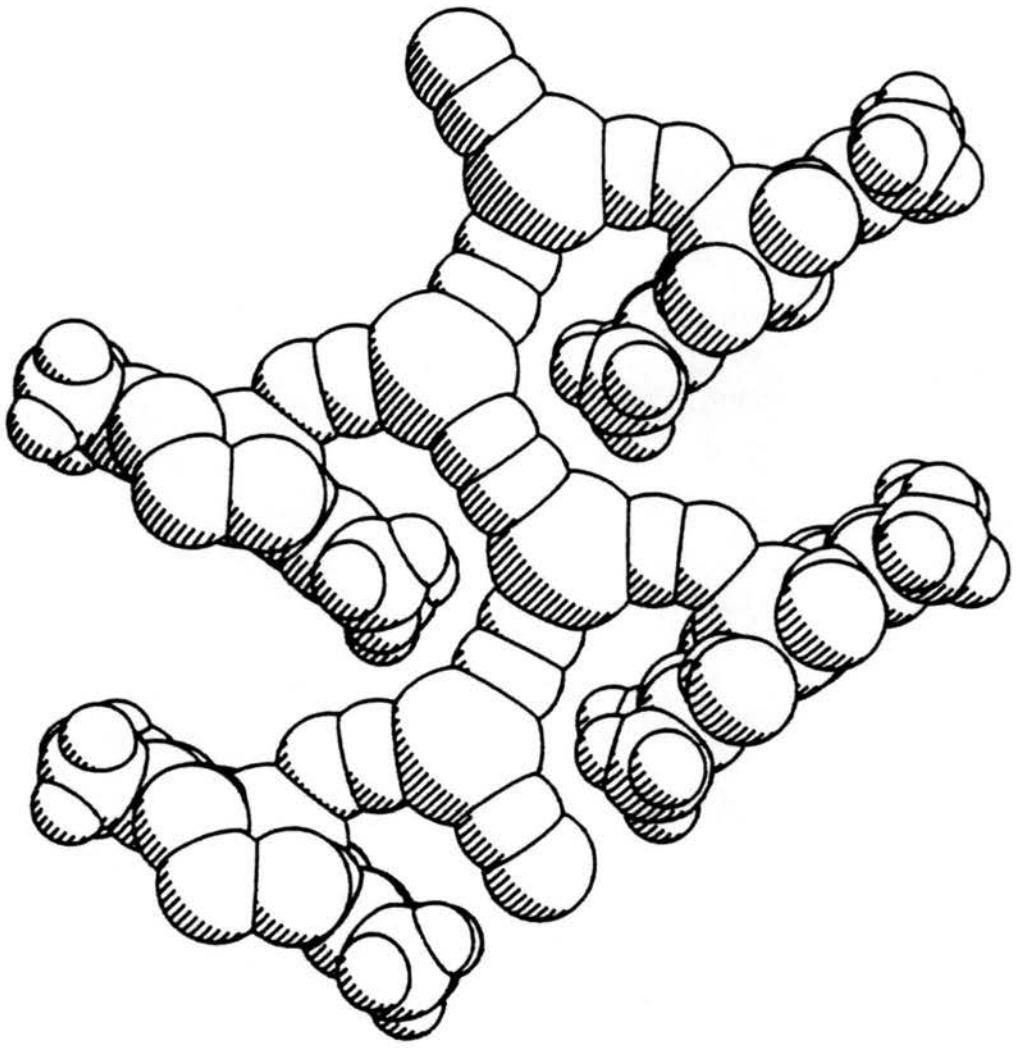

Figure 1.7. Space-filling plot of a portion of the chain in $Cu(\mathbf{1})(\mu\text{-}NC)Cu(\mu\text{-}CN)]_n$ (**5b**), viewed perpendicular to the *b* axis.

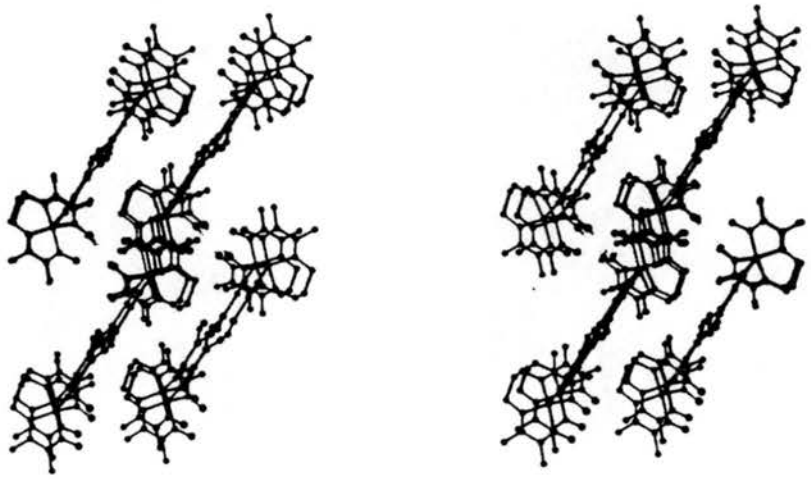

Figure 1.8. Stereoview of the structure of $[Cu(\mathbf{1})(\mu\text{-NC})Cu(\mu\text{-CN})]_n$ (**5b**), viewed parallel to the *b* axis. Bonds are represented as solid lines. Atoms are represented as solid circles.

the next by a twofold screw operation parallel to *b*. The *c* glide plane (with reflection through the *ab* face) relates two $[Cu(\mathbf{1})]^+$ complexes of adjacent polymer chains in such a way as to interweave the units along the *b* axis with the oxime oxygen atoms directed away from the chain propagation axis. The twist angle of the $[Cu(\mathbf{1})]^+$ unit (see above) is 89.6°. Unlike the structure of **5a**, the polymeric layers in **5b** are interwoven with layers adjacent to them. The cavities of the interwoven layers are filled by units above and below them.

Structure of 5c. The structure of **5c** cannot be described in the same detail as was done for **5a** and **5b**. As was the case for **5a** and **5b**, **5c** consists of $[Cu(CN)_2]^-$ repeat units bridged by one of the two cyano ligands to form a polymeric chain (see Figure 1.9). The structural details involving the dicyanocuprate(I) chain are clear. The coordination geometry about the copper(I) atom in the dicyanocuprate(I) chain is roughly trigonal planar with two sites occupied by carbon atoms of bridging cyano ligands. The copper(I) atom, the two carbon atoms, and the nitrogen atom bound to the copper(I) atom form a plane ($0.116(5)x - 1.32(7)y + 23.03(4)z = 9.064(14)$; $\Sigma\Delta^2 = 0.001$, $\sigma^2 = 0.017$); the deviations of the atoms from that plane are as follows: Cu1, –0.029(2) Å; C1, 0.01(2) Å; C2, 0.01(2) Å; N1, –0.01(2) Å. As before, the third coordination site is occupied by a nitrogen-bound cyano ligand from an adjacent symmetry-related repeat unit. The angles about copper(I) (C2–Cu1–C1 = 119.8(6)°; C2–Cu1–N1 = 118.3(6)°; C1–Cu1–N1 = 121.8(6)°) are very close to the ideal angle of 120° for trigonal planar coordination. The Cu(I)–N and Cu(I)–C bond lengths do not differ significantly (Cu1–N1 = 1.964(13) Å; Cu1–C1 = 1.956(14) Å; Cu1–C2 = 1.971(17) Å), nor do the C–N bond lengths (C1–N1 = 1.103(19) Å; C2–N2 = 1.135(22) Å). The carbon-bound and nitrogen-bound cyano ligands form bonds to copper(I) that are nearly linear (N1–C1–Cu1 = 174(1)°; Cu1–C2–N2 = 163(2)°; Cu1–N1–C1 = 176(2)°). The repeat units are related by an *a* glide operation.

The copper(II) atom is coordinated by **1** and by the nitrogen atom of the bridging cyano ligand. Nitrogen atoms of **1** occupy four of the five coordination sites on the

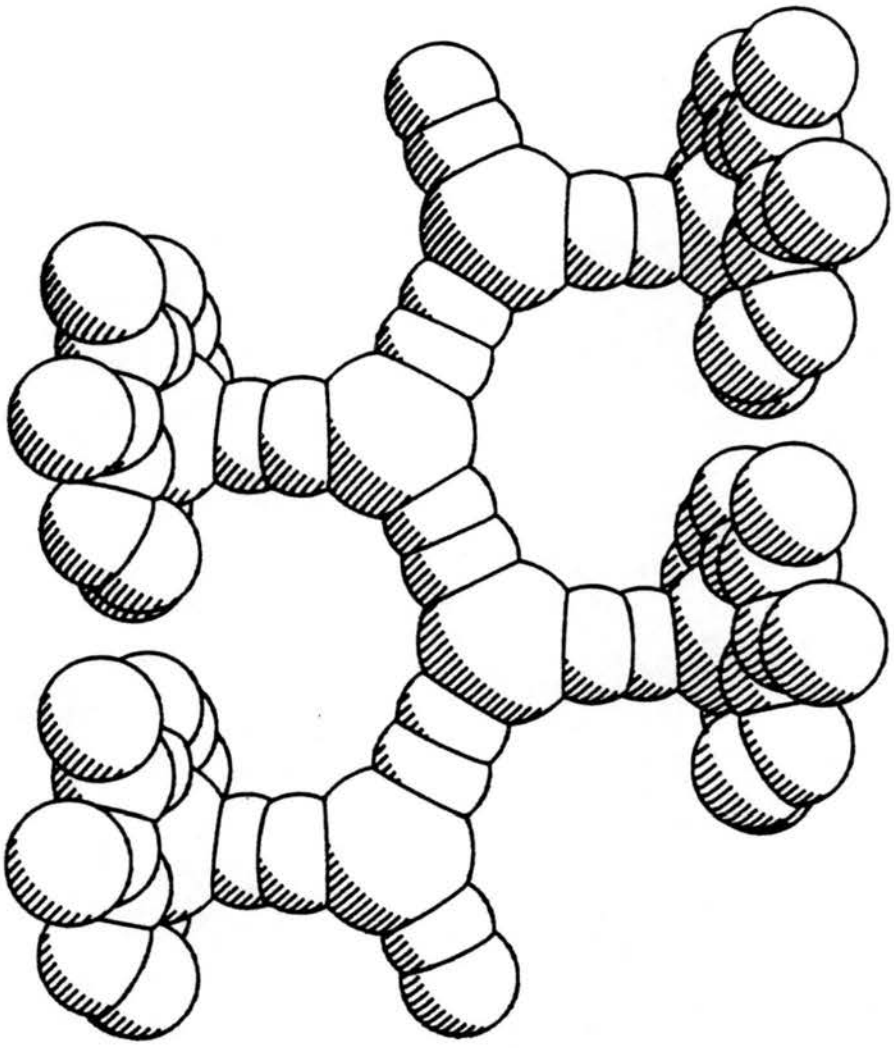

Figure 1.9. Space-filling plot of a portion of the chain in $Cu(\mathbf{1})(\mu\text{-NC})Cu(\mu\text{–CN})]_n$ (**5c**), viewed parallel to the *c* axis.

pentacoordinate copper(II) atom, and the remaining site is occupied by the nitrogen atom of the cyano ligand. The coordination geometry cannot be discussed in detail, due to the disordered nature of ligand **1**.

Structure of 6. Compound **6** also consists of $[Cu(CN)_2]^-$ repeat units which are bridged by one of the two cyano ligands to form an infinite polymer chain. The coordination geometry about the copper(I) atoms in the polymer chain is roughly trigonal planar. The copper(I) atom, the cyano carbon atoms, and the cyano nitrogen atom bound to copper(I) form a plane ($11.2(3)x - 0.010(9)y + 3.174(8)z = 3.154(7)$; $\Sigma\Delta^2 = 0.000$, $\sigma^2 = 0.002$); deviations of atoms from that plane are as follows: Cu1, 0.003(1) Å; C1(N1), 0.001(4) Å; N1(C1), 0.0009(4) Å; C2, 0.0009(4) Å. One coordination site about the copper(I) is occupied by a carbon-bound cyano ligand, which bridges to a $[Cu(\mathbf{2})]^+$ complex (see Figure 1.10). The remaining sites are occupied by the disordered atoms of the cyano ligand which bridges the copper(I) atoms. The Cu(I)–C(N) bond lengths involving the disordered atoms are not equivalent (Cu1–C1(N1) = 1.938(3)Å; Cu1–N1(C1) = 1.951(3)Å). However, the average of the two bond lengths (1.944 Å) is close to the average of copper(I)-bridging cyano bond lengths for **5a** and **5b** (1.941 Å). The C–N distances in the disordered cyano ligands are equivalent (C1(N1)–C1(N1) = 1.166(6) Å, N1(C1)–N1(C1) = 1.170(6) Å). The C2–N2 bond length (1.133(4) Å) is significantly shorter than the C–N distances in the disordered cyano ligands. The repeating units of the chain are related by inversion centers, and the chain is propagated parallel to the *b* axis.

The coordination geometry about the copper(II) atom is distorted square pyramidal. As was the case for **5a–c**, the apical site is occupied by the nitrogen atom of the bridging cyano ligand. The basal positions are occupied by nitrogen atoms of ligand **2**. The basal nitrogen atoms form a plane (see Table S-1.10), with the copper(II) atom displaced by 0.462(2) Å toward the apical ligand. The coordination geometry is distorted in such a way as to force the vector that bisects the Cu2–N4 and Cu2–N5 bonds towards the vector

Figure 1.10. Thermal ellipsoid plot (50% probability) and the numbering scheme of $[Cu(\mathbf{2})(\mu\text{-}NC)Cu(\mu\text{-}CN) \cdot 1/2(C_6H_6)]_n$ (**6**). Hydrogen atoms have been included as spheres of fixed, arbitary radius. The molecule of benzene sits on a crystallographic inversion center. Only the repeat unit of the polymer chain is represented.

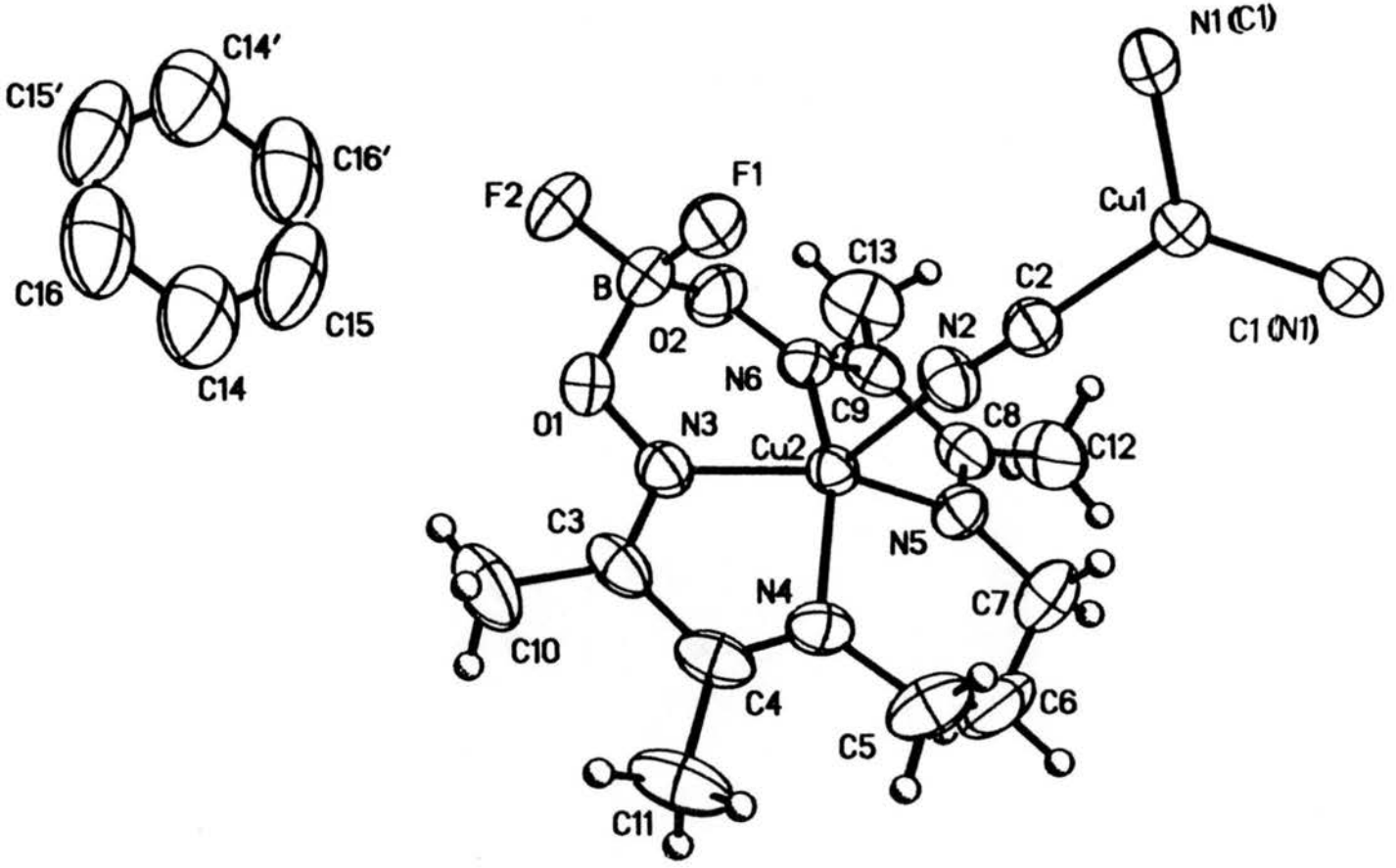
C14'
C15'
C16'
C16
C15
C14
N1 (C1)
Cu1
F2
F1
C13
C2
B
O2
N2
C1 (N1)
N6
C9
O1
N3
Cu2
C8
C12
C3
N5
N4
C7
C10
C4
C6
C5
C11

formed by the Cu2-N2 bond. The angle between the normal to the plane formed by the basal nitrogen atoms and the vector formed by the apical Cu2–N2 bond is 11.7°. This distortion is also reflected in the N(ax)–Cu2–N(basal) bond angles. The angles N2–Cu2–N4 and N2–Cu2–N5 are smaller than the angles N2–Cu2–N3 and N2–Cu2–N6. The bond between copper(II) and the apical nitrogen atom is significantly longer than the Cu2–N(basal) bonds. The remaining bond lengths and angles do not differ from expected values.

As was the case in **5a** and **5b**, formation of the chain is sterically restrictive, and binding the large $[Cu(\mathbf{2})]^+$ complexes creates distortions (see Figure 1.11). To accommodate the bulky complex, the coordination geometry about copper(II) distorts (see above), allowing the $[Cu(\mathbf{2})]^+$ units to swing in towards the chain by pivoting at the copper(II) atom; in this manner the chain effectively stacks the $[Cu(\mathbf{2})]^+$ complexes and fills the intrachain voids.

The occluded molecule of benzene was seen to occupy an inversion center, halfway between the faces of two $[Cu(\mathbf{2})]^+$ moieties of adjacent polymer chains. The benzene molecule thus fills the void between the chains (see Figure 1.12).

Infrared Studies. Infrared absorption spectroscopy has proved to be a useful tool in the investigation of copper cyanide complexes.[35] The frequencies and band shapes that arise from the stretching modes of carbon–nitrogen triple bonds allows ready identification of cyano ligands in the infrared absorption spectrum. The frequencies seen for C–N stretching modes in inorganic compounds fall between 2500 cm^{-1} and 2000 cm^{-1}.[31,32]

In an X-ray diffraction experiment, a single crystal is chosen to represent the bulk sample. To assess whether that crystal is representative of the bulk sample, one must rely on means other than the X-ray experiment. Comparison of the infrared absorption spectrum of the bulk sample to the spectrum obtained from a single crystal is one such means of verifying that the crystal chosen for the X-ray experiment does represent the

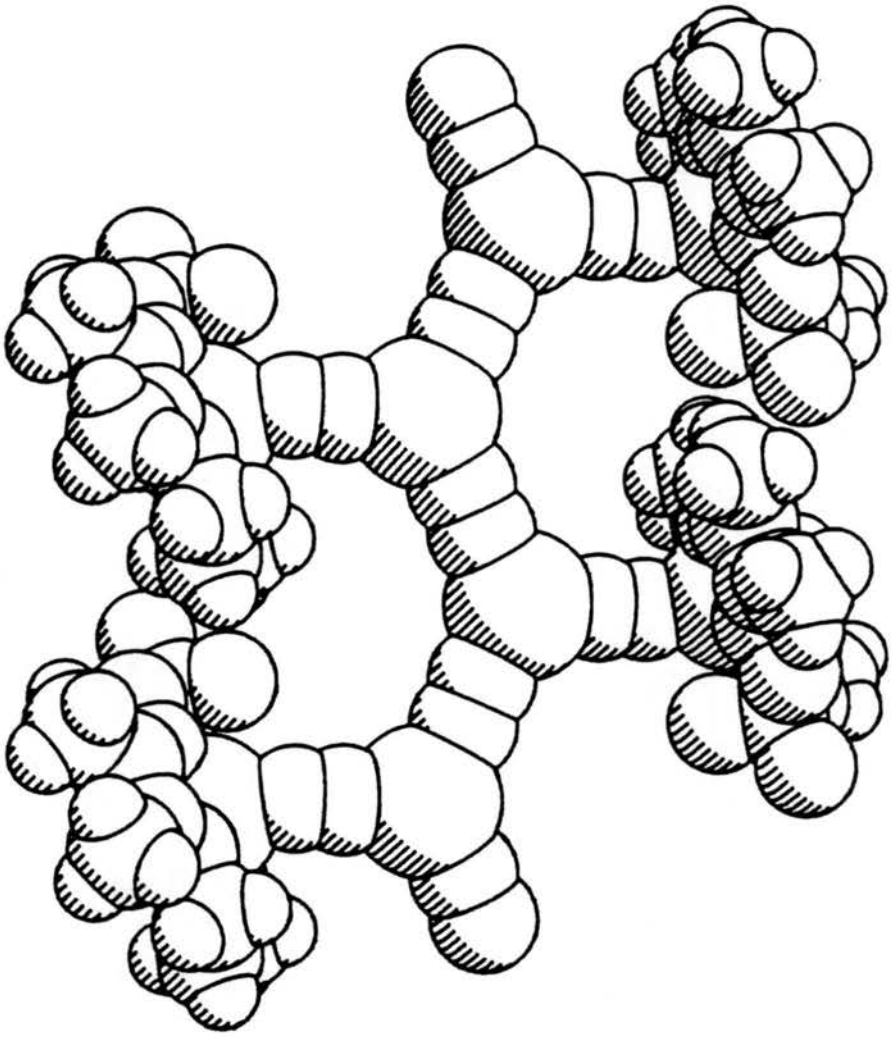

Figure 1.11. Space-filling plot of a portion of the chain in Cu(**2**)(μ-NC)Cu(μ-CN) · $1/2(C_6H_6)]_n$ (**6**), viewed parallel to the *a* axis.

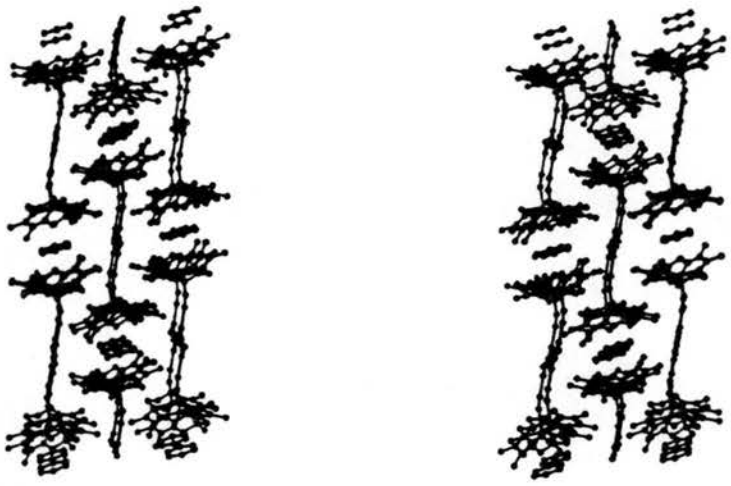

Figure 1.12. Stereoview of the structure of $[Cu(\mathbf{2})(\mu\text{-NC})Cu(\mu\text{-CN}) \cdot 1/2(C_6H_6)]_n$ (**6**), viewed parallel to the *b* axis. Bonds are represented as solid lines. Atoms are represented as solid circles.

entire sample. Single crystal FT-IR spectroscopy has been used (see the Experimental Section) to probe this question.

The frequencies, ν_{CN}, for **4**, **5a**, **5b**, **5c**, and **6**, together with those for other cyanocuprate compounds, are summarized in Table S-1.11. The infrared absoption spectra between 2500 cm^{-1} and 1950 cm^{-1} for bulk samples and single crystal samples of **4** (Figure 1.13), **5a** (Figure 1.14), **5b** (Figure 1.15), **5c** (Figure 1.16), and **6** (Figure 1.17) can be examined to determine whether the single crystal and the bulk sample contain similar structural components. Close examination of all of the spectra indicates no substantial differences in the shape or position of the infrared bands in the single crystal spectra and the bulk spectra. From this evidence it can be concluded that the samples used for the X-ray experiments were truly representative of the bulk samples. The single crystal IR spectrum of **6** from 4000 cm^{-1} to 400 cm^{-1} (see Figure 1.18) was recorded without mulling. Mulled samples proved more useful in the identification and comparison of samples, due to negative effects often seen in single crystal infrared investigations.[33,34]

As discussed above, **4** consists of two chemically equivalent $[Cu(\mathbf{1})]^+$ complexes, which are coordinated to the $[Cu(CN)_3]^{2-}$ group in structurally inequivalent fashions. This gives rise to three inequivalent cyano ligands: a terminal, nonbridging ligand; a linear bridging ligand; and a nonlinear bridging ligand. The three peaks seen in the cyanide stretching region for **4** correspond to these three ligand types.

The C–N stretching frequencies for **4** are on average 20 cm^{-1} higher in energy than those reported for the anion $[Cu(CN)_3]^{2-}$.[35] The shift toward higher energy is expected for bridging cyano ligands, due to the additional constraints placed on the vibrational motions.[36,37] Of the three bands in the spectrum of **4**, the two higher frequency bands at 2128 cm^{-1} and 2112 cm^{-1} are assigned to the bridging cyano ligands, while the band at 2095 cm^{-1} is due to the terminal cyano ligand.

5a, **5b**, and **5c** are structural variations of the same compound. The cyano ligands in these structures are in different environments. Two bands in the single crystal and bulk

Figure 1.13. Infrared spectra (2200 cm^{-1} to 2000 cm^{-1}) of mulls made from a single crystal (bottom line) and a bulk sample (top line) of $[Cu(\mathbf{1})(\mu\text{-}NC)]_2Cu(CN) \cdot H_2O$ (**4**).

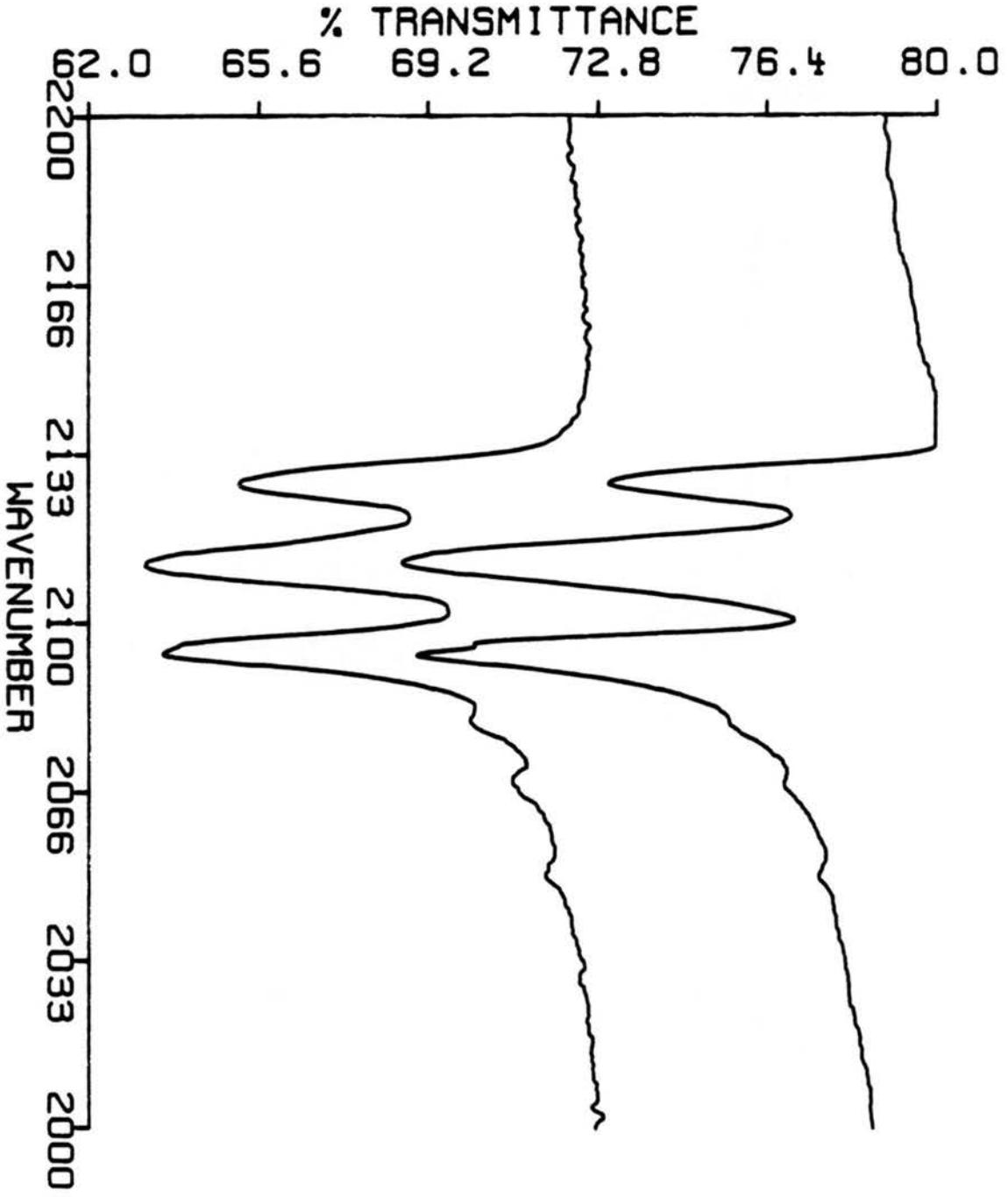
% TRANSMITTANCE
62.0
65.6
69.2
72.8
76.4
80.0
2200
2166
2133
2100
2066
2033
2000
WAVENUMBER

Figure 1.14. Infrared spectra (2290 cm^{-1} to 1920 cm^{-1}) of mulls made from a single crystal (bottom line) and a bulk sample (top line) of $[Cu(\mathbf{1})(\mu\text{-}NC)Cu(\mu\text{-}CN)]_n$ (**5a**).

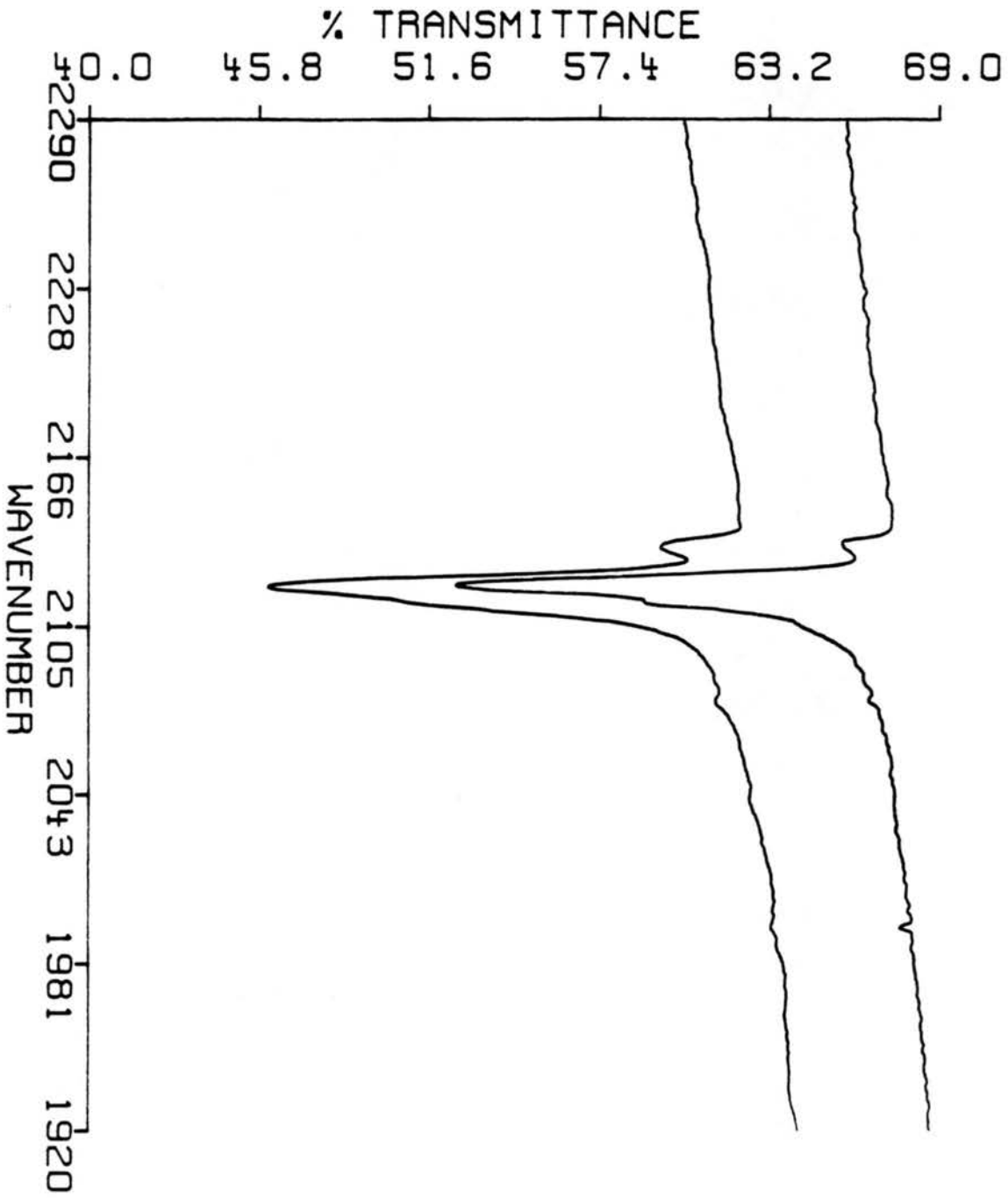
% TRANSMITTANCE
40.0
45.8
51.6
57.4
63.2
69.0
2290
2228
2166
2105
2043
1981
1920
WAVENUMBER

Figure 1.15. Infrared spectra (2290 cm^{-1} to 1920 cm^{-1}) of mulls made from a single crystal (top line) and a bulk sample (bottom line) of $[Cu(\mathbf{1})(\mu\text{-}NC)Cu(\mu\text{-}CN)]_n$ (**5b**).

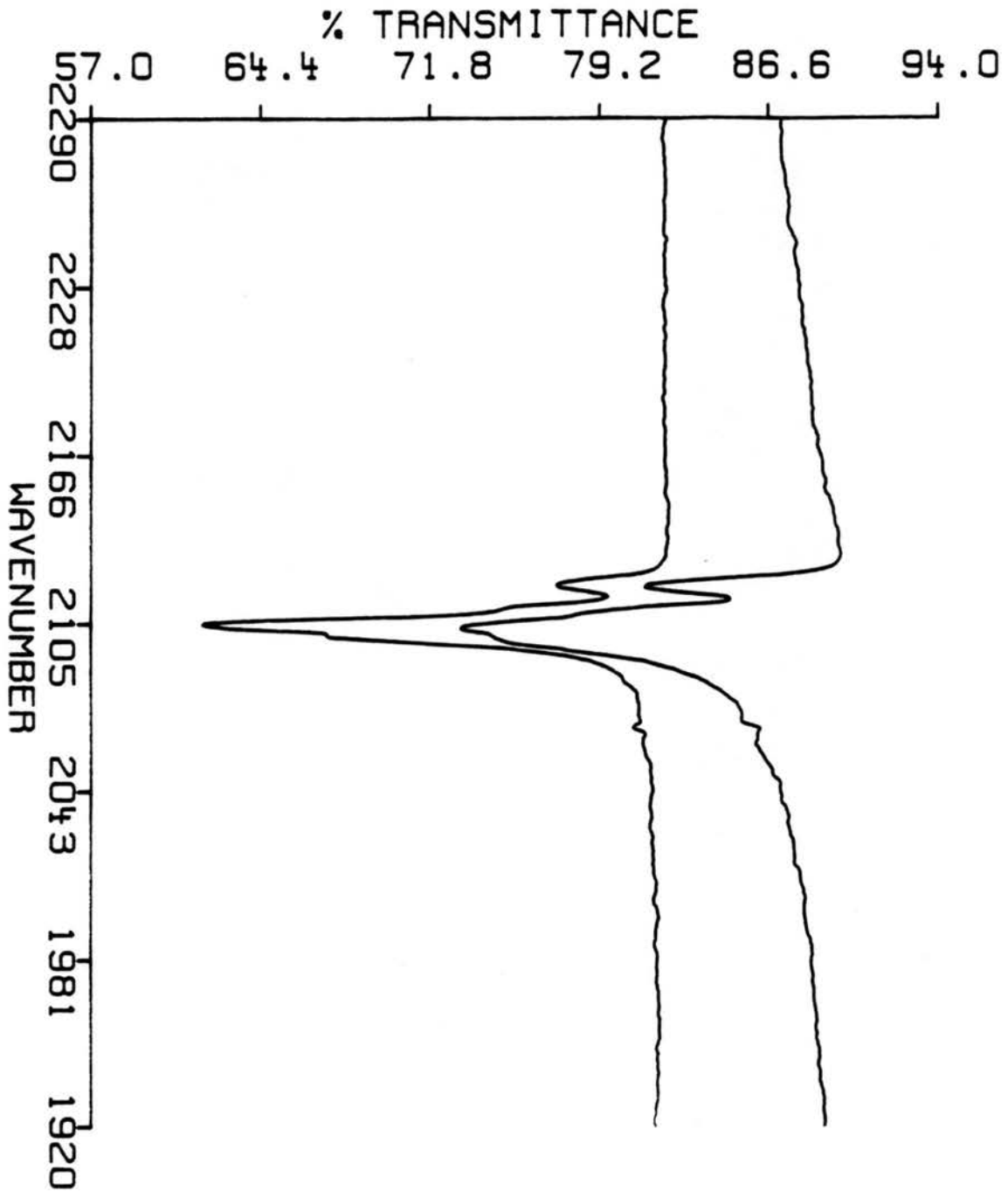
% TRANSMITTANCE
57.0
64.4
71.8
79.2
86.6
94.0
2290
2228
2166
2105
2043
1981
1920
WAVENUMBER

Figure 1.16. Infrared spectra (2290 cm^{-1} to 1920 cm^{-1}) of mulls made from a single crystal (bottom line) and a bulk sample (top line) of $[Cu(\mathbf{1})(\mu\text{-}NC)Cu(\mu\text{-}CN)]_n$ (**5c**).

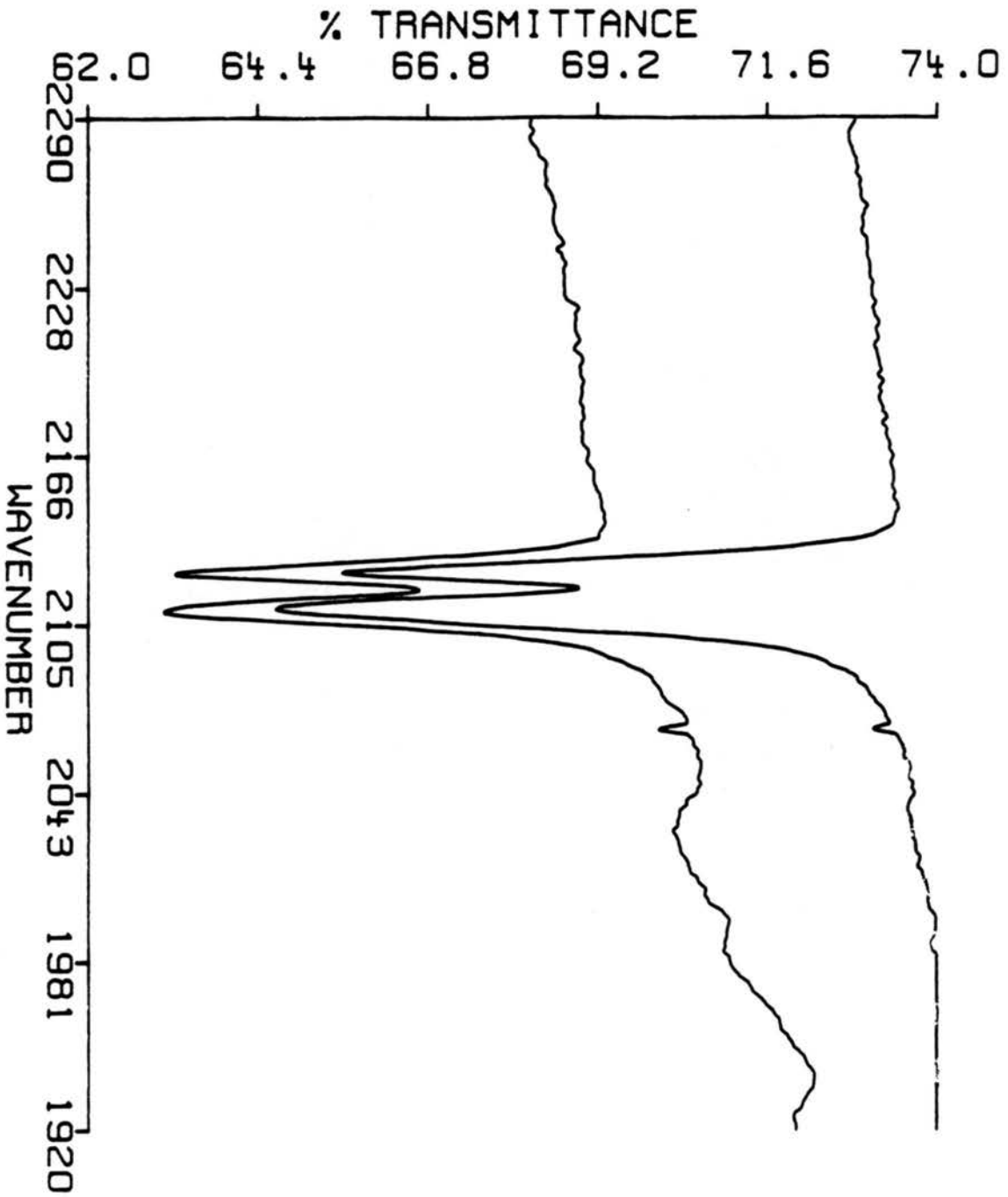
% TRANSMITTANCE
62.0
64.4
66.8
69.2
71.6
74.0
WAVENUMBER
2290
2228
2166
2105
2043
1981
1920

Figure 1.17. Infrared spectra (2200 cm^{-1} to 2000 cm^{-1}) of mulls made from a single crystal (top line) and a bulk sample (bottom line) of [Cu(**2**)(μ-NC)Cu(μ-CN) · $1/2(C_6H_6)]_n$ (**6**).

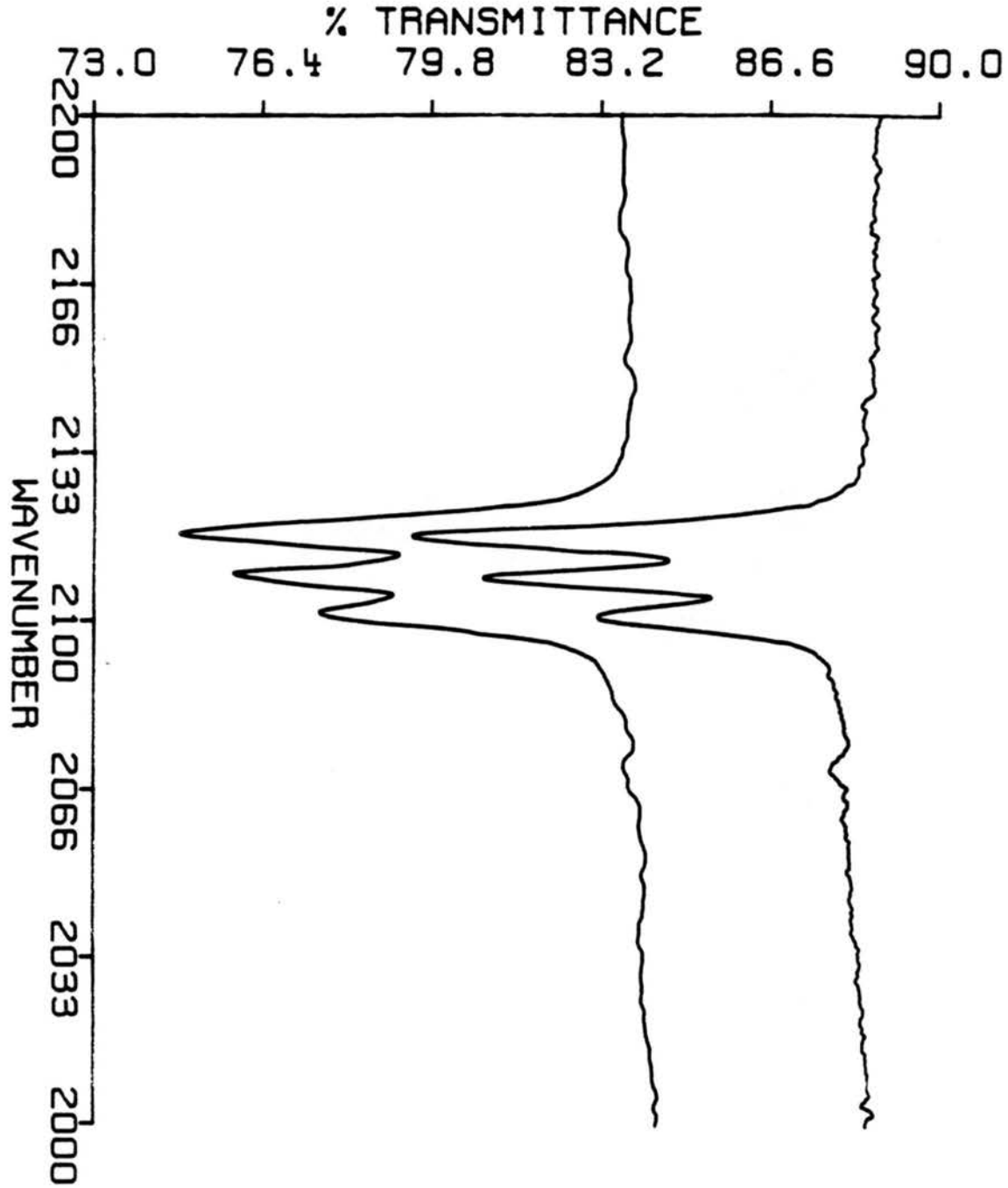
% TRANSMITTANCE
73.0
76.4
79.8
83.2
86.6
90.0
2200
2166
2133
2100
2066
2033
2000
WAVENUMBER

Figure 1.18. Infrared spectra (4000 cm^{-1} to 500 cm^{-1}) of a single crystal of [Cu(**2**)(μ-NC)Cu(μ-CN) · 1/2(C_6H_6)]$_n$ (**6**).

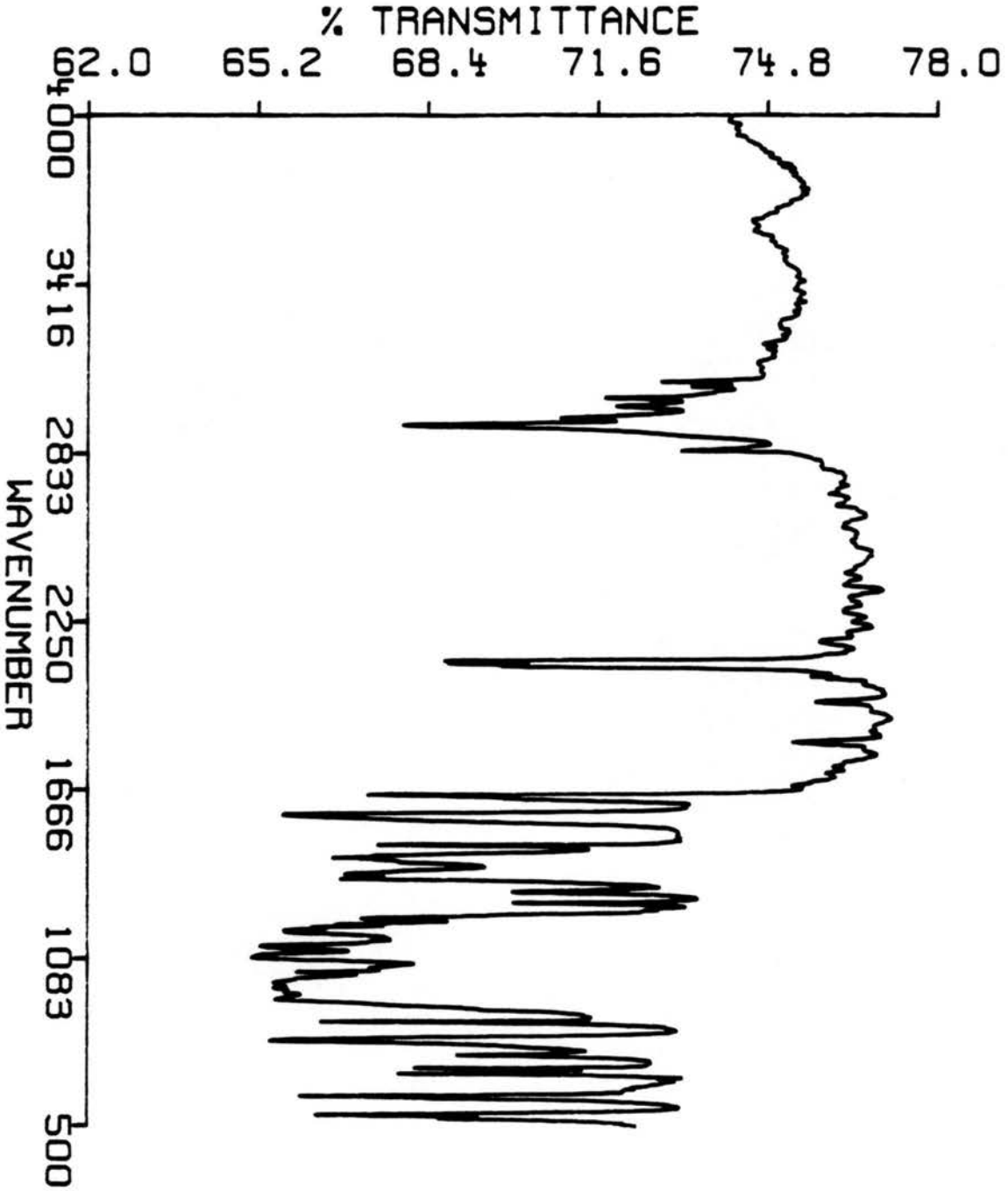
% TRANSMITTANCE
62.0
65.2
68.4
71.6
74.8
78.0
4000
3416
2833
2250
1666
1083
500
WAVENUMBER

sample spectra are seen in each case (see Figures 1.14 – 1.16). The two bands in **5a** are higher in energy than those for **5a** and **5c**; this may result from the different bridging environments of the cyano ligands.[36]

A shoulder is seen on the lower frequency absorption band in the cyano stretching region of the infrared spectra for **5a**, **5b**, and **5c**. The lower frequency band probably consists of two overlapping absorption bands, which result from the coupling of the skeletal stretching modes of the polymer with the site symmetry and the unit cell symmetry.[3,38]The coupling is similar to that seen for crystalline polyethylene[38] and a Cu(**L**)(μ–CN) polymeric adduct (**L** = 2,9-dimethyl-1,10-phenanthroline)[3].

The infrared absorption spectrum of **6** in the cyano stretching region shows three distinct bands (see Figure 1.17). Two of these bands arise from the correlation of the bands of the cyanocuprate(I) polymer with the site symmetry and unit cell symmetry just as for **5a**, **5b**, and **5c**. The three bands are lower in frequency than those seen for **5a**, **5b**, and **5c**, which is a result of the coordination of cyanide to the more easily reduced $[Cu(\mathbf{2})]^+$ complex.[28,30,40]

In summary, the terminal cyano ligands in $[Cu(CN)_3]^{2-}$ and $[Cu(CN)_2]^-$ can be used to coordinate metal complexes. This is due, in part, to the flexibility of the cyanocuprate(I) backbone and to the facile bridging nature of the cyano ligand.

Chapter 2

Dinuclear Copper(II) Complexes with Copper–Copper Separations of Less than 3.5 Å. Models for the Active Site of Oxidized Hemocyanin

Introduction

Hemocyanin (Hc) is found in arthropods and molluscs, and is a copper-containing dioxygen transport protein.[41–43] EXAFS studies[44,45] of the oxygenated protein (oxyHc) suggest that the active site contains two copper(II) atoms which are separated by a distance of approximately 3.6 Å (3.55 Å in *Megathura crenulata* (a mollusc),[45] 3.66 Å in *Busycon* (a mollusc),[44] 3.58 Å in *Limulus*.(an arthropod),[44] and 3.62 Å in *Cancer* (an arthropod)[44]). The low frequency (750 cm^{-1}) of the O–O stretch in the resonance Raman spectrum[46] of oxyHc suggests that dioxygen binds to the active site as a peroxide. The peroxo ligand (O_2^{2-}) to metal (Cu^{2+}) charge transfer spectrum ($\pi_v^* \rightarrow d_{x^2-y^2}$, 570 nm; $\pi_\sigma^* \rightarrow d_{x^2-y^2}$, 345 nm) has been investigated utilizing a transition dipole model.[47] The model suggests that the peroxo anion binds to the copper(II) centers through both oxygen atoms (referred to as the **EE** mode). EXAFS studies of oxyHc suggest that a second bridge between the copper(II) atoms is formed by a single oxygen atom, which may be from a tyrosine residue.[48,49] The copper(II) atoms in oxyHc are thought to be five-coordinate; four of the sites about each copper(II) atom are probably occupied by two nitrogen atoms of histidine residues,[44] an oxygen atom of the peroxo ligand,[46,47] and an oxygen atom from a tyrosine residue.[48] The fifth site may be occupied by an oxygen atom of a coordinated water molecule.[50] The bridging phenolato and peroxo groups provide

exchange pathways for the unpaired electron density on the copper(II) atoms. As a result, the two copper(II) atoms are antiferromagnetically coupled. Previous work[51] indicated that the coupling constant ($2J$) characterizing the exchange interaction was ~620 cm^{-1}. A broad absorption band in the resonance Raman spectrum centered at 1075 cm^{-1} may be associated with the singlet to triplet transition in the ground state of the dimer.[41,51] As a result of the strong antiferromagnetic coupling between the copper(II) atoms, the oxyHc protein is EPR silent.[41,49]

Model systems that display the proposed structural features of Hc have been of considerable interest in achieving an understanding of how dioxygen is incorporated in the protein. A suitable ligand for such a model system must be capable of binding two copper atoms with a copper–copper separation of greater than 3.0 Å. It should provide at least two histidine-like residues, as well as a bridging phenoxo oxygen atom. The model ligand should be flexible enough to allow either square pyramidal or trigonal bipyramidal coordination of the metals, so that the metal coordination can respond to changes in the nature of other ligands.

Model ligands which fulfill most of the above criteria have been synthesized, and 2,6-bis[bis(2-(1-pyrazolyl)ethyl)amine]-*p*-cresol (N_6OH) and 2,6-bis[[bis(2-(1-pyrazolyl)ethyl)amino]methyl]-*p*-cresol, (N_6'OH) are just such binucleating ligands.[52,53]

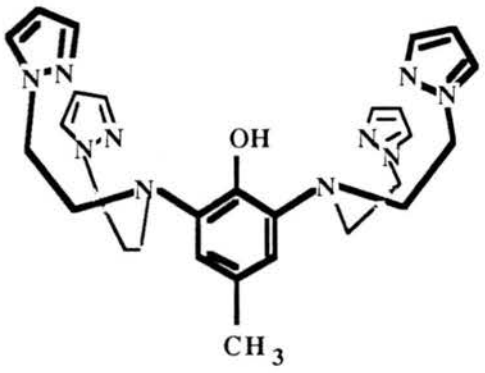

N_6O

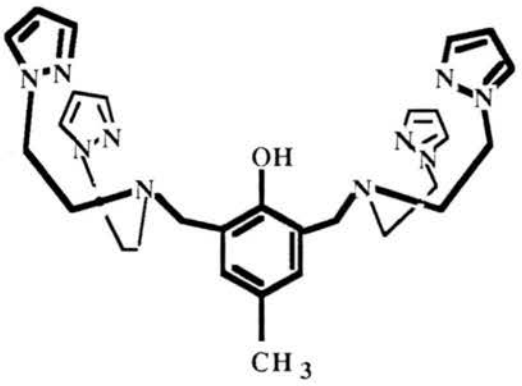

$N_6'O$

Both compounds contain coordination sites for two copper(II) atoms. Each such site would involve two pyrazole groups and an aliphatic amine, and the deprotonated phenolate oxygen atom may be shared between the two metal centers. The only difference between the two ligands is the presence or absence of a methylene group that bridges between the amine nitrogen atoms and the cresol moiety.

This difference in the ligands should result in a difference in the distance between the metal atoms bound to the coordination sites. Previous work[54–56] with copper(II) complexes similar to N_6O^- has shown that binucleating ligands that form five-membered chelate rings (see **A** below) are capable of separating metal centers by a minimum of 3.3 Å.[54–55] Likewise, copper(II) complexes similar to $N_6'O^-$ contain six-membered chelate rings and are capable of bringing the metal centers closer together (see **B** below).[52,57–59]

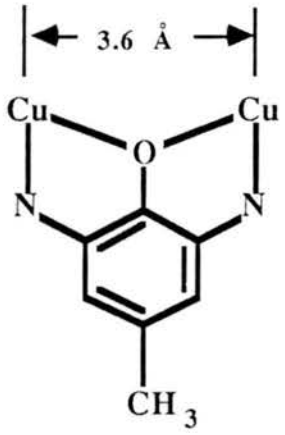

N_6O^-

(A)

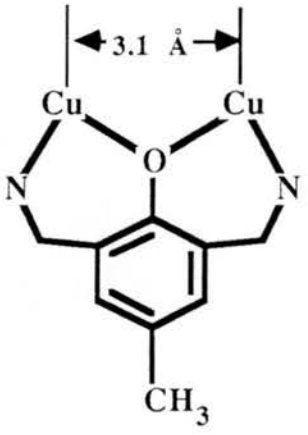

$N_6'O^-$

(B)

One of the goals in modeling the active site of hemocyanin is to mimic the magnetic properties of the protein. Magnetic coupling in the azido derivatives of metHc, where the azide ion has replaced dioxygen at the binding site of oxyHc, involves an exchange pathway through the HOMO π_g orbital (orbital energy = –1.83 eV)[60] of the azido ligand.[61] Other filled orbitals ($2\sigma_u$, orbital energy = –8.51 eV; $2\sigma_g$, orbital energy = –10.39 eV; π_u, orbital energy = –11.25 eV) are much lower in energy, and are not close to the metal *d* orbitals in energy. As a result, they are not involved in a significant way in magnetic exchange pathways.[60] Antiferromagnetic coupling in dinuclear azido-bridged copper(II) compounds involves the overlap of the orbitals on the copper(II) atoms which contain the unpaired electrons with the lobes of the π_g orbital of the bridging azido ligand.

The magnetic coupling constant ($2J$) describes the energy difference between the singlet state ($S = 0$) and the triplet state ($S = 1$) for d^9 metal dimers. The J term is composed of an antiferromagnetic negative component (J_{AF}) and a ferromagnetic positive component (J_F). J_{AF} is proportional to the overlap density between the ligand orbitals and the metal orbitals which contain the unpaired electron, while J_F is dependent on the two-electron exchange integral.[61–63]

An azido ligand can bridge between two copper(II) centers using both terminal nitrogen atoms (**EE**, end-to-end) or only one terminal nitrogen atom (**EO**, end-on).[62] The separation of the metal centers in dinuclear copper(II) complexes is crucial to the mode of azido binding. For the **EO** mode to occur, the metal centers must be less than 3.1 Å apart for the azido ligand to provide an effective bridge.[58,64,65] The **EE** mode demands that the metal centers be separated by at least 3.4 Å.[54]

A hydroxo ligand or the phenolato moieties of ligands such as N_6O^- and $N_6'O^-$ can also provide a magnetic exchange pathway between two copper(II) centers through the 2*p* orbital on oxygen.[66] However, only one bridging mode is possible.[52,57,65,67-71]

Previous work designed to create complexes that might serve as models for the active site of hemocyanin resulted in the synthesis of the perchlorate salts of the binuclear complex ions (μ-1,3-azido)[2,6-bis[bis[2-(1-pyrazolyl)ethyl]amino]-*p*-cresolato]dicopper(II) ($[Cu_2(N_6O)(\mu\text{-}1,3\text{-}N_3)]^{2+}$, referred to herein as **7**),[9] (μ-O,O'-acetato)[2,6-bis[bis[2-(1-pyrazolyl)ethyl]amino]-*p*-cresolato]dicopper(II) ($[Cu_2(N_6O)(\mu\text{-}O,O'\text{-}CH_3CO_2)]^{2+}$, referred to herein as the acetato complex),[53] the tetrafluoroborate salt of the binuclear complex ion (μ-1,1-azido)[2,6-bis[bis[2-(1-pyrazolyl)ethyl]amino]methyl]-*p*-cresolato]dicopper(II) ($[Cu_2(N_6'O)(\mu\text{-}1,1\text{-}N_3)]^{2+}$, referred to herein as **8**),[53] and the tetrafluoroborate salt of the binuclear complex ion (μ-hydroxo)[2,6-bis[bis[2-(1-pyrazolyl)ethyl]amino]methyl]-*p*-cresolato]dicopper(II) ($[Cu_2(N_6'O)(OH)]^{2+}$, referred to herein as **9**).[52] **9** exists in a brown form (**9b**, $[Cu_2(N_6O)(OH)](BF_4)_2$), which has been characterized by X-ray crystallography, as well as by spectroscopic and magnetic studies.[52] A green form of the compound (**9a**) also exists.[8] Crystals of this green form (**9a**) contain an occluded THF solvent molecule, and are thus formulated as $[Cu_2(N_6O)(OH)](BF_4)_2 \cdot (THF)]$.

7 has the largest reported antiferromagnetic coupling constant of these compounds ($2J = -1800\ cm^{-1}$), and is currently being used as a model compound in the EXAFS studies of azido-metHc.[53] The acetato complex, in contrast, displays negligible magnetic

interaction between the copper(II) atoms even though the two structures have the same binucleating ligand (N_6O^-) and similar copper(II) coordination spheres.[53] The antiferromagnetic coupling constant for **8** ($2J = -450\ cm^{-1}$)[53] is one-fourth that observed for **7**. A study of the structures of **7** and **8** was undertaken in an effort to understand the differences in the magnetic properties of these complexes.

The apparently minor difference between **9a** and **9b** (the presence of an occluded THF molecule in **9a**) results in physical properties that are significantly different for the two forms. Of particular interest is the fact that the magnetic coupling between the two copper(II) atoms varies from $2J = -420\ cm^{-1}$ for **9b** to $2J = -300\ cm^{-1}$ (see below) for **9a**. In an attempt to understand these differences, the determination of the structure of **9a** was undertaken.

Experimental

Synthesis and Crystallization. The syntheses of (μ-1,3-azido)[2,6-bis[bis[2-(1-pyrazolyl)ethyl]amino]-*p*-cresolato]dicopper(II) (**7**), (μ-1,1-azido)[2,6-bis[bis[2-(1-pyrazolyl)ethyl]amino]methyl]-*p*-cresolato]dicopper(II) (**8**), and (μ-hydroxo)[2,6-bis[bis[2-(1-pyrazolyl)ethyl]amino]methyl]-*p*-cresolato]dicopper(II) (**9**) have been previously reported.[52,53] Crystals of **7**, **8**, and **9** were furnished by T. N. Sorrell. Structural modification **9a** was crystallized by the vapor diffusion of tetrahydrofuran into an acetonitrile solution of **9b**.

X-Ray Structure Determinations. The crystallographic experiments were carried out on a Nicolet *R*3*m* X-ray diffractometer utilizing the software provided with the instrument. The SHELXTL program package (Rev. 4.1, 1983, written by G. M. Sheldrick and supplied by Nicolet XRD for the Data General Eclipse S/140 computer) was used for data reduction, structure solution, refinement, and plotting. Neutral atom scattering factors and anomalous dispersion terms were taken from Ref. 39.

Structure Determination for 7. Many crystals of **7** were examined. Most crystals were unsuitable for intensity data collection, due to broadened peaks and satellite reflections. The green, cube-shaped crystal chosen for data collection was mounted on a glass fiber and centered on the X-ray diffractometer. The unit cell constants reported in Table 2.1 were calculated from a least squares fit to the setting angles for 25 independent reflections ($2\theta_{ave} = 13.7°$). Three control reflections monitored every 97 reflections during data collection showed no significant variation in intensity.

Data were corrected for Lorentz and polarization factors, as well as for absorption effects. The analytical absorption correction resulted in $T_{min} = 0.65$ and $T_{max} = 0.85$.

Table 2.1. Details of the Crystallographic Experiments and Computations for **7**, **8**, and **9a**.

Compound	**7**	**8**	**9a**
Formula	$C_{31}H_{41}N_{13}Cl_2Cu_2O_{10}$	$C_{33}H_{45}N_{13}B_2Cu_2F_8O_2$	$C_{33}H_{46}N_{10}B_2Cu_2F_8O_3$
Molecular weight (g mol^{-1})	953.7	956.5	931.5
Crystal system	orthorhombic	orthorhombic	monoclinic
Space group	$P2_12_12_1$	$P\,2_1cn$	$P\,2_1/n$
Lattice constants			
a (Å)	12.977(2)	10.222(2)	12.457(3)
b (Å)	13.188(3)	16.683(4)	10.222(3)
c (Å)	22.033(6)	23.517(7)	30.397(10)
β (deg)			91.63(2)
V (Å^3)	3771	4010	3869
Temperature (°C)	−130(1)	−130(1)	−130(1)
Z	4	4	4
ρ (calculated, g cm^{-3})	1.65	1.58	1.60
Crystal dimensions	(001→ 00$\bar{1}$) 0.12 mm ×	(001 → 00$\bar{1}$) 0.19 mm ×	(001 → 00$\bar{1}$) 0.12 mm ×
	(010→ 0$\bar{1}$0) 0.28 mm ×	(010 → 0$\bar{1}$0) 0.20 mm ×	(010 → 0$\bar{1}$0) 0.32 mm ×
	(100 → $\bar{1}$00) 0.41mm	(100 → $\bar{1}$00) 0.46 mm	(100 → $\bar{1}$00) 0.28 mm

Table 2.1 (continued)

Radiation	$MoK_\alpha(\lambda = 0.71073$ Å)	MoK_α	MoK_α
Monochromator	graphite	graphite	graphite
Scan type	θ–2θ	θ–2θ	θ–2θ
Geometry	bisecting	bisecting	bisecting
μ (cm^{-1})	13.5	11.4	11.9
Scan speed (deg min^{-1})	2.0 – 29.3	2.0 – 29.3	2.0 – 29.3
2θ range (deg)	3.5 – 50.0	3.5 – 50.0	3.5 to 50.0
Index restrictions	$0 \le h \le 16$; $-16 \le k \le 0$; $-27 \le l \le 0$	$0 \le h \le 13$; $-20 \le k \le 0$; $0 \le l \le 28$	$-15 \le h \le 15$; $-13 \le k \le 0$; $-37 \le l \le 0$
Total number of reflections	3828	4136	7645
Number of unique, observed reflections	3093	2938	5156
Observed reflection criterion	$F \ge 2.5\ \sigma\|F\|$	$F \ge 2.5\ \sigma\|F\|$	$F \ge 2.5\ \sigma\|F\|$
Number of least-squares parameters	507	506	537
Data to parameter ratio	6.1	5.8	9.7
R	0.072	0.100	0.072
R_w	0.075	0.101	0.077
S	1.59	2.41	1.56
g	0.001(fixed)	0.0005(fixed)	9.0×10^{-4} (refined)
Slope, normal probability plot	1.37	1.83	1.37

Systematic reflection conditions (*h00*, $h = 2n$; *0k0*, $k = 2n$; *00l*, $l = 2n$) required the space group to be $P2_12_12_1$.

The structure was solved readily by Patterson map interpretation. The positions of two independent copper(II) atoms were obtained from the Patterson map. Atomic coordinates for all other nonhydrogen atoms were obtained from subsequent electron density maps. Near the end of the refinement, a molecule of tetrahydrofuran was discovered in the asymmetric unit. Examination of the difference electron density map at this point revealed two prominent peaks (~ 3.0 e $Å^{-3}$) in the immediate vicinity of the two copper atoms of **7**. In addition, examination of bond lengths and angles revealed significant differences in chemically equivalent parameters (for example, N11–N12 = 1.13 Å, N12–N13 = 1.20 Å for the azido ligand; N–N(pyrazole) distances varied from 1.32 to 1.40 Å).

The origin of these two peaks is uncertain. It is possible that the cation is disordered to a minor extent, although the bulk of this species would seem to make this unlikely. It is also possible that unresolved scattering from a small twin fragment might cause such anomalous electron density to appear. Most likely, however, is that these peaks reflect the cocrystallization of a minor amount of a structurally similar cationic impurity. This last possibility is favored by the fact that the magnetic susceptibility experiments revealed the presence of a small amount of a paramagnetic impurity in crystalline samples of **7**.[53]

The prominence of these two peaks and the distance separating them (~ 3.7 Å, compared to Cu1–Cu2 ~ 3.8 Å for **7**) led to a decision to interpret them to be two copper atoms of a binuclear impurity. The structural model was then revised to accommodate the additional copper atoms by allowing the site occupancy factors of the atoms of the original cation to be refined as a single number (SOF). The site occupancy factor for the extra copper atoms was constrained to be (1.0 – SOF). At convergence, the value of SOF was 0.915. Because of the low level at which the extra cation was present (~8.5%), other

atoms of that cation were not detectable. The site occupancy factors of the perchlorate anions were fixed at 1.0.

The SOF value for the atoms of the THF molecule refined to a value not significantly different from one, and was subsequently fixed at 1.0. The large thermal parameters for the atoms of the THF molecule resulted in bond lengths that deviated significantly from expected values. As a consequence, the bond lengths in the THF molecule were constrained to maintain ideal C–C and C–O distances, while the atomic positions and thermal parameters were further refined.

Two enantiomorph assignments are possible for the data collection crystal in the noncentrosymmetric space group. The correctness of the enantiomorph was checked by refinement of the multiplicative factor (*df*) of the imaginary components of the atomic scattering factors. A strong indication ($df = 1.05(6)$) of the correctness of the assignment was obtained.

Inclusion of the minor contribution of the extra copper(II) atoms in the final structural refinement cycles improved the residual indices significantly (before addition of extra copper(II) atoms, $R = 0.0815$, $R_w = 0.0920$; after, $R = 0.0710$, $R_w = 0.0745$). More importantly, most of the of the differences in the chemically equivalent bond lengths that had been present before the inclusion of the extra copper atoms disappeared.

All nonhydrogen atoms were refined with anisotropic thermal parameters. Hydrogen atoms bound to carbon were placed in idealized positions (C–H = 0.96 Å, $U_{iso}(H) = 1.2 \times U_{iso}(C)$). The weighted [$w = (\sigma^2(F) + g(F)^2)^{-1}$] least squares refinement on F yielded the residual values listed in Table 2.1 at convergence (for the last ten cycles, mean shift/e.s.d = 0.078, max shift/e.s.d. = 0.794 for U_{22} of C5b). The height of the highest peak in the final ΔF map was +0.93 e Å^{-3} (near Cu2), while the minimum was –0.60 e Å^{-3}.

Structure Determination for 8. Many crystals of **8** were examined. Nearly all displayed diffraction phenomena arising from twinned or cracked crystals (*i.e.*, broad

peaks and/or satellite reflections in the axial photographs). After much effort, a green parallelepiped was chosen in which the occurrence of these phenomena was minimal. This crystal was mounted on a glass fiber and centered on the X-ray diffractometer. The unit cell constants reported in Table 2.1 were calculated from a least squares fit to the setting angles for 25 independent reflections ($2\theta_{ave} = 19.6°$). Three control reflections monitored every 97 reflections showed no significant variation in intensity during data collection.

Data were corrected for Lorentz and polarization factors. An analytical absorption correction was applied to the data ($T_{min} = 0.74$; $T_{max} = 0.81$). Systematic reflection conditions (*hk0*, $h + k = 2n$; *h0l*, $l = 2n$; *h00*, $h = 2n$; *0k0*, $k = 2n$; *00l*, $l = 2n$) required that the space group was either $P2_1cn$ or *Pmcn*. Attempts to solve the structure in the centrosymmetric space group, *Pmcn*, failed. Statistical tests (mean $|E^2 - 1| = 0.86$) suggested that the noncentrosymmetric space group was the correct choice.

The structure was solved readily by Patterson map interpretation. During refinement, two BF_4^- anions and one THF molecule were located in general positions. Their respective atoms were included in the final refinement.

Due to the large amplitude of thermal motion of atoms of the anions, bond lengths and angles for the tetrafluroborate groups deviated significantly from those expected. Therefore the B–F bond lengths in these anions were constrained to an idealized value (B–F = 1.36 Å, see reference 52 and the results for **9a**) using the DFIX option of the SHELXTL refinement program.

The atoms of the occluded THF molecule were given isotropic thermal parameters; hydrogen atoms associated with this molecule were not included in the final structural model. As with the tetrafluroborate anions, large amplitude thermal motion resulted in bond lengths which were significantly different from those expected, and the DFIX option was again used to constrain the C–C and C–O bond lengths to idealized values (C–O = 1.39 Å, C–C = 1.54 Å).[72]

Due to the large amplitude of the thermal motion for C6c, B1, and B2, these atoms were refined with isotropic thermal parameters.

All other nonhydrogen atoms were refined with anisotropic thermal parameters. Hydrogen atoms bound to carbon were placed in idealized positions (C–H = 0.96 Å, $U_{iso}(H) = 1.2 \times U_{iso}(C)$). The first enantiomorph was refined to a residual R_w value of 0.1076. The correctness of the enantiomorph was checked by refinement of the multiplicative factor of the imaginary components of the structural factors. A strong indication that the assignment was incorrect was seen ($df = -1.4(1)$). All coordinates were changed by an inversion operation (MOVE 1 1 1 –1 in the program X of the SHELXTL program package) and the structure was rerefined. A significant drop in the value of R_w was seen (see Table 2.1). The weighted [$w = (\sigma^2(F) + g(F)^2)^{-1}$] least squares refinement on F yielded the residual values listed in Table 2.1 at convergence (for the last twenty cycles, mean shift/e.s.d = 0.126, max shift/e.s.d. = 0.86 for x/a of C6b). The height of the highest peak in the final ΔF map was 1.05 e Å^{-3} (near B2), while the minimum was –0.62 e Å^{-3}.

Structure Determination for 9a. A parallelepiped of **9a** was mounted on a glass fiber and centered on the X-ray diffractometer. The unit cell constants reported in Table 2.1 were calculated from a least squares fit to the setting angles for 25 independent reflections ($2\theta_{ave} = 16.0°$). Three control reflections monitored every 97 reflections showed no significant variation in intensity during data collection. Data were corrected for Lorentz and polarization factors. Due to the small value of μt_{max} (~ 0.4), no correction for absorption effects was performed. Systematic reflection conditions (*h0l*, $h + l = 2n$; *0k0*, $k = 2n$) required that the space group be $P2_1/n$. The structure was solved readily by Patterson map interpretation.

One of the two tetrafluoroborate anions was disordered. In the final model for this anion, two of the fluorine atoms were shared between two units involving B2, F22, and F23 (site occupancy factor refined to 0.631(4)) on the one hand, and B2', F22', and F23'

(site occupancy factor = 0.369(4)) on the other hand. The DFIX option of the refinement program was employed to constrain all B–F distances in this disordered unit to a value of 1.36 Å. Near the end of the least squares refinement, a molecule of THF was located in the asymmetric unit; its site occupancy factor attained a final refined value of 0.984(7). Atoms of this occluded THF molecule were given anisotropic thermal parameters; hydrogen atoms associated with this molecule were not included in the final structural model.

All nonhydrogen atoms were refined with anisotropic thermal parameters. Hydrogen atoms bound to carbon were placed in idealized positions (C–H = 0.96 Å, $U_{iso}(H) = 1.2 \times U_{iso}(C)$). The weighted [$w = (\sigma^2(F) + g(F)^2)^{-1}$] least squares refinement on F yielded the residual values listed in Table 2.1 at convergence (for the last ten cycles, mean shift/e.s.d = 0.009, max shift/e.s.d. = 0.416 for rotation about y for the Cb4–Cbp bond). The height of the highest peak in the final ΔF map was +0.95 e Å^{-3} (near B2), while the minimum was –0.70 e Å^{-3}.

Results and Discussion

Each of the complex cations in **7**, **8**, and **9a** contains two five-coordinate copper(II) metal atoms. Two aspects of the coordination geometry about these metal atoms must be taken into account in deciding on the best description (square pyramidal or trigonal bipyramidal) of the coordination array in each case. Examination of the bond lengths and bond angles involving each copper(II) atom is the first step in this process. In idealized square pyramidal geometry, the bond from Cu(II) to the atom in the apical position is normally 0.2 – 0.4 Å longer than a similar bond in one of the four basal positions. In the idealized trigonal bipyramidal geometry, the Cu(II)–L(axial) bonds are usually 0.05 – 0.10 Å shorter than similar Cu(II)–L(equatorial) bonds.[73] The second step involves examination of the degree of planarity of various collections of ligand atoms. The presence of a highly planar group of four ligand atoms implies a square pyramidal geometry, while the presence of three ligand atoms coplanar with the copper(II) atom defines the equatorial plane of a trigonal bipyramidal coordination array.

The planarity of a group of atoms is normally discussed in terms of the least-squares plane through a set of four or more atoms; calculation of the equation for such a plane involves minimizing $\Sigma\Delta_m^2$ (where Δ_m is the perpendicular distance of the mth atom from the plane). The variance of the plane is calculated as $\sigma^2_{plane} = \Sigma\Delta^2/(m-3)$. The equation of such a plane takes the form $A(\sigma_A)x + B(\sigma_B)y + C(\sigma_C)z = D(\sigma_D)$ (where the σ_i are the estimated standard deviations in the coefficients A, B, C, and D). In all discussions presented in this work, A, B, C, and D refer to the crystallographic coordinate system. A small value for $\Sigma\Delta^2$ (and in turn σ^2_{plane}) indicates that the atoms in question do form are close to coplanar.

For five-coordinate systems, the labels **A** through **E** may be used to represent the five coordination sites about the central metal atom **M**. The coordination site **A** is chosen such that the two largest **M**-centered angles, designated α and β, are opposite the **M–A** bond. In this scheme, the angle β is assigned such that the value of β is greater than or equal to the value of α. Thus, the angles α and β are between sites **C** and **D**, and **B** and **E**, respectively (see below). These angles are sensitive indicators of whether the geometry is closer to square pyramidal or trigonal bipyramidal.[74]

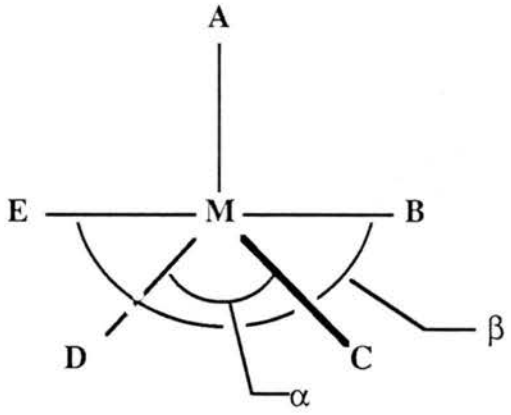

For ideally square pyramidal geometry, $\alpha = \beta = 180°$, whereas for ideally trigonal bipyramidal geometry, $\alpha = 120°$ and $\beta = 180°$. The ratio τ (where $\tau = (\beta - \alpha)/60$) can be used to assign the coordination geometry. For ideal square pyramidal geometry, τ is equal to zero, while τ equals one for idealized trigonal bipyramidal geometry. A listing of τ values for selected compounds, together with assignments of their coordination geometries, is given in Table 2.2.[75]

The pattern of the perpendicular deviations from the least-squares plane (Δ) can also provide information on the nature and distortion of the coordination geometry. In the scheme outlined above, the four coordination sites **B** through **E** can be used to calculate a

Table 2.2. τ values for selected copper(II) complexes.

compound	α	β	τ	assignment[a]	ref
$[Cu(\mathbf{1})OH_2]ClO_4$	174.1(3)	174.4(3)	0.005	sp	88
Ni(**2**)I	164.2(2)	166.6(2)	0.04	sp	89
$[Cu(\mathbf{2})OH_2]ClO_4$	160.9(4)	164.1(4)	0.05	sp	88
Cu(**2**)I	155.4(3)	158.4(3)	0.05	sp	90
$[Cu(BnAO)OH_2]^+$	163.4(2)	172.5(2)	0.15	distorted sp	106
$Ni(P(Ph)(OPh)_2)_3(CN)_2$	133.5	170.8	0.62	distorted tbp	109
[Cu(bipy)I]I	135.5(8)	174.7(10)	0.65	distorted tbp	108
$[Ni(TAP)CN]ClO_4$	120.3	178.4	0.97	tbp	107
$[CuCl_5]^{3-}$	120	180	1.00	regular tbp	73

[a] sp = square pyramidal
tbp = trigonal bypryamidal

potential square pyramidal basal plane. The average of the metal-centered angles between the four basal sites **B** through **E** and the apical site **A** for ideal square pyramidal geometry is 90°, while for trigonal bipyramidal geometry the average metal-centered angle between the equatorial site **A** and the remaining four sites would be 105°. As the ideal square pyramidal geometry distorts toward trigonal bipyramidal, one would expect two sites (**B** and **E**) to display perpendicular deviations from the potential basal plane which are opposite in direction from the deviations that are seen for **C** and **D.** Such a distortion is often referred to as a tetrahedral (T_d) distortion. Those atoms which deviate on the side of the central metal atom **M** would become the axial ligand atoms in the trigonal bipyramidal geometry, while those that deviate on the side away from **M** become equatorial ligand atoms of the trigonal bipyramid. The average of the three **M**-centered angles (**A–M–C**, **A–M–D**, and **C–M–D**) is 120° for ideal trigonal bipyramidal geometry. Thus, the set of three atoms with the average metal-centered angle between its members closest to the ideal value of 120° can be taken to define the equatorial plane of the trigonal bipyramidal.

The Structure of 7. The structure of $[Cu_2(N_6O)(\mu\text{-}1,3\text{-}N_3]^{2+}$, the cation of **7**, is plotted in Figure 2.1, while Figure 2.2 displays a closeup view of the primary coordination sphere. Tables 2.3, 2.4, and 2.5 contain atomic coordinates, bond lengths, and bond angles for **7**, respectively. Tables S-2.1 and S-2.2 (see the Appendix) contain the anisotropic thermal parameters and hydrogen atom coordinates for **7**.

The cation of **7** contains two five-coordinate copper(II) atoms, separated by 3.765(2) Å. The copper(II) atoms are simultaneously chelated by the binucleating ligand N_6O^- and coordinated to the terminal nitrogen atoms of the azido ligand. Bridging between the two copper(II) atoms is accomplished by the azido ligand (in the **EE** mode) and by the phenolate oxygen atom of the N_6O^- ligand.

To assign the coordination geometry about the copper(II) metal atoms, the structural evidence for both square pyramidal and trigonal bipyramidal coordination will be presented. The results will then be compared to previous work on structurally

Figure 2.1. Thermal ellipsoid plot (50% probability) of the cation of **7**, $\{Cu_2(N_6O)N_3\}^{2+}$. Hydrogen atoms have been omitted for clarity.

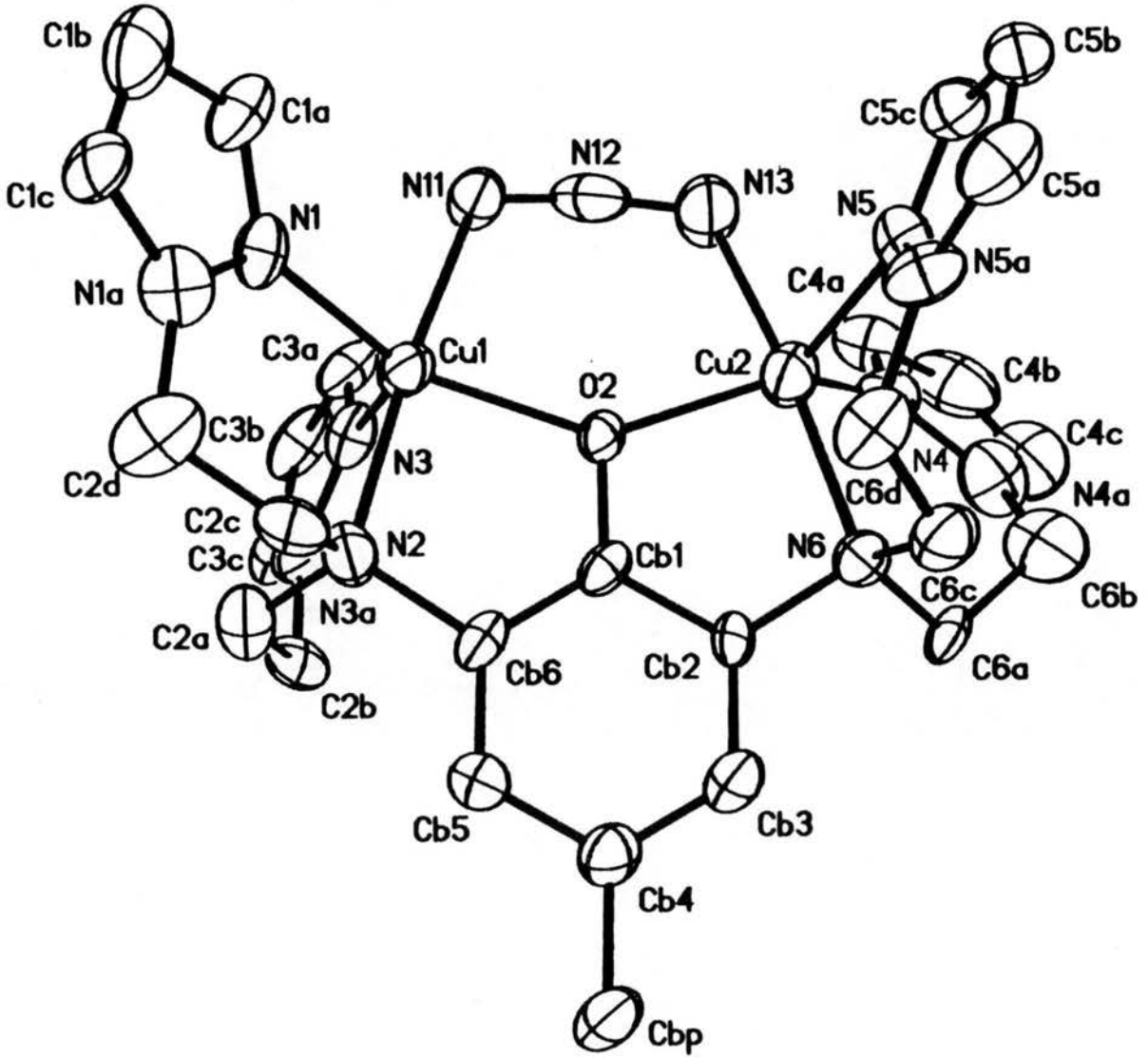
C1b
C1a
C1c
N1
N1a
C3a
Cu1
N11
N12
N13
O2
Cu2
C4a
N5
C5c
C5b
C5a
N5a
C4b
C4c
N4
N4a
C6d
C6c
C6b
C6a
N6
C3b
C2d
N3
C2c
C3c
N2
N3a
C2a
C2b
Cb1
Cb6
Cb2
Cb5
Cb3
Cb4
Cbp

Figure 2.2. Ball and stick plot of the primary coordination sphere of the copper(II) ions in $\{Cu_2(N_6O)N_3\}^{2+}$.

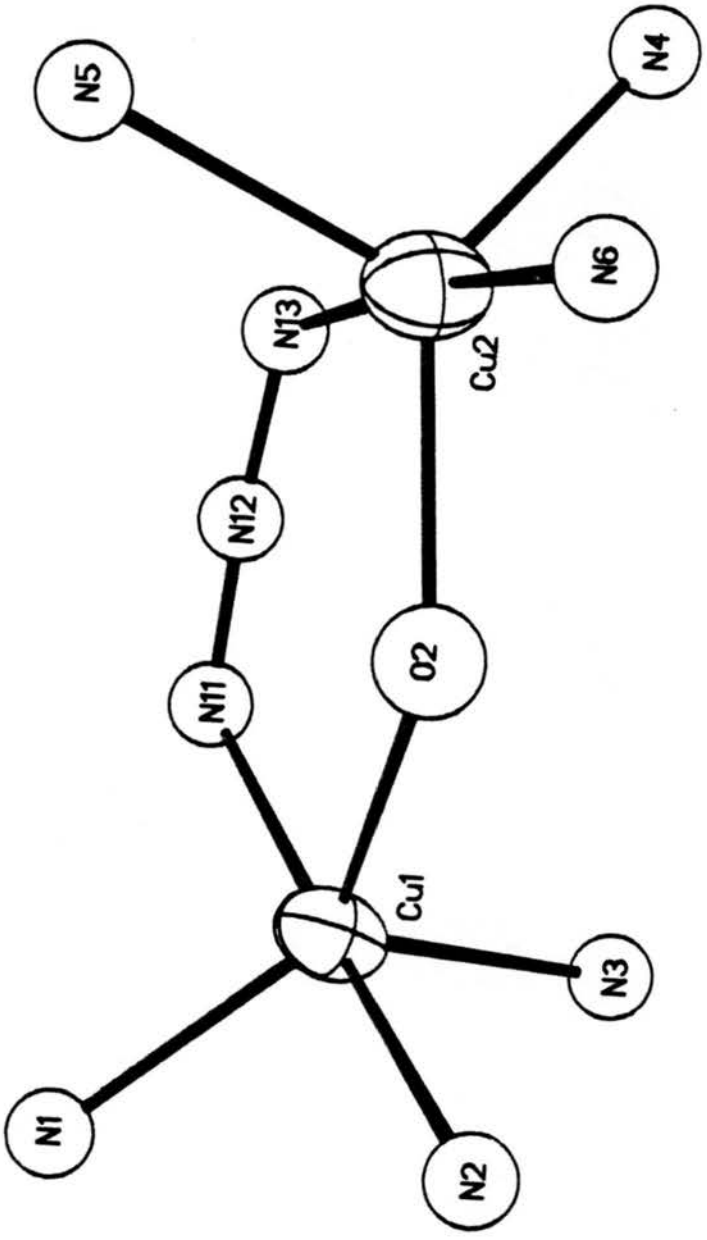
N5
N4
N6
N13
Cu2
N12
O2
N11
Cu1
N3
N1
N2

Table 2.3. Atomic coordinates ($\times 10^4$) and isotropic thermal parameters ($Å^2 \times 10^3$)[a] for **7**.

atom	*x*	*y*	*z*	U_{iso}[b]
Cu1	7152(1)	5760(1)	8706(1)	35(1)
Cu2	9798(1)	6213(1)	9348(1)	41(1)
Cu2'	9439(7)	5707(8)	9522(4)	2(3)
Cu1'	7331(17)	6082(16)	8426(10)	66(7)
O2	8662(4)	5559(4)	8864(3)	24(2)
N11	7128(7)	6920(6)	9297(4)	40(3)
N12	7930(8)	7132(6)	9488(4)	47(3)
N13	8797(7)	7269(7)	9642(5)	56(3)
N1	5805(6)	5296(6)	9054(4)	34(3)
N1a	5376(6)	4384(6)	8995(4)	41(3)
C1a	5255(7)	5766(9)	9473(5)	47(4)
C1b	4461(8)	5153(10)	9679(6)	61(5)
C1c	4569(7)	4290(9)	9362(4)	46(4)
N3	7049(6)	6834(6)	7976(4)	38(3)
N3a	7086(6)	6573(6)	7370(4)	38(3)
C3a	6837(7)	7794(8)	8000(5)	41(4)
C3b	6757(8)	8194(8)	7414(5)	49(4)
C3c	6931(7)	7389(8)	7048(5)	47(4)
N2	7296(6)	4549(6)	8139(4)	42(3)
C2a	6838(8)	4742(7)	7550(5)	42(4)
C2b	7371(8)	5527(6)	7188(4)	35(3)
C2c	6787(7)	3633(6)	8445(4)	36(3)
C2d	5687(8)	3722(7)	8543(5)	54(4)
N4	10774(7)	7348(7)	9179(3)	42(3)
N4a	11827(7)	7226(7)	9061(4)	53(3)
C4a	10635(10)	8331(8)	9149(5)	51(4)
C4b	11535(12)	8849(11)	9026(5)	71(5)
C4c	12222(12)	8117(10)	8996(6)	71(5)
N5	9966(6)	5701(6)	10254(3)	33(3)
N5a	10027(7)	4713(6)	10372(4)	41(3)
C5a	10066(8)	4560(8)	10964(5)	50(4)
C5b	9993(7)	5462(8)	11243(5)	46(4)
C5c	9921(7)	6187(7)	10784(4)	38(3)
N6	10728(6)	5053(6)	8998(4)	35(3)
C6a	11705(6)	5486(7)	8713(4)	30(3)
C6b	12217(9)	6270(9)	9106(5)	66(5)
C6c	10998(8)	4301(8)	9455(5)	45(4)
C6d	10094(8)	3982(7)	9843(5)	42(3)
Cb1	9043(6)	4841(7)	8498(4)	26(3)
Cb2	10092(7)	4568(7)	8524(4)	30(3)
Cb3	10458(7)	3822(8)	8138(5)	45(4)
Cb4	9833(8)	3353(7)	7725(4)	37(3)
Cb5	8787(7)	3591(6)	7707(4)	29(3)
Cb6	8422(6)	4341(7)	8084(4)	28(3)
Cbp	10233(8)	2507(9)	7309(5)	55(4)
Cl1	3973(2)	6489(2)	7731(1)	39(1)
O1	4583(6)	6594(7)	7206(4)	81(3)
O3	4290(7)	7242(6)	8152(4)	81(3)

Table 2.3. (continued)

atom	*x*	*y*	*z*	U_{iso}[b]
O4	4136(6)	5523(5)	7988(4)	72(3)
O5	1661(8)	2129(8)	10104(4)	105(4)
C12	2296(2)	1633(2)	9669(1)	53(1)
O6	2618(7)	726(7)	9947(5)	107(4)
O7	1647(6)	1467(7)	9146(4)	86(4)
O8	3143(6)	2232(6)	9500(4)	71(3)
O9	2911(6)	6605(6)	7588(4)	76(3)
O10	7860(10)	10045(10)	9146(4)	168(5)
C30	7893(11)	11101(10)	9131(8)	127(6)
C40	8921(11)	11418(11)	8874(7)	116(6)
C60	8400(11)	9867(10)	8609(8)	171(9)
C50	9233(11)	10602(10)	8389(8)	173(9)

[a] Estimated standard deviations in the least significant digits are given in parentheses.

[b] Equivalent isotropic U for anisotropic atoms is defined as one-third the trace of the orthogonalized U_{ij} tensor.

Table 2.4. Bond lengths (Å)[a] for **7**.

Cu1–Cu1'	0.782(22)	Cu1–O2	2.011(5)
Cu1–N11	2.008(8)	Cu1–N1	2.006(8)
Cu1–N3	2.145(8)	Cu1–N2	2.034(8)
Cu2–Cu2'	0.899(10)	Cu2–O2	2.013(6)
Cu2–N13	2.012(9)	Cu2–N4	1.998(9)
Cu2–N5	2.114(8)	Cu2–N6	2.096(8)
Cu2'–O2	1.774(11)	Cu2'–N5	1.750(12)
Cu1'–O2	2.097(22)	Cu1'–N3	1.449(23)
Cu1'–N2	2.119(23)	O2–Cb1	1.339(10)
N11–N12	1.158(13)	N12–N13	1.191(13)
N1–N1a	1.331(11)	N1–C1a	1.321(13)
N1a–C1c	1.328(13)	N1a–C2d	1.384(14)
C1a–C1b	1.386(16)	C1b–C1c	1.342(17)
N3–N3a	1.377(12)	N3–C3a	1.295(13)
N3a–C3c	1.303(14)	N3a–C2b	1.483(12)
C3a–C3b	1.398(16)	C3b–C3c	1.352(16)
N2–C2a	1.449(14)	N2–C2c	1.533(12)
N2–Cb6	1.493(11)	C2a–C2b	1.478(13)
C2c–C2d	1.450(15)	N4–N4a	1.401(13)
N4–C4a	1.309(14)	N4a–C4c	1.290(16)
N4a–C6b	1.362(15)	C4a–C4b	1.381(19)
C4b–C4c	1.316(21)	N5–N5a	1.331(11)
N5–C5c	1.331(12)	N5a–C5a	1.319(15)
N5a–C6d	1.513(13)	C5a–C5b	1.341(15)
C5b–C5c	1.393(14)	N6–C6a	1.526(11)
N6–C6c	1.454(13)	N6–Cb2	1.475(12)
C6a–C6b	1.503(15)	C6c–C6d	1.512(14)
Cb1–Cb2	1.411(12)	Cb1–Cb6	1.384(12)
Cb2–Cb3	1.383(14)	Cb3–Cb4	1.367(14)
Cb4–Cb5	1.396(13)	Cb4–Cbp	1.533(15)
Cb5–Cb6	1.376(13)	Cl1–O1	1.406(8)
Cl1–O3	1.418(8)	Cl1–O4	1.411(8)
Cl1–O9	1.423(8)	Cl2–O5	1.422(10)
Cl2–O6	1.407(10)	Cl2–O7	1.444(9)
Cl2–O8	1.406(8)	O10–C30	1.393(19)
O10–C60	1.393(20)	C30–C40	1.510(21)
C40–C50	1.567(22)	C60–C50	1.530(21)

[a] Estimated standard deviations in the least significant digits are given in parentheses.

Table 2.5. Bond angles (deg)[a] for **7**.

Cu1'–Cu1–O2	85.3(16)	Cu1'–Cu1–N11	95.6(16)
O2–Cu1–N11	90.1(3)	Cu1'–Cu1–N1	136.5(16)
O2–Cu1–N1	138.2(3)	N11–Cu1–N1	88.4(3)
Cu1'–Cu1–N3	21.9(16)	O2–Cu1–N3	106.1(3)
N11–Cu1–N3	88.9(3)	N1–Cu1–N3	115.6(3)
Cu1'–Cu1–N2	85.3(16)	O2–Cu1–N2	85.0(3)
N11–Cu1–N2	175.0(3)	N1–Cu1–N2	94.3(3)
N3–Cu1–N2	93.8(3)	Cu2'–Cu2–O2	61.8(6)
Cu2'–Cu2–N13	92.4(7)	O2–Cu2–N13	89.5(3)
Cu2'–Cu2–N4	164.7(6)	O2–Cu2–N4	133.5(3)
N13–Cu2–N4	87.2(4)	Cu2'–Cu2–N5	54.3(6)
O2–Cu2–N5	115.9(3)	N13–Cu2–N5	89.2(4)
N4–Cu2–N5	110.4(3)	Cu2'–Cu2–N6	85.1(7)
O2–Cu2–N6	85.2(3)	N13–Cu2–N6	174.8(4)
N4–Cu2–N6	96.4(3)	N5–Cu2–N6	93.1(3)
Cu2–Cu2'–O2	91.7(7)	Cu2–Cu2'–N5	101.0(8)
O2–Cu2'–N5	166.5(7)	Cu1–Cu1'–O2	72.9(15)
Cu1–Cu1'–N3	146.5(24)	O2–Cu1'–N3	138.4(14)
Cu1–Cu1'–N2	73.1(15)	O2–Cu1'–N2	80.8(8)
N3–Cu1'N2	116.4(13)	Cu1–O2–Cu2	138.7(3)
Cu1–O2–Cu2'	133.0(4)	Cu2–O2–Cu2'	26.5(3)
Cu1–O2–Cu1'	21.8(6)	Cu2–O2–Cu1'	135.0(6)
Cu2'–O2–Cu1'	143.9(7)	Cu1–O2–Cb1	110.5(5)
Cu2–O2–Cb1	110.4(5)	Cu2'–O2–Cb1	111.0(6)
Cu1'–O2–Cb1	105.2(8)	Cu1–N11–N12	113.9(7)
N11–N12–N13	172.6(10)	Cu2–N13–N12	114.6(7)
Cu1–N1–N1a	127.1(6)	Cu1–N1–C1a	126.5(7)
N1a–N1–C1a	105.3(8)	N1–N1a–C1c	110.9(8)
N1–N1a–C2d	121.1(8)	C1c–N1a–C2d	127.4(9)
N1–C1a–C1b	110.9(10)	C1a–C1b–C1c	104.3(10)
N1a–C1c–C1b	108.6(10)	Cu1–N3–Cu1'	11.6(9)
Cu1–N3–N3a	123.8(6)	Cu1'–N3–N3a	118.8(11)
Cu1–N3–C3a	128.8(7)	Cu1'–N3–C3a	133.9(12)
N3a–N3–C3a	107.0(8)	N3–N3a–C3c	108.3(8)
N3–N3a–C2b	120.2(7)	C3c–N3a–C2b	131.2(8)
N3–C3a–C3b	110.3(9)	C3a–C3b–C3c	103.9(9)
N3a–C3c–C3b	110.5(10)	Cu1–N2–Cu1'	21.6(6)
Cu1–N2–C2a	111.8(6)	Cu1'–N2–C2a	96.2(8)
Cu1–N2–C2c	108.0(6)	Cu1'–N2–C2c	129.0(8)
C2a–N2–C2c	110.7(7)	Cu1–N2–Cb6	106.5(6)
Cu1'–N2–Cb6	100.3(8)	C2a–N2–Cb6	111.3(8)
C2c–N2–Cb6	108.3(7)	N2–C2a–C2b	114.3(8)
N3a–C2b–C2a	112.9(8)	N2–C2c–C2d	115.3(8)
N1a–C2d–C2c	116.4(9)	Cu2–N4–N4a	124.6(6)

Table 2.5. (continued)

Cu2–N4–C4a	131.5(8)	N4a–N4–C4a	103.8(9)
N4–N4a–C4c	107.7(10)	N4–N4a–C6b	117.1(9)
C4c–N4a–C6b	134.6(11)	N4–C4a–C4b	112.5(11)
C4a–C4b–C4c	102.8(13)	N4a–C4c–C4b	113.0(14)
Cu2–N5–Cu2'	24.7(3)	Cu2–N5–N5a	120.1(6)
Cu2'–N5–N5a	101.9(7)	Cu2–N5–C5c	131.9(6)
Cu2'–N5–C5c	141.8(8)	N5a–N5–C5c	107.6(8)
N5–N5a–C5a	110.1(8)	N5–N5a–C6d	118.5(8)
C5a–N5a–C6d	131.2(8)	N5a–C5a–C5b	108.3(9)
C5a–C5b–C5c	106.4(9)	N5–C5c–C5b	107.5(8)
Cu2–N6–C6a	111.0(5)	Cu2–N6–C6c	112.5(6)
C6a–N6–C6c	109.7(7)	Cu2–N6–Cb2	104.6(5)
C6a–N6–Cb2	109.8(7)	C6c–N6–Cb2	109.1(7)
N6–C6a–C6b	112.9(8)	N4a–C6b–C6a	115.5(9)
N6–C6c–C6d	113.1(8)	N5a–C6d–C6c	107.6(8)
O2–Cb1–Cb2	120.9(8)	O2–Cb1–Cb6	121.1(7)
Cb2–Cb1–Cb6	118.0(8)	N6–Cb2–Cb1	117.3(8)
N6–Cb2–Cb3	123.3(8)	Cb1–Cb2–Cb3	119.2(8)
Cb2–Cb3–Cb4	121.7(9)	Cb3–Cb4–Cb5	119.7(9)
Cb3–Cb4–Cbp	121.7(9)	Cb5–Cb4–Cbp	118.5(9)
Cb4–Cb5–Cb6	118.7(8)	N2–Cb6–Cb1	115.6(8)
N2–Cb6–Cb5	121.3(8)	Cb1–Cb6–Cb5	122.5(8)
O1–Cl1–O3	107.7(5)	O1–Cl1–O4	109.4(5)
O3–Cl1–O4	109.0(5)	O1–Cl1–O9	110.8(5)
O3–Cl1–O9	110.5(5)	O4–Cl1–O9	109.3(5)
O5–Cl2–O6	105.8(6)	O5–Cl2–O7	105.4(5)
O6–C12–O7	113.1(6)	O5–C12–O8	112.0(6)
O6–Cl2–O8	111.1(5)	O7–Cl2–O8	109.3(5)
C30–O10–C60	97.7(11)	O10–C30–C40	108.3(12)
C30–C40–C50	107.0(12)	O10–C60–C50	121.1(13)
C40–C50–C60	92.2(12)		

[a] Estimated standard deviations in the least significant digits are given in parentheses.

characterized square pyramidal and trigonal bipyramidal copper(II) coordination compounds. Because the copper(II) atoms in **7** (Cu1 and Cu2) are crystallographically independent they will be reviewed separately.

The structural evidence with respect to square pyramidal coordination geometry about Cu1 may be summarized as follows. The longest bond between Cu1 and the five coordinated atoms is Cu1–N3(pyrazole) (2.145(8) Å). The four remaining ligand atoms form significantly shorter bonds to Cu1 (Cu1–N1(pyrazole), 2.006(8) Å; Cu1–N2(amine), 2.034(8) Å; Cu1–N11(azido), 2.008(8) Å; Cu1–O2, 2.011(5) Å). The two largest metal-centered angles are found opposite the Cu1–N3 bond, and are assigned as α (O2–Cu1–N1 = 138.2(3)°) and β (N2–Cu1–N11 = 175.0(3)°). The value of $\Sigma\Delta^2$ for the plane formed by the atoms O2, N1, N2, and N11 is 0.441 (see Appendix, Table S-2.3). The set of atoms O2, N1, N2, and N11 are not planar within experimental error. In fact, the four atoms are tetrahedrally distorted from the above least-squares plane, with the atoms O2 and N1 above the plane by 0.3 Å and the atoms N2 and N11 below the plane by 0.3 Å (and on the same side of the plane as Cu1). The average of the four metal-centered angles involving N3 is 101.1°.

The structural evidence for trigonal bipyramidal geometry about Cu1 may be summarized as follows. The three atoms (N1, N3, and O2) which formed metal-centered angles with an average closest to the ideal value of 120° (see reference 73 and discussion above) were chosen to be the atoms that defined the equatorial plane. Cu1 is nearly coplanar with those three ligand atoms. (see Appendix Table S-2.3). The value of $\Sigma\Delta^2$ for the plane formed by the atoms O2, N1, N3, and Cu1 is 0.0007. The metal-centered angles involving O2, N1, and N3 range from 138.2(3)° (O2–Cu1–N1) to 106.1(3)° (N1–Cu1–O2). With this assignment of the equatorial ligand atoms, N11 and N2 would be the axial ligand atoms; the angle N11–Cu1–N2 (175.0(3)°) is close to the ideal value of 180°.

The Cu1–N2(amine) bond length (2.034(8) Å) is significantly longer than Cu1–N11(azido) (2.008(8) Å), but is shorter than typical basal copper(II)–N(amine) distances seen in square pyramidal copper(II) complexes ($Cu(II)–N(amine)_{ave}$ = 2.06 Å).[52,53,56,58,69,76] In fact, the Cu1–N2 bond length is very similar to Cu(II)–N(amine) bond lengths in trigonal bipyramidal complexes ($Cu(II)–N(amine)_{ave}$ = 2.03 Å).[52,53,56] The Cu1–N11(azido) bond is significantly shorter than the basal Cu(II)–N(azido) bond (2.08(1) Å) in the compound Cu_2[N,N,N',N',-tetrakis(2-(1-ethylbenzimidazolyl))-2-hydroxo-1,3-diaminopropano)(μ-N_3)]$(BF_4)_2$. This compound contained a dimeric copper(II) complex cation in which the copper(II) atoms were bridged by an **EE** azido ligand.[54] The Cu1–O2 bond (2.011(5) Å) in **7** is significantly longer than basal Cu(II)–O(phenoxo) bonds ($Cu(II)–O(phenoxo)_{ave}$ = 1.946 Å),[52,56,58,62] but equivalent in length to equatorial Cu(II)–O(phenoxo) bonds ($Cu(II)–O(phenoxo)_{ave}$ = 2.009 Å).[52,53,56] The Cu1–N1(pyrazole) bond (2.006(8) Å) is significantly longer than the basal Cu(II)–N(pyrazole) bond reported for **9b** (1.959(10) Å),[52] and is equivalent in length to the equatorial Cu(II)–N(pyrazole) bonds found in the acetato compound (2.007(8) Å and 2.004(9) Å)[9] and in **9b** (2.002(8) Å)[52]. The bond length pattern about Cu1 most closely resembles that characteristic of trigonal bipyramidal copper(II) complexes.

The τ value for the coordination sphere about Cu1 (τ = 0.61 for α =138.2(3)°, O2–Cu1–N3; β = 175.0(3)°, N2–Cu1–N11) is closer to the ideal trigonal bipyramidal value than to the square pyramidal value. Based on this τ value, the least squares planes, and the bond lengths and angles about the metal ion, the coordination geometry about Cu1 is best described as distorted trigonal bipyramidal. The axial sites are occupied by an azido nitrogen atom (N11) and an amine nitrogen atom (N2), while the equatorial sites are occupied by the two pyrazole nitrogen atoms (N1, N3) and the oxygen atom (O2) of the bridging phenoxo group.

The structural evidence for square pyramidal coordination geometry about Cu2 may be summarized as follows. The longest bond formed between Cu2 and the five ligand

atoms is Cu2–N5(pyrazole) (2.114(8) Å). The four remaining ligand atoms form significantly shorter bonds to Cu2 (Cu2–O2, 2.013(6) Å; Cu2–N13(azido), 2.012(9) Å; Cu2–N4(pyrazole), 1.998(9) Å; Cu2–N6(amine), 2.096(8) Å). The two largest metal-centered angles are opposite the Cu2–N5 bond and are assigned as α (O2–Cu2–N4 = 133.5(3)°) and β (N13–Cu2–N6 = 174.8(4)°). The value of $\Sigma\Delta^2$ for the plane formed by the atoms O2, N13, N6, and N4 is 0.570 (see Appendix, Table S-2.3). These four atoms are not planar within experimental error. Just like those about Cu1, the four atoms are tetrahedrally distorted from the least-squares plane, with the atoms O2 and N4 above the plane by 0.3 Å and the atoms N6 and N11 below the plane by 0.3 Å on the same side as Cu2. The average of the four metal-centered angles involving N5 is 102.1°.

The structural evidence for trigonal bipyramidal geometry about Cu2 is more compelling. The three atoms which formed metal-centered angles with an average closest to the ideal value of 120° (N4, N5, and O2) were chosen as the equatorial atoms. Cu2 is nearly coplanar with those three ligand atoms (see Appendix, Table S-2.3). The value of $\Sigma\Delta^2$ for the plane formed by the atoms O2, N4, N5, and Cu2 is 0.0018. The metal-centered angles involving O2, N4, and N5 range from 133.5(3)° (O2–Cu2–N4) to 110.4(3)° (N4–Cu2–O5). With this assignment of the equatorial atoms, N6 and N13 would be axial ligands; the angle N13–Cu2–N6 equals 174.8(3)°.

The Cu2–N6(amine) bond (2.096(8) Å) is significantly longer than Cu2–N13(azido) (2.012(9) Å), and is similar to typical basal copper(II)–N(amine) bonds seen for square pyramidal copper(II) complexes ($Cu(II)–N(aliphatic)_{ave}$ = 2.06 Å).[52,53,56,58,69,76] The Cu2–N13(azido) bond is equal to the Cu1–N11(azido) bond in length, and the Cu2–O2 bond (2.013(6) Å) is identical to Cu1–O2 in length within experimental error. The Cu2–N4(pyrazole) bond (1.998(9) Å) also exhibits the same length as the Cu1–N1 bond (2.006(8) Å). As was the case for Cu1, the bond lengths and angles about Cu2 most closely resemble those characteristic of trigonal bipyramidal copper(II) complexes.

The τ value for the coordination sphere about Cu2 (τ = 0.69 for α =133.5(3)°, O2–Cu2–N4; β = 174.8(3)°, N6–Cu2–N13) is also closer to the ideal trigonal bipyramidal value. Based on the τ value, the quality of the least-squares planes, and the bond lengths and angles about the metal atom, the coordination geometry about Cu2 is best described as distorted trigonal bipyramidal. The axial sites are occupied by an azido nitrogen atom (N13) and an amine nitrogen atom (N6), while the equatorial sites are occupied by the two pyrazole nitrogen atoms (N4, N5) and the oxygen atom (O2) of the bridging phenoxo group.

In idealized trigonal bipyramidal coordination, the d_z2 orbital of a d^9 metal is expected to contain the unpaired electron density. For the unpaired electron on one metal center to be able to couple to the unpaired electron on the adjacent metal center through a bridging ligand, the d_z2 orbitals on each metal atom must be nonorthogonal to the appropriate orbitals of the ligand; *i.e.*, the orientation of the metal d_z2 orbitals must be such as to allow for overlap with the appropriate orbitals of the bridging ligand or ligands.

The geometry of each copper(II) coordination site in the cation of **7** would position the copper(II) d_z2 orbital, which contains the unpaired electron, in such a way as to promote overlap with the orbitals of the azido ligand. In fact it appears that a major lobe of the d_z2 orbital on each metal atom would overlap with a π^* orbital of the bridging azido ligand. Likewise, the minor lobe of each d_z2 orbital would overlap the p_x orbital of the bridging phenoxo oxygen atom. However, the magnetic coupling through the phenoxo oxygen atom should be much smaller than the interaction through the azide group, as a result of the smaller degree of overlap of the minor lobes of the d_z2 orbitals with the phenoxo oxygen p_x orbital.[53,54]

It is of interest to compare the structure of the cation of **7** with the previously reported structures of the cations $[Cu_2(N_6O)OAc]^{2+}$ and Cu_2[N,N,N',N',-tetrakis(2-(1-ethylbenzimidazolyl))-2-hydroxo-1,3-diaminopropane)(μ-N_3)]$^{2+}$. In each of these three cations the copper(II) atoms are held more than 3.5 Å apart.[53,54] Each cation contains two

copper(II) atoms that are bridged by an oxygen atom from a phenoxo or alkoxo group and by an **EE** bound azide anion or by an acetate anion. For the two azido derivatives, the magnetic coupling between the copper(II) atoms is strong ($2J$ values < -1000 cm^{-1}) while for the acetato derivative there is no noticeable interaction. The coordination geometry for all copper(II) atoms in these cations is trigonal bipyramidal, with the axial positions occupied by amine nitrogen atoms and nitrogen or oxygen atoms of the azido or acetato bridging ligands. It is clear from these results that the azido ligand is a much better mediator for magnetic coupling than the acetato ligand. The results also indicate that magnetic coupling pathways through the azido ligand are of major importance in distorted trigonal bipyramidal structures in which the azido nitrogen atoms occupy axial sites.

The Structure of 8. The structure of $[Cu_2(N_6'O)(\mu\text{-}1,1\text{-}N_3)]^{2+}$, the cation of **8**, is displayed in Figure 2.3, while Figure 2.4 displays a closeup view of the primary coordination sphere. Tables 2.6, 2.7, and 2.8 contain the atomic coordinates, bond lengths, and bond angles for **8**, respectively. Tables of anisotropic thermal parameters and hydrogen atom coordinates for **8** can be found in the Appendix as Tables S-2.4 and S-2.5.

The cation of **8** contains two copper(II) atoms separated by 3.146(2) Å, a distance which is dramatically shorter than the Cu–Cu separation in the cation of **7** (3.765(2) Å). The copper(II) atoms are simultaneously chelated by the binucleating ligand $N_6'O^-$ and coordinated to one of the terminal nitrogen atoms (N11) of the azido ligand. In this case, bridging between the copper atoms is accomplished by the azido ligand (in the **EO** mode) and by the phenoxo oxygen atom of the $N_6'O^-$ ligand.

As was done for the cation of **7**, the assignment of the coordination geometries of the copper(II) atoms in **8** will be based upon the examination of the structural parameters which would characterize a square pyramid or a trigonal bipyramid. Since the two copper(II) atoms in **8** (Cu1, Cu2) are crystallographically independent, they will be reviewed separately.

Figure 2.3. Thermal ellipsoid plot (20% probability) of the cation of **8**, $\{Cu_2(N_6'O)N_3\}^{2+}$. Hydrogen atoms have been omitted for clarity.

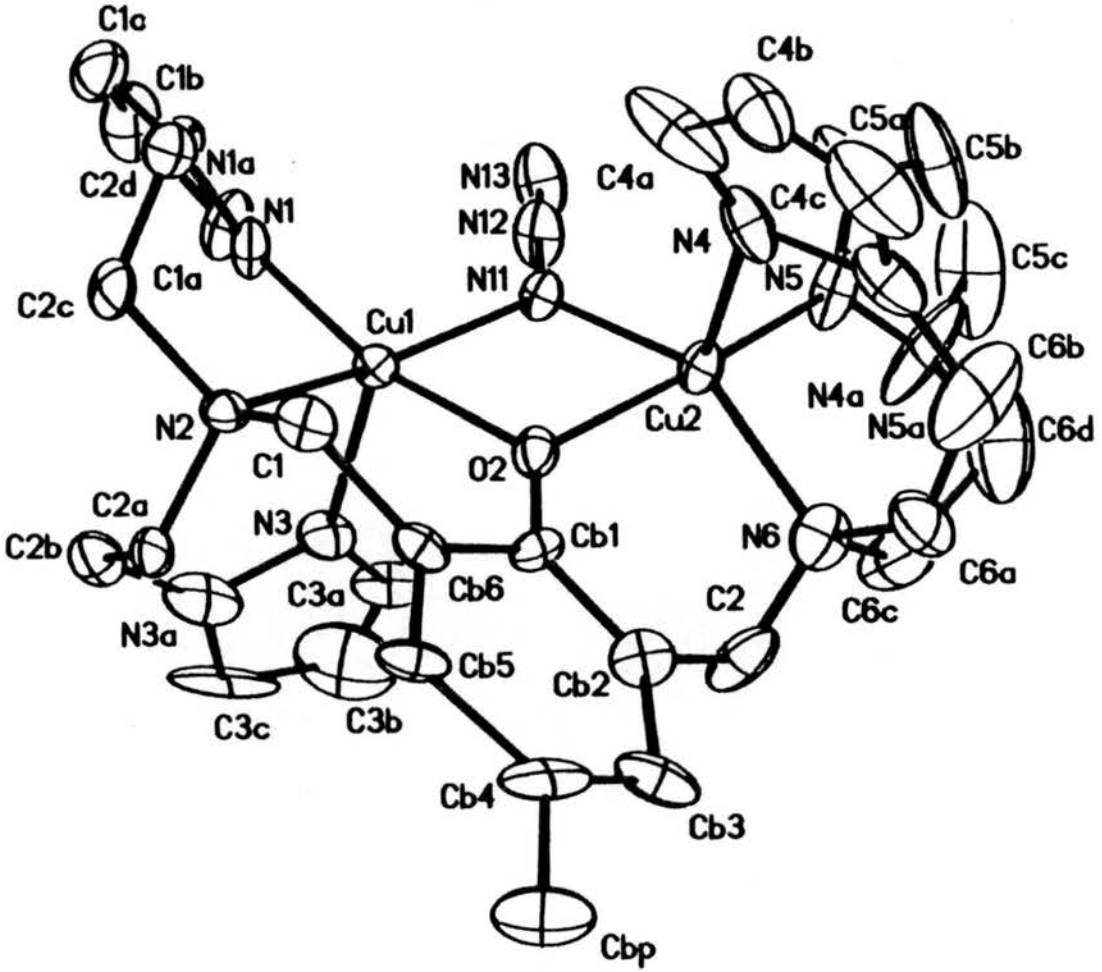
C1a
C1b
N1a
C2d
N1
C1a
C2c
Cu1
N2
C1
C2a
C2b
N3
C3a
N3a
C3c
C3b
Cb6
Cb5
Cb4
Cbp
Cb3
Cb2
Cb1
O2
N13
N12
N11
C4a
C4b
C5a
C5b
C4c
N4
N5
C5c
C6b
N4a
N5a
C6d
Cu2
N6
C6a
C6c
C2

Figure 2.4. Ball and stick plot of the primary coordination sphere of the copper(II) ions in $\{Cu_2(N_6'O)N_3\}^{2+}$.

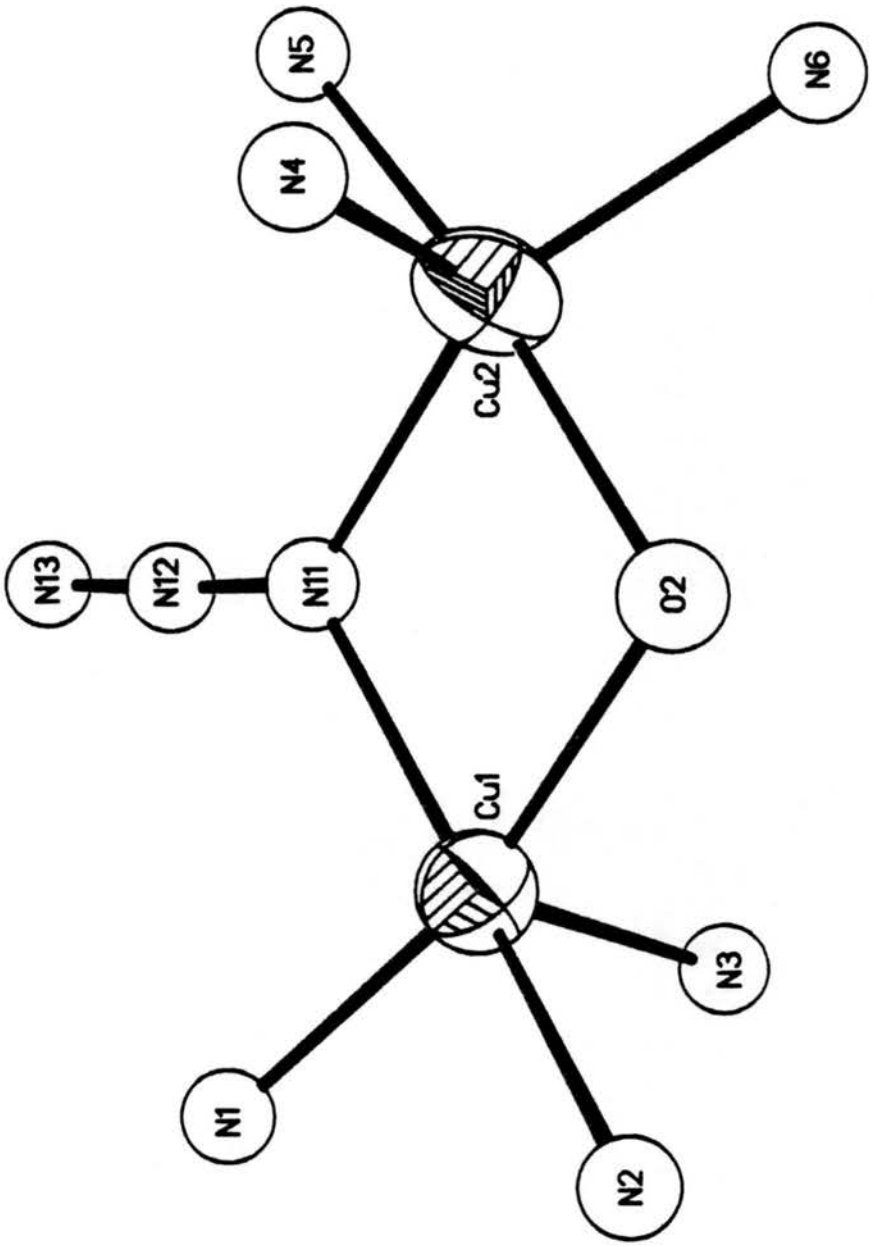
N5
N6
N4
Cu2
N13
N12
N11
O2
Cu1
N3
N1
N2

Table 2.6. Atomic coordinates ($\times 10^4$) and isotropic thermal parameters ($Å^2 \times 10^3$)[a] for **8**.

atom	*x*	*y*	*z*	U_{iso}[b]
Cu1	4822(6)	6257(1)	7861(1)	42(1)
Cu2	3844(6)	7805(1)	8485(1)	50(1)
N11	5118(11)	7455(6)	7873(4)	42(4)
N12	5853(15)	7818(7)	7589(6)	70(5)
N13	6644(16)	8186(9)	7335(8)	97(7)
O2	3794(12)	6640(5)	8502(4)	54(3)
N1	5704(16)	6084(7)	7140(5)	63(5)
N1a	4909(20)	5818(7)	6679(5)	77(5)
C1a	6833(20)	6264(11)	6931(8)	78(7)
C1b	6907(32)	6033(12)	6332(9)	127(12)
C1c	5635(26)	5759(10)	6204(8)	98(9)
N3	6488(13)	5829(8)	8339(5)	65(5)
N3a	6768(15)	5024(10)	8344(6)	90(6)
C3a	7391(15)	6240(16)	8626(8)	75(8)
C3b	8209(47)	5950(20)	8818(18)	183(22)
C3c	8097(23)	5145(22)	8668(9)	165(15)
N2	3877(13)	5155(6)	7822(4)	43(4)
C2a	4586(17)	4536(8)	8167(6)	54(6)
C2b	6006(18)	4458(10)	8035(7)	68(7)
C2c	3678(19)	4864(8)	7217(5)	60(6)
C2d	3663(22)	5513(9)	6800(7)	77(7)
N4	1918(14)	7905(7)	8134(8)	76(6)
N4a	968(18)	8216(8)	8601(7)	90(7)
C4a	1297(25)	7616(12)	7720(15)	149(15)
C4b	−144(28)	7640(10)	7873(9)	95(8)
C4c	−214(26)	7999(11)	8304(12)	139(12)
N5	4327(14)	8934(8)	8424(6)	82(6)
N5a	4806(33)	9391(14)	8816(8)	208(14)
C5a	4386(18)	9440(11)	7991(14)	135(12)
C5b	4938(36)	10132(12)	8089(15)	189(16)
C5c	5098(31)	10117(14)	8559(15)	225(19)
N6	3472(15)	7856(9)	9326(6)	82(6)
C6a	2259(24)	8107(13)	9463(9)	108(10)
C6b	1404(23)	8387(26)	9128(11)	253(25)
C6c	4575(47)	8568(12)	9560(8)	223(22)
C6d	4274(30)	9434(13)	9291(14)	188(18)
C1	2515(14)	5258(8)	8066(6)	48(5)
C2	3769(26)	7154(11)	9612(6)	97(8)
Cb1	3101(13)	6213(9)	8867(5)	43(5)
Cb2	2993(14)	6435(10)	9426(7)	56(6)
Cb3	2303(18)	6025(11)	9837(8)	72(7)
Cb4	1643(16)	5327(14)	9639(7)	86(8)
Cb5	1749(15)	5029(9)	9042(6)	51(5)
Cb6	2478(14)	5494(8)	8676(6)	48(5)
Cbp	755(20)	4812(13)	10045(9)	93(8)
B1	8352(39)	2746(20)	8738(14)	219(22)

Table 2.6 (continued)

atom	*x*	*y*	*z*	U_{iso}[b]
F1	7254(18)	3136(8)	8939(5)	146(8)
F2	8458(38)	2077(8)	9026(8)	445(31)
F3	8395(25)	2564(13)	8238(7)	238(13)
F4	9473(25)	3253(15)	8853(22)	943(58)
B2	8010(34)	9451(24)	9615(15)	178(18)
F5	7267(19)	9289(13)	10072(6)	208(11)
F6	7774(25)	9000(9)	9172(8)	252(14)
F7	7415(26)	10173(12)	9521(10)	259(15)
F8	9230(18)	9476(17)	9799(11)	301(17)
O100	8207(11)	7108(17)	10977(4)	279(16)
C101	6974(7)	7092(35)	10604(6)	572(17)
C102	7459(11)	7030(22)	9992(4)	288(24)
C103	8901(11)	6778(19)	10033(6)	239(18)
C104	9200(8)	7101(18)	10630(6)	202(34)

[a] Estimated standard deviations in the least significant digits are given in parenthesis.

[b] Equivalent isotropic U for anisotropic atoms is defined as one-third the trace of the orthogonalized U_{ij} tensor.

Table 2.7. Bond lengths (Å)[a] for **8**.

Cu1–N11	2.027(10)	Cu1–O2	1.943(10)
Cu1–N1	1.940(14)	Cu1–N3	2.157(14)
Cu1–N2	2.082(12)	Cu2–N11	2.024(11)
Cu2–O2	1.950(9)	Cu2–N4	2.134(16)
Cu2–N5	1.958(14)	Cu2–N6	2.016(15)
N11–N12	1.172(18)	N12–N13	1.176(22)
O2–Cb1	1.321(16)	N1–N1a	1.424(20)
N1–C1a	1.286(25)	N1a–C1c	1.342(26)
N1a–C2d	1.397(29)	C1a–C1b	1.461(28)
C1b–C1c	1.407(40)	N3–N3a	1.376(21)
N3–C3a	1.332(24)	N3a–C3c	1.565(28)
N3a–C2b	1.424(23)	C3a–C3b	1.065(48)
C3b–C3c	1.397(50)	N2–C2a	1.501(18)
N2–C2c	1.516(16)	N2–C1	1.510(19)
C2a–C2b	1.484(25)	C2c–C2d	1.463(21)
N4–N4a	1.554(24)	N4–C4a	1.257(36)
N4a–C4c	1.438(33)	N4a–C6b	1.347(32)
C4a–C4b	1.511(38)	C4b–C4c	1.179(33)
N5–N5a	1.293(27)	N5–C5a	1.325(31)
N5a–C5c	1.388(35)	N5a–C6d	1.243(39)
C5a–C5b	1.307(31)	C5b–C5c	1.118(51)
N6–C6a	1.343(28)	N6–C2	1.388(23)
C6a–C6b	1.264(36)	C6c–C6d	1.611(32)
C1–Cb6	1.488(20)	C2–Cb2	1.503(26)
Cb1–Cb2	1.372(20)	Cb1–Cb6	1.432(20)
Cb2–Cb3	1.376(25)	Cb3–Cb4	1.425(29)
Cb4–Cb5	1.494(22)	Cb4–Cbp	1.572(28)
Cb5–Cb6	1.378(20)	B1–F1	1.377(41)
B1–F2	1.312(37)	B1–F3	1.217(38)
B1–F4	1.448(46)	B2–F5	1.341(39)
B2–F6	1.309(41)	B2–F7	1.369(45)
B2–F8	1.316(40)	O100–C101	1.531(15)
O100–C104	1.300(15)	C101–C102	1.524(17)
C102–C103	1.530(20)	C103–C104	1.533(24)

[a] Estimated standard deviations in the least significant digits are given in parenthesis.

Table 2.8. Bond angles (deg)[a] for **8**.

N11–Cu1–O2	75.1(4)	N11–Cu1–N1	95.2(5)
O2–Cu1–N1	167.4(5)	N11–Cu1–N3	101.8(5)
O2–Cu1–N3	97.4(5)	N1–Cu1–N3	92.4(6)
N11–Cu1–N2	160.9(6)	O2–Cu1–N2	94.4(5)
N1–Cu1–N2	92.5(5)	N3–Cu1–N2	95.3(5)
N11–Cu2–O2	75.1(4)	N11–Cu2–N4	109.7(6)
O2–Cu2–N4	93.6(5)	N11–Cu2–N5	93.8(5)
O2–Cu2–N5	166.6(6)	N4–Cu2–N5	97.2(5)
N11–Cu2–N6	146.2(6)	O2–Cu2–N6	91.0(5)
N4–Cu2–N6	101.7(7)	N5–Cu2–N6	94.4(6)
Cu1–N11–Cu2	101.6(5)	Cu1–N11–N12	126.9(10)
Cu2–N11–N12	131.6(10)	N11–N12–N13	175.6(18)
Cu1–O2–Cu2	107.4(5)	Cu1–O2–Cb1	127.9(8)
Cu2–O2–Cb1	124.6(9)	Cu1–N1–N1a	116.7(12)
Cu1–N1–C1a	135.5(12)	N1a–N1–C1a	106.9(14)
N1–N1a–C1c	110.1(18)	N1–N1a–C2d	118.3(12)
C1c–N1a–C2d	130.1(16)	N1–C1a–C1b	110.7(19)
C1a–C1b–C1c	104.1(21)	N1a–C1c–C1b	107.8(18)
Cu1–N3–N3a	119.5(10)	Cu1–N3–C3a	129.4(14)
N3a–N3–C3a	111.0(15)	N3–N3a–C3c	93.3(17)
N3–N3a–C2b	122.2(14)	C3c–N3a–C2b	143.6(19)
N3–C3a–C3b	121.3(30)	C3a–C3b–C3c	105.6(36)
N3a–C3c–C3b	108.5(28)	Cu1–N2–C2a	111.4(9)
Cu1–N2–C2c	112.8(8)	C2a–N2–C2c	110.4(10)
Cu1–N2–C1	107.9(8)	C2a–N2–C1	108.4(10)
C2c–N2–C1	105.7(12)	N2–C2a–C2b	114.6(13)
N3a–C2b–C2a	111.5(14)	N2–C2c–C2d	113.0(12)
N1a–C2d–C2c	113.5(16)	Cu2–N4–N4a	108.9(11)
Cu2–N4–C4a	137.0(15)	N4a–N4–C4a	111.3(17)
N4–N4a–C4c	95.3(15)	N4–N4a–C6b	121.1(18)
C4c–N4a–C6b	141.0(21)	N4–C4a–C4b	107.1(24)
C4a–C4b–C4c	106.1(25)	N4a–C4c–C4b	119.7(25)
Cu2–N5–N5a	127.8(14)	Cu2–N5–C5a	133.2(14)
N5a–N5–C5a	98.8(17)	N5–N5a–C5c	106.7(20)
N5–N5a–C6d	120.7(28)	C5c–N5a–C6d	115.7(24)
N5–C5a–C5b	116.7(28)	C5a–C5b–C5c	102.5(28)
N5a–C5c–C5b	114.8(25)	Cu2–N6–C6a	114.9(13)
Cu2–N6–C2	113.5(11)	C6a–N6–C2	110.4(17)
N6–C6a–C6b	126.9(22)	N4a–C6b–C6a	136.1(33)
N5a–C6d–C6c	102.6(22)	N2–C1–Cb6	114.8(11)
N6–C2–Cb2	114.9(17)	O2–Cb1–Cb2	121.3(13)
O2–Cb1–Cb6	119.2(11)	Cb2–Cb1–Cb6	119.5(13)
C2–Cb2–Cb1	117.0(14)	C2–Cb2–Cb3	117.6(15)
Cb1–Cb2–Cb3	125.3(15)	Cb2–Cb3–Cb4	114.9(16)
Cb3–Cb4–Cb5	123.0(16)	Cb3–Cb4–Cbp	121.5(16)
Cb5–Cb4–Cbp	115.4(17)	Cb4–Cb5–Cb6	116.0(14)
C1–Cb6–Cb1	120.9(12)	C1–Cb6–Cb5	117.8(12)
Cb1–Cb6–Cb5	121.1(13)	F1–B1–F2	107.1(29)

Table 2.8. (continued)

F1–B1–F3	118.6(31)	F2–B1–F3	106.4(28)
F1–B1–F4	107.4(26)	F2–B1–F4	109.8(33)
F3–B1–F4	107.3(35)	F5–B2–F6	114.7(30)
F5–B2–F7	93.4(26)	F6–B2–F7	107.4(28)
F5–B2–F8	106.0(38)	F6–B2–F8	116.9(31)
F7–B2–F8	116.2(32)	C101–O100–C104	106.1(9)
O100–C101–C102	106.1(7)	C101–C102–C103	105.6(11)
C102–C103–C104	98.7(14)	O100–C104–C103	115.1(12)

[a] Estimated standard deviations in the least significant digits are given in parenthesis.

The structural evidence for square pyramidal coordination geometry about Cu1 may be summarized as follows. The longest bond between Cu1 and the five ligand atoms is Cu1–N3(pyrazole) (2.157(14) Å). The four remaining coordinated atoms form significantly shorter bonds to Cu1 (Cu1–O2, 1.943(10) Å; Cu1–N11(azido), 2.024(11) Å; Cu1–N2(amine), 2.082(12) Å; Cu1–N1(pyrazole), 1.940(14) Å). The two largest metal-centered angles are found opposite the Cu1–N3 bond, and are assigned as α (N2–Cu1–N11 = 160.9(6)°) and β (N1–Cu1–O2 = 167.4(5)°). The value of $\Sigma\Delta^2$ for the plane formed by the atoms O2, N1, N2, and N11 is 0.019 (see Appendix, Table S-2.3). The average of the four metal-centered angles involving N3 is 96.7°.

The structural evidence for trigonal bipyramidal geometry about Cu1 is not as compelling. As was done previously, the equatorial ligand atoms were chosen to be those with metal-centered angles closest, on average, to the ideal value of 120°. N1, N2, and N11 were assigned as equatorial on this basis; Cu1 is nearly coplanar with these atoms (see Appendix, Table S-2.3). The orientation of this plane dictates that the axial sites be occupied by the phenoxo oxygen atom (O2) and by a pyrazole nitrogen atom (N3). The value of $\Sigma\Delta^2$ for the plane formed by the atoms N1, N2, N11 and Cu1 is 0.019.

The Cu1–N2(amine) bond (2.082(12) Å) is longer than the Cu1–N11(azido) bond (2.027(10) Å), but is similar to basal copper(II)–N(amine) bonds in square pyramidal copper(II) complexes (Cu(II)–N(amine)$_{ave}$ = 2.06 Å).[52,53,56,58,69,76] The Cu1–N2 bond length is significantly longer than other Cu(II)–N(aliphatic) bond lengths in trigonal bipyramidal complexes (Cu(II)–N(aliphatic)$_{ave}$ = 2.03Å),[52,53,56] The Cu1–N11 bond is significantly shorter than the basal Cu(II)–N(azido) bond (2.08(1) Å) in Cu_2[N,N,N',N',-tetrakis(2-(1-ethylbenzimidazolyl))-2-hydroxo-1,3-diaminopropane)(μ-N_3)](BF_4)$_2$ (**EE** azido ligand bridging),[54] and is similar in length to the basal Cu(II)–N(azido) bond (2.024(12) Å) reported in [Cu_2(*m*-xyl-py_2)(μ-1,1-N_3)]$^{2+}$ (**EO** azido ligand bridging).[58] The Cu1–O2 bond (1.943(10) Å) is not significantly longer than other basal Cu(II)–O(phenoxo) bonds (Cu(II)–O(phenoxo)$_{ave}$ = 1.946 Å),[52,56,58,62] but does differ

significantly in length from equatorial Cu(II)–O(phenoxo) bonds (Cu(II)–O(phenoxo)$_{ave}$ = 2.009 Å).[52,53,56] The Cu1–N1(pyrazole) bond (1.940(14) Å) is not different in length from basal Cu(II)–N(pyrazole) bonds reported for **9b** (1.959(10) Å),[53] but does differ in length from the equatorial Cu(II)–N(pyrazole) bonds found in the acetato compound (2.007(8) Å and 2.004(9) Å)[53] and in **9b** (2.002(8) Å)[52]. The bond length pattern about Cu1 most closely resembles that characteristic of square pyramidal copper(II) complexes.

The τ value for the coordination sphere about Cu1 (τ = 0.11 for α =160.9(6)°, N2–Cu1–N11; β = 167.4(5)°, O2–Cu1–N1) is very close to the ideal τ value for the square pyramidal. Based on this τ value, the least-squares planes, and the bond lengths and angles about Cu1, the coordination geometry about this metal atom is best described as slightly distorted square pyramidal. The apical site is occupied by a pyrazole nitrogen atom (N3), while the basal sites are occupied by a pyrazole nitrogen atom (N1), an amine nitrogen atom (N2), an azido nitrogen atom, and the oxygen atom (O2) of the bridging phenoxide group.

The structural evidence for square pyramidal coordination about Cu2 is as follows. The longest bond formed between Cu2 and the five coordinated atoms is Cu2–N4(pyrazole) (2.134(16) Å). The four remaining coordinated atoms form significantly shorter bonds to Cu2 (Cu2–O2, 1.950(9) Å; Cu2–N11(azido), 2.024(11) Å; Cu2–N6(amine), 2.016(15) Å; Cu2–N5(pyrazole), 1.958(14) Å). The two largest metal-centered angles are opposite the Cu2–N4 bond, and are assigned as α (N6–Cu2–N11 = 146.2(6)°) and β (N5–Cu2–O2 = 166.6(6)°). The value of $\Sigma\Delta^2$ for the plane formed by the atoms O2, N5, N6, and N11 is 0.143 (see Appendix, Table S-2.3).

The structural evidence for trigonal bipyramidal coordination about Cu2 is as follows. The three atoms (N11, N4, and N6) which formed metal-centered angles with an average value closest to the ideal value of 120° were assigned as the equatorial ligand atoms. Cu2 occupied a position very close to the plane of these atoms (see Appendix,

Table S-2.3). The orientation of this plane dictated that the axial sites be occupied by the phenoxo oxygen atom (O2) and a pyrazole nitrogen atom (N5).

The Cu2–N6(amine) bond (2.016(15) Å) is equivalent in length to the Cu1–N11(azido) bond (2.024(11) Å) bond. The Cu2–N6 bond is significantly different in length from Cu(II)–N(amine) bonds in trigonal bipyramidal complexes ($Cu(II)–N(amine)_{ave}$ = 2.03 Å).[52,53,56] The Cu2–N11 bond does not differ from the Cu1–N11 bond in length, but is significantly shorter than the basal Cu(II)–N(azido) bond (2.08(1) Å) in Cu_2[N,N,N',N',-tetrakis(2-(1-ethylbenzimidazolyl))-2-hydroxo-1,3-diaminopropane)(μ-N_3)](BF_4)$_2$ (**EE** azido ligand bridging)[54]. Cu2–N11 is equivalent in length to the basal Cu(II)–N(azido) bond (2.024(12) Å) in the compound [Cu_2(*m*-xyl-py_2)(μ-1,1-N_3)]$^{2+}$, in which the azido ligand bridges in the **EO** mode.[58] The Cu2–O2 bond (1.950(10) Å) does not differ significantly in length from the Cu1–O2 bond. The Cu2–N5(pyrazole) bond (1.958(14) Å) is equivalent in length to the basal Cu(II)–N(pyrazole) bond in **9b** (1.959(10) Å)[52], and is significantly shorter than the equatorial Cu(II)–N(pyrazole) bonds found in the acetato compound (2.007(8) Å and 2.004(9) Å)[53] and in **9b** (2.002(8) Å)[52]. Thus, the bond length pattern about Cu2 also most closely resembles that characteristic of square pyramidal copper(II) complexes.

The τ value for the coordination sphere about Cu2 (τ = 0.34 for α = 146.2(6)°, N6–Cu2–N11; β = 166.6(6)°, O2–Cu2–N5) is closer to the τ value characteristic of square pyramidal coordination than to that characteristic of trigonal bipyramidal coordination. As was the case for Cu1, the τ value, the least squares planes, and the bond lengths and bond angles for the coordination sphere indicate that the coordination geometry about Cu2 is best described as distorted square pyramidal. The apical site is occupied by a pyrazole nitrogen atom (N4), while the basal sites are occupied by a pyrazole nitrogen atom (N5), an amine nitrogen atom (N6), an azido nitrogen atom, and the oxygen atom of the bridging phenoxo group (O2).

In the case of square pyramidal coordination about copper(II), the metal $d_{x^2-y^2}$ orbital is expected to contain the unpaired electron density. In such square pyramidal systems, coupling of the unpaired electron on one Cu(II) atom to the unpaired electron on an adjacent Cu(II) through a bridging ligand must be achieved by overlap of the metal $d_{x^2-y^2}$ orbitals with appropriate orbitals of the bridging ligand or ligands.

The geometry about each metal atom in **8** would position the $d_{x^2-y^2}$ orbital on each copper(II) so as to promote overlap between the $d_{x^2-y^2}$ orbitals and orbitals of the bridging azido and phenoxo ligand atoms. In fact, it appears that lobes of a $d_{x^2-y^2}$ orbital would overlap with both the π^* orbital of the bridging azido ligand and a *p* orbital of the phenoxo oxygen atom.

The Structure of 9a. The structure of $[Cu_2(N_6'O)(\mu\text{-}OH)]^{2+}$, the cation of **9a**, is displayed in Figure 2.5, while Figure 2.6 displays a closeup view of the primary coordination sphere about the two copper(II) atoms. Tables 2.9, 2.10, and 2.11 contain atomic coordinates, bond lengths, and bond angles, respectively, for **9a**, . Tables of anisotropic thermal parameters and hydrogen atom coordinates can be found in the Appendix as Tables S-2.6 and S-2.7.

The $[Cu_2(N_6'O)(\mu\text{-}OH)]^{2+}$ cation contains two copper(II) atoms separated by 3.079(1) Å, a distance which is significantly shorter than the Cu–Cu distances in both **7** and **8**. The copper(II) atoms are simultaneously chelated by the binucleating ligand $N_6'O^-$ and coordinated the bridging hydroxo ligand, as well as to the phenoxide oxygen atom of the $N_6'O^-$ species.

As usual, assignment of the coordination geometries for the copper(II) atoms will be accomplished by comparison of the structural parameters characteristic of **9a** with those of ideal square pyramids or trigonal bipyramids. Again, since the two copper(II) atoms in **9a** (Cu1, Cu2) are crystallographically independent they must be discussed separately.

The structural evidence for square pyramidal coordination about Cu1 is as follows. The longest metal–ligand bond is Cu1–N3(pyrazole) (2.099(6) Å). The four remaining

Figure 2.5. Thermal ellipsoid plot (50% probability) of the cation of **9a**, $\{Cu_2(N_6'O)OH\}^{2+}$. Hydrogen atoms have been omitted for clarity.

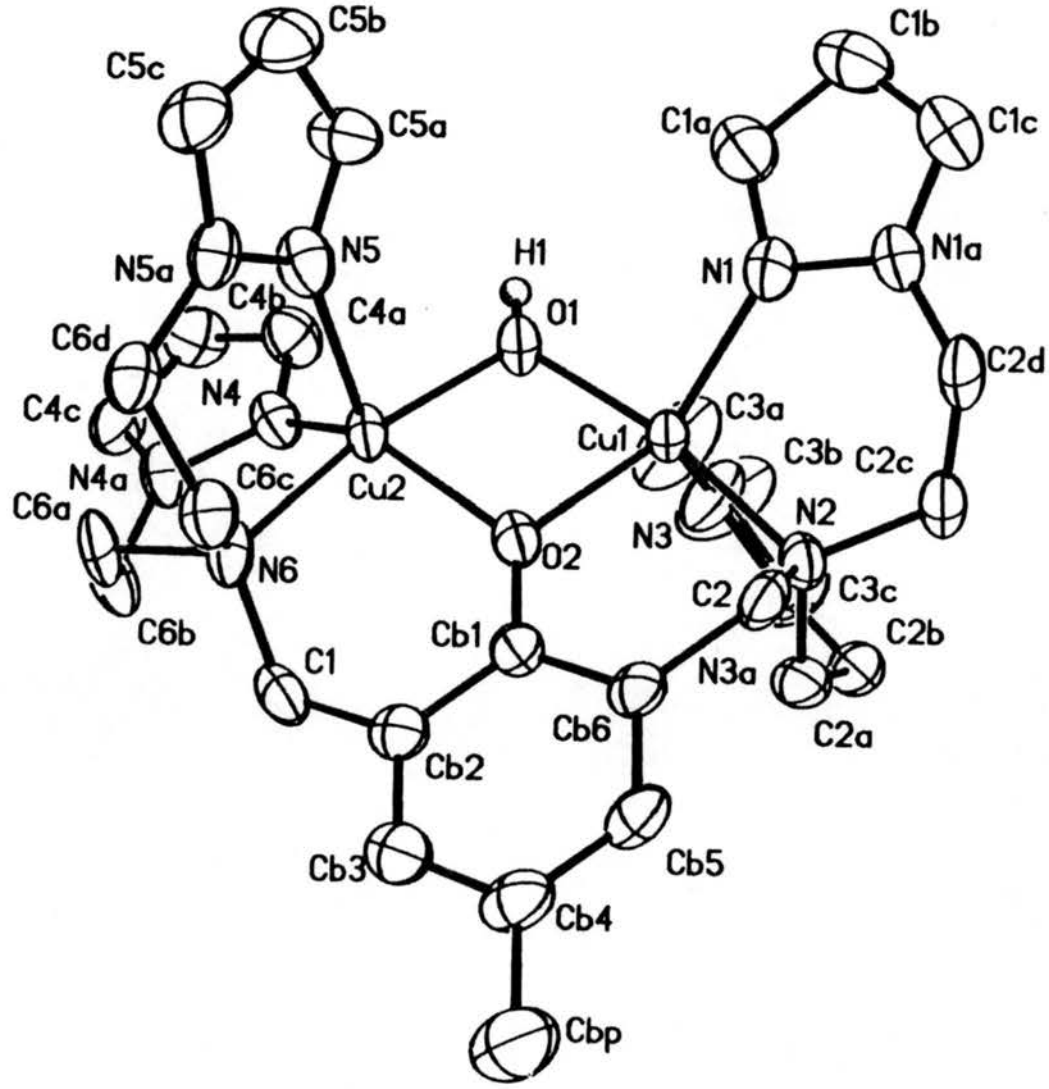
C5b
C5c
C5a
C1b
C1a
C1c
N5a
N5
H1
N1
N1a
C4b
C4a
O1
C6d
C2d
N4
C4c
C3a
Cu1
C3b
C2c
N4a
C6c
Cu2
C6a
N3
N2
N6
O2
C2
C3c
C6b
Cb1
C2b
C1
N3a
Cb6
C2a
Cb2
Cb3
Cb5
Cb4
Cbp

Figure 2.6. Ball and stick plot of the primary coordination sphere of the copper(II) ions in $\{Cu_2(N_6'O)OH\}^{2+}$ (**9a**).

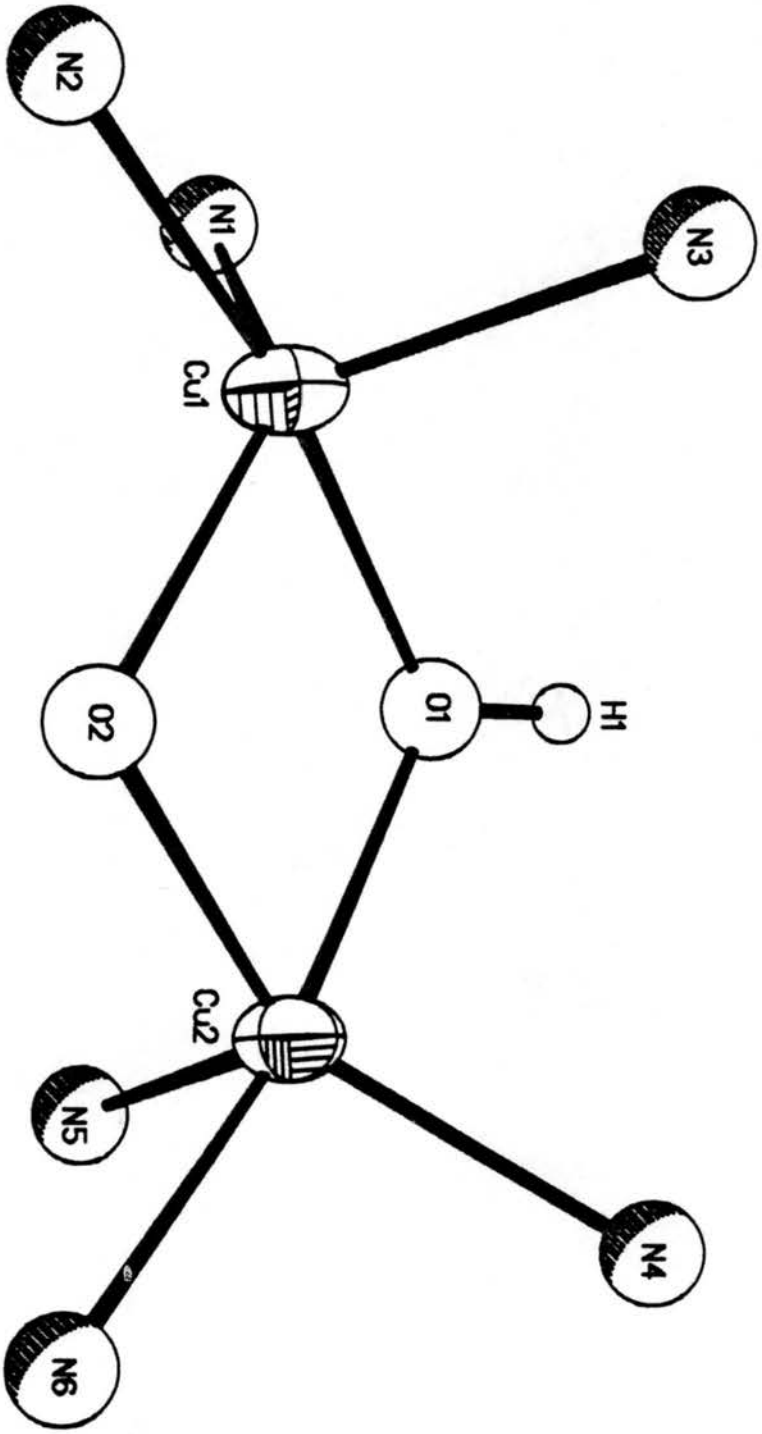
N2
N1
N3
Cu1
O2
O1
H1
Cu2
N5
N4
N6

Table 2.9. Atomic coordinates ($\times 10^4$) and thermal parameters ($Å^2 \times 10^3$)[a] for **9a**.

atom	*x*	*y*	*z*	U_{iso}[b]
Cu1	1273(1)	2221(1)	1108(1)	28(1)
Cu2	–1097(1)	3087(1)	1056(1)	28(1)
O1	86(3)	2703(4)	1458(1)	32(1)
O2	96(3)	2580(4)	653(1)	32(1)
Cb1	105(4)	2480(5)	215(2)	31(2)
Cb6	901(4)	1746(6)	9(2)	31(2)
Cb5	890(5)	1666(6)	–452(2)	37(2)
Cb4	112(5)	2249(7)	–714(2)	44(2)
Cb3	–668(5)	2956(6)	–507(2)	40(2)
Cb2	–686(4)	3095(6)	–53(2)	33(2)
Cbp	95(6)	2119(8)	–1211(2)	62(3)
C2	1733(4)	1015(6)	280(2)	34(2)
C1	–1494(4)	3961(6)	166(2)	37(2)
C6c	–2513(4)	2020(5)	375(2)	34(2)
C6d	–3297(4)	1316(6)	655(2)	37(2)
C6a	–3052(4)	4199(6)	624(2)	43(2)
C6b	–2744(5)	5544(6)	792(2)	47(2)
C2a	2698(5)	3029(6)	432(2)	37(2)
C2b	3475(4)	3864(6)	709(2)	40(2)
C2c	3268(4)	1018(6)	797(2)	42(2)
C2d	2992(5)	–277(6)	1005(2)	49(2)
C5a	–1866(5)	861(6)	1665(2)	44(2)
C5b	–2612(5)	–152(6)	1703(3)	52(3)
C5c	–3220(5)	–125(6)	1324(2)	46(2)
C4c	–2760(5)	6238(6)	1583(2)	43(2)
C4b	–2191(5)	5877(6)	1951(2)	46(2)
C4a	–1479(5)	4914(6)	1814(2)	44(2)
C1c	2746(6)	–886(8)	1794(3)	64(3)
C1b	2069(7)	–499(8)	2111(3)	68(3)
C1a	1432(6)	498(7)	1915(2)	56(3)
C3c	3408(6)	5458(7)	1336(3)	64(3)
C3b	2821(7)	5582(8)	1700(3)	88(4)
C3a	2055(7)	4598(9)	1659(3)	84(4)
N1	1708(4)	700(5)	1496(2)	44(2)
N1a	2525(4)	–160(5)	1432(2)	47(2)
N2	2309(3)	1787(4)	633(2)	31(2)
N4a	–2400(4)	5505(4)	1248(2)	36(2)
N3	2173(4)	3876(6)	1298(2)	51(2)
N3a	3008(4)	4451(5)	1098(2)	41(2)
N4	–1604(4)	4674(5)	1389(2)	36(2)
N5a	–2839(4)	841(4)	1071(2)	33(2)
N5	–2010(4)	1471(5)	1281(2)	39(2)
N6	–2114(4)	3339(4)	531(2)	34(2)

Table 2.9. (continued)

atom	*x*	*y*	*z*	U_{iso}[b]
B1	5264(6)	7615(8)	2299(2)	42(3)
F1	5133(4)	6256(5)	2342(2)	105(2)
F2	4574(3)	8248(4)	2569(1)	57(1)
F3	6306(3)	7869(4)	2418(1)	58(1)
F4	5083(4)	7915(5)	1865(1)	86(2)
B2	5145(5)	7792(5)	393(1)	32(3)
F21	5127(4)	7553(5)	834(1)	89(2)
F22	4460(5)	8793(5)	293(2)	50(2)
F23	5091(4)	6606(5)	160(2)	109(2)
F24	6170(4)	8264(5)	383(2)	49(2)
F24'	3692(7)	7135(9)	497(3)	43(3)
F22'	4862(13)	8470(14)	94(4)	85(5)
B2'	4701(6)	7545(8)	422(2)	45(5)
O101	5082(5)	2566(6)	1537(2)	93(3)
C105	5687(7)	3334(9)	1770(3)	75(4)
C104	5678(10)	3209(10)	2261(3)	103(5)
C103	5081(12)	1889(17)	2304(4)	170(8)
C102	4471(12)	1721(15)	1866(5)	158(8)

[a] Estimated standard deviations in the least significant digits are given in parenthesis.

[b] Equivalent isotropic U for anisotropic atoms is defined as one-third the trace of the orthogonalized U_{ij} tensor.

Table 2.10. Bond lengths (Å)[a] for **9a.**

Cu1–O1	1.907(4)	Cu1–O2	2.020(4)
Cu1–N1	2.013(5)	Cu1–N2	2.011(5)
Cu1–N3	2.099(6)	Cu2–O1	1.926(4)
Cu2–O2	2.018(4)	Cu2–N4	2.020(5)
Cu2–N5	2.126(5)	Cu2–N6	2.024(5)
O2–Cb1	1.333(7)	Cb1–C5c	1.403(8)
Cb1–Cb2	1.409(8)	Cb6–Cb5	1.400(8)
Cb6–C2	1.503(8)	Cb5–Cb4	1.373(9)
Cb4–Cb3	1.377(9)	Cb4–Cbp	1.513(9)
Cb3–Cb2	1.386(8)	Cb2–C1	1.507(8)
C2–N2	1.497(7)	C1–N6	1.509(8)
C6c–C6d	1.496(8)	C6c–N6	1.507(7)
C6d–N5a	1.454(8)	C6a–C6b	1.510(9)
C6a–N6	1.493(7)	C6b–N4a	1.438(8)
C2a–C2b	1.525(8)	C2a–N2	1.493(7)
C2b–N3	1.452(8)	C2c–C2d	1.509(9)
C2c–N2	1.501(7)	C2d–N1a	1.441(9)
C5a–C5b	1.396(9)	C5a–N5	1.328(8)
C5b–C5c	1.361(10)	C5c–N5a	1.344(8)
C4c–C4b	1.359(9)	C4c–N4a	1.349(8)
C4b–C4a	1.395(9)	C4a–N4	1.317(8)
C1c–C1b	1.355(11)	C1c–N1a	1.34810)
C1b–C1a	1.411(11)	C1a–N1	1.342(9)
C3c–C3b	1.347(12)	C3c–N3a	1.350(9)
C3b–C3a	1.387(12)	C3a–N3	1.332(11)
N1–N1a	1.362(7)	N4a–B40	1.363(6)
N3–N3a	1.357(7)	N5a–N5	1.359(7)
B1–F1	1.403(10)	B1–F2	1.367(8)
B1–F3	1.360(8)	B1–F4	1.368(9)
B2–F21	1.361(5)	B2–F22	1.360(8)
B2–F23	1.403(7)	B2–F24	1.364(8)
F21–B2'	1.344(6)	F22–B2'	1.364(10)
F23–B2'	1.345(9)	F24–B2'	1.350(12)
F22'–B2'	1.391(15)	O101–C105	1.286(11)
O101–C102	1.538(16)	C105–C104	1.498(13)
C104–C103	1.546(20)	C103–C102	1.523(19)

[a] Estimated standard deviations in the least significant digits are given in parenthesis.

Table 2.11. Bond angles (deg)[a] for **9a**.

O1–Cu1–O2	77.0(2)	O1 -Cu1–N1	94.2(2)
O2–Cu1–N1	135.9(2)	O1–Cu1–N2	167.9(2)
O2–Cu1–N2	90.0(2)	N1–Cu1–N2	94.8(2)
O1–Cu1–N3	93.2(2)	O2–Cu1–N3	114.4(2)
N1–Cu1–N3	109.1(2)	N2–Cu1–N3	91.5(2)
O1–Cu2–O2	76.7(2)	O1–Cu2–N4	95.2(2)
O2–Cu2–N4	139.0(2)	O1–Cu2–N5	92.5(2)
O2–Cu2–N5	113.9(2)	N4–Cu2–N5	106.4(2)
O1–Cu2–N6	167.1(2)	O2–Cu2–N6	90.5(2)
N4–Cu2–N6	95.5(2)	N5–Cu2–N6	91.4(2)
Cu1–O1–Cu2	106.9(2)	Cu1–O2–Cu2	99.4(2)
Cu1–O2–C1	129.9(3)	Cu2–O2–C1	130.7(3)
O2–Cb1–C2	120.9(5)	O2–Cb1–Cb2	121.1(5)
Cb6–Cb1–Cb2	118.0(5)	Cb1–Cb6–Cb5	119.5(5)
Cb1–Cb6–C2	120.2(5)	Cb5–Cb6–C2	120.4(5)
Cb6–Cb5–Cb4	122.8(6)	Cb53–Cb4–Cb3	117.1(6)
Cb5–Cb4–Cbp	122.1(6)	Cb3–Cb4–Cbp	120.8(6)
Cb4–Cb3–Cb2	122.7(6)	Cb1–Cb2–Cb3	119.9(5)
Cb1–6–C1	118.1(5)	Cb3–Cb2–C1	121.8(5)
Cb6–C2–N2	116.1(5)	Cb2–C1–N6	116.0(5)
C6d–C6c–N6	117.7(5)	C6c–C6d–N5a	114.1(5)
C6b–C6a–N6	113.9(5)	C6a–C6b–N4a	111.4(5)
C2b–C2a–N2	117.1(5)	C2a–C2b–N3a	114.4(5)
C2d–C2c–N2	114.1(5)	C2c–C2d–N1a	114.0(5)
C5b–C5a–N5	110.4(6)	C5a–C5b–C5c	105.6(6)
C5b–C5c–N5a	107.6(6)	C4b–C4c–N4a	107.1(5)
C4c–C4b–C4a	105.4(6)	C4b–C4a–N4	111.4(6)
C1b–C1c–N1a	107.6(7)	C1c–C1b–C1a	105.3(7)
C1b–C1a–N1	110.8(6)	C3b–C3c–N3a	108.4(7)
C3c–C3b–C3a	104.3(8)	C3b–C3a–N3	112.4(8)
Cu1–N1–C1a	127.0(5)	Cu1–N1–N1a	127.1(4)
C1a–N1–N1a	104.3(5)	C2d–N1a–C1c	127.6(6)
C2d–N1a–N1	120.2(5)	C1c–N1a–N1	112.0(6)
Cu1–N2–C2	109.0(3)	Cu1–N2–C2a	109.2(3)
C2–N2–C2a	107.9(4)	Cu1–N2–C2c	113.4(4)
C2–N2–C2c	108.8(4)	C2a–N2–C2c	108.4(4)
C6b–N4a–C4c	127.8(5)	C6b–N4a–N4	121.0(5)
C4c–N4a–N4	111.2(5)	Cu1–N3–C3a	127.0(5)
Cu1–N3–N3a	129.2(4)	C3a–N3–N3a	103.9(6)
C2b–N3a–C3c	127.0(5)	C2b–N3a–N3	121.3(5)
C3c–N3a–N3	110.9(5)	Cu2–N4–C4a	127.6(4)
Cu2–N4–N4a	125.1(4)	C4a–N4–N4a	104.9(5)
C6d–N5a–C5c	127.2(5)	C6d–N5a–N5	121.5(5)
C5c–N5a–N5	110.8(5)	Cu2–N5–C5a	125.9(4)
Cu2–N5–N5a	128.4(4)	C5a–N5–N5a	105.7(5)
Cu2–N6–C1	108.2(3)	Cu2–N6–C6c	109.1(3)
C1–N6–C6c	108.4(4)	Cu2–N6–C6a	113.6(4)
C1–N6–C6a	108.1(4)	C6c–N6–C6a	109.4(4)

Table 2.11. (continued)

F1–B1–F2	109.6(6)	F1–B1–F3	106.1(6)
F2–B1–F3	111.2(6)	F1–B1–F4	107.1(6)
F2–B1–F4	112.6(6)	F3–B1–F4	110.0(6)
F21–B2–F22	109.1(5)	F21–B2–F23	109.9(5)
F22–B2–F23	120.9(5)	F21–B2–F24	97.3(5)
F22–B2–F24	108.0(5)	F23–B2–F24	109.0(5)
F21–B2'–F24'	100.9(6)	F23–B2'–F24'	103.4(7)
F21–B2'–F22'	126.9(9)	F23–B2'–F22'	89.9(7)
F22'–B2'–F24'	119.1(9)	C105–O101–C102	106.0(8)
O101–C105–C104	118.4(8)	C105–C104–C103	100.1(8)
C104–C103–C102	104.6(11)	O101–C102–C103	105.2(11)

[a] Estimated standard deviations in the least significant digits are given in parentheses.

ligand atoms form significantly shorter bonds to Cu1 (Cu1–N1(pyrazole), 2.013(5) Å; Cu1–N2(amine), 2.011(5) Å; Cu1–O1(hydroxo), 1.907(4) Å; Cu1–O2(phenoxo), 2.020(4) Å). The two largest metal-centered angles are opposite the Cu1–N3 bond and are assigned as α (O2–Cu1–N1 = 135.9(2)°) and β (N2–Cu1–O1 = 167.9(1)°). These four potential basal ligand atoms are far from coplanar, as evidenced by the large value for $\Sigma\Delta^2$ (0.450) for the least-squares plane formed by O2, N1, N2, and O1 (see Appendix, Table S-2.3). These four atoms are tetrahedrally distorted from that plane, with the atoms O2 and N1 above the plane by 0.3 Å and N2 and O2 below the plane by 0.3 Å (on the same side as Cu1).

The structural evidence for trigonal bipyramidal geometry about Cu1 may be summarized as follows. The atoms which formed metal-centered angles with an average value closest to the ideal trigonal bipyramidal value of 120° were assigned to be the equatorial ligand atoms. Those three coordinated atoms (N1, N3, and O2) are nearly coplanar with Cu1 (see Appendix, Table S-2.3). The near planarity of these atoms is attested to by the low value of $\Sigma\Delta^2$ (0.0056) for the least squares plane through N1, N3, O2, and Cu1. The metal-centered angles involving O2, N1, and N3 range from 135.9(2)° (O2–Cu1–N1) to 109.1(2)° (N1–Cu1–O2); these values are close to those expected for a trigonal bipyramidal complex.[73] The angle N11–Cu1–N2 (167.9(2)°) is also close to the L(ax)–Cu–L(ax) angle expected.

The Cu1–N2(amine) bond (2.011(5) Å) is significantly longer than the Cu1–O1(hydroxo) bond (1.907(4) Å), but is shorter than the typical basal copper(II)–N(amine) bond in square pyramidal copper(II) complexes ($Cu(II)–N(amine)_{ave}$ = 2.06 Å).[52,53,56,58,69,76] The Cu1–N2 bond is very similar in length to those reported for Cu(II)–N(amine) bonds in trigonal bipyramidal complexes ($Cu(II)–N(amine)_{ave}$ = 2.03 Å).[52,53,56] The Cu1–O1 bond is significantly shorter than the typical basal Cu(II)–O(hydroxo) bonds (1.90(1) Å).[52,57,70,71] The Cu1–O2 bond (2.020(4) Å) is significantly longer than basal Cu(II)–O(phenoxo) bonds ($Cu(II)–O(phenoxo)_{ave}$ = 1.946

Å),[52,56,58,62] and slightly longer than equatorial Cu(II)–O(phenoxo) bonds ($Cu(II)–O(phenoxo)_{ave}$ = 2.009 Å).[52,53,56] The Cu1–N1(pyrazole) bond (2.013(5) Å) is significantly longer than the basal Cu(II)–N(pyrazole) bond reported in **9b** (1.959(10) Å),[52] but does not differ significantly from the equatorial Cu(II)–N(pyrazole) bonds found in the acetato compound (2.007(8) Å and 2.004(9) Å).[53] The bond length pattern about Cu1 most closely resembles that characteristic of trigonal bipyramidal copper(II) complexes.[73]

The τ value for the coordination sphere about Cu1 (τ = 0.53 for α = 135.9(2)°, O2–Cu1–N1; β = 167.9(1)°, N2–Cu1–O1) is very close to the midpoint value for the τ range. While the τ value is inconclusive, the least-squares planes and the bond lengths and angles for the coordination sphere about Cu1 suggest that the coordination geometry about Cu1 is best described as distorted trigonal bipyramidal. The axial sites are occupied by an hydroxo oxygen atom (O1) and an amine nitrogen atom (N2), while the equatorial sites are occupied by the two pyrazole nitrogen atoms (N1, N3) and the oxygen atom of the bridging phenoxo group (O2).

The structural evidence for square pyramidal coordination geometry about Cu2 is as follows. The longest bond formed between Cu2 and its five coordinated atoms is Cu1–N5(pyrazole) (2.126(5) Å). The four remaining ligand atoms form significantly shorter bonds to Cu2 (Cu2–N6(amine), 2.024(5) Å; Cu2–N4(pyrazole), 2.020(5) Å; Cu2–O1(hydroxo), 1.926(4) Å; Cu2–O2(phenoxo), 2.018(4) Å). The two largest metal-centered angles are found opposite the Cu2–N5 bond, and are assigned as α (O2–Cu2–N4 = 139.0(2)°) and β (N6–Cu2–O1 = 167.1(2)°). The value of $\Sigma\Delta^2$ for the plane formed by O2, N4, N6, and O1 is 0.407 (see Appendix, Table S-2.3.). Based on this information, that set of four atoms is not planar within experimental error. In fact, the four atoms are tetrahedrally distorted from the plane, with the atoms O2 and N6 above the plane by 0.3 Å and the atoms N4 and O2 below the plane by 0.3 Å (on the same side as Cu2).

The structural evidence for trigonal bipyramidal coordination about Cu2 is examined next. The atoms (N1, N3, and O2) which formed the metal-centered angle with an average closest to the ideal value of 120° were assigned as the equatorial ligand atoms. The near planarity of Cu2, N1, N3, and O2 is demonstrated by the value of $\Sigma\Delta^2$ (0.0062) for the plane formed by those atoms (see Appendix, Table S-2.3). The metal-centered angles involving O2, N4, and N5 range from 139.0(2)° (O2–Cu2–N4) to 106.4(2)° (N4–Cu2–N5), and are all close to the values expected for an ideal trigonal bipyramidal complex.[73] The angle O1–Cu2–N6 (167.1(2)°) is close to the expected L(ax)–Cu–L(ax) angle.

The Cu2–N6(amine) bond (2.024(5) Å) is significantly longer than the Cu2–O1(hydroxo) bond (1.926(4) Å), but is shorter than typical basal copper(II)–N(amine) bonds in square pyramidal copper(II) complexes ($Cu(II)–N(amine)_{ave}$ = 2.06 Å).[52,53,56,58,69,76] The Cu2–O1(hydroxo) bond is equivalent in length to basal Cu(II)–O(hydroxo) bonds (1.92(1) Å)[57,70,71] and to the Cu(II)–O(hydroxo) bonds in **9b**,[8] but is significantly longer than the Cu1–O1(hydroxo) bond length. The Cu2–O2 (phenoxo) bond (2.018(4) Å) is significantly longer than basal Cu(II)–O(phenoxo) bonds ($Cu(II)–O(phenoxo)_{ave}$ = 1.946 Å)[52,56,58,62] and equatorial Cu(II)–O(phenoxo) bonds ($Cu(II)–O(phenoxo)_{ave}$ = 2.009 Å),[52,53,56] but does not differ from the Cu1–O2(phenoxo) bond in length. The Cu2–N4(pyrazole) bond (2.020(5) Å) is significantly longer than the basal Cu(II)–N(pyrazole) bond in **9b** (1.959(10) Å)[52] and the equatorial Cu(II)–N(pyrazole) bonds in the acetato compound (2.007(8) Å and 2.004(9) Å).[53] Thus, the bond length pattern about Cu2 most closely resembles that characteristic of trigonal bipyramidal copper(II) complexes.[73]

The τ value for the coordination sphere about Cu2 (τ = 0.47 for α = 139.0(2)°, O2–Cu1–N4; β = 167.1(1)°, N6–Cu1–O1) is very close to the midpoint value for the τ range. While the τ value is again inconclusive, the least squares planes and the bond lengths and angles about Cu2 suggest that the coordination geometry about Cu2 is best

described as distorted trigonal bipyramidal. The axial sites are occupied by an hydroxo oxygen atom (O1) and an amine nitrogen atom (N6), while the equatorial sites are occupied by the two pyrazole nitrogen atoms (N4, N5) and the oxygen atom of the bridging phenoxo group (O2).

The occluded THF solvent molecule is located closer to Cu1 than to Cu2. Its presence between N1 and N3 undoubtedly changes the packing forces about the complex cation, as compared to the structure of the brown form **9b** (see Figures 2.7.a and 2.7.b). This would seem to be the most likely cause of the changes in coordination geometry which result in the observed differences in color and magnetic properties for **9a** and **9b**. The closest approach of the THF molecule to a copper(II) ion occurs between Cu1 and C104 (4.5 Å); closest approach to the $N_6'O^-$ ligand occurs between C4b and C104 (3.8 Å). The geometry of each copper(II) coordination site in **9a** positions the copper(II) d_z2 orbital, which contains the unpaired electron, so as to promote overlap of a major lobe with a *p* orbital of the bridging hydroxo ligand. Likewise, the minor lobes of the d_z2 orbitals are nonorthogonal to a *p* orbital of the bridging phenoxide oxygen atom; however, the difference in overlap should make the magnetic coupling through the phenoxo oxygen atoms much smaller than the interaction through the bridging hydroxo group.[53,54]

It is of interest to compare the structure of the cation of **9a** with the previously reported structure of the cation of **9b**. The coordination geometry about each of the copper(II) atoms in the cation of **9a** is trigonal bipyramidal, with the axial positions being occupied by amine nitrogen atoms and the oxygen atom of the bridging hydroxo ligand. The coordination geometry for one of the two copper(II) atoms in the cation of **9b** is also trigonal bipyramidal, with the axial sites occupied by the amine nitrogen atom and the hydroxo oxygen atom. However, the remaining coordination site in the cation of **9b** is square pyramidal, with the basal sites occupied by a pyrazole nitrogen atom, an amine nitrogen atom, and the oxygen atoms of the hydroxo and phenoxo groups.

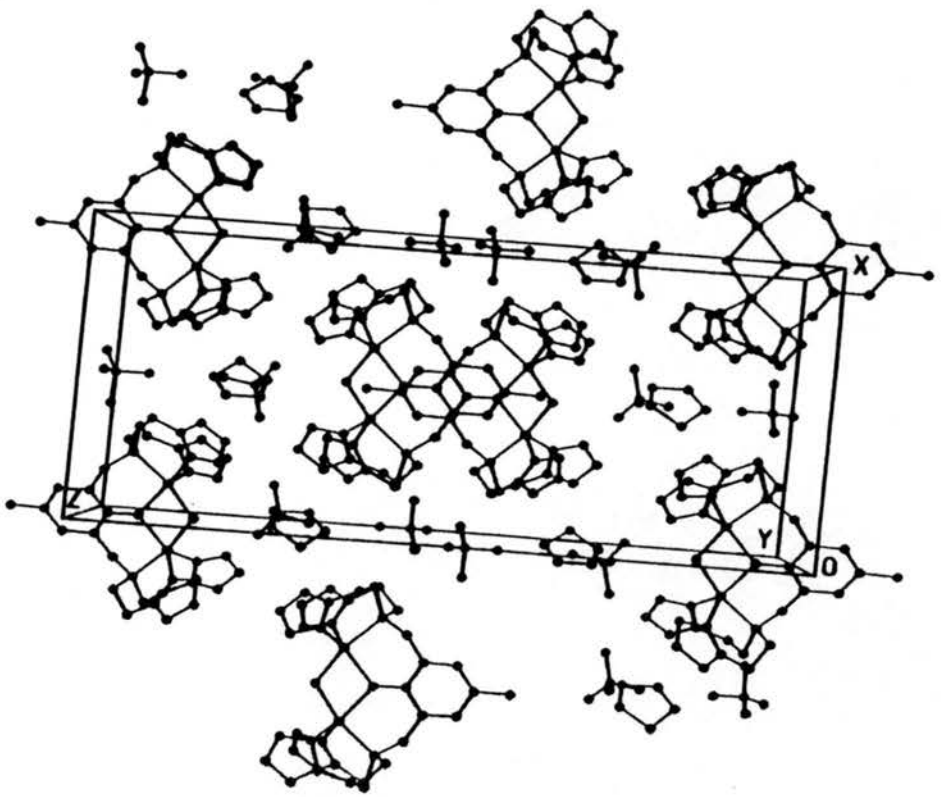

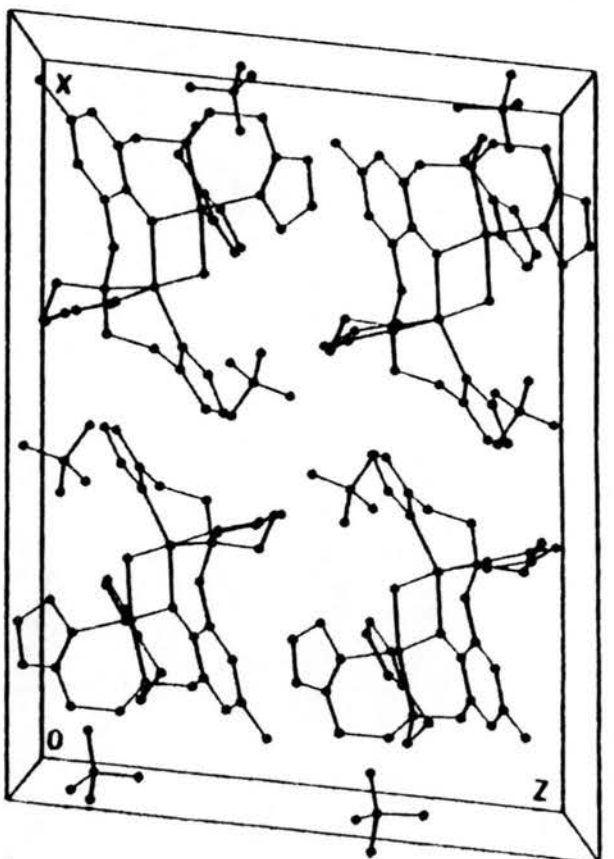

Figure 2.7.a Packing diagram for **9a**, viewed parallel to the *b* axis. Bonds are represented as solid lines. Atoms are represented as solid circles.

2.7.b Packing diagram for **9b**, viewed parallel to the *b* axis. Bonds are represented as solid lines. Atoms are represented as solid circles.

The magnetic coupling constant ($2J$) for **9a** is -300 cm^{-1}.[52] Hatfield and Hodgson have found a linear dependence of the coupling constant on the Cu–O–Cu bond angle for di-μ-hydroxo-bridged dimeric copper(II) complexes.[77,78] For **9a**, the bridging angle at the phenoxide oxygen atom is 99.4(2)°, while the angle at the hydroxide oxygen atom is 106.9(2)°. The Hatfield-Hodgson plot would predict a coupling constant, $2J$, of approximately -600 cm^{-1} for **9a**. This value does not agree with the experimental value of -300 cm^{-1}. On the other hand, the coupling constant for **9b**, for which the bond angle at the hydroxo oxygen atom is 103.6(3)° and the angle at the phenoxo oxygen atom is 101.9(4)°, is consistent with the Hatfield-Hodgson plot.[52] In fact, the Hatfield-Hodgson plot suggests that the $2J$ value for **9a** should be larger in magnitude that that for **9b**, not smaller by a factor of 0.7. Clearly, the coupling cannot be readily explained by only taking into account the angle at the hydroxide oxygen atom, as was done for **9b**.[52] An exchange mechanism operating through the phenoxide oxygen atom must mediate to some degree the overall coupling of the copper(II) atoms. Although the structural analysis of this binuclear complex would predict that major lobes of the orbitals containing the unpaired electrons on both copper(II) atoms would be directed toward the hydroxide bridge, the stronger coupling that this would predict is not seen.

The difference between the coupling constants for **9a** and **9b** must in part be due to the differences in their respective coordination geometries. The coordination environment in **9b**, which includes both square pyramidal and trigonal bipyramidal structures for copper(II), is somehow a more favorable environment for magnetic coupling than is that for **9a,** in which only trigonal bipyramidal geometries are seen.

Chapter 3

A Dinuclear Monoiodo-Bridged Copper(II) Complex

Introduction

Many examples of di-μ-chloro and di-μ-hydroxo copper(II) complexes are known, but structurally characterized binuclear copper(II) species bridged by a single atom are rare.[79–82] Singly bridged binuclear complexes represent the simplest examples of ligand bridging in which metal–metal interactions are unimportant. Many proteins contain two copper(II) atoms that are bridged by a single ligand.[41] Monobridged copper(II) complexes provide models for EPR studies, magnetic studies, and UV-visible spectroscopic studies of bridge-mediated interactions between metal ions.[79–87]

Previous studies have been concerned with the synthesis of dinuclear $[Cu_2(L)_2X]ClO_4$ complexes (L = $Me_4BO_2F_2$[14]teteneN$_4$ (cyclops),[79] hereafter known as **2**, or triethylenetriamine[83]; X^- = bridging ligand (CN^-, OH^-, Br^-, N_3^-, and I^-)]. In these complexes, both square pyramidal and trigonal bipyramidal coordination geometries are possible. The copper(II) cyclops complexes are expected to exhibit square pyramidal coordination geometry.[88–91] Magnetic studies have shown that such complexes display very weak antiferromagnetic interactions, with $2J$ values between –1.0 and –2.0 cm^{-1}. The weak magnetic coupling in these complexes is attributed to the fact that the *d* orbitals that contain the unpaired electrons of the copper(II) atoms are orthogonal to the orbitals of the bridging ligands that would be effective in creating a spin exchange pathway between the metal ions. The fact that any coupling is seen has been postulated to be the result of off-axis binding of the apical bridging ligand, with a Cu–X–Cu angle much larger than 90°.

Magnetic exchange through halogen atoms is postulated to take place through the filled *p* orbitals of the bridging ligand. A Cu–X–Cu angle of 180° would imply that the bonding interaction involved a single *p* orbital on the bridging X ligand, while an angle of 90° would imply that orthogonal *p* orbitals were involved. In order to verify the expected geometry of the copper(II) coordination sphere and structurally characterize a rare example of a copper(II) dimer with a single bridging atom, an X-ray diffraction study of the compound $[Cu_2(\mathbf{2})_2I]ClO_4 \cdot 2MeOH$ was undertaken.

Experimental

Synthesis of $\{[Cu(2)]_2I\}ClO_4 \cdot 2MeOH$ (10). A 0.101 g (0.228 mmol) sample of $[Cu(\mathbf{2})OH_2]ClO_4$ (see Chapter 1) was dissolved in 6 mL of hot (60°C) MeOH. A 0.041 g (0.111 mmol) sample of *n*-butylammonium iodide (Aldrich) was dissolved in this solution, which resulted in a slow color change from violet to blue. The solution was stirred for 30 min and then cooled to –19 °C. Over the course of 12 h, large blue crystals formed. The unit cell constants for those crystals matched those of the mononuclear [Cu(**2**)I] complex.[90] If, however, the crystals remained in the mother liquor for two weeks, at –19 °C, a change in composition was seen, as shown by a change in the cell constants. Apparently the original crystals redissolved in the mother liquor and the dimeric complex **10** formed. These crystals were collected by filtration and washed in ethanol. Yield 0.010 g (7.0%).

Structure Determination for 10. A crystal of **10** was mounted on a glass fiber and centered on the X-ray diffractometer. The cell constants reported in Table 3.1 were calculated from a least squares fit to the setting angles for 25 independent reflections ($2\theta_{ave} = 21.7°$). Three control reflections monitored every 97 reflections showed no significant variation in intensity during data collection. Data were corrected for Lorentz and polarization factors, as well as for absorption effects. The intensities of a small number of reflections ($2\theta_{min} = 6.3°$, $2\theta_{max} = 30.98°$, $2\theta_{ave} = 17.62°$) were measured as a function of Ψ and were used in the empirical absorption correction. The R_{merge}[92] value of the azimuthal data set was 0.048 before correction, and 0.017 after the correction was applied.

Table 3.1. Details of the Crystallographic Experiment and Computations for **10**.

Formula	$C_{26}H_{46}N_8B_2ClCu_2F_4IO_{10}$
Formula weight (g mol^{-1})	1018
Crystal system	monoclinic
Space group	*C2/c*
Lattice constants	
a (Å)	21.564(3)
b (Å)	11.920(2)
c (Å)	14.831(2)
β (deg)	96.83(1)
V (Å^3)	3785
Temperature (°C)	20(1)
Z	4
ρ(calculated, g cm^{-3})	1.79
Crystal dimensions	0.20 mm × 0.34 mm × 0.38 mm
Radiation	$MoK_\alpha(\lambda = 0.71073$ Å)
Monochromator	graphite
μ (cm^{-1})	20.7
Scan type	θ–2θ
Geometry	bisecting
Scan speed (deg min^{-1})	2.0 – 29.3
2θ range (deg)	3.5 – 50.0
Index restrictions	$-26 \le h \le 26$; $-15 \le k \le 0$; $-18 \le l \le 0$
Total number of reflections	3795
Number of unique, observed reflections	2920
Observed reflection criterion	$\|F\| \ge 2.5\ \sigma\|F\|$
Data to parameter ratio	10.7
R	0.044
R_w	0.060
S	1.44
g (fixed)	0.0010

Slope, normal probability plot 1.23

The crystal was taken to be ellipsoidal in shape ($\mu r_{ave} = 0.34$), resulting in $T_{min} = 0.34$ and $T_{max} = 0.45$ for the entire data set.

Systematic reflection conditions (*hkl*, $h+k = 2n$; *h0l* , $l = 2n$) suggested that the space group was either *C*2/*c* or *Cc*. The structure was solved readily in *C*2/*c* by Patterson map interpretation.

The chlorine atom of the perchlorate anion was found to sit on a crystallographic inversion center. The four oxygen atoms of the perchlorate anion are thus disordered eight positions, four of which are related to the other four by the inversion operation. The site occupancy factor of each oxygen atom in the unique portion was fixed at 0.5.

The elbow carbon atom (C6) was found to be disordered between two structurally reasonable positions. In the final stages of refinement the disorder about C6 was modeled as two independent atoms (C6 and C6'). The site occupancy factor of each atom (C6 and C6') was fixed at 0.50.

An occluded molecule of methanol was located during the final stages of refinement. Refinement of the site occupancy factor of the methanol molecule converged at a value of 0.98; in the final refinement calculation this value was fixed at 1.0.

All nonhydrogen atoms were refined using anisotropic thermal parameters. Hydrogen atoms bound to carbon were placed in idealized positions (C–H = 0.96 Å, $U_{iso}(H) = 1.2 \times U_{iso}(C)$). The weighted [$w = (\sigma^2(F) + g(F)^2)^{-1}$] least squares refinement on *F* yielded the residual values listed in Table 3.1 at convergence (for the last twenty cycles, mean shift/e.s.d = 0.038, max shift/e.s.d. = 0.302 (for rotation of the methyl group C15)). The height of the highest peak in the final ΔF map was +0.78 e Å^{-3} (near O3), while the minimum was –0.48 e Å^{-3}.

Results and Discussion

The structure of $[Cu_2(\mathbf{2})_2I]^+$ is displayed in Figure 3.1. The packing diagram, viewed along the *b* axis, is shown in Figure 3.2a, as is the copper(II) coordination polyhedron (Figure 3.2b). Tables 3.2, 3.3, and 3.4 contain the atomic coordinates, bond lengths, and bond angles for **10**, respectively. Tables of anisotropic thermal parameters and hydrogen atom coordinates are given in the Appendix as Tables S-3.1 and S-3.2.

The dinuclear cation contains two five-coordinate copper(II) atoms. The coordination geometry about each copper atom is, as expected, square pyramidal, with the nitrogen atoms of **2** occupying the four basal sites and the bridging iodo ligand occupying the apical site. The two copper(II) complexes in the cation of **10** are related by a twofold crystallographic axis that passes through the iodo ligand. The Cu–I–Cu angle is far from linear (118.9(1)°), and is significantly less obtuse than the bridging angle in *catena*-μ-iodo-bis-{μ-{[2-(3-aminopropyl)amino]ethanolato-N,N', μ-O}copper(II)} (145.0(2)°), in which two copper(II) atoms are bridged by an apical iodine atom.[93] I is also less obtuse than the bridging angle reported for the Cu-Cl-Cu bridge in $[Cu_2(tet\text{-}b)_2Cl](ClO_4)_2$ (174.2°).[94]

The orientation of ligand **2** with respect to the Cu–I–Cu plane can be described in terms of the vector from the copper(II) atom to the elbow carbon atom C6. If the angle between this vector and the normal to the Cu–I–Cu plane were 90°, C6 would be in the Cu–I–Cu plane, while if the angle were 0° or 180°, C6 would be offset from this plane to the maximum degree. The angle seen between the Cu···C6 vector and the normal to the Cu–I–Cu plane is 46.4°. The orientation of ligand **2** with respect to the Cu–I–Cu plane is such as to direct the polar BF_2 group and the C6 carbon atom away from that plane at

Figure 3.1. Thermal ellipsoid plot (40% probability) of the cation of **10**, $\{[Cu(\mathbf{2})]_2I\}^+$. Hydrogen atoms have been omitted for clarity.

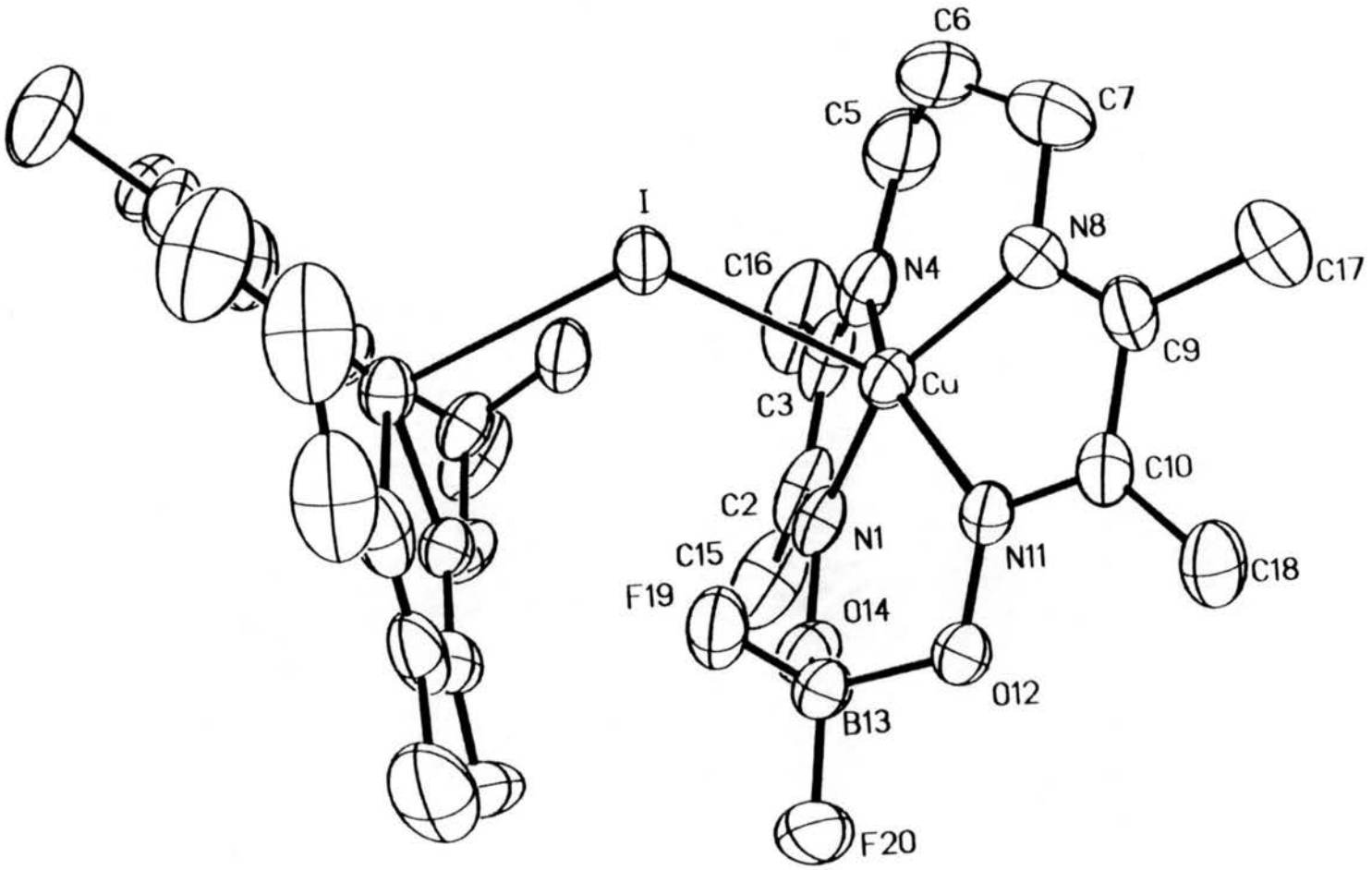
C6
C5
C7
I
N8
C16
N4
C17
C9
Cu
C3
C10
C2
N1
N11
C15
C18
F19
O14
O12
B13
F20

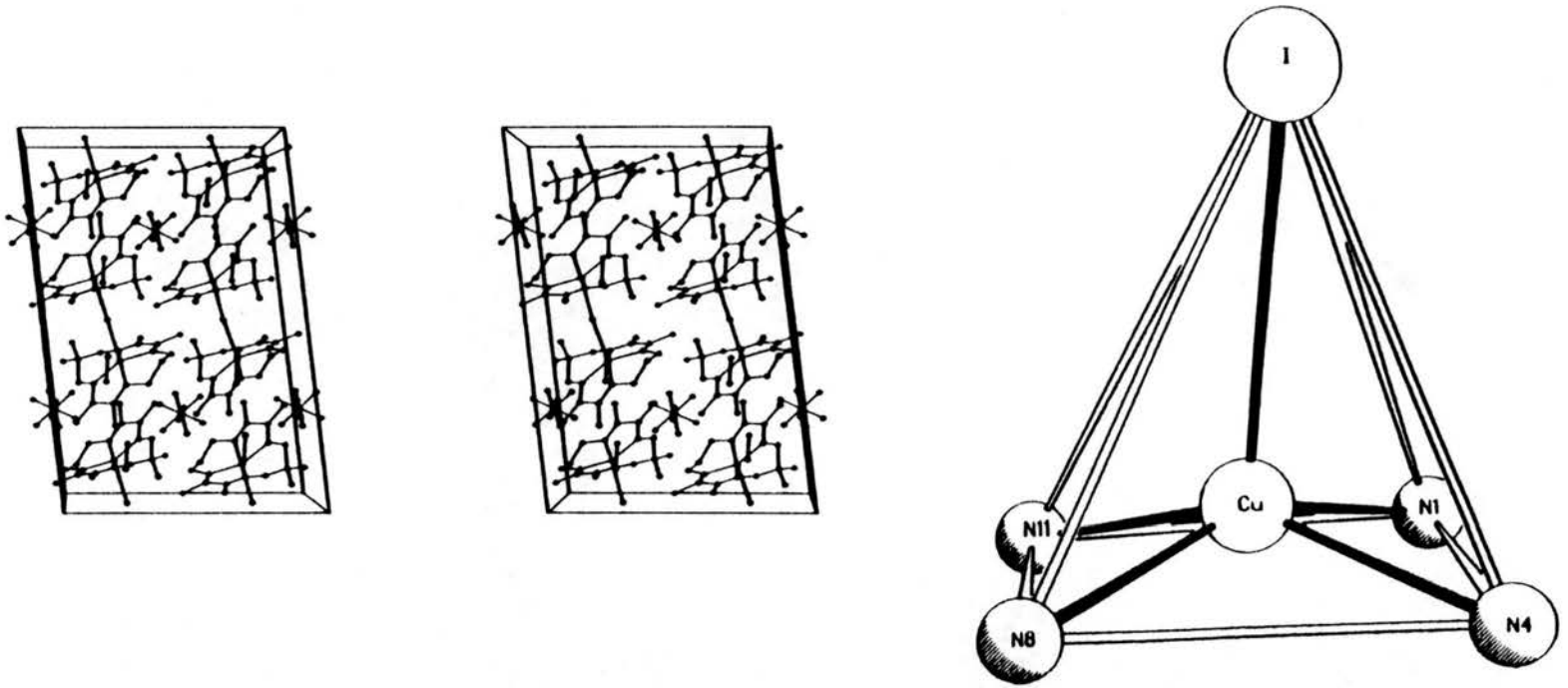

Figure 3.2.a Stereoview of the structure of $\{[Cu(2)]_2I\}(ClO_4) \cdot MeOH$, viewed parallel to the *b* axis. Bonds are represented as solid lines. Atoms are represented as solid circles.

3.2.b Ball and stick plot of the polyhedron about the copper(II) ion in the cation of **10**, $\{[Cu(2)]_2I\}^+$.

Table 3.2. Atomic coordinates ($\times 10^4$) and isotropic thermal parameters ($Å^2 \times 10^3$)[a] for **10**.

atom	*x*	*y*	*z*	U_{iso}[b]
I	0	4954(1)	2500	53(1)
Cu	–1096(1)	3734(1)	2823(1)	48(1)
N1	–831(2)	2174(3)	2837(3)	52(1)
C2	–659(2)	1749(5)	3628(4)	72(2)
C3	–650(2)	2600(6)	4371(3)	78(2)
N4	–843(2)	3551(4)	4135(2)	69(2)
C5	–899(3)	4487(8)	4792(4)	105(3)
C6	–1078(6)	5566(11)	4359(7)	111(5)
C6'	–1470(15)	5264(20)	4503(16)	80(9)
C7	–1651(4)	5684(7)	3756(5)	118(3)
N8	–1692(2)	4950(4)	2940(3)	68(2)
C9	–2163(2)	4963(4)	2350(4)	67(2)
C10	–2166(2)	4105(4)	1595(3)	50(1)
N11	–1680(1)	3474(3)	1709(2)	45(1)
O12	–1669(1)	2585(2)	1140(2)	51(1)
B13	–1057(2)	1995(5)	1225(4)	54(2)
O14	–894(1)	1445(3)	2119(2)	60(1)
C15	–498(3)	559(5)	3790(5)	105(3)
C16	–402(4)	2216(9)	5307(4)	127(4)
C17	–2721(3)	5722(6)	2340(6)	102(3)
C18	–2684(2)	3964(5)	873(4)	66(2)
F19	–602(1)	2711(3)	1048(2)	67(1)
F20	–1129(2)	1120(3)	622(2)	89(1)
Cl	2500	2500	0	222(4)
O1	2701(9)	1369(9)	88(19)	704(38)
O2	2243(8)	2814(17)	818(8)	257(14)
O3	2955(6)	2347(24)	796(10)	437(28)
O4	1982(5)	1807(12)	115(13)	163(9)
Cme	1795(8)	8132(11)	2726(10)	197(8)
Ome	1139(10)	8026(12)	2622(11)	356(12)

[a] Estimated standard deviations in the least significant digits are given in parentheses.

[b] The equivalent isotropic U_{iso} is defined as one-third of the trace of the U_{ij} tensor.

Table 3.3. Bond lengths (Å)[a] for **10**.

I–Cu	2.863(1)	Cu–N1	1.945(4)
Cu–N4	1.970(4)	Cu–N8	1.960(4)
Cu–N11	1.979(3)	N1–C2	1.291(6)
N1–O14	1.369(5)	C2–C3	1.495(8)
C2–C15	1.474(9)	C3–N4	1.244(8)
C3–C16	1.500(8)	N4–C5	1.495(9)
C5–C6	1.468(15)	C5–C6'	1.559(30)
C6–C7	1.444(14)	C6'–C7	1.236(24)
C7–N8	1.488(9)	N8–C9	1.259(7)
C9–C10	1.516(7)	C9–C17	1.504(8)
C10–N11	1.286(5)	C10–C18	1.463(6)
N11–O12	1.356(4)	O12–B13	1.486(6)
B13–O14	1.484(6)	B13–F19	1.350(6)
B13–F20	1.371(6)	Cl–O1	1.418(12)
Cl–O2	1.442(14)	Cl–O3	1.454(13)
Cl–O4	1.415(13)	Cme–Ome	1.411(27)

[a] Estimated standard deviations in the least significant digits are given in parentheses.

Table 3.4. Bond angles (deg)[a] for **10**.

Cu–I–Cua	118.9	I–Cu–N1	103.9(1)
I–Cu–N4	94.9(1)	N1–Cu–N4	80.6(2)
I–Cu–N8	101.7(1)	N1–Cu–N8	154.4(2)
N4–Cu–N8	95.8(2)	I–Cu–N11	113.3(1)
N1–Cu–N11	90.9(1)	N4–Cu–N11	151.8(2)
N8–Cu–N11	80.2(2)	Cu–N1–C2	115.9(3)
Cu–N1–O14	126.6(3)	C2–N1–O14	116.7(4)
N1–C2–C3	112.4(5)	N1–C2–C15	124.2(5)
C3–C2–C15	123.4(5)	C2–C3–N4	115.9(4)
C2–C3–C16	116.5(6)	N4–C3–C16	127.6(6)
Cu–N4–C3	115.0(4)	Cu–N4–C5	121.8(4)
C3–N4–C5	123.2(4)	N4–C5–C6	113.9(6)
N4–C5–C6'	112.7(9)	C5–C6–C7	121.2(10)
C5–C6'–C7	130.0(22)	C6–C7–N8	114.2(7)
C6'–C7–N8	118.2(13)	Cu–N8–C7	122.1(4)
Cu–N8–C9	115.5(4)	C7–N8–C9	121.5(5)
N8–C9–C10	116.0(4)	N8–C9–C17	126.3(6)
C10–C9–C17	117.7(5)	C9–C10–N11	111.4(4)
C9–C10–C18	123.7(4)	N11–C10–C18	124.7(4)
Cu–N11–C10	116.5(3)	Cu–N11–O12	125.8(2)
C10–N11–O12	116.7(3)	N11–O12–B13	113.4(3)
O12–B13–O14	113.5(4)	O12–B13–F19	110.1(4)
O14–B13–F19	110.7(4)	O12–B13–F20	105.9(3)
O14–B13–F20	104.1(4)	F19–B13–F20	112.5(4)
N1–O14–B13	113.9(3)	O1–Cl–O2	108.3(14)
O1–Cl–O3	68.7(15)	O2–Cl–O3	68.8(9)
O1–Cl–O4	70.8(10)	O2–Cl–O4	70.3(10)
O3–Cl–O4	107.1(11)	O2–Cl–O1a	71.7(14)
O3–Cl–O1a	111.3(15)	O4–Cl–O1a	109.2(10)
O1–Cl–O2a	71.7(14)	O3–Cl–O2a	111.2(9)
O4–Cl–O2a	109.7(10)	O1a–Cl–O2a	108.3(14)
O1–Cl–O3a	111.3(15)	O2–Cl–O3a	111.2(9)
O4–Cl–O3a	72.9(11)	O1a–Cl–O3a	68.7(15)
O2a–Cl–O3a	68.8(9)	O1–Cl–O4a	109.2(10)
O2–Cl–O4a	109.7(10)	O3–Cl–O4a	72.9(11)
O1a–Cl–O4a	70.8(10)	O2a–Cl–O4a	70.3(10)
O3a–Cl–O4a	107.1(11)		

[a] Estimated standard deviations in the least significant digits are given in parentheses.

almost a 45° angle. This orientation places the electronegative BF_2 group above the π system of the symmetry-related Cu(II) complex (F19····C2 = 3.01(1) Å).

The Cu–I bond in each coordination sphere (see Figure 3.2b) is tilted toward the BF_2 group and the Cu–N1 bond. A similar tilt of the apical ligand toward the BF_2 group has been reported for the polymeric species $[Cu(\mathbf{2})(\mu\text{-CN})Cu(\mu\text{-CN})]_n$ (see Ch. 1), while a tilt of the Cu–I bond away from the BF_2 group is seen for monomeric [Cu(**2**)L] complexes.[88–91] The four nitrogen atoms of **2** form a plane ($17.6(1)x + 5.69(5)y - 6.25(6)z = -2.02(2)$; $\Sigma\Delta^2 = 0.0024$, $\sigma^2 = 0.025$); the maximum deviation from this plane is seen for N1 (0.025(4) Å) and N11 (–0.025(3) Å). The tilt of the apical ligand away from the ideal square pyramidal position is reflected in the angle between the vector from the centroid of the basal plane to the apical position and the vector normal to that basal plane. That angle in the cation of **10** is 8.7°. The same angle is 10.1° for [Cu(**2**)I][90] and 9° for $[Cu(\mathbf{2})OH_2]^+$,[4] but as noted the sense of the tilt is very different in those complexes. The copper(II) atom is displaced away from the basal plane toward the bridging iodo ligand by 0.445(2) Å, a distance that is significantly longer than that seen for the monomeric iodo complex (0.38 Å)[90] or the aqua complex (0.321 Å)[88] but shorter than that reported for the cyanato complex [Cu(**2**)(NCO)] (0.57 Å).[95] The large out-of-plane displacement of the copper(II) atom is rather surprising, given that the Cu–I bond length in the dimer (2.863(1) Å) is significantly longer than that reported for the monomer (Cu–I = 2.742(2) Å).

The perchlorate counterions in **10** packs into the voids between the dinuclear complexes (see Figure 3.2a). The closest approach of the perchlorate anion to the dimeric complex involves contacts between O1 and C5 (3.26(1) Å) and between O2 and a symmetry-related C17 (3.36(1) Å).

The average Cu–N bond length in the dimer is 1.963(3) Å, which is equivalent to that reported for [Cu(**2**)I], where $Cu–N_{ave}$ = 1.956(7) Å. Unlike [Cu(**2**)I], in which the four Cu–N bonds were equal within experimental error,[90] the Cu–N bonds in the cation of **10** display significant differences in their bond lengths. Three long Cu–N bonds are

equivalent in length (Cu–N4, 1.970(4) Å; Cu–N11, 1.979(3) Å; Cu–N8, 1.960(4) Å), while one bond is significantly shorter. (Cu–N1, 1.945(4) Å). These differences appear to be the result of the distortion of the coordination sphere about each copper(II) atom in the dimer.

The surprisingly large displacement of the copper(II) atom from the basal plane cannot be readily explained. Clearly, the out-of-plane displacement in the cation of **10** does not correlate well with the relationship between out-of-plane displacement and apical bond strength established for the monomeric complexes.[88–90] It may be that dinuclear complexes containing single bridging ligands cannot be expected to follow the trends seen in the mononuclear complexes; however, the lack of structural information on such dinuclear complexes limits the conclusions that can be drawn.

A study of the magnetic properties of the dimer was previously carried out, in order to determine the magnitude of the exchange coupling through the iodo ligand.[79] The $2J$ value (-1.8 cm^{-1}, $g_{ave} = 2.08$) reported was small and is consistent with the tetragonal symmetry seen for the dinuclear complex. The unpaired electron on each copper(II) atom should be in the $d_{x^2-y^2}$ orbital. The fact that any coupling is seen must be due to the small distortion in the copper(II) coordination sphere, which allows for overlap of the $d_{x^2-y^2}$ orbital with p orbitals of the bridging ligand.

Chapter 4

A Polynuclear Copper(II) Compound Utilizing the Ligand Pre-H

Introduction

Phase transitions in solids may be either first or second order. First order phase transitions involve the discontinuous reconstruction of the solid crystalline lattice.[96,97] Substances undergoing first order phase changes also display discontinuous changes in physical properties at a well-defined temperature (T_{th}). At that transition point, the two different phases are believed to be in equilibrium. First order transitions need not involve a change in symmetry of the crystalline lattice, but it is also possible that the symmetries of the lattice before and after the phase transition may have nothing in common.

If the structure of the solid changes continuously during the phase transition, the transition is second order.[96] Such a phase transition is accompanied by a change in the crystal symmetry. Although the phase transition is continuous over a range of temperature, the symmetry of the lattice undergoes a sudden change at the transition point. Unlike first order phase transitions, in which the two phases are believed to be in equilibrium at the transition point, for second order transitions the two phases are identical at the transition point.

Phase transitions for inorganic copper(II) coordination complexes may be either first or second order, and are often characterized by a color change. This behavior, known as thermochromism, is a result of a change in the copper(II) coordination sphere. The coordination sphere transformations generally involve alterations in connectivity or geometric distortions of the primary coordination sphere about the copper(II) atom.[98–104]

Previous work described the synthesis and the room temperature structural characterization of the perchlorate salt of the copper(II) complex involving the ligand **1** (see Ch. 1) and methanol. The complex was reported to form infinite chain polymers.[105] The monomer units are connected by weak Cu–O(oxime) bonds, and every other copper(II) complex along the chain was accompanied by a molecule of methanol which was weakly bonded to the metal. However, reevaluation of the previous work has found that the triclinic unit cell which was reported was incorrect, and that the true cell at room temperature is monoclinic. Further investigation showed that the compound underwent a phase change when cooled to –130 °C. This phase change is not accompanied by detectable thermochromic behavior. To correct the misassigned structure, investigate the apparent lack of thermochromic behavior, and fully characterize the phase change of this copper(II) complex the structural characterization of the room temperature form and the low temperature form was undertaken.

Experimental

Synthesis of $[\{[Cu(1)MeOH]Cu(1)\}(ClO_4)_2]_n$ (11). A 0.091 g (0.22 mmol) sample of $[Cu(\mathbf{1})OH_2]ClO_4$ (see Chapter 1) was dissolved in 10 mL of methanol. The solution was stirred under argon atmosphere for 24 h and filtered into a crystallization vial. The solution was then cooled to –19 °C. Large brown crystals of **11** formed during a 12 h period; these crystals were collected by filtration and washed with cold methanol. Yield 0.011 g (12 %).

The Determination of the Structure of 11a. A crystal of **11** was mounted on a glass fiber and centered on the X-ray diffractometer. The cell constants reported in Table 4.1 were calculated from a least squares fit to the setting angles for 25 independent reflections ($2\theta_{ave} = 20.35°$). The intensities of three control reflections were measured every 97 reflections during data collection; these intensities decreased by 16% during the period of data collection. A correction for this decay in intensity was applied during data reduction, as were corrections for Lorentz and polarization factors. No absorption correction was applied.

Systematic reflection conditions (*hkl*, $h+k = 2n$; *h0l*, $l = 2n$) required that the space group be *C*2/*c* or *Cc*. The structure was solved readily in *C*2/*c* by Patterson map interpretation.

The elbow carbon (C6) was found to be disordered between two structurally reasonable positions. In the final stages of refinement the disorder about C6 was modeled as two independent atoms (C6 and C6'). The site occupancy factor of each atom (C6 and C6') was fixed at 0.50.

All nonhydrogen atoms were refined with anisotropic thermal parameters. Hydrogen atoms bound to carbon were placed in idealized positions (C–H = 0.96 Å,

Table 4.1. Details of the Crystallographic Experiment and Computations for **11a** and **11b**.

Phase	**11a**	**11b**
Formula	$C_{11.5}H_{21}N_4ClCuO_{6.5}$	$C_{23}H_{42}N_8Cl_2Cu_2O_{13}$
Formula weight (g mol^{-1})	418.3	836.6
Crystal system	monoclinic	triclinic
Space group	$C\,2/c$	$P\,\bar{1}$
Lattice constants		
a (Å)	23.018(3)	6.850(2)
b (Å)	6.903(1)	11.886(3)
c (Å)	22.511(3)	22.303(5)
α(deg)		75.26(2)
β (deg)	105.48(1)	88.97(2)
γ(deg)		73.38(2)
V (Å^3)	3447(1)	1680(1)
Temperature (°C)	20(1)	–130(1)
Z	8	2
ρ(calculated, g cm^{-3})	1.61	1.65
Crystal dimensions	0.20 mm × 0.34 mm × 0.38 mm	0.16 mm × 0.21 mm × 0.36 mm
Radiation	MoK$_\alpha$(λ = 0.71073 Å)	MoK$_\alpha$
Monochromator	graphite	graphite
μ (cm^{-1})	15.0	15.2
Scan type	θ–2θ	θ–2θ
Geometry	bisecting	bisecting
Scan speed (deg min^{-1})	2.0 – 29.3	2.0 – 29.3
2θ range (deg)	3.5 – 50.0	3.5 – 50.0
Index restrictions	$-28 \le h \le 28$, $-9 \le k \le 0$, $-27 \le l \le 0$	$-9 \le h \le 9$, $-15 \le k \le 15$, $0 \le l \le 27$
Total no. of reflections	3537	6316
No. of unique, observed reflections	2351	5161
Observed reflection criterion	$\|F\| \ge 3.0\ \sigma(\|F\|)$	$\|F\| \ge 2.5\ \sigma\ (\|F\|)$
No. of parameters	285	489
Data/parameter ratio	8.3	10.5
R	0.073	0.058
R_w	0.080	0.083
S	2.17	1.96
g	5.0×10^{-4} (fixed)	9.0×10^{-4} (refined)
Slope, normal probability plot	1.82	1.51

$U_{iso}(H) = 1.2 \times U_{iso}(C)$). The weighted [$w = (\sigma^2(F) + g(F)^2)^{-1}$] least squares refinement on F yielded the residual values listed in Table 4.1 at convergence (for the last fourteen cycles, mean shift/e.s.d = 0.035, max shift/e.s.d. = 0.361 for rotation of methyl group C13). The height of the highest peak found in the final ΔF map was +0.68 e Å^{-3} (near Cl), while the minimum was –0.66 e Å^{-3}.

The previously reported triclinic cell (a = 6.897(3) Å, b = 12.023(4) Å, c = 22.646(7) Å, α = 100.81(3)°, β = 98.69(3)°, γ = 106.73(3)°)[105] can be transformed by the matrix (–1 –1 0 / –1 –1 –1/ 1 0 0) to the reduced cell (a = 12.016(4) Å, b = 22.536(7) Å, c = 6.897(3) Å, α = 90.04(3)°, β = 106.62(3)°, γ = 75.08(3)°) for the true monoclinic C-centered cell (a = 23.028(8) Å, b = 6.897(3) Å, c = 22.536(7) Å, β = 105.57(3)°). The reduced cell is transformed to the monoclinic cell by the transformation matrix (2 0 1 / 0 0 1 / 0 –1 0). Two supposedly independent [Cu(**1**)]$^+$ complexes were found in the asymmetric unit of the triclinic unit cell; in the true monoclinic cell these [Cu(**1**)]$^+$ units are related by a center of inversion.

The Determination of the Structure of 11b. A crystal of **11** was mounted on a glass fiber, cooled to –130(1) °C, and centered on the X-ray diffractometer. The cell constants reported in Table 4.1 were calculated from a least squares fit to the setting angles for 25 independent reflections ($2\theta_{ave}$ = 18.59°). The intensities of three control reflections were monitored every 97 reflections; these intensities showed no significant variation during the course of data collection. The data were corrected for Lorentz and polarization factors, but not for absorption effects. The space group was $P1$ or $P\bar{1}$. The structure was solved readily by Patterson map interpretation in $P\bar{1}$. All nonhydrogen atoms were refined with anisotropic thermal parameters. Hydrogen atoms bound to carbon were placed in idealized positions (C–H = 0.96 Å, $U_{iso}(H) = 1.2 \times U_{iso}(C)$). The weighted [$w = (\sigma^2(F) + g(F)^2)^{-1}$] least squares refinement on F yielded the residual values listed in Table 4.1 at convergence (for the last twenty cycles, mean shift/e.s.d = 0.025, max shift/e.s.d. = 0.30

for rotation of methyl group C117). The height of the highest peak in the final ΔF map was +1.0 e $Å^{-3}$ (near O1), while the minimum was –0.688 e $Å^{-3}$.

Results and Discussion

The structure of **11a** is displayed in Figure 4.1. A plot displaying the one-dimensional polymeric chain, which consists of repeating units of the cation above, is shown in Figure 4.2. Tables 4.2, 4.3, and 4.4 list the atomic coordinates, bond lengths, and bond angles, respectively. Tables of anisotropic thermal parameters and hydrogen atom coordinates are included in the appendix as Tables S-4.1 and S-4.2, respectively.

At room temperature, crystals of **11** contain an infinite polymer, the basic repeat unit of which is the $[Cu(\mathbf{1})]^+$ cation (see Figure 4.2). Bridging between the $[Cu(\mathbf{1})]^+$ cations is accomplished through oxime atoms (Cu–N–O–Cu) with propagation of the chain parallel to the *b* axis. Each copper(II) ion is six-coordinate, with five coordination sites occupied by the nitrogen atoms of ligand **1** and the oxime oxygen atom of an adjacent $[Cu(\mathbf{1})]^+$ cation. The sixth site is occupied by the methanol oxygen atom; however the formula for **11a** is consistent with two copper(II) atoms per molecule of methanol. The methanol molecule is disordered between $[Cu(\mathbf{1})]^+$ moieties in the adjacent polymeric chains in such a way as to locate its oxygen atom near one of the $[Cu(\mathbf{1})]^+$ units, only half the time. The remaining time the site is unoccupied. The oxygen atom of the occluded methanol molecule is *trans* to the bridging O2(oxime) atom and could possibly be viewed as "semi-coordinated" to the copper(II) atom.[82]

The four nitrogen atoms of ligand **1** (N1, N4, N8, N11) form a plane ($18.94(6)x + 3.55(13)y - 10.16(8)z = 3.98(2)$; $\Sigma\Delta^2 = 0.0031$, $\sigma^2 = 0.03$) with maximum deviations for these four atoms from this plane seen for N1 (0.028(4) Å) and N11 (–0.028(4) Å). The copper(II) atom is displaced from this plane (by 0.117(2) Å) in the direction of the bridging oxime oxygen atom. The average of the four equatorial Cu–N bond lengths is 1.94(1) Å. Two of the Cu–N bonds (Cu–N1 = 1.951(4) Å and Cu–N4 = 1.954(4) Å) are

Figure 4.1. Thermal ellipsoid plot (50% probability) of the cation of **11a**. Hydrogen atoms have been omitted for clarity.

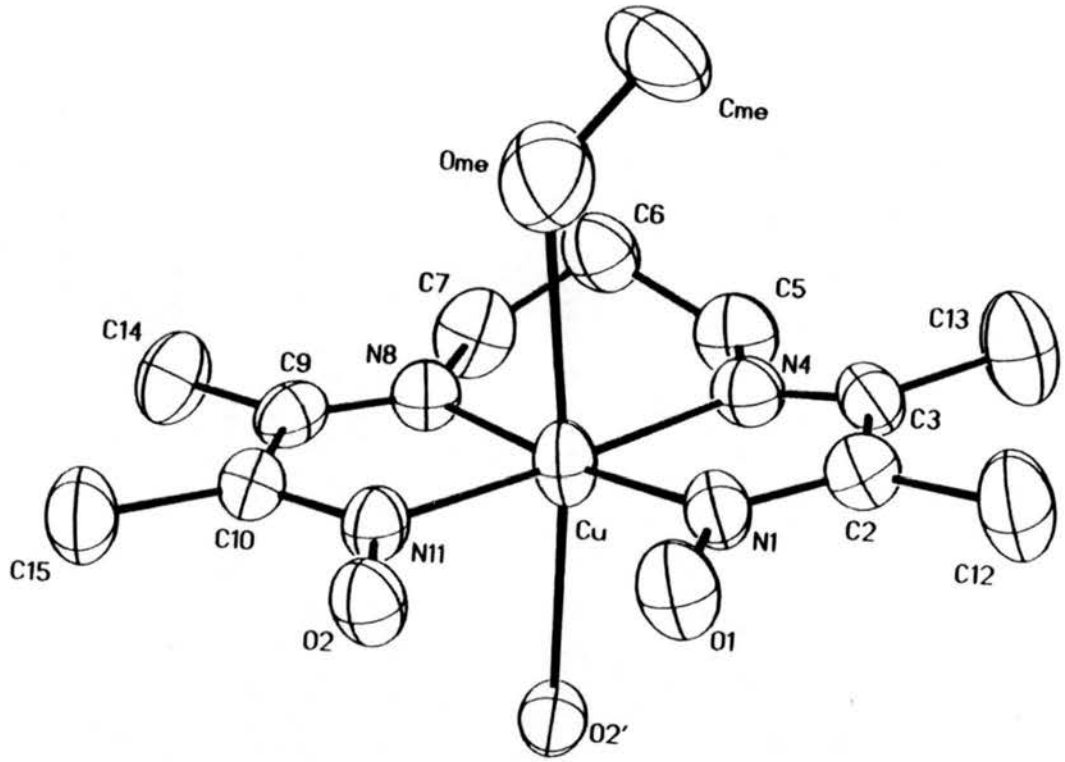
Cme
Ome
C6
C7
C5
C14
C9
N8
N4
C13
C3
C10
N11
Cu
N1
C2
C15
C12
O2
O1
O2'

Figure 4.2. Ball and stick plot of a portion of the one-dimensional polymer chain in **11a**. Hydrogen atoms have been omitted for clarity.

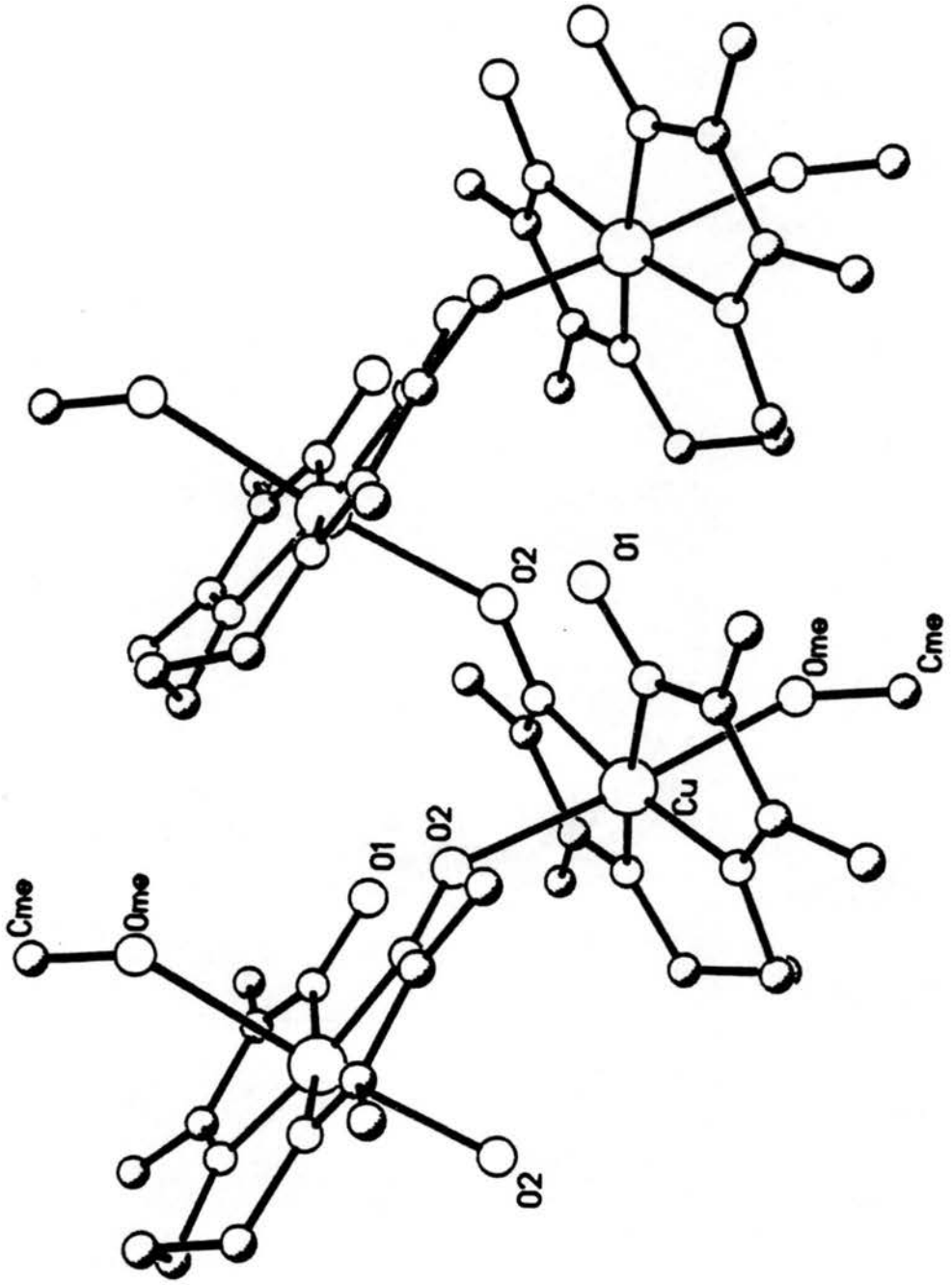
O2
O1
Ome
Cme
Cu
O2
O1
Cme
Ome
O2

Table 4.2. Atomic coordinates ($\times 10^4$) and isotropic thermal parameters ($Å^2 \times 10^3$)[a] for **11a**.

atom	*x*	*y*	*z*	U_{iso}[b]
Cu	3340(1)	371(1)	2555(1)	57(1)
N1	3530(2)	1924(7)	3306(2)	51(2)
C2	3942(3)	1259(9)	3761(3)	55(2)
C3	4205(2)	–591(8)	3615(3)	55(2)
N4	3970(2)	–1252(7)	3075(2)	55(2)
C5	4148(3)	–3069(9)	2830(3)	79(3)
C6	4142(3)	–2835(13)	2141(4)	74(3)
C6'	3733(17)	–3796(49)	2326(14)	72(14)
C7	3545(3)	–2717(10)	1711(3)	78(3)
N8	3231(2)	–899(7)	1769(2)	52(2)
C9	2873(3)	–38(9)	1318(2)	52(2)
C10	2618(3)	1832(8)	1474(2)	53(2)
N11	2777(2)	2196(7)	2055(2)	49(2)
C12	4134(4)	2183(12)	4385(3)	84(3)
C13	4704(3)	–1494(12)	4096(3)	97(4)
C14	2697(4)	–749(11)	660(3)	82(3)
C15	2204(3)	3082(12)	997(3)	77(3)
O1	3239(2)	3583(6)	3365(2)	64(2)
O2	2587(2)	3806(6)	2288(2)	57(1)
Cl	4049(1)	3254(3)	696(1)	71(1)
O3	3746(8)	4850(18)	373(7)	256(16)
O4	3805(5)	2827(16)	1198(5)	157(8)
O5	4032(6)	1640(15)	335(5)	148(8)
O6	4656(4)	3802(26)	969(7)	225(12)
O3'	4149(5)	1515(12)	1036(5)	252(16)
O4'	3464(4)	3909(18)	612(7)	145(11)
O5'	4465(6)	4639(15)	1018(7)	144(11)
O6'	4171(7)	2911(23)	123(4)	166(13)
Cme	4844(5)	2176(23)	2280(5)	109(5)
Ome	4237(5)	2186(17)	2280(5)	109(5)

[a] Estimated standard deviations in the least significant digits are given in parentheses.
[b] The equivalent isotropic U_{iso} is defined as one–third of the trace of the U_{ij} tensor.

Table 4.3. Bond lengths (Å)[a] for **11a**.

Cu–N1	1.951(4)	Cu–N4	1.954(4)
Cu–N8	1.930(5)	Cu–N11	1.938(4)
Cu–Ome	2.628(12)	Cu–O2a	2.499(4)
N1–C2	1.281(6)	N1–O1	1.351(6)
C2–C3	1.487(9)	C2–C12	1.498(9)
C3–N4	1.276(7)	C3–C13	1.489(9)
N4–C5	1.472(8)	C5–C6	1.556(11)
C5–C6'	1.369(31)	C6–C7	1.458(9)
C6'–C7	1.528(32)	C7–N8	1.471(8)
N8–C9	1.271(6)	C9–C10	1.498(8)
C9–C14	1.510(8)	C10–N11	1.287(7)
C10–C15	1.503(8)	N11–O2	1.351(6)
Cl–O3	1.400(14)	Cl–O4	1.419(13)
Cl–O5	1.373(11)	Cl–O6	1.419(9)
Cl–O3'	1.409(9)	Cl–O4'	1.385(9)
Cl–O5'	1.409(11)	Cl–O6'	1.413(12)
Cme–Ome	1.365(15)		

[a] Estimated standard deviations in the least significant digits are given in parentheses.

Table 4.4. Bond angles (deg)[a] for **11a**.

N1–Cu–N4	80.6(2)	N1–Cu–N8	171.3(2)
N4–Cu–N8	100.5(2)	N1–Cu–N11	96.1(2)
N4–Cu–N11	174.1(2)	N8–Cu–N11	82.0(2)
N1–Cu–Ome	86.2(3)	N4–Cu–Ome	84.9(3)
N8–Cu–Ome	85.3(3)	N11–Cu–Ome	89.9(3)
N1–Cu–O2a	96.8(2)	N4–Cu–O2a	101.1(2)
N8–Cu–O2a	91.5(2)	N11–Cu–O2a	84.2(2)
Ome–Cu–O2a	173.6(2)	Cu–Ome–Cme	132.2(12)
Cu–N1–C2	116.3(4)	Cu–N1–O1	123.3(3)
C2–N1–O1	120.4(5)	N1–C2–C3	112.9(5)
N1–C2–C12	124.5(6)	C3–C2–C12	122.6(5)
C2–C3–N4	115.1(5)	C2–C3–C13	118.6(5)
N4–C3–C13	126.3(6)	Cu–N4–C3	115.1(4)
Cu–N4–C5	120.1(3)	C3–N4–C5	124.8(5)
N4–C5–C6	110.8(6)	N4–C5–C6'	114.8(16)
C5–C6–C7	115.1(7)	C5–C6'–C7	122.6(25)
C6–C7–N8	112.8(6)	C6'–C7–N8	111.3(15)
Cu–N8–C7	121.5(3)	Cu–N8–C9	114.7(4)
C7–N8–C9	123.9(5)	N8–C9–C10	115.3(5)
N8–C9–C14	125.3(6)	C10–C9–C14	119.3(5)
C9–C10–N11	112.5(5)	C9–C10–C15	122.8(5)
N11–C10–C15	124.6(6)	Cu–N11–C10	115.5(4)
Cu–N11–O2	123.1(3)	C10–N11–O2	121.5(4)
O3–Cl–O4	109.3(9)	O3–Cl–O5	113.5(7)
O4–Cl–O5	110.4(7)	O3–Cl–O6	108.1(10)
O4–Cl–O6	105.3(8)	O5–Cl–O6	109.9(9)
O3'–Cl–O4'	111.4(8)	O3'–Cl–O5'	108.0(7)
O4'–Cl–O5'	110.6(7)	O3'–Cl–O6'	108.0(8)
O4'–Cl–O6'	110.7(9)	O5'–Cl–O6'	108.0(9)

[a] Estimated standard deviations in the least significant digits are given in parentheses.

longer, than the other two (Cu-N8 = 1.930(5) Å, Cu–N11 = 1.938(4) Å). The Cu–O2a (axial) bond length is long (2.499(4) Å) compared to similar compounds.[106] Only one of the two oxime oxygen atoms is deprotonated and the bridging oxime oxygen atom must also serve as a hydrogen bond acceptor.[105] Thus, a weaker bond is formed to the adjacent copper(II) atom.

The perchlorate counterion was found to be disordered between two crystallographically unrelated positions. The counterions fill the space between the one-dimensional polymeric chains. The anion does not appear likely to influence the structure of the cations, as the closest contact between any perchlorate atom and the $[Cu(\mathbf{1})]^+$ unit occurs between O4 and N8 (3.30(1) Å).

The structure of **11b** is displayed in Figure 4.3. A plot of the intermolecular units is shown in Figure 4.4. Tables of atomic coordinates, bond lengths, and bond angles for **11b** are included as Tables 4.5, 4.6, and 4.7 respectively. Tables of anisotropic thermal parameters and hydrogen atom coordinates are found in the Appendix as Tables S-4.3 and S-4.4, respectively.

At –130 °C, crystals of **11** contain dimeric copper(II) units (see Figure 4.3). The asymmetric unit consists of two crystallographically unique $[Cu(\mathbf{1})]^+$ cations. Bridging between the copper(II) atoms to form the dimer is accomplished through oxime atoms (Cu1–N11–O12–Cu2).

One of the copper(II) atoms, Cu2, is five-coordinate, with four coordination sites occupied by the nitrogen atoms of ligand **1** and the fifth site occupied by an oxime oxygen atom from the adjacent $[Cu(\mathbf{1})]^+$ unit. The coordination geometry about Cu2 is square pyramidal, with the basal nitrogen atoms (N101, N104, N108, and N111) forming a plane $[3.38(4)x - 7.74(2)y - 10.32(6)z = -9.13(1);\ \Sigma\Delta^2 = 0.0012,\ \sigma^2 = 0.017]$; the maximum deviation from this plane occurs for N101 (0.018(5) Å) and N111 (–0.018(5) Å). The Cu2 atom is displaced from this plane by 0.210(2) Å in the direction of the bridging apical oxime oxygen atom (O12) of the adjacent $[Cu(\mathbf{1})]^+$ unit. The average basal

Figure 4.3. Thermal ellipsoid plot (50% probability) of the dimeric cation of **11b**. Hydrogen atoms have been omitted for clarity.

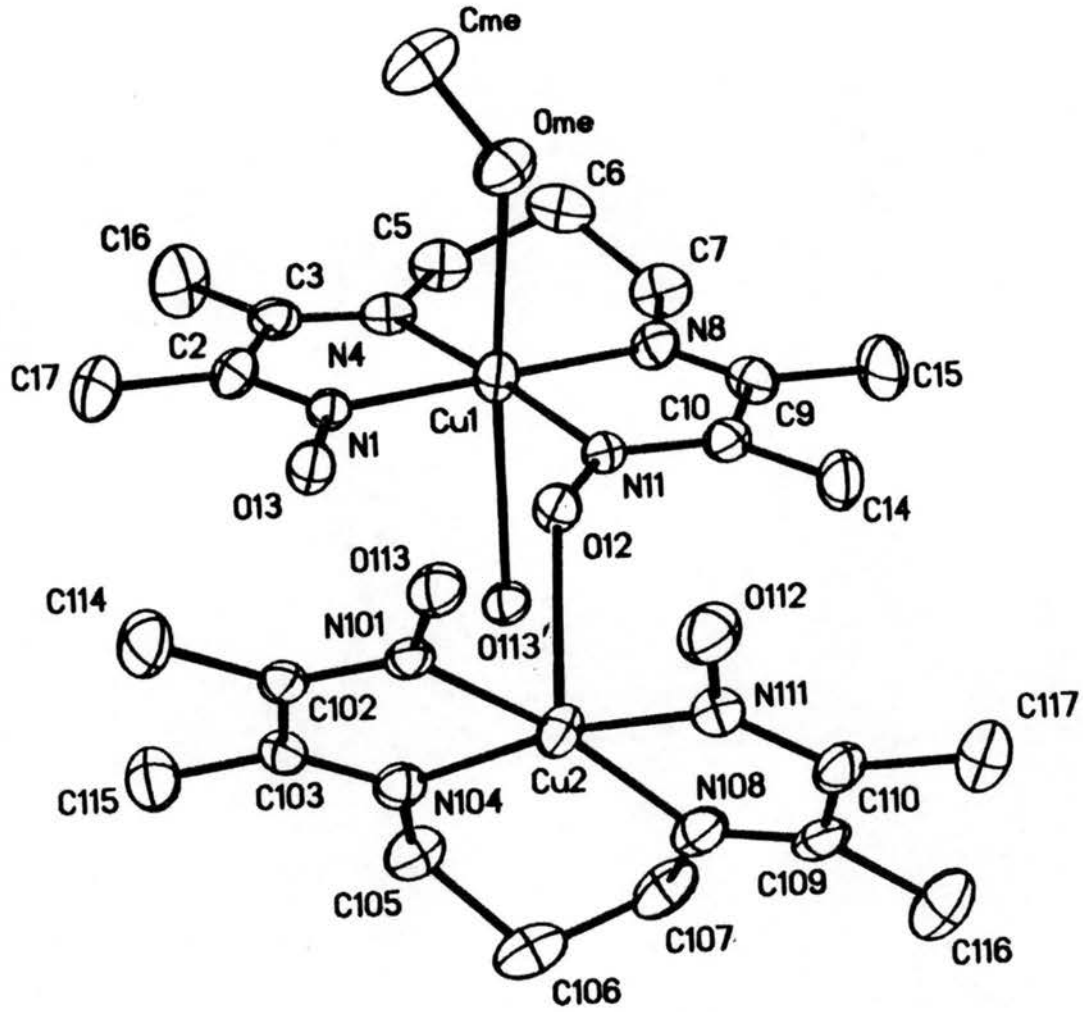
Cme
Ome
C6
C5
C16
C7
C3
N8
C2
N4
C17
C15
C10
C9
Cu1
N1
N11
O13
C14
O12
O113
C114
O112
N101
O113'
N111
C102
C117
C115
C103
N104
Cu2
N108
C110
C105
C109
C107
C116
C106

Figure 4.4. Ball and stick plot showing interactions between the cations of **11b**. Hydrogen atoms have omitted for clarity.

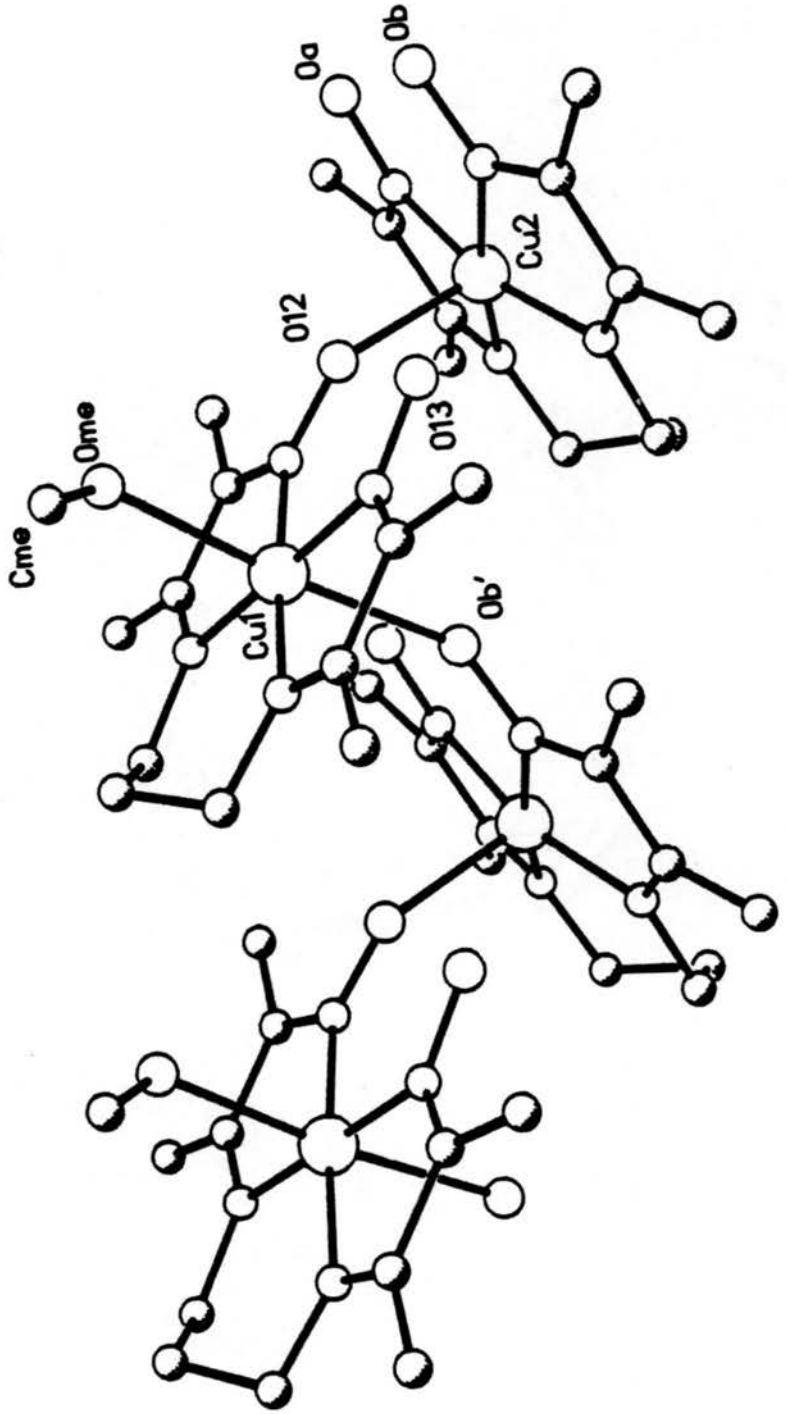
Oa
Ob
Cu2
O12
O13
Ome
Cme
Cu1
Ob'

Table 4.5. Atomic coordinates ($\times 10^4$) and isotropic thermal parameters ($Å^2 \times 10^3$)[a] for **11b**.

atom	*x*	*y*	*z*	U_{iso}[b]
Cu1	2808(1)	3301(1)	2558(1)	25(1)
Cu2	–3603(1)	6672(1)	2452(1)	25(1)
N1	1499(6)	2988(3)	3346(2)	20(1)
C2	2563(7)	2213(4)	3806(2)	25(2)
C3	4756(8)	1718(4)	3649(2)	28(2)
N4	5144(6)	2129(4)	3089(2)	24(1)
C5	7155(8)	1739(5)	2833(3)	35(2)
C6	6967(8)	1780(5)	2147(3)	36(2)
C7	6229(8)	3024(5)	1704(3)	35(2)
N8	4081(6)	3622(4)	1769(2)	26(2)
C9	2855(8)	4393(5)	1319(2)	27(2)
C10	736(7)	4887(4)	1487(2)	23(2)
N11	448(6)	4514(3)	2072(2)	21(1)
O12	–1381(5)	4857(3)	2308(2)	23(1)
O13	–517(5)	3531(3)	3408(2)	26(1)
C14	–904(9)	5714(5)	1008(2)	35(2)
C15	3467(9)	4802(6)	672(3)	41(2)
C16	6212(10)	825(6)	4155(3)	51(3)
C17	1825(9)	1843(5)	4442(3)	39(2)
N101	–5002(6)	5604(3)	2980(2)	20(1)
C102	–4505(7)	5299(4)	3562(2)	21(2)
C103	–2861(7)	5784(4)	3713(2)	23(2)
N104	–2255(6)	6486(4)	3254(2)	24(1)
C105	–738(8)	7084(5)	3317(3)	32(2)
C106	–1253(8)	8361(5)	2864(3)	36(2)
C107	–1061(8)	8384(5)	2181(3)	36(2)
N108	–2667(6)	8008(4)	1944(2)	29(2)
C109	–3663(8)	8513(4)	1404(3)	27(2)
C110	–5250(8)	7983(4)	1265(2)	28(2)
N111	–5471(6)	7117(4)	1726(2)	24(1)
O112	–6842(6)	6525(3)	1679(2)	32(1)
O113	–6494(5)	5255(3)	2756(2)	26(1)
C114	–5489(9)	4562(5)	4050(3)	36(2)
C115	–2033(9)	5465(5)	4370(2)	35(2)
C116	–3271(10)	9519(5)	923(3)	46(2)
C117	–6451(10)	8384(5)	661(3)	39(2)
Cl1	2797(2)	8145(1)	4236(1)	32(1)
O1	3256(7)	7873(4)	3640(2)	57(2)
O2	1142(8)	9213(4)	4123(3)	81(2)
O3	4531(9)	8305(7)	4475(4)	145(5)
O4	2250(11)	7178(5)	4621(3)	107(4)
C12	842(2)	1969(1)	668(1)	29(1)
O5	1286(14)	904(6)	1170(3)	110(6)
O5'	2385(15)	2106(12)	1020(5)	117(13)

Table 4.5. (continued)

atom	*x*	*y*	*z*	U_{iso}[b]
O6	2550(11)	1954(8)	307(4)	125(6)
O6'	97(19)	1021(10)	1012(6)	72(9)
O7	–858(13)	2017(9)	314(4)	186(10)
O7'	1636(16)	1677(10)	119(4)	53(4)
O8	359(13)	2973(6)	912(4)	121(7)
O8'	–768(14)	3051(8)	503(5)	85(8)
Ome	1830(6)	1692(3)	2292(2)	36(1)
Cme	2537(10)	432(5)	2600(3)	49(3)

[a] Estimated standard deviations in the least significant digits are given in parentheses.
[b] The equivalent isotropic U is defined as one-third of the trace of the U_{ij} tensor.

Table 4.6. Bond lengths (Å)[a] for **11b**.

Cu1–N1	1.958(4)	Cu1–N4	1.964(3)
Cu1–N8	1.948(4)	Cu1–N11	1.950(3)
Cu1–O11a	2.642(1)	Cu1–Ome	2.404(1)
Cu2–N101	1.952(4)	Cu2–N104	1.960(4)
Cu2–N108	1.964(4)	Cu2–N111	1.947(4)
Cu2–O12	2.352(3)		
N1–C2	1.263(5)	N1–O13	1.368(5)
C2–C3	1.518(7)	C2–C17	1.498(7)
C3–N4	1.273(7)	C3–C16	1.490(7)
N4–C5	1.476(6)	C5–C6	1.525(9)
C6–C7	1.505(7)	C7–N8	1.462(6)
N8–C9	1.293(6)	C9–C10	1.482(7)
C9–C15	1.495(8)	C10–N11	1.296(6)
C10–C14	1.499(6)	N11–O12	1.343(5)
N101–C102	1.280(6)	N101–O113	1.353(6)
C102–C103	1.483(8)	C102–C114	1.494(8)
C103–N104	1.291(6)	C103–C115	1.497(7)
N104–C105	1.444(8)	C105–C106	1.541(7)
C106–C107	1.520(9)	C107–N108	1.454(8)
N108–C109	1.305(6)	C109–C110	1.475(8)
C109–C116	1.475(8)	C110–N111	1.297(6)
C110–C117	1.487(8)	N111–O112	1.344(6)
Cl1–O1	1.454(5)	Cl1–O2	1.408(4)
Cl1–O3	1.391(8)	Cl1–O4	1.390(6)
Cl2–O5	1.421(6)	Cl2–O5'	1.397(13)
Cl2–O6	1.407(8)	Cl2–O6'	1.412(13)
Cl2–O7	1.398(10)	Cl2–O7'	1.416(9)
Cl2–O8	1.388(9)	Cl2–O8'	1.403(8)
Ome–Cme	1.422(6)		

[a] Estimated standard deviations in the least significant digits are given in parentheses.

Table 4.7. Bond angles (deg)[a] for **11b**.

N1–Cu1–N4	80.3(2)	N1–Cu1–N8	179.4(2)
N4–Cu1–N8	100.4(2)	N1–Cu1–N11	97.1(2)
N4–Cu1–N11	176.4(2)	N8–Cu1–N11	82.2(2)
N1–Cu1–Ome	89.7(1)	N4–Cu1–Ome	91.4(1)
N8–Cu1–Ome	90.1(1)	N11–Cu1–Ome	90.1(1)
N1–Cu1–O11a	91.7(1)	N4–Cu1–O11a	95.6(1)
N8–Cu1–O11a	88.3(1)	N11–Cu1–O11a	82.0(1)
Cu1–Ome–Cme	126.5(1)	Cu2–O12–N11	136.8(3)
N101–Cu2–N104	81.4(2)	N101–Cu2–N108	168.5(2)
N104–Cu2–N108	99.3(2)	N101–Cu2–N111	95.3(2)
N104–Cu2–N111	166.5(2)	N108–Cu2–N111	81.4(2)
N101–Cu2–O12	84.6(1)	N104–Cu2–O12	93.5(1)
N108–Cu2–O12	106.8(1)	N111–Cu2–O12	99.3(1)
Cu1–N1–C2	117.7(3)	Cu1–N1–O13	122.9(2)
C2–N1–O13	119.4(4)	N1–C2–C3	111.7(4)
N1–C2–C17	125.4(4)	C3–C2–C17	122.9(4)
C2–C3–N4	115.2(4)	C2–C3–C16	117.7(5)
N4–C3–C16	127.1(5)	Cu1–N4–C3	115.0(3)
Cu1–N4–C5	120.9(3)	C3–N4–C5	124.1(4)
N4–C5–C6	112.1(4)	C5–C6–C7	116.3(5)
C6–C7–N8	112.1(4)	Cu1–N8–C7	121.9(3)
Cu1–N8–C9	113.9(3)	C7–N8–C9	124.2(4)
N8–C9–C10	115.3(4)	N8–C9–C15	124.2(5)
C10–C9–C15	120.5(4)	C9–C10–N11	114.0(4)
C9–C10–C14	121.6(4)	N11–C10–C14	124.3(4)
Cu1–N11–C10	114.3(3)	Cu1–N11–O12	123.0(3)
C10–N11–O12	122.4(3)	Cu2–N101–C102	116.0(4)
Cu2–N101–O113	122.7(3)	C102–N101–O113	121.2(4)
N101–C102–C103	112.9(4)	N101–C102–C114	124.7(5)
C103–C102–C114	122.4(4)	C102–C103–N104	116.2(4)
C102–C103–C115	119.8(4)	N104–C103–C115	124.1(5)
Cu2–N104–C103	113.4(4)	Cu2–N104–C105	122.7(3)
C103–N104–C105	123.9(5)	N104–C105–C106	111.1(4)
C105–C106–C107	115.2(5)	C106–C107–N108	111.9(5)
Cu2–N108–C107	120.9(3)	Cu2–N108–C109	113.4(4)
C107–N108–C109	125.7(5)	N108–C109–C110	116.1(4)
N108–C109–C116	125.4(6)	C110–C109–C116	118.5(5)
C109–C110–N111	112.7(4)	C109–C110–C117	123.8(5)
N111–C110–C117	123.5(6)	Cu2–N111–C110	116.2(4)
Cu2–N111–O112	122.8(3)	C110–N111–O112	120.8(4)

Table 4.7. (continued)

O1–Cl1–O2	106.9(3)	O1–Cl1–O3	107.9(4)
O2–Cl1–O3	111.8(4)	O1–Cl1–O4	107.9(3)
O2–Cl1–O4	110.3(3)	O3–Cl1–O4	111.8(4)
O5–Cl2–O5'	77.1(7)	O5–Cl2–O6	109.7(5)
O5'–Cl2–O6'	109.9(7)	O5–Cl2–O7	108.8(6)
O6–Cl2–O7	111.1(5)	O5'–Cl2–O7'	109.5(7)
O6'–Cl2–O7'	108.9(7)	O5–Cl2–O8	108.3(5)
O6–Cl2–O8	110.3(6)	O7–Cl2–O8	108.5(6)
O5'–Cl2–O8'	110.6(7)	O6'–Cl2–O8'	109.3(6)
O7'–Cl2–O8'	108.6(6)		

[a] Estimated standard deviations in the least significant digits are given in parentheses.

Cu2–N bond length is 1.956(7) Å, which may be longer than that seen in **11a** (1.94(1)). Three of the four Cu2–N bonds (Cu2–N101 = 1.952(4) Å, Cu2–N104 = 1.960(4) Å, Cu2–N108 = 1.948(4) Å) are equivalent in length within experimental error, while the Cu2–N111 bond (1.947(4) Å) may be shorter than Cu2–N104 and Cu2–N108. The bond length to the apical oxygen atom (Cu2–O12 = 2.352(3) Å) is significantly shorter than that seen in **11a** (Cu–O2a = 2.499(4) Å), which suggests a stronger bonding interaction between the copper(II) atoms in the dimeric unit.

The coordination sphere about the adjacent copper(II) atom (Cu1) is quite different than that about Cu2. The Cu1 atom is six-coordinate with four sites occupied by nitrogen atoms of **1**. The fifth and sixth sites, however, are occupied by a methanol oxygen atom and an oxime oxygen atom of an adjacent dimeric unit.

The coordination geometry about Cu1 might thus be described as Jahn-Teller distorted octahedral, with the equatorial sites occupied by the nitrogen atoms (N1, N4, N8, N11) of ligand **1**. These atoms form a plane ($3.47(5)x + 11.16(5)y + 10.16(7)z = 7.27(2)$; $\Sigma\Delta^2 = 0.0019$, $\sigma^2 = 0.022$). The maximum deviations from this plane occur for N1 (–0.022(5) Å) and N11 (0.022(5) Å). The axial sites are occupied by the oxime and methanol oxygen atoms. The copper(II) atom is displaced from the equatorial plane of the four nitrogen atoms by 0.019(2) Å in the direction of the methanol oxygen atom. The average equatorial Cu1–N bond length (1.956(7) Å) may be longer than Cu–N_{ave} in **11a** but is equivalent to the Cu2–N_{ave} in this structure. As was the case for Cu2, three of the four Cu1–N bonds are equivalent (Cu1–N1 = 1.958(4) Å, Cu1–N4 = 1.964(3) Å, Cu1–N11 = 1.950(3) Å) while the remaining bond (Cu1–N8 = 1.948(4) Å) may be shorter than Cu1–N4. The methanol oxygen atom forms a shorter bond to Cu1 (Cu1–O(methanol) = 2.404(1) Å) than does the "semi-coordinated" oxime oxygen atom (Cu1–O113 = 2.642(1)) Å).

Of the two perchlorate counterions one (containing Cl1) is ordered, while the oxygen atoms of the other (containing Cl2) are disordered between two sets of positions

which are not related by symmetry. The counterions reside between the dimeric units and do not appear to influence their structure; the closest contact distances for any perchlorate atoms are between O1 and C102 (3.01(1) Å) and between O8 and C9 (3.06(1) Å).

Summary

The crystals of **11** undergo a structural change upon cooling. This structural change involves the disruption of the one-dimensional polymeric chain of $[Cu(\mathbf{1})]^+$ cations seen at room temperature into units more appropriately described as dimers at low temperature. This structural change involves two adjacent $[Cu(\mathbf{1})]^+$ units. In the first unit (Cu1) the Cu–O2 bond length of 2.499(2) Å at room temperature is elongated to 2.642(1) Å (Cu1–O113) at low temperature. Along with the elongation of the Cu–O(oxime) bond, a contraction of the Cu–O(methanol) bond occurs; the value of 2.62(1) Å seen in the room temperature structure decreases to 2.404(1) Å at low temperature. The displacement of the copper(II) atom from the equatorial plane of the four nitrogen atoms changes from 0.117(2) Å in the direction of the oxime oxygen atom at room temperature, to 0.019(2) Å in the direction of the methanol oxygen atom at low temperature. The adjacent copper(II) unit, Cu2 (related by the centering operation in the room temperature structure) undergoes a very different structural change. The Cu–O(oxime) bond shortens from 2.499(2) Å at room temperature to 2.352(3) Å at low temperature. The copper(II) atom is pulled further out of the basal nitrogen atom plane by this change; the metal's displacement from that plane increases from 0.117(2) Å at room temperature to 0.210(2) Å at –130 °C.

These structural changes explain why thermochromic behavior was not observed for **11**. In undergoing the structural transformation that accompanies the phase change, the copper(II) atoms trade one environment with weakly bonded axial oxygen ligands for another environment with similarly weak axial coordination. The absence of any major change in the coordination environments results in the lack of observable change in the color of this material.

References

1. Kappenstein, C.; Hugel, R. P. *Inorg. Chem.* **1977**, *16*, 250.
2. Dyason, J. C.; Healy, P. C.; Engelhardt, K. M.; Pakawatchai, C.; Patrick, V. A.; White, A. H. *J. Chem. Soc. Dalton Trans.* **1985**, 839.
3. Morpurgo, G. O.; Dessy, G.; Fares, V. *J. Chem. Soc. Dalton Trans.* **1984**, 785.
4. Morris, D. F. *Acta Cryst.* **1961**, *14*, 547.
5. Chaudhuri, P.; Oder, K.; Wieghardt, K.; Weiss, J.; Reedijk, J.; Hinrichs, W.; Wood, J.; Ozarowski, A.; Stratemaier, H.; Reinen, D. *Inorg. Chem.* **1986**, *25*, 2951.
6. Kappenstein, C.; Hugel, R. P. *Inorg. Chem.* **1978**, *17*, 1945.
7. Shriver, D. F. *Struct. Bond.* (Berlin) **1966**, *1*, 33.
8. Shriver, D. F.; Posner, J. *J. Am. Chem. Soc.* **1966**, *88*, 1672.
9. Peng, Shie-ming; Liaw, Der-Shin *Inorg. Chim. Acta* **1986**, *113*, L11.
10. Cromer, D. T.; Larson, A. C.; Roof, R. B. *Acta Cryst.* **1965**, *19*, 192.
11. Fronczek, F. R.; Schaefer, W. P. *Inorg. Chem.* **1974**, *13*, 727.
12. Wang, Bi-Cheng; Schaefer, W. P.; Marsh, R. E. *Inorg. Chem.* **1971**, *10*, 1492.
13 Cromer, D. T. *J. Phys. Chem.* **1957**, *61*, 1388.
14 Cromer, D. T.; Douglas, R. M.; Staritzky, E. *Anal. Chem.* **1957**, *29*, 316.
15 Dessy, G.; Fares, V.; Imperatori, P.; Morpurgo, G. *J. Chem. Soc. Dalton Trans.* **1985**, 1285.
16. Williams, R. J.; Cromer, D. T.; Larson, A. C. *Acta Cryst.* **1971**, *B27*, 1701.
17. Connor, J. A.; Gibson, D.; Price, R. *J. Chem. Soc. Dalton Trans.* **1986**, 346.
18. Cromer, D. T.; Larson, A. C.; Roof, R. B. *Acta Cryst.* **1966**, *20*, 279.
19. Cromer, D. T.; Larson, A. C. *Acta Cryst.* **1972**, *B28*, 1052.

20. Kirfel, A. *Acta Cryst.* **1977**, *B33*, 2788.

21. Vrabel, V.; Garaj, J.; Kutschabsky, L. *Acta Cryst.* **1979**, *B35*, 357.

22. Kappenstein, C.; Schubert, U. *J. Chem. Soc. Chem. Commun.* **1980**, 1116.

23. Roof, R. B.; Larson, A. C.; Cromer, D. T. *Acta Cryst.* **1968**, *B24*, 269.

24. Wicholas, M.; Wolford,T. *Inorg. Nucl. Chem. Letters* **1975**, *11*, 157.

25. Anderson, O. P.; Packard, A. B. *Inorg. Chem.* **1980**, *19*, 2941.

26. Schlemper, E. O.; Hussain, M. S.; Murmann, K. R. *Acta Cryst.* **1981**, *B37*, 234.

27. Jungst, R.; Stucky, G. *Inorg. Chem.* **1974**, *13*, 2404.

28. Wicholas, M.; Wolford, T. *Inorg. Chem.* **1974**, *13*, 316.

29. Pascal constants taken from: Drago, R. S. *Physical Methods in Chemistry*; Saunders, W. B.: Phiadelphia, 1975; p 413.

30. Nishida, Y.; Takeuchi, M.; Oishi, N.; Kida, S. *Inorg. Chim. Acta* **1985**, *96*, 81.

31 Griffths, P. R.; deHaseth, J. A. *Fourier Transform Infrared Spectrometry*; John Wiley & Sons: New York, **1985**.
Gillete, P. C.; Lando, J. B.; Koenig, J. G. in *Fourier Transform Spectroscopy*; Ferraro, J. R.; Basile, L. B., Ed.; Academic Press: New York, 1985; Vol. 4, pp 1-47.

32. Griffiths, P. R. *Science* **1983**, *221*, 297.

33. Wood, D. L.; Mitra, S. S. *J. Am. Opt. Soc.* **1958**, *48*, 537.

34. Charney, E. *J. Am. Opt. Soc.* **1955**, *45*, 980.

35. Sharpe, A. G. *The Chemistry of Cyano Complexeses of the Transition Metals*; Academic Press: New York, 1976; pp 10–14.

36. El-Sayed, M. F.; Sheline, R. K. *J. Inog. Nucl. Chem.* **1958**, *6*, 187.

37. Dows, D. A.; Haim, A.; Wilmarth, W. K. *J. Inorg. Nucl. Chem.* **1961**, *21*, 33.

38. Liang, C.Y.; Krimm, S.; Sutherland, G.M. *J. Chem. Phys.* **1956**, *25*, 543.

39. *International Tables for X-ray Crystallograpy* **1974**, *4* , pp 55,99,149.

40. Gagne, R. R.; Allison, J. L.; Gall, R. S.; Koval, C. A. *J. Am. Chem. Soc.* **1977**, *99*, 7170.

41. Solomon, E. I. in *Copper Proteins;* Spiro T. G., Ed.; Wiley: New York, 1981; pp 41-108.

42. Redfield, A. G.; Collige, T.; Montgomery, H. *J. Biol. Chem.* **1928**, *76*, 197.

43. Van Holde, K. E.; Miller, K. I. *Q. Rev. Biophys.* **1982**, *15*, 1.

44. Woolery, G. L.; Powers, L.; Winkler, M.; Solomon, E. I.; Spiro T.G. *J. Am. Chem. Soc.* **1984**, *106*, 86.

45. Co, M. S.; Hodgson K. E.; Eccles, T. K.; Lontie, R. *J. Am. Chem. Soc.* **1981**, *103*, 984.

46. Brown, J. M.; Powers, L.; Kincaid, B.; Larrabee, J. A.; Spiro, T. G.; *J. Am. Chem. Soc.* **1980** *102*, 4210.

47. Eickman, N. C.; Himmelwright, R. S.; Soloman, E. I *Proc. Natl. Acad. Sci. U.S.A.* **1979**, *76*, 2094.

48. Dooley, D. M.; Scott, R. A.; Ellinghaus, J.; Solomon, E. I.; Gray, H. B. *Proc. Natl. Acad. Sci. U.S.A.* **1978**, *75*, 3019.

49. Soloman, E. I; Penfield, K. W.; Wilcox, D. E. *Struct. Bond.* (Berlin) **1983**, *53*, 1.

50. Solomon, E. I; Dooley, D. M.; Wang, R.; Gray, H. B.; Cerdonio, M.; Mogno, F; Romani, G. L.; *J. Am. Chem. Soc.* **1976**, *98*, 1029.

51. Larrabee, J. A.; Spiro, T. G. *J. Am. Chem. Soc.*, **1980** *102*, 4217.

52. Sorrell, T. N.; Jameson, D. L.; O'Connor, C. J. *Inorg. Chem.* **1984**, *23*, 190.

53. Sorrell, T. N.; O'Connor, C. J.; Anderson, O. P.; Reibenspies, J. H. *J. Am. Chem. Soc.* **1985**, *107*, 4199.

54. McKee, V.; Zvagulis, M.; Dagdigan, J. V.; Patch, M. G.; Reed, C. A. *J. Am. Chem. Soc.* **1984**, *106*, 93.

55. McKee, V.; Zvagulis, M.; Reed, C. A. *Inorg. Chem.*, **1985**, *24*, 2914.

56. Nishida, Y.; Takeuchi, M.; Takahashi, K; Kida, S. *Chem. Lett.* **1985**, 631.

57. Karlin, K. D.; Hayes, J. C.; Gultneh, Y.; Cruse, R. W.; McKown, J. W.; Hutchinson, J. P.; Zubieta J. *J. Am. Chem. Soc.* **1984**, *106*, 2121.

58. Karlin, K. D.; Hayes, J. C.; Hutchinson, J. P.; Zubieta, J. *J. Chem. Soc. Chem. Commun.* **1983**, 376.

59. Nishida, Y.; Shimo, H.; Maehara, H.; Kida, S. *J. Chem. Soc. Dalton Trans.* **1985**, 1945.

60. Wyatt, J. F.; Hillier, V. R. ; Saunders, R.; Connor, J. A.; Barber, M. *J. Chem. Phys.* **1971**, *54*, 5311.

61. Kahn, O *Inorg. Chim. Acta.* **1982**, *62*, 3.

62. Dori, Z.; Ziolo, R. *Chem. Rev.* **1973**, *73*, 247.

63. Kahn, O.; Sikorav, S.; Gouteron, J.; Jeannin, S.; Jeannin, Y. *Inorg. Chem.* **1983**, *22*, 2877.

64. Sikorav, S.; Waksman-Bkouche, I; Kahn, O. *Inorg. Chem.* **1984**, *23*, 490.

65. Mallah, T.; Boillot, M.; Kahn, O.; Gouteron, J.; Jeannin, S.; Jeannin, Y *Inorg. Chem.* **1986**, *25*, 3058.

66. Hay, P. J.; Thibeault, J. C.; Hoffmann, R. *J . Am. Chem. Soc.* **1975**, *97*, 4884.

67. Thompson, L. K.; Sanat, K; Gabe, E. J.; Charland J. *J. Chem. Soc. Chem. Commun.* **1986**, 1537.

68. Coughlin, P.K.; Lippard, S. J. *J. Am. Chem. Soc.* **1981**, *103*, 3228.

69. Karlin, K. D; Gultneh, Y.; Hayes, J. C.; Zubieta, J. *Inorg. Chem.* **1984**, *23*, 519.

70. Haddad, M. S.; Wilson, S. R.; Hodgson, D. J.; Hendrickson, D. N. *J. Am. Chem. Soc.* **1981**, *103*, 384.

71. Burk, P. L; Osborn, J. A.; Youinou, M.; Agnus, Y.; Louis, R.; Weiss, R *J. Am. Chem. Soc.* **1981**, *103*, 1273.

72. Huttner, G.; Gartzke, W.; Allinger K. *J. Organometallic Chem.* **1975**, *91*, 47.

73. Raymond, K. N.; Meek, D. W.; Ibers, J.A. *Inorg. Chem.* **1968**, *7*, 1111.

74. Addison, A. W; Nageswara, R. T.; Reedijk J.; vanRijn, J.; Verschoor G.C. *J. Chem. Soc. Dalton Trans.* **1984**, 1349.

75. a more rigorous approach in defining the 5 atom polyhedron is to calculate dihedral angles between the six faces of the polyhedron. Muetterties, E. L.; Guggenberger, L. J. *J. Am. Chem. Soc.* **1974**, *96*, 1748.

76. Sorrell, T. N.; Jameson D. L. *Inorg. Chem.* **1982**, *21*, 1014.

77. Crawford, V. H.; Richardson, H. W.; Wasson J. R.; Hodgson, D. J.; Hatfield, W.E. *Inorg. Chem.* **1976**, *15*, 2107.

78. Hodgson, D. J. *Prog. Inorg. Chem.*, **1975**, *19*, 173.

79. Addison, A. W.; Landee, C. P., Willet, R. D.; Wicholas, M. *Inorg. Chem.* **1980**, *19*, 1921.

80. Duggan, D. M; Jungst, R. G.; Mann, K. R.; Stucky, G. D.; Hendrickson, D. N. *J. Am. Chem. Soc.* **1974**, *96*, 3443.

81. Bauer, R. A.; Robinson, W. R.; Margerum, D. W. *J. Chem. Soc. Chem. Commun.* **1973**, 289.

82. Brown, D. S.; Lee, J. D.; Melson, B. G. A.; Hathaway, B. J.; Procter, I. M.; Tomlinson, A. A. *J. Chem. Soc. Chem. Commun.* **1967**, 369.

83. Bieksza, D. S; Hendrickson, D. N. *Inorg. Chem.* **1977**, *16*, 924.

84. Haddad, M. S.; Hendrickson, D. N. *Inorg Chim Acta* **1978**, *28*, L121.

85. Haddad, M. S.; Hendrickson, D. N. *Inorg. Chem.* **1978**, *17*, 2622.

86. Felthouse, T. R.; Hendrickson, D. N. *Inorg. Chem.* **1978**, *17*, 2636.

87. Haddad, M. S.; Hendrickson, D. N.; Cannady, J. P.; Drago, R.S.; Bieksza, D.S. *J . Am. Chem. Soc.* **1979**, *101*, 898.

88. Anderson, O. P.; Packard, A. B. *Inorg. Chem.* **1979**, *18*, 1940.

89. Anderson, O. P. *Acta Cryst.* **1981**, *B37*, 1194.

90. Anderson, O. P.; Packard A. B. *Inorg. Chem.* **1979**, *18*, 3064.

91. Gange, R. R; Allison, J. L.; Gall, R. S.; Koval, C. A. *J. Am. Chem. Soc.* **1977**, *99*, 7170.

92. $R_{merge} = (\Sigma(N\Sigma(w(F(mean)-F)^2/\Sigma((N-1)\Sigma(wF^2))$, where N = the number of symmetry equivalent reflections.

93. Nieminen, K.; Nasakkala, M. *Acta Chem. Scan.* **1980**, *A34*, 375.

94. Drew, M. G.; McCann, M.; Nelson, S. M. *J. Chem. Soc. Chem. Commun.* **1979**, 481.

95 Anderson, O. P.; Marshall, J. C. *Inorg. Chem.* **1978**, *17*, 1258.

96. Landau, L. D.; Lifshitz, E. M. *Statistical Physics*; Pergamon Press LTD: London, 1958; pp 134–138.

97. Cocharn, W. in *Structural Phase Transitions and Soft Modes, Proceeding of the NATO Advanced Study Institute at Geilo Norway*; Samuelsen, E. J; Andersen, E.; Feder, J., Ed.; Universitetsforlaget: Oslo, 1971; pp. 1-15.

98. Roberts S. A.; Bloomquist, D. R.; Willet, R. D.; Dodgen, H. W. *J. Am. Chem. Soc.* **1981**, *103*, 2603.

99. Grenthe, I.; Paoletti, P.; Sandstrom, M.; Glikberg, S. *Inorg. Chem.* **1979**, *10*, 2687.

100. Ferraro, J. R.; Basile, L. J.; Gracia-Ineguez, L. R; Paoletti, P.; Fabbrizzi, L. *Inorg. Chem.* **1976**, *15*, 2342.

101. Willet, R. D.; Hangen, J. A.; Lebsack, J. A.; Morrey, J. *Inorg. Chem.* **1974**, *15*, 2510

102. Fabbrizzi, L.; Micheloni, M.; Paoletti, P. *Inorg. Chem.* **1974**, *13*, 3019.

103. Menabue, L.; Pellacani, G. C.; Battaglia, L. P.; Corradi A. B.; Motori, A.; Sandrolini, F.; Pylkki, R. J.; Willet, R. D. *J. Chem. Soc. Dalton Trans.* **1984**, 2187.

104. Yamaki, S.; Fukuda, Y.; Sone, K. *Chem. Lett.*, **1982**, 269.

105. Bertrand, J. A.; Smith, J. H.; VanDerveer, D. G. *Inorg. Chem.* **1977**, *16*, 1484.

106. Pal, J.; Murmann, R. K.; Schlemper, E. O.; Fair, C. K. *Inorg. Chim. Acta* **1986**, *115*, 153.

107. Stevenson, D. L.; Dahl, L. F. *J. Am. Chem. Soc.* **1967**, *89*, 3424.

108. Johnson, J. E.; Jacobson, J. E. *J. Chem. Soc. Dalton Trans.* **1973**, 580.

109. Sttaalnick, J. K.; Ibers, J. A. *Inorg. Chem.* **1969**, *8*, 1084.

APPENDIX

Table S-1.1. Anisotropic thermal parameters ($Å^2 \times 10^3$)[a,b] for atoms of **4**.

atom	U_{11}	U_{22}	U_{33}	U_{23}	U_{13}	U_{12}
Cu1	50(1)	43(1)	45(1)	7(1)	15(1)	0(1)
C11	59(3)	47(2)	41(2)	–1(2)	15(2)	–1(2)
N11	64(2)	62(2)	56(2)	–5(2)	28(2)	–10(2)
C12	64(3)	64(3)	63(3)	–5(2)	28(2)	–10(2)
N12	104(4)	104(4)	110(4)	–31(3)	39(3)	–47(3)
C13	46(2)	41(2)	51(2)	9(2)	15(2)	–6(2)
N13	55(2)	47(2)	50(2)	1(2)	19(2)	–13(2)
Cu2	28(1)	32(1)	44(1)	8(1)	8(1)	0(1)
N21	30(2)	33(2)	59(2)	7(1)	9(1)	0(1)
N22	37(2)	38(2)	48(2)	11(1)	11(1)	5(1)
N23	26(2)	41(2)	51(2)	9(1)	6(1)	4(1)
N24	30(2)	37(2)	51(2)	14(1)	5(1)	3(1)
O21	29(1)	43(2)	88(2)	15(1)	2(1)	–1(1)
O22	32(2)	44(2)	84(2)	24(1)	–2(1)	5(1)
C21	42(2)	36(2)	53(2)	0(2)	19(2)	–5(2)
C22	55(3)	34(2)	44(2)	4(2)	18(2)	–2(2)
C23	43(2)	54(3)	83(3)	28(2)	10(2)	13(2)
C24	29(4)	33(4)	57(5)	7(3)	8(3)	14(3)
C24'	55(7)	107(9)	123(10)	61(9)	–12(7)	19(6)
C25	39(2)	53(3)	94(3)	26(2)	1(2)	13(2)
C26	35(2)	44(2)	43(2)	10(2)	12(2)	–5(2)
C27	32(2)	34(2)	48(2)	8(2)	8(2)	–1(2)
C28	48(3)	60(3)	87(3)	8(2)	30(2)	–13(2)
C29	78(3)	50(3)	77(3)	29(2)	24(3)	–3(2)
C30	37(2)	53(3)	73(3)	13(2)	–2(2)	–14(2)
C31	45(2)	38(2)	85(3)	18(2)	12(2)	–1(2)
Cu3	41(1)	52(1)	44(1)	0(1)	12(1)	–6(1)
N31	50(2)	54(2)	49(2)	–2(2)	16(2)	–5(2)
N32	49(2)	51(2)	50(2)	1(2)	15(2)	–3(2)
N33	51(2)	61(2)	48(2)	3(2)	15(2)	–13(2)
N34	56(2)	58(2)	58(2)	9(2)	23(2)	3(2)
O31	71(2)	68(2)	76(2)	–16(2)	30(2)	–2(2)
O32	60(2)	74(2)	79(2)	7(2)	19(2)	12(2)
C32	48(2)	59(3)	46(2)	3(2)	9(2)	–11(2)
C33	46(2)	57(3)	56(3)	13(2)	13(2)	1(2)
C34	61(3)	62(3)	76(3)	–6(2)	20(3)	7(2)
C35	81(4)	55(3)	64(3)	–7(2)	25(3)	–4(2)
C36	77(3)	69(3)	54(3)	–16(2)	24(2)	–15(3)
C37	51(3)	75(3)	48(2)	17(2)	13(2)	–15(2)
C38	48(3)	77(3)	56(3)	26(2)	9(2)	–2(2)
C39	76(4)	97(4)	67(3)	–26(3)	5(3)	–21(3)

Table S-1.1. (continued)

atom	U_{11}	U_{22}	U_{33}	U_{23}	U_{13}	U_{12}
C40	52(3)	85(4)	111(5)	1(3)	–6(3)	8(3)
C41	75(4)	105(4)	56(3)	6(3)	0(3)	–21(3)
C42	64(4)	131(5)	81(4)	28(4)	11(3)	14(3)
O51	100(4)	138(5)	153(5)	39(4)	33(4)	15(3)

[a] Estimated standard deviations in the least significant digits are given in parentheses.
[b] The anisotropic thermal parameter exponent takes the form

$$-2\pi^2(h^2a^{*2}U_{11} + k^2b^{*2}U_{22} + \ldots + 2hka^*b^*U_{12})$$

Table S-1.2. Hydrogen atom coordinates ($\times 10^4$)[a] and thermal parameters ($Å^2 \times 10^3$) for **4**.

atom	*x*	*y*	*z*	U_{iso}
H2	795(62)	3953(74)	4855(50)	179(24)
H28a	–1325	120	5794	80
H28b	–1492	1506	5653	80
H28c	–798	1192	6570	80
H29a	1033	–220	7085	86
H29b	2525	–666	7025	86
H29c	1177	–1157	6290	86
H30a	6070	6093	6601	76
H30b	7088	5086	6379	76
H30c	6543	5115	7218	76
H31a	4351	6854	5588	72
H31b	3749	6781	6399	72
H31c	2714	6613	5481	72
H3	4907(58)	5295(38)	1731(33)	109(20)
H34a	8785	1905	141	85
H34b	8933	1109	890	85
H35a	6501	566	455	86
H35b	7280	86	–258	86
H36a	5260	743	–956	86
H36b	6431	1772	–957	86
H39a	9704	4802	3357	103
H39b	8760	5904	3141	103
H39c	10017	5645	2702	103
H40a	10993	3868	1998	106
H40b	10749	2468	1584	106
H40c	10511	2871	2504	106
H41a	2766	2707	–1703	100
H41b	2178	1639	–1295	100
H41c	3522	1465	–1665	100
H42a	1780	4006	–873	113
H42b	1836	4867	–6	113
H42c	1214	3486	–150	113

[a] Estimated standard deviations in the least significant digits are given in parentheses. Hydrogen atoms without standard deviations were placed in idealized positions.

Table S-1.3. Anisotropic thermal parameters ($Å^2 \times 10^3$)[a,b] for the atoms of **5a**.

atom	U_{11}	U_{22}	U_{33}	U_{23}	U_{13}	U_{12}
Cu1	21(1)	24(1)	21(1)	2(1)	2(1)	–3(1)
Cu2	16(1)	16(1)	21(1)	–1(1)	–2(1)	1(1)
C1	21(2)	26(2)	23(2)	7(2)	4(1)	–1(2)
N1	24(2)	47(2)	29(1)	9(2)	–1(1)	–4(2)
C2	22(2)	28(2)	23(2)	6(2)	–4(1)	4(2)
N2	24(2)	31(2)	25(1)	7(1)	3(1)	3(2)
O1	27(1)	22(1)	37(2)	–6(1)	–6(1)	–3(1)
O2	24(1)	24(1)	33(1)	–6(1)	–11(1)	0(1)
N3	25(2)	23(2)	23(2)	0(1)	2(1)	2(1)
N4	21(2)	24(2)	26(2)	3(1)	2(1)	3(1)
N5	17(1)	23(2)	22(1)	–2(1)	–6(1)	–3(1)
N6	21(2)	19(2)	19(1)	–4(1)	0(1)	–1(1)
C3	30(2)	24(2)	24(2)	2(2)	3(2)	6(2)
C4	29(2)	31(2)	22(2)	5(2)	4(2)	8(2)
C5	16(2)	34(2)	41(2)	4(2)	–8(1)	1(2)
C6	30(2)	36(2)	36(2)	–2(2)	–10(2)	–1(2)
C7	23(2)	28(2)	38(2)	–2(2)	–9(2)	–6(2)
C8	22(2)	20(2)	17(2)	–2(1)	1(1)	–1(2)
C9	24(2)	23(2)	20(2)	1(2)	–3(1)	3(2)
C10	47(3)	24(2)	42(2)	–3(2)	10(2)	7(2)
C11	36(2)	37(3)	44(2)	1(2)	0(2)	18(2)
C12	35(2)	22(2)	27(2)	–3(2)	–4(2)	4(2)
C13	32(2)	27(2)	46(3)	–4(2)	–18(2)	6(2)

[a] Estimated standard deviations in the least significant digits are given in parentheses.

[b] The anisotropic thermal parameter exponent takes the form

$$-2\pi^2(h^2a^{*2}U_{11} + k^2b^{*2}U_{22} + \ldots + 2hka^*b^*U_{12})$$

Table S-1.4. Hydrogen atom coordinates ($\times 10^4$)[a] and thermal parameters ($Å^2 \times 10^3$) for **5a**.

atom	*x*	*y*	*z*	U_{iso}
H1	2111(56)	–4910(38)	2861(29)	40(13)
H5a	8804	–4326	4846	38
H5b	8866	–3629	4077	38
H6a	8353	–2742	5308	40
H6b	6554	–3283	5347	40
H7a	7441	–1903	4135	35
H7b	6339	–1612	4896	35
H10a	5813	–7424	3627	38
H10b	6019	–6975	2753	38
H10c	4174	–7167	3110	38
H11a	8575	–6404	3479	45
H11b	8349	–6499	4420	45
H11c	9600	–5681	4059	45
H12a	2838	–495	4060	38
H12b	4342	–337	3438	38
H12c	4760	–559	4350	38
H13a	394	–1282	3455	39
H13b	159	–2145	2811	39
H13c	1435	–1247	2641	39

[a] Estimated standard deviations in the least significant digits are given in parentheses. Hydrogen atoms without standard deviations were placed in idealized positions.

Table S-1.5. Anisotropic thermal parameters ($Å^2 \times 10^3$)[a,b] for the atoms of **5b**.

atom	U_{11}	U_{22}	U_{33}	U_{23}	U_{13}	U_{12}
Cu1	62(1)	50(1)	52(1)	6(1)	18(1)	8(1)
Cu2	38(1)	47(1)	47(1)	–1(1)	6(1)	2(1)
C1	69(4)	41(3)	45(3)	–3(2)	21(3)	–7(3)
N1	89(4)	61(3)	62(3)	4(3)	28(3)	–12(3)
C2	65(4)	37(3)	62(4)	–6(3)	19(3)	–2(3)
N2	77(3)	49(3)	71(3)	1(2)	40(3)	–2(2)
N3	47(2)	51(3)	48(2)	–2(2)	10(2)	10(2)
N4	38(2)	55(3)	69(3)	7(2)	11(2)	4(2)
N5	56(3)	56(3)	48(3)	–1(2)	–4(2)	–8(2)
N6	45(2)	49(2)	44(2)	–6(2)	6(2)	1(2)
O1	56(2)	71(3)	54(2)	–13(2)	–2(2)	20(2)
O2	44(2)	73(3)	59(2)	–13(2)	–1(2)	18(2)
C3	56(3)	37(3)	55(3)	9(2)	25(3)	7(2)
C4	43(3)	43(3)	76(4)	17(3)	26(3)	5(2)
C5	42(3)	98(5)	92(5)	5(4)	–9(3)	3(3)
C6	63(9)	90(11)	77(10)	17(8)	–28(7)	9(8)
C7	69(4)	100(5)	77(5)	–2(4)	–24(4)	1(4)
C8	68(4)	58(3)	44(3)	–2(3)	8(3)	–18(3)
C9	61(3)	45(3)	46(3)	–8(2)	18(3)	–8(3)
C10	81(4)	52(3)	59(4)	–2(3)	31(3)	9(3)
C11	48(3)	77(4)	97(5)	8(4)	32(3)	17(3)
C12	107(6)	107(6)	57(4)	–25(4)	8(4)	–11(5)
C13	79(5)	76(4)	67(4)	–17(4)	22(4)	11(4)
C6'	46(7)	107(11)	77(9)			

[a] Estimated standard deviations in the least significant digits are given in parentheses.

[b] The anisotropic thermal parameter exponent takes the form

$$-2\pi^2(h^2a^{*2}U_{11} + k^2b^{*2}U_{22} + \ldots + 2hka^*b^*U_{12})$$

Table S-1.6. Hydrogen atom coordinates ($\times 10^4$) and thermal parameters ($Å^2 \times 10^3$) for **5b**.

atom	*x*	*y*	*z*	U_{iso}
H10a	4935	515	–777	68
H10b	5189	2259	–968	68
H10c	3409	1712	–799	68
H11a	7583	764	–395	67
H11b	8477	343	148	67
H11c	8832	1980	–110	67
H12a	3579	7526	2007	99
H12b	5235	6541	2149	99
H12c	3488	5970	2336	99
H13a	382	6510	1626	90
H13b	124	6911	1035	90
H13c	1359	7940	1399	90

Table S-1.7. Anisotropic thermal parameters ($Å^2 \times 10^3$)[a,b] for the atoms of **5c**.

atom	U_{11}	U_{22}	U_{33}	U_{23}	U_{13}	U_{12}
Cu1	47(1)	52(1)	105(2)	5(1)	4(2)	1(1)
Cu2	55(1)	60(1)	57(1)	–1(1)	–1(1)	–12(1)
N1	27(7)	39(8)	132(16)	8(11)	53(11)	–8(6)
C1	43(8)	80(10)	178(18)	31(13)	40(12)	–6(7)
C2	33(9)	77(11)	87(14)	0(13)	–8(11)	–9(9)
N2	66(11)	47(7)	113(13)	–25(11)	–27(12)	–16(7)
O1	23(6)	251(21)	294(26)	–160(21)	25(11)	7(10)
O2	244(23)	165(17)	143(17)	–67(14)	129(18)	–109(17)
N3	36(8)	142(14)	99(13)	–86(13)	–16(9)	17(9)
C3	162(23)	99(16)	37(12)	–36(11)	–42(13)	36(15)
C4	76(11)	50(9)	71(12)	–9(9)	–17(10)	–5(9)
N4	50(9)	51(9)	80(12)	–19(8)	21(22)	4(7)
C5	159(26)	105(17)	158(27)	–48(18)	21(22)	–73(18)
C6	132(37)	188(37)	672(131)	–212(61)	140(60)	–1(7)
C7	25(11)	534(86)	473(89)	282(74)	–25(27)	–51(26)
N5	260(32)	46(10)	126(20)	10(12)	–96(21)	–33(14)
C8	362(55)	29(12)	107(29)	–12(15)	–170(36)	43(22)
C9	795(128)	99(24)	0(9)	–1(11)	–3(40)	64(50)
N6	196(26)	123(17)	98(17)	–31(16)	97(20)	–58(18)
C10	68(25)	2178(282)	246(58)	–396(117)	–85(32)	245(82)
C11	179(28)	185(25)	58(14)	–53(17)	19(17)	37(23)
C12	1696(225)	1051(174)	146(50)	305(82)	–229(94)	–1111(180)
C13	393(67)	314(47)	430(75)	276(51)	–212(61)	34(49)

[a] Estimated standard deviations in the least significant digits are given in parentheses.

[b] The anisotropic thermal parameter exponent takes the form

$$-2\pi^2(h^2a^{*2}U_{11} + k^2b^{*2}U_{22} + \ldots + 2hka^*b^*U_{12})$$

Table S-1.8. Anisotropic thermal parameters ($Å^2 \times 10^3$)[a,b] for the atoms of **6**.

atom	U_{11}	U_{22}	U_{33}	U_{23}	U_{13}	U_{12}
Cu1	62(1)	41(1)	40(1)	–2(1)	15(1)	–6(1)
Cu2	30(1)	35(1)	37(1)	1(1)	8(1)	1(1)
C1(N1)	67(2)	50(2)	50(2)	–3(1)	25(2)	–8(2)
N1(C1)	102(3)	46(2)	43(2)	–5(1)	26(2)	–6(2)
C2	53(2)	37(2)	43(2)	3(1)	12(2)	4(1)
N2	55(2)	51(2)	37(1)	6(1)	8(1)	12(1)
O1	76(2)	43(1)	66(2)	–13(1)	31(1)	–2(1)
O2	50(1)	54(2)	72(2)	–17(1)	9(1)	–15(1)
B	74(3)	41(2)	64(3)	–13(2)	21(2)	–12(2)
F1	100(2)	43(1)	69(1)	4(1)	31(1)	4(1)
F2	119(2)	51(1)	109(2)	–32(1)	43(2)	–33(1)
N3	43(2)	40(1)	44(2)	4(1)	13(1)	5(1)
N4	33(1)	53(2)	52(2)	3(1)	5(1)	–8(1)
N5	46(2)	34(1)	48(2)	1(1)	5(1)	4(1)
N6	35(1)	41(1)	42(1)	1(1)	8(1)	–3(1)
C3	43(2)	61(2)	49(2)	10(2)	20(2)	19(2)
C4	33(2)	70(2)	51(2)	22(2)	7(2)	4(2)
C5	60(3)	70(3)	98(3)	–6(2)	–5(2)	–29(2)
C6	92(3)	48(2)	98(3)	–10(2)	5(3)	–32(2)
C7	84(3)	41(2)	83(3)	–12(2)	8(2)	–3(2)
C8	50(2)	41(2)	48(2)	11(1)	18(2)	15(2)
C9	32(2)	55(2)	44(2)	9(2)	8(1)	6(2)
C10	76(3)	101(4)	84(3)	–8(3)	42(3)	25(3)
C11	42(2)	120(4)	103(4)	33(3)	30(2)	2(3)
C12	74(3)	57(3)	114(4)	11(2)	45(3)	28(2)
C13	35(2)	106(4)	95(3)	6(3)	–4(2)	5(2)
C14	193(7)	101(5)	50(3)	–7(3)	15(3)	10(5)
C15	230(8)	67(4)	51(3)	–3(3)	3(4)	32(5)
C16	170(7)	108(5)	52(3)	–12(3)	4(4)	41(5)

[a] Estimated standard deviations in the least significant digits are given in parentheses.

[b] The anisotropic thermal parameter exponent takes the form

$$-2\pi^2(h^2a^{*2}U_{11} + k^2b^{*2}U_{22} + \ldots + 2hka^*b^*U_{12})$$

Table S-1.9. Hydrogen atom coordinates ($\times 10^4$) and thermal parameters ($Å^2 \times 10^3$) for **6**.

atom	*x*	*y*	*z*	U_{iso}
H5a	2369	9817	7534	95
H5b	2794	10321	6854	95
H6a	986	11241	6485	92
H6b	1555	12050	7145	92
H7a	–324	11799	7211	89
H7b	342	10734	7754	89
H10a	2511	5956	5265	100
H10b	1693	4642	5411	100
H10c	2893	4841	5859	100
H11a	3482	8912	5859	103
H11b	3838	7262	6046	103
H11c	3985	8503	6606	103
H12a	–2923	10645	7283	98
H12b	–2911	11032	6516	98
H12c	–2007	11770	7070	98
H13a	–3831	8344	6675	97
H13b	–3547	6959	6245	97
H13c	–3555	8565	5932	97
H14	1673	1438	4931	120
H15	–39	2556	5169	114
H16	1671	–1167	4744	112

Table S–1.10. Selected least–squares planes for **4**, **5a**, **5b**, and **6**.

Plane one for **4**
Least squares plane for N21, N22, N23, N24
Equation of plane $-3.07(2)x + 2.99(3)y + 12.77(1)z = 8.514(8)$

$\Sigma_w\Delta^2 = 0.004$[b] $\quad {}_w\sigma^2 = 0.004$[b]

$\Sigma\Delta^2 = 0.0001$ $\quad \sigma^2 = 0.004$

deviations from plane[a,b]

atom	dev.	atom	dev.[a,c]
N21	0.004(3)	N22	–0.004(3)
N23	0.004(3)	N24	–0.004(3)
Cu2	–0.441(1)		

Plane two for **4**
Least squares plane for N31, N32, N33, N34
Equation of plane two[a] $4.32(2)x + 7.64(3)y - 11.72(8)z = 4.20(1)$

$\Sigma_w\Delta^2 = 0.003$[b] $\quad {}_w\sigma^2 = 0.010$[b]

$\Sigma\Delta^2 = 0.0004$ $\quad \sigma^2 = 0.010$

deviations from plane

atom	dev.	atom	dev.[a,c]
N31	–0.010(3)	N32	0.009(3)
N33	–0.010(3)	N34	0.010(3)
Cu3	–0.326(1)		

Table S–1.10. (continued)

Plane one for **5a**.
Least squares plane for N3, N4, N5, N6

Equiation of plane one.[a]: $3.57(3)x + 2.63(4)y - 14.28(4)z = -4.68(2)$

$\Sigma_w\Delta^2 = 0.012$[b] $\quad {}_w\sigma^2 = 0.020$[b]

$\Sigma\Delta^2 = 0.0002$ $\quad \sigma^2 = 0.020$

deviations from plane

atom	dev.[a,c]	atom	dev.[a,c]
N3	–0.020(3)	N4	0.020(3)
N5	–0.020(3)	N6	0.021(3)
Cu2	–0.294(2)		

Plane one for **5b**.
Least squares plane for N3, N4, N5, N6

Equiation of plane one.[a]: $3.39(2)x + 6.77(3)y - 11.43(11)z = 3.200(1)$

$\Sigma_w\Delta^2 = 0.025$[b] $\quad {}_w\sigma^2 = 0.010$[b]

$\Sigma\Delta^2 = 0.0004$ $\quad \sigma^2 = 0.010$

deviations from plane

atom	dev.[a,c]	atom	dev.[a,c]
N3	–0.010(4)	N4	0.009(5)
N5	–0.009(4)	N6	0.010(4)
Cu2	–0.301(1)		

Table S–1.10. (continued)

Plane one for **6**
Least squares plane for N3, N4, N5, N6
Equation of plane $0.47(10)x - 3.12(2)y + 18.36(2)z = 9.79(1)$

$\Sigma_w\Delta^2 = 0.005$[b] $\quad {}_w\sigma^2 = 0.014$[b]

$\Sigma\Delta^2 = 0.0008$ $\quad \sigma^2 = 0.014$

deviations from plane[a,b]

atom	dev.	atom	dev.[a,c]
N3	–0.014(4)	N4	0.014(4)
N23	–0.014(4)	N24	0.014(4)
Cu2	0.462(2)		

---

[a] Estimated standard deviations in the least significant digits are given in parenthese.

[b] The weights used in the calculations were derived from the atomic numbers of the respective elements.

[c] in Å, estimated standard deviations in the least significant digits are given in parenthese

Table S-1.11. Infrared C–N stretching frequencies for selected compounds.[a,b]

Compound	ν_1	ν_2	ν_3
NaCN[c]	2090		
[Cu(cyclops)CN][d]	2134		
$Na[Cu(CN)(\mu\text{-}CN)]_n$[c]	2126	2113	
$Na_2[Cu(CN)_3]$[c]	2109	2090	2049
$K_3[Cu(CN)_4]$[c]	2109	2092	2075
$[Cu(\mathbf{1})(\mu\text{-}NC)]_2Cu(CN)$ (**4**)	2128	2112	2095
$[Cu(\mathbf{1})(\mu\text{-}NC)Cu(\mu\text{-}CN)]_n$ (**5a**)	2134	2120	
$[Cu(\mathbf{1})(\mu\text{-}NC)Cu(\mu\text{-}CN)]_n$ (**5b**)	2120	2105	
$[Cu(\mathbf{1})(\mu\text{-}NC)Cu(\mu\text{-}CN)]_n$ (**5c**)	2125	2111	
$[Cu(\mathbf{2})(\mu\text{-}NC)Cu(\mu\text{-}CN)\cdot(1/2\ C_6H_6)]_n$ (**6**)	2117	2109	2102

[a] Frequencies are in units of cm^{-1}

[b] Spectra taken of solid samples, mulled in mineral oil.

[c] See reference 35

[d] See reference 25

Table S-2.1 Anisotropic thermal parameters ($Å^2 \times 10^3$)[a,b] for the atoms of **7**.

atom	U_{11}	U_{22}	U_{33}	U_{23}	U_{13}	U_{12}
Cu1	26(1)	32(1)	46(1)	–12(1)	4(1)	–0(1)
Cu2	33(1)	42(1)	48(1)	–5(1)	–5(1)	6(1)
O2	21(3)	29(3)	22(3)	5(3)	–2(3)	4(3)
N11	29(4)	32(4)	60(6)	–20(4)	–0(5)	0(4)
N12	58(6)	45(5)	37(5)	–14(4)	17(5)	–5(5)
N13	44(5)	51(6)	73(7)	–27(5)	–14(5)	13(5)
N1	26(4)	31(4)	46(5)	11(4)	–6(4)	2(4)
N1a	49(5)	22(4)	52(5)	10(4)	–5(5)	2(4)
C1a	29(5)	54(6)	57(7)	13(6)	9(5)	–1(5)
C1b	37(6)	80(9)	66(8)	15(7)	–13(6)	6(6)
C1c	31(5)	69(7)	39(6)	9(6)	11(5)	–16(5)
N3	25(4)	38(5)	50(6)	5(4)	–3(4)	3(4)
N3a	31(4)	54(5)	31(5)	8(4)	4(4)	8(4)
C3a	28(5)	50(7)	44(7)	10(5)	12(5)	7(5)
C3b	32(5)	35(5)	79(8)	24(6)	8(6)	12(5)
C3c	25(6)	66(7)	50(7)	–2(6)	–1(5)	5(5)
N2	33(5)	44(5)	48(5)	–16(4)	–12(4)	6(4)
C2a	38(6)	26(5)	63(8)	–3(5)	–13(5)	2(5)
C2b	48(6)	36(5)	20(5)	2(4)	–3(5)	3(5)
C2c	50(6)	20(5)	37(6)	–8(4)	2(5)	0(4)
C2d	55(7)	31(5)	76(8)	11(6)	16(6)	7(5)
N4	45(5)	61(6)	20(4)	13(4)	8(4)	5(5)
N4a	65(6)	42(5)	52(6)	9(5)	–12(5)	1(5)
C4a	64(7)	49(7)	39(7)	–4(5)	9(6)	–4(6)
C4b	102(11)	69(9)	42(7)	–1(7)	14(8)	–26(9)
C4c	75(9)	74(9)	65(9)	8(8)	8(8)	–16(9)
N5	34(4)	28(4)	37(5)	2(4)	–3(4)	–14(4)
N5a	40(5)	36(5)	47(5)	6(4)	20(5)	–4(4)
C5a	44(7)	41(6)	66(8)	17(6)	10(6)	11(5)
C5b	32(5)	77(8)	28(5)	7(6)	8(5)	–9(5)
C5c	35(6)	35(5)	44(6)	–5(5)	6(5)	–2(5)
N6	36(5)	33(4)	37(5)	–6(4)	–7(4)	17(4)
C6a	13(4)	41(5)	35(5)	6(5)	3(4)	2(4)
C6b	48(7)	94(10)	56(7)	–8(7)	22(6)	–38(8)
C6c	40(6)	52(6)	43(7)	1(6)	1(5)	14(5)
C6d	39(6)	25(5)	61(7)	13(5)	7(5)	0(5)

Table S-2.1. (continued)

atom	U_{11}	U_{22}	U_{33}	U_{23}	U_{13}	U_{12}
Cb1	21(5)	27(5)	29(5)	9(4)	3(4)	7(4)
Cb2	23(5)	38(5)	29(5)	–4(4)	–12(4)	12(4)
Cb3	30(5)	62(7)	43(6)	–6(6)	–2(5)	15(5)
Cb4	34(5)	42(5)	34(6)	3(5)	–1(5)	9(5)
Cb5	33(5)	26(5)	28(5)	2(4)	2(4)	–4(4)
Cb6	18(4)	34(5)	31(5)	10(5)	3(4)	4(4)
Cbp	36(6)	84(9)	45(7)	–13(6)	–1(6)	26(6)
Cl1	37(1)	35(1)	47(1)	5(1)	3(1)	0(1)
O1	58(5)	117(7)	69(5)	6(5)	24(4)	–15(5)
O3	94(6)	60(5)	88(6)	–27(5)	10(5)	–8(5)
O4	69(5)	44(4)	103(7)	5(4)	–10(5)	7(4)
O5	110(8)	138(9)	65(6)	18(6)	21(6)	44(7)
C12	48(1)	44(1)	68(2)	4(1)	–3(1)	4(1)
O6	60(5)	66(5)	195(10)	52(7)	–8(6)	9(5)
O7	67(6)	124(8)	67(6)	–1(6)	–4(5)	–23(6)
O8	63(5)	66(5)	85(6)	15(5)	–8(4)	–15(4)
O9	37(4)	92(6)	98(6)	42(5)	–18(4)	–4(4)

[a] estimated standard deviations in the least significant digits are given in parentheses.

[b] the anisotropic thermal parameter exponent takes the form:

$$-2\pi^2(h^2a^{*2}U_{11}+k^2b^{*2}U_{22}+....+2hka^*b^*U_{12})$$

Table S-2.2. Hydrogen coordinates ($\times 10^4$) and thermal parameters ($Å^2 \times 10^3$) for **7**.

atom	*x*	*y*	*z*	U_{iso}
H1A	5300	6428	9653	58
H1B	3994	5396	9984	87
H1C	4192	3664	9356	70
H3A	6736	8256	8332	49
H3B	6611	8902	7357	63
H3C	6955	7316	6613	59
H2AA	6841	4121	7322	57
H2AB	6140	4958	7613	57
H2BA	8100	5445	7238	53
H2BB	7193	5434	6768	53
H2CA	7110	3534	8833	44
H2CB	6905	3050	8194	44
H2DA	5432	3061	8645	75
H2DB	5382	3942	8168	75
H4A	9939	8549	9214	62
H4B	11531	9574	8987	89
H4C	12952	8137	8929	86
H5A	10122	3969	11217	63
H5B	9985	5684	11658	66
H5C	9865	6887	10899	46
H6AA	11531	5793	8331	42
H6AB	12180	4939	8645	42
H6BA	12931	6296	8995	63
H6BB	12155	6057	9522	63
H6CA	11264	3712	9252	67
H6CB	11519	4581	9715	67
H6DA	9472	4008	9607	50
H6DB	10197	3305	9991	50
H3BE	11174	3770	8241	52
H5BE	8205	3359	7476	37
H1MA	9674	2217	7082	59
H1MB	10523	2002	7572	59
H1MC	10751	2745	7032	59
H30A	7350	11356	8878	80
H30B	7813	11360	9536	80
H40A	8879	12072	8683	80
H40B	9424	11438	9193	80
H60A	8759	9244	8689	80
H60B	7915	9764	8286	80
H50A	9929	10371	8432	80
H50B	9117	10819	7978	80

Table S-2.3. Selected least-squares planes for **7**, **8**, and **9a**.

plane I of **7** formed by O2, N1, N2, N11

A	B	C	D
1.9(3)	–8.2(4)	16.9(3)	11.8(2)

atom	Δ_m	σ_m
O2	0.345	0.006
N1	0.319	0.008
N2	-.329	0.008
N11	-.334	0.008
Cu1	-.385	0.002

$\Sigma\Delta^2 = 0.441$ $\sigma^2_{plane} = 0.332$ σ^2_m (mean square value) $= 6 \times 10^{-5}$

$\Sigma\Delta^2/\ \sigma^2_m = 7350$

plane II of **7** formed by O2, N1, N3, Cu1

A	B	C	D
0.02(3)	10.00(2)	14.33(2)	18.28(1)

atom	Δ_m	σ_m
O2	0.008	0.006
N1	0.009	0.008
N3	0.006	0.008
Cu1	–0.023	0.002

$\Sigma\Delta^2 = 0.0007$ $\sigma^2_{plane} = 0.0132$ σ^2_m (mean square value) $= 4 \times 10^{-5}$

$\Sigma\Delta^2/\ \sigma^2_m = 17.5$

Table S-2.3. (continued)

Plane III of **7** formed by O2, N4, N6, N13

A	B	C	D
1.2(3)	–1.8(4)	20.4(3)	16.8(3)

atom	Δ_m	σ_m
O2	–0.393	0.006
N4	–0.360	0.007
N6	0.361	0.009
N13	0.392	0.011
Cu2	0.414	0.002

$\Sigma\Delta^2 = 0.570$ $\sigma^2_{plane} = 0.376$ σ^2_m (mean square value) $= 7 \times 10^{-5}$

$\Sigma\Delta^2/\ \sigma^2_m = 8143$

plane IV of **7** formed by O2, N4, N5, Cu2

A	B	C	D
8.61(2)	–8.90(3)	–7.14(2)	–3.18(2)

atom	Δ_m	σ_m
O2	–0.014	0.006
N4	–0.013	0.009
N5	–0.010	0.008
Cu1	0.037	0.002

$\Sigma\Delta^2 = 0.0018$ $\sigma^2_{plane} = 0.0212$ σ^2_m (mean square value) $= 5 \times 10^{-5}$

$\Sigma\Delta^2/\ \sigma^2_m = 38.9$

Table S-2.3. (continued)

plane I of **8** formed by O2, N1, N2, N11

A	B	C	D
7.9(1)	–4.65(8)	13.14(6)	11.03(5)

atom	Δ_m	σ_m
O2	0.076	0.011
N1	0.063	0.015
N2	-0.063	0.012
N11	-0.076	0.011
Cu1	0.229	0.005

$\Sigma\Delta^2 = 0.019$ $\sigma^2_{plane} = 0.070$ σ^2_m (mean square value) $= 2 \times 10^{-4}$

$\Sigma\Delta^2/\ \sigma^2_m = 95$

plane II of **8** formed by N2, N3, N11, Cu1

A	B	C	D
4.73(8)	–2.10(6)	–20.61(5)	–15.32(4)

atom	Δ_m	σ_m
N2	–0.040	0.010
N3	-0.012	0.014
N11	–0.042	0.010
Cu1	0.095	0.004

$\Sigma\Delta^2 = 0.0125$ $\sigma^2_{plane} = 0.0559$ σ^2_m (mean square value) $= 8 \times 10^{-5}$

$\Sigma\Delta^2/\ \sigma^2_m = 156$

Table S-2.3. (continued)

plane III of **8** formed by O2, N5, N6, N11

A	B	C	D
9.1(3)	–1.6(4)	10.5(2)	11.5(1)

atom	Δ_m	σ_m
O2	–0.209	0.012
N5	-0.167	0.014
N6	0.173	0.015
N11	0.204	0.011
Cu1	0.111	0.006

$\Sigma\Delta^2 = 0.143$ $\sigma^2_{plane} = 0.189$ σ^2_m (mean square value) $= 2 \times 10^{-4}$

$\Sigma\Delta^2/\ \sigma^2_m = 715$

plane IV of **8** formed by N11, N4, N6, Cu2

A	B	C	D
2.0(1)	16.32(7)	–2.18(6)	11.54(5)

atom	Δ_m	σ_m
N11	–0.051	0.011
N4	–0.026	0.012
N6	–0.049	0.015
Cu2	0.126	0.006

$\Sigma\Delta^2 = 0.022$ $\sigma^2_{plane} = 0.074$ σ^2_m (mean square value) $= 2 \times 10^{-4}$

$\Sigma\Delta^2/\ \sigma^2_m = 110$

Table S-2.3. (continued)

plane I of **9a** formed by O2, N1, N2, O1

A	B	C	D
6(2)	8(1)	8(2)	3.1(2)

atom	Δ_m	σ_m
O2	–0.371	0.005
N1	–0.296	0.005
N2	0.299	0.005
O1	0.368	0.004
Cu1	–0.342	0.001

$\Sigma\Delta^2 = 0.450$ $\sigma^2_{plane} = 0.335$ σ^2_m (mean square value) $= 2 \times 10^{-5}$

$\Sigma\Delta^2/\ \sigma^2_m = 19800$

plane II of **9a** formed by O2, N1, N3, Cu1

A	B	C	D
8.4(2)	–2.5(1)	–21.7(2)	–1.97(2)

atom	Δ_m	σ_m
O2	–0.024	0.003
N1	–0.024	0.006
N3	–0.017	0.006
Cu1	0.065	0.002

$\Sigma\Delta^2 = 0.0056$ $\sigma^2_{plane} = 0.0375$ σ^2_m (mean square value) $= 1 \times 10^{-5}$

$\Sigma\Delta^2/\ \sigma^2_m = 178$

Table S-2.3. (continued)

plane III of **9a** formed by O2, N4, N6, O1

A	B	C	D
6(1)	8.2(7)	–9(2)	1.2(2)

atom	Δ_m	σ_m
O2	0.357	0.005
N4	0.277	0.005
N6	–0.329	0.005
O1	–0.349	0.005
Cu1	–0.375	0.002

$\Sigma\Delta^2 = 0.407$ $\sigma^2_{plane} = 0.319$ σ^2_m (mean square value) $= 3 \times 10^{-5}$

$\Sigma\Delta^2/\ \sigma^2_m = 13570$

plane IV of **9a** formed by O2, N4, N5, Cu1

A	B	C	D
7.7(2)	–7.1(1)	22.7(2)	1.09(3)

atom	Δ_m	σ_m
O2	0.026	0.003
N4	0.025	0.005
N5	0.017	0.006
Cu1	–0.068	0.002

$\Sigma\Delta^2 = 0.0062$ $\sigma^2_{plane} = 0.039$ σ^2_m (mean square value) $= 7 \times 10^{-5}$

$\Sigma\Delta^2/\ \sigma^2_m = 87$

Table S-2.4. Anisotropic thermal parameters ($Å^2 \times 10^3$)[a,b] for the atoms of **8**.

atom	U_{11}	U_{22}	U_{33}	U_{23}	U_{13}	U_{12}
Cu1	41(1)	42(1)	42(1)	0(1)	3(1)	–4(1)
Cu2	47(1)	50(1)	52(1)	–13(1)	7(1)	–13(1)
N11	35(7)	40(5)	50(6)	–5(5)	–6(6)	–11(5)
N12	60(9)	41(7)	109(11)	–14(7)	38(9)	–31(7)
N13	59(10)	66(10)	166(16)	–16(10)	11(11)	–13(9)
O2	54(6)	53(6)	55(6)	–15(5)	–10(6)	8(6)
N1	85(10)	36(7)	69(8)	–7(6)	35(9)	–2(7)
N1a	114(12)	62(8)	54(7)	–11(6)	–11(10)	–21(11)
C1a	62(13)	95(14)	77(12)	–22(11)	28(11)	–7(12)
C1b	192(28)	88(15)	102(16)	12(12)	83(19)	–12(18)
C1c	172(24)	59(11)	63(11)	–9(9)	7(14)	–19(13)
N3	45(8)	83(9)	68(9)	11(7)	–6(7)	17(8)
N3a	50(9)	118(13)	103(12)	42(10)	6(9)	33(9)
C3a	21(8)	126(19)	79(12)	36(12)	–30(8)	–9(11)
C3b	175(41)	130(27)	242(43)	53(28)	14(34)	–43(31)
C3c	73(16)	325(40)	97(16)	142(23)	28(13)	123(23)
N2	50(7)	43(6)	37(6)	2(5)	–6(7)	–1(7)
C2a	70(12)	42(8)	50(9)	–2(7)	20(8)	17(8)
C2b	69(12)	56(10)	78(12)	10(9)	15(10)	9(10)
C2c	66(11)	44(8)	68(10)	–19(7)	–21(9)	–10(9)
C2d	104(15)	57(10)	71(10)	–10(9)	–19(12)	0(12)
N4	37(8)	41(8)	149(14)	3(9)	11(10)	6(7)
N4a	80(12)	48(8)	142(15)	39(9)	–10(12)	–14(9)
C4a	95(19)	60(14)	293(40)	29(18)	–141(24)	–35(13)
C4b	87(15)	60(10)	138(17)	–11(11)	–41(16)	3(15)
C4c	75(15)	75(13)	268(31)	79(17)	–10(23)	–29(15)
N5	67(10)	79(10)	101(11)	–52(8)	44(8)	–43(8)
N5a	283(31)	220(24)	120(14)	–129(16)	112(20)	–191(25)
C5a	52(11)	51(12)	302(33)	76(16)	60(16)	–9(9)
C5b	163(27)	54(12)	349(38)	13(19)	168(31)	1(19)
C5c	172(30)	88(16)	414(46)	–101(23)	191(34)	–94(20)

Table S-2.4. (continued)

atom	U_{11}	U_{22}	U_{33}	U_{23}	U_{13}	U_{12}
N6	70(11)	85(10)	91(11)	–11(9)	8(9)	0(9)
C6a	114(19)	89(16)	122(17)	–13(14)	–43(16)	26(15)
C6b	43(15)	587(69)	128(23)	–109(34)	27(15)	33(29)
C6c	520(64)	75(14)	72(13)	–52(11)	–146(27)	20(26)
C6d	120(27)	103(18)	340(42)	–82(23)	24(27)	–30(18)
C1	35(8)	46(8)	64(9)	12(7)	6(7)	–19(7)
C2	132(18)	113(15)	47(9)	–16(10)	33(13)	–54(16)
Cb1	30(7)	71(10)	28(7)	5(7)	9(6)	3(8)
Cb2	24(8)	78(12)	67(10)	0(9)	–12(8)	–11(8)
Cb3	44(10)	77(13)	96(15)	44(11)	–11(11)	–5(10)
Cb4	28(9)	169(20)	61(11)	51(13)	4(9)	42(12)
Cb5	31(8)	70(10)	52(9)	31(8)	5(7)	3(8)
Cb6	31(8)	45(8)	69(10)	12(7)	–10(8)	7(7)
Cbp	66(13)	119(17)	94(13)	55(12)	–5(12)	–32(13)
F1	222(18)	118(10)	100(9)	–29(8)	5(11)	54(12)
F2	940(88)	134(14)	261(22)	–96(14)	–317(37)	244(30)
F3	272(30)	297(22)	146(14)	–113(16)	–54(17)	10(23)
F4	408(55)	177(22)	2243(163)	–36(59)	769(85)	15(29)
F5	180(17)	350(27)	93(10)	7(13)	82(12)	20(19)
F6	363(35)	129(13)	263(22)	–39(14)	202(24)	–30(17)
F7	285(32)	196(20)	296(27)	–34(20)	69(26)	9(22)
F8	143(18)	418(39)	343(30)	–260(30)	61(18)	64(20)

[a] Estimated standard deviations in the least significant digits are given in parentheses.

[b] The anisotropic thermal parameter exponent takes the form:

$$-2\pi^2(h^2a^{*2}U_{11}+k^2b^{*2}U_{22}+....+2hka^*b^*U_{12})$$

Table S-2.5. Hydrogen atom coordinates ($\times 10^4$) and thermal parameters ($Å^2 \times 10^3$) for **8**.

atom	*x*	*y*	*z*	U_{iso}
H1a	7545	6495	7141	92
H1b	7641	6080	6078	172
H1c	5349	5553	5844	115
H3a	7295	6808	8665	92
H3b	8905	6186	9036	196
H3c	8702	4720	8750	166
H2aA	4499	4670	8561	67
H2aB	4170	4030	8098	67
H2bA	6145	4540	7635	88
H2bB	6280	3928	8137	88
H2cA	2857	4583	7197	75
H2cB	4382	4506	7123	75
H2dA	3127	5938	6947	96
H2dB	3282	5314	6455	96
H4a	1665	7414	7373	165
H4b	–860	7419	7659	102
H4c	–1057	8133	8459	148
H5a	4053	9301	7622	144
H5b	5149	10548	7823	234
H5c	5376	10580	8768	279
H6aA	2400	8531	9732	101
H6aB	1852	7662	9651	101
H6bA	616	8351	9351	57
H6bB	1658	8938	9092	57
H6cA	5468	8404	9500	855
H6cB	4411	8620	9960	855
H6dA	4643	9842	9529	147
H6dB	3365	9550	9221	147
H1A	2056	4760	8025	60
H1B	2075	5663	7848	60
H2A	4684	7041	9556	106
H2B	3604	7236	10010	106
HbpA	435	4302	9920	109
HbpB	99	5213	9977	109
HbpC	946	4789	10445	109

Table S-2.6. Anisotropic thermal parameters ($Å^2 \times 10^3$)[a,b] for the atoms of **9a**.

atom	U_{11}	U_{22}	U_{33}	U_{23}	U_{13}	U_{12}
Cu1	20(1)	30(1)	34(1)	4(1)	2(1)	5(1)
Cu2	20(1)	25(1)	38(1)	0(1)	–3(1)	4(1)
O1	22(2)	37(2)	37(2)	–3(2)	–2(2)	6(2)
O2	26(2)	38(2)	33(2)	2(2)	–3(2)	6(2)
Cb1	26(3)	32(3)	36(3)	6(.3)	1(2)	–2(2)
Cb6	25(3)	37(3)	32(3)	3(3)	2(2)	–10(2)
Cb5	29(3)	50(4)	34(4)	–6(3)	7(3)	–11(3)
Cb4	36(4)	62(5)	33(4)	0(3)	2(3)	–19(3)
Cb3	35(3)	45(4)	41(4)	7(3)	–6(3)	–14(3)
Cb2	30(3)	35(3)	33(3)	2(3)	–2(3)	–9(3)
Cbp	50(4)	95(6)	43(4)	–1(4)	3(3)	–18(4)
C2	27(3)	36(3)	39(4)	–1(3)	14(3)	5(3)
C1	31(3)	35(3)	44(4)	9(3)	–14(3)	0(3)
C6c	30(3)	32(3)	41(4)	–6(3)	–5(3))	–4(3)
C6d	26(3)	36(3)	48(4)	–4(3)	–1(3)	–3(3)
C6a	28(3)	48(4)	53(4)	–5(3)	–10(3)	21(3)
C6b	44(4)	31(4)	65(5)	0(3)	–11(3)	22(3)
C2a	31(3)	45(4)	37(4)	11(3)	–3(3)	–7(3)
C2b	29(3)	43(4)	48(4)	12(3)	2(3)	–7(3)
C2c	26(3)	44(4)	55(4)	6(3)	4(3)	10(3)
C2d	33(4)	48(4)	67(5)	6(4)	12(3)	21(3)
C5a	53(4)	43(4)	36(4)	8(3)	–7(3)	–11(3)
C5b	59(5)	40(4)	58(5)	10(3)	0(4)	–13(3)
C5c	41(4)	39(4)	60(5)	1(3)	3(3)	–13(3)
C4c	39(4)	32(3)	59(5)	2(3)	11(3)	5(3)
C4b	55(4)	44(4)	39(4)	–6(3)	5(3)	4(3)
C4a	48(4)	39(4)	43(4)	–3(3)	–2(3)	8(3)
C1c	56(5)	66(5)	70(6)	21(4)	1(4)	22(4)
C1b	78(6)	77(6)	51(5)	27(4)	9(4)	22(5)
C1a	57(5)	62(5)	51(5)	10(4)	6(4)	17(4)
C3c	60(5)	49(5)	84(6)	–15(4)	13(4)	–28(4)
C3b	108(7)	73(6)	84(7)	–40(5)	39(6)	–47(5)
C3a	75(6)	86(7)	91(7)	–45(6)	31(5)	–36(5)
N1	34(3)	53(4)	45(3)	5(3)	8(2)	14(3)
N1a	38(3)	49(3)	53(4)	10(3)	6(3)	18(3)
N2	20(2)	31(3)	42(3)	6(2)	–3(2)	1(2)
N4a	31(3)	27(3)	49(3)	–6(2)	–4(2)	8(2)
N3	40(3)	50(4)	63(4)	–11(3)	19(3)	–13(3)
N3a	36(3)	42(3)	46(3)	2(3)	3(2)	–5(2)
N4	35(3)	32(3)	41(3)	4(2)	–5(2)	7(2)
N5a	23(2)	33(3)	43(3)	–10(2)	–1(2)	–3(2)
N5	34(3)	32(3)	51(3)	–3(2)	–8(2)	–3(2)
N6	23(2.	26(3)	53(3)	–5(2)	O(2)	4(2)

Table S–2.6. (continued)

atom	U_{11}	U_{22}	U_{33}	U_{23}	U_{13}	U_{12}
B1	33(4)	59(5)	33(4)	–2(4)	6(3)	2(4)
F1	107(4)	66(3)	146(5)	–11(3)	50(4)	–21(3)
F2	41(2)	82(3)	48(2)	–9(2)	10(2)	14(2)
F3	43(2)	74(3)	56(3)	–12(2)	3(2)	6(2)
F4	64(3)	148(5)	46(3)	2(3)	4(2)	38(3)
F21	102(4)	101(4)	65(3)	1(3)	–4(3)	41(3)
F22	67(4)	42(4)	40(4)	4(3)	–12(3)	8(3)
F23	58(3)	119(4)	149(5)	–94(4)	18(3)	–33(3)
F24	39(3)	43(4)	64(4)	–13(3)	5(3)	–8(3)
O101	110(5)	85(4)	81(5)	–11(4)	–33(4)	19(4)
C105	67(6)	86(7)	71(6)	–9(5)	–9(4)	–2(5)
C104	170(12)	70(7)	67(7)	4(5)	–27(7)	–33(7
C103	156(13)	261(19)	91(9)	51(10)	–39(8)	–80(13)
C102	148(12)	175(14)	148(13)	79(11)	–47(10	–79(11)

[a] estimated standard deviations in the least significant digits are given in parentheses.

[b] the anisotropic thermal parameter exponent takes the form:

$$-2\pi^2(h^2a^{*2}U_{11}+k^2b^{*2}U_{22}+....+ 2hka^*b^*U_{12})$$

Table S–2.7. Hydrogen atom coordinates ($\times 10^4$) and thermal parameters ($Å^2 \times 10^3$) for **9a**.

atom	*x*	*y*	*z*	U_{iso}
Hb5A	1511	1141	–509	40
H3b	–1286	3445	–608	44
HbpA	234	2986	–1315	68
HbpB	–563	1797	–1343	68
HbpC	677	1549	–1287	68
HC2a	2263	690	84	35
HC2b	1382	292	418	35
HC1a	–1116	4704	286	40
HC1b	–2002	4251	–57	40
H6cA	–1896	1462	349	40
H6cB	–2850	2141	90	40
H6dA	–3573	579	492	40
H6dB	–3874	1906	717	40
H6aA	–3474	4301	357	51
H6aB	–3476	3776	842	51
H6bA	–3355	6114	761	54
H6bB	–2168	5878	621	54
H2aA	3055	2799	166	38
H2aB	2079	3557	360	38
H2bA	3737	4556	526	47
H2bB	4064	3320	806	47
H2cA	3717	851	551	49
H2cB	3656	1537	1011	49
H2dA	3639	–785	1036	58
H2dB	2489	–725	813	58
H5a	–1369	986	1908	48
H5b	–2605	–679	1965	61
H5c	–3818	–634	1214	50
H4c	–3322	6865	1525	50
H4b	–2191	6136	2255	52
H4a	–1003	4556	2037	49
H1c	3305	–1532	1785	82
H1b	1956	–751	2411	75
H1a	902	891	2096	63
H3c	4017	5927	1229	72
H3b	2834	6157	1950	102
H3a	1554	4553	1984	94

Table S-3.1. Anisotropic thermal parameters ($Å^2 \times 10^3$)[a,b] for the atoms of **10**.

atom	U_{11}	U_{22}	U_{33}	U_{23}	U_{13}	U_{12}
I	40(1)	54(1)	66(1)	0	13(1)	0
Cu	37(1)	59(1)	47(1)	–7(1)	0(1)	–3(1)
N1	31(2)	64(2)	57(2)	11(2)	–8(1)	–7(2)
C2	39(2)	89(4)	84(3)	36(3)	–10(2)	–19(2)
C3	38(2)	142(5)	52(3)	26(3)	–2(2)	–25(3)
N4	45(2)	118(4)	44(2)	–6(2)	3(2)	–22(2)
C5	80(4)	175(7)	61(3)	–49(4)	9(3)	–20(5)
C6	94(9)	139(10)	103(7)	–81(7)	22(6)	–24(7)
C7	100(5)	128(6)	127(6)	–78(5)	13(4)	11(5)
N8	56(2)	72(3)	80(3)	–28(2)	16(2)	–1(2)
C9	41(2)	59(3)	102(4)	–7(3)	15(3)	10(2)
C10	35(2)	52(2)	63(3)	8(2)	7(2)	3(2)
N11	32(2)	51(2)	51(2)	–0(2)	2(1)	0(1)
O12	39(1)	59(2)	50(2)	–8(1)	–9(1)	8(1)
B13	38(2)	61(3)	60(3)	–15(3)	–10(2)	6(2)
O14	48(2)	49(2)	79(2)	–4(2)	–15(2)	2(1)
C15	77(4)	93(5)	133(5)	65(5)	–32(4)	–16(4)
C16	85(5)	233(10)	61(4)	48(5)	–4(3)	–25(6)
C17	67(4)	91(5)	146(6)	–28(5)	11(4)	27(3)
C18	46(3)	78(3)	73(3)	8(3)	–4(2)	15(2)
F19	41(1)	93(2)	66(2)	–0(1)	5(1)	1(1)
F20	65(2)	92(2)	101(2)	–48(2)	–22(2)	20(2)
Cl	132(4)	171(5)	377(10)	45(5)	98(6)	21(3)
O1	622(55)	143(18)	1512(97)	273(35)	813(64)	180(24)
O2	170(17)	344(31)	280(23)	154(24)	128(19)	158(20)
O3	133(17)	961(79)	212(22)	47(37)	–5(16)	–177(32)
O4	139(14)	149(13)	200(17)	24(12)	15(12)	5(10)
Cme	238(15)	151(11)	233(15)	35(11)	151(13)	–1(11)
Ome	470(25)	297(17)	349(19)	114(15)	253(18)	48(16)

[a] Estimated standard deviations in the least significant digits are given in parentheses.

[b] The anisotropic thermal parameter exponent takes the form

$$-2\pi^2(h^2a^{*2}U_{11}+k^2b^{*2}U_{22}+....2hka^*b^*U_{12})$$

Table S-3.2. Hydrogen atom coordinates ($\times 10^4$) and thermal parameter ($Å^2 \times 10^3$) for **10**.

atom	*x*	*y*	*z*	U_{iso}
H15A	–756	223	4200	108
H15B	–69	532	4052	108
H15C	–545	156	3226	108
H16A	–442	1429	5177	117
H16B	–654	2408	5775	117
H16C	27	2388	5508	117
H17A	–3108	5614	1957	114
H17B	–2536	6419	2188	114
H17C	–2799	5739	2963	114
H18A	–2757	4641	526	72
H18B	–3064	3737	1100	72
H18C	–2550	3383	492	72

Table S-4.1. Anisotropic thermal parameters ($Å^2 \times 10^3$)[a,b] for the atoms of **11a**.

atom	U_{11}	U_{22}	U_{33}	U_{23}	U_{13}	U_{12}
Cu	65(1)	55(1)	43(1)	–5(1)	2(1)	15(1)
N1	46(3)	58(3)	43(2)	1(2)	3(2)	4(2)
C2	49(3)	61(4)	51(3)	–2(3)	11(3)	–1(3)
C3	42(3)	60(4)	56(3)	11(3)	2(3)	0(3)
N4	52(3)	51(3)	62(3)	–2(2)	15(2)	8(2)
C5	82(5)	62(4)	92(5)	2(4)	24(4)	20(4)
C6	61(5)	80(6)	76(5)	–9(5)	11(4)	13(5)
C6'	94(28)	48(20)	48(20)	–22(16)	–23(18)	6(20)
C7	104(5)	58(4)	75(5)	–14(4)	27(4)	9(4)
N8	58(3)	47(3)	52(3)	–3(2)	15(3)	6(2)
C9	58(4)	58(4)	44(3)	–9(3)	19(3)	–12(3)
C10	56(3)	60(4)	44(3)	6(3)	14(3)	3(3)
N11	51(3)	56(3)	38(3)	–5(2)	6(2)	–1(2)
C12	81(5)	99(6)	58(4)	–12(4)	–8(3)	15(5)
C13	92(6)	90(6)	85(5)	1(5)	–15(4)	26(5)
C14	112(6)	88(5)	43(4)	–13(4)	14(4)	–3(5)
C15	82(5)	96(6)	50(4)	12(4)	9(3)	22(4)
O1	70(3)	59(3)	57(2)	–10(2)	5(2)	18(2)
O2	60(2)	57(2)	51(2)	–7(2)	8(2)	16(2)
Cl	71(1)	79(1)	67(1)	–6(1)	23(1)	1(1)
O3	328(34)	250(24)	188(18)	72(16)	63(21)	114(22)
O4	131(112)	126(10)	246(16)	–8(10)	107(10)	–36(9)
O5	153(12)	136(12)	164(14)	–56(11)	61(10)	17(9)
O6	110(11)	261(20)	2306(25)	–166(23)	59(13)	–8(13)
O3'	186(19)	390(37)	219(22)	123(25)	121(16)	106(24)
O4'	107(12)	155(19)	180(22)	–98(17)	51(13)	–3(12)
O5'	93(12)	153(17)	208(21)	–91(16)	78(14)	–57(13)
O6'	119(14)	284(32)	113(12)	–9(7)	65(11)	16(18)
Cme	37(12)	110(11)	145(15)	33(13)	2(13)	4(7)
Ome	108(8)	112(9)	99(8)	22(7)	13(6)	–25(7)

[a] Estimated standard deviations in the least significant digits are given in parentheses.

[b] The anisotropic thermal parameter exponent takes the form:

$$-2\pi^2(h^2a^{*2}U_{11}+k^2b^{*2}U_{22}+....2\ hka^*b^*U_{12})$$

Table S-4.2. Hydrogen atom coordinates ($\times 10^4$) and thermal parameter ($Å^2 \times 10^3$) for **11a**.

atom	*x*	*y*	*z*	U_{iso}
H5A	4233	–4015	3154	90
H5B	4507	–2822	2702	90
H7A	3590	–2801	1300	84
H7B	3305	–3783	1784	84
H12A	3946	1574	4670	90
H12B	4032	3534	4353	90
H12C	4563	2039	4531	90
H13A	4973	–587	4354	111
H13B	4934	–2411	3931	111
H13C	4478	–2166	4334	111
H14A	2286	–453	450	93
H14B	2746	–2127	704	93
H14C	2958	–260	425	93
H15A	1893	2213	782	83
H15B	2403	3631	713	83
H15C	2027	4100	1182	83

Table S-4.3. Anisotropic thermal parameters ($Å^2 \times 10^3$)[a,b] for the atoms of **11b**.

atom	U_{11}	U_{22}	U_{33}	U_{23}	U_{13}	U_{12}
Cu1	19(1)	26(1)	23(1)	–2(1)	3(1)	–0(1)
Cu2	28(1)	21(1)	23(1)	1(1)	–1(1)	–10(1)
N1	19(2)	17(2)	22(2)	–4(2)	3(2)	–0(2)
C2	23(3)	24(3)	26(3)	–1(2)	–2(2)	–7(2)
C3	29(3)	20(2)	30(3)	–8(2)	–6(2)	2(2)
N4	13(2)	22(2)	38(3)	–11(2)	0(2)	–2(2)
C5	21(3)	35(3)	47(4)	–14(3)	0(2)	–2(2)
C6	17(3)	41(3)	58(4)	–27(3)	9(2)	–8(2)
C7	20(3)	38(3)	48(4)	–14(3)	14(2)	–8(2)
N8	24(2)	25(2)	29(2)	–5(2)	6(2)	–10(2)
C9	30(3)	30(3)	29(3)	–13(2)	10(2)	–15(2)
C10	26(3)	20(2)	24(3)	–5(2)	3(2)	–8(2)
N11	25(2)	18(2)	21(2)	–5(2)	3(2)	–6(2)
O12	19(2)	23(2)	23(2)	–4(1)	5(1)	–3(1)
O13	23(2)	25(2)	25(2)	–2(1)	5(1)	–1(1)
C14	42(3)	33(3)	21(3)	–2(2)	7(2)	0(2)
C15	43(3)	50(4)	28(3)	–8(3)	14(3)	–16(3)
C16	36(3)	54(4)	42(4)	1(3)	–11(3)	11(3)
C17	45(4)	38(3)	27(3)	3(3)	–3(3)	–10(3)
N101	20(2)	14(2)	24(2)	–5(2)	6(2)	–2(2)
C102	22(2)	17(2)	23(3)	–6(2)	8(2)	–3(2)
C103	24(2)	21(2)	22(3)	–8(2)	3(2)	–4(2)
N104	21(2)	21(2)	27(2)	–5(2)	–1(2)	–2(2)
C105	29(3)	27(3)	39(3)	–5(2)	–7(2)	–8(2)
C106	25(3)	25(3)	58(4)	–6(3)	–8(3)	–11(2)
C107	27(3)	25(3)	53(4)	2(3)	4(3)	–14(2)
N108	29(2)	20(2)	34(2)	–2(2)	7(2)	–6(2)
C109	28(3)	14(2)	34(3)	–4(2)	10(2)	–1(2)
C110	30(3)	19(2)	26(3)	–1(2)	4(2)	4(2)
N111	26(2)	21(2)	24(2)	–6(2)	1(2)	–5(2)
O112	39(2)	26(2)	32(2)	–4(2)	–5(2)	–13(2)
O113	31(2)	23(2)	27(2)	–5(1)	1(2)	–14(2)
C114	47(3)	37(3)	29(3)	–6(2)	10(3)	–25(3)
C115	41(3)	41(3)	27(3)	–7(3)	2(2)	–18(3)
C116	47(4)	34(3)	47(4)	7(3)	6(3)	–14(3)
C117	48(4)	34(3)	28(3)	3(2)	–3(3)	–10(3)
Cl1	30(1)	25(1)	42(1)	–12(1)	–5(1)	–4(1)
O1	60(3)	52(3)	58(3)	–24(2)	9(2)	–8(2)
O2	89(4)	48(3)	82(4)	–22(3)	13(3)	22(3)
O3	92(5)	188(8)	192(9)	–106(7)	–43(5)	–47(5)
O4	144(6)	79(4)	77(4)	11(3)	26(4)	–29(4)
C12	36(1)	27(1)	21(1)	–9(1)	3(1)	–2(1)

Table S-4.3. (continued)

atom	U_{11}	U_{22}	U_{33}	U_{23}	U_{13}	U_{12}
O5	128(11)	99(8)	54(6)	9(5)	36(7)	15(7)
O5'	150(19)	212(23)	61(11)	–54(13)	38(12)	–151(19)
O6	119(9)	87(7)	89(8)	31(6)	59(7)	44(7)
O6'	87(14)	83(13)	92(14)	–47(11)	52(11)	–76(12)
O7	274(18)	176(13)	122(10)	37(9)	–121(11)	–143(13)
O8	125(9)	110(8)	200(12)	–118(8)	98(9)	–80(7)
O8'	86(12)	62(10)	66(11)	10(8)	46(10)	16(9)
Ome	36(2)	31(2)	42(2)	–5(2)	–1(2)	–14(2)
Cme	42(4)	31(3)	68(5)	2(3)	–6(3)	–10(3)

[a] Estimated standard deviations in the least significant digits are given in parentheses.

[b] The anisotropic thermal parameter exponent takes the form:

$$-2\pi^2(h^2a^{*2}U_{11}+k^2b^{*2}U_{22}+....2hka^*b^*U_{12})$$

Table S-4.4. Hydrogen atom coordinates ($\times 10^4$) and thermal parameter ($Å^2 \times 10^3$) for **11b.**

atom	*x*	*y*	*z*	U_{iso}
H5A	7941	2266	2880	23
H5B	7845	920	3060	23
H6A	6029	1338	2101	21
H6B	8289	1382	2030	21
H7A	6391	2944	1287	33
H7B	7038	3516	1784	33
H14A	–910	5337	676	28
H14B	–511	6444	859	28
H14C	–2246	5909	1161	28
H15A	3061	4300	452	32
H15B	4926	4625	684	32
H15C	2855	5643	464	32
H16A	5958	63	4176	40
H16B	6242	938	4566	40
H16C	7501	824	3979	40
H17A	2502	2058	4750	33
H17B	2127	975	4537	33
H17C	378	2201	4441	33
H10A	–684	7158	3734	18
H10B	567	6604	3229	18
H10C	–348	8774	2972	24
H10D	–2635	8790	2918	24
H10E	237	7843	2132	26
H10F	–1141	9197	1948	26
H11A	–5990	4969	4367	31
H11B	–4513	3792	4235	31
H11C	–6605	4434	3850	31
H11D	–2083	4679	4609	26
H11E	–2744	6072	4574	26
H11F	–636	5469	4335	26
H11G	–4572	10126	822	43
H11H	–2879	9177	577	43
H11I	–2267	9885	1012	43
H11J	–5439	8205	368	34
H11K	–7221	9227	531	34
H11L	–7351	7889	681	34

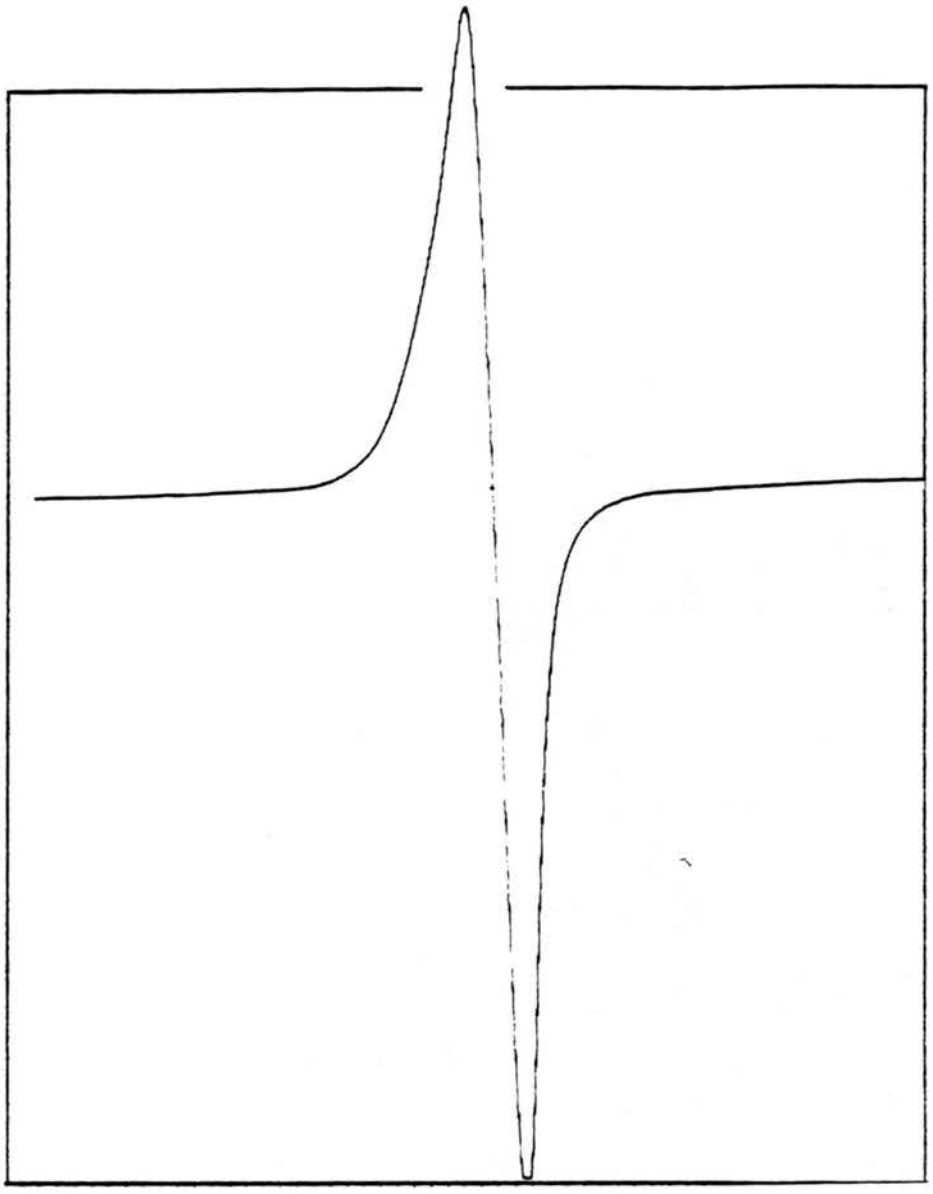

Figure S-1.1. EPR spectrum of a powder of [Cu(**1**)(μ-NC)Cu(μ-CN)]$_n$ (**5a**) at –174 °C.

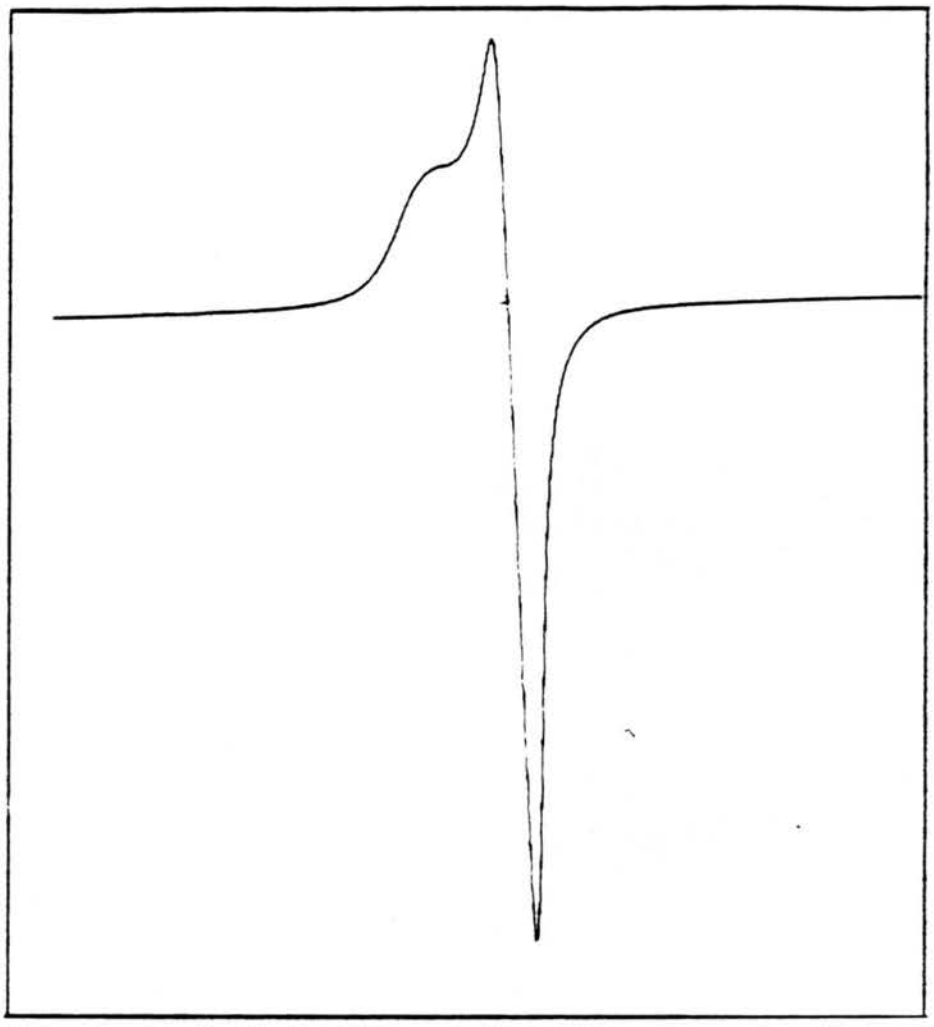

Figure S-1.2. EPR spectrum of a powder of [Cu(**1**)(μ-NC)Cu(μ-CN)]$_n$ (**5b**) at –174 °C.

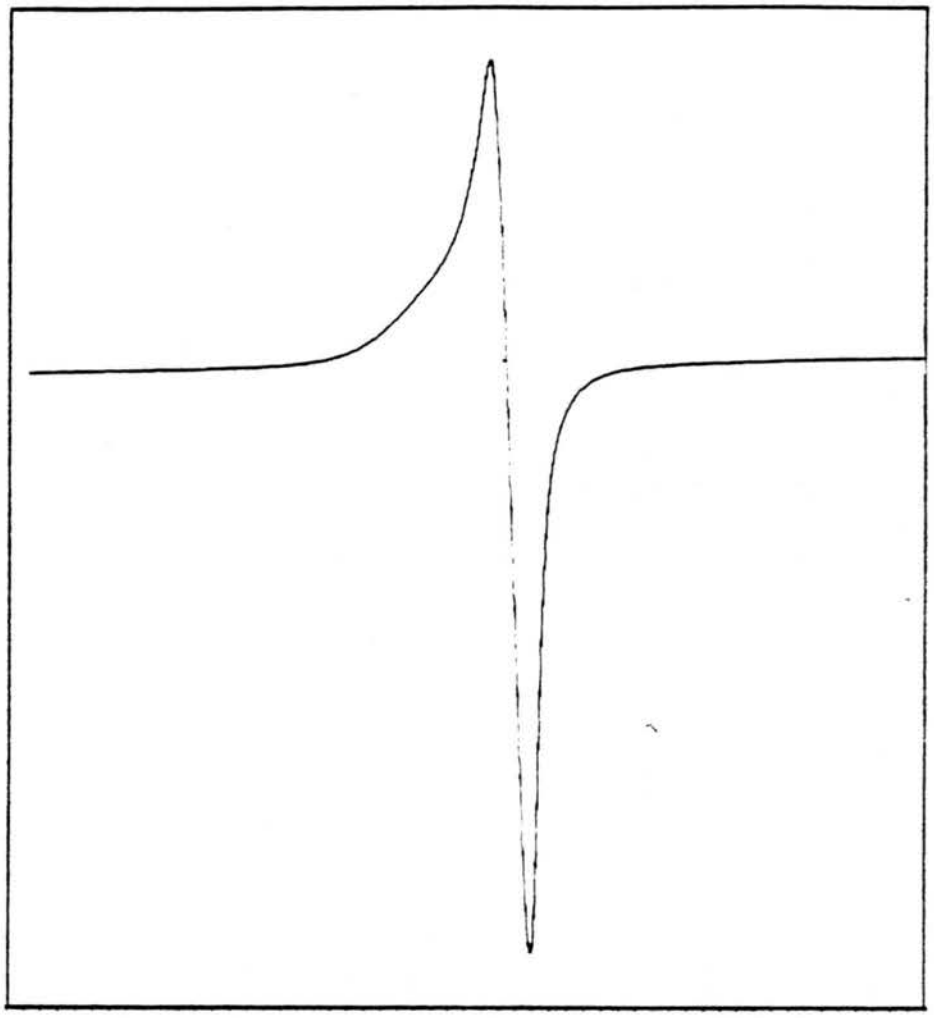

Figure S-1.3. EPR spectrum of a powder of [Cu(**1**)(μ-NC)Cu(μ-CN)]$_n$ (**5c**) at –174 °C.

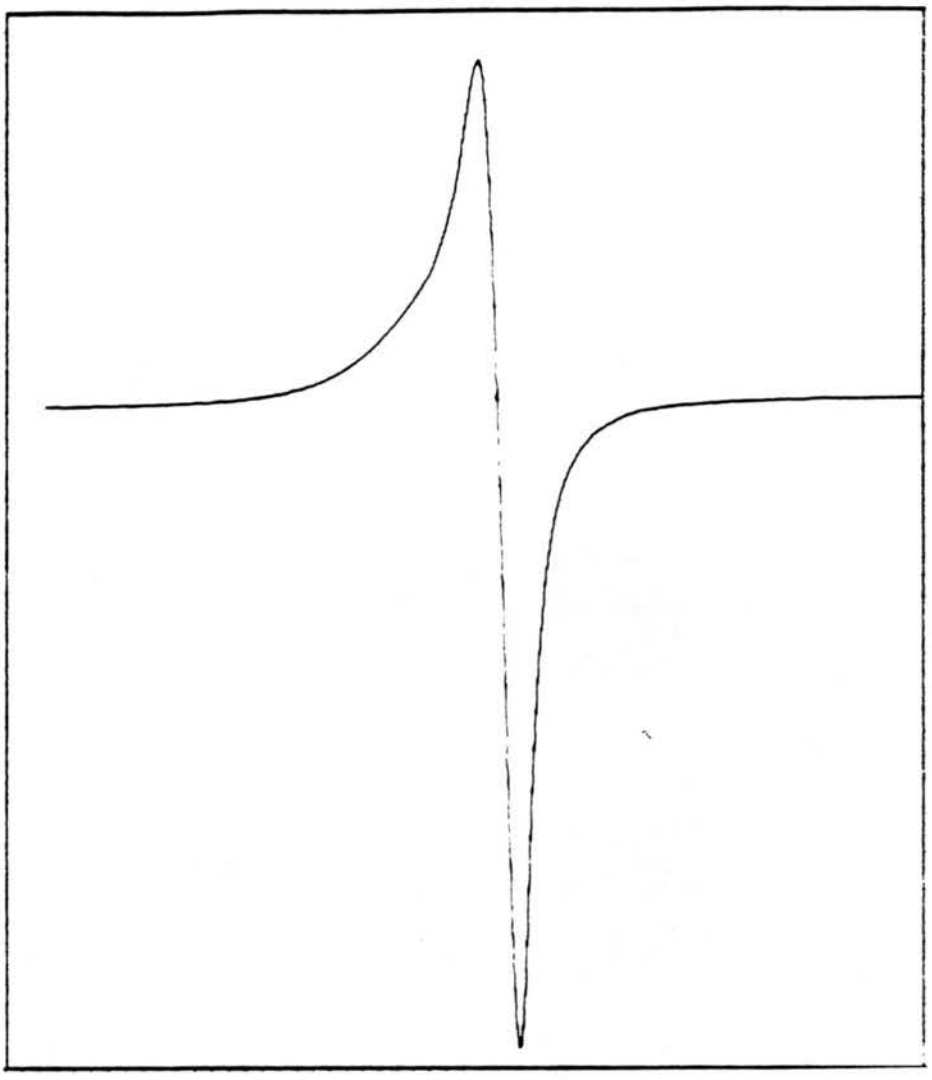

Figure S-1.4. EPR spectrum of a powder of $[Cu(\mathbf{2})(\mu\text{-NC})Cu(\mu\text{-CN})]_n$ (**6**) at –174 °C.